

AFRL-VS-HA-TR-98-0041

**DIGITAL DATABASE DEVELOPMENT AND SEISMIC
CHARACTERIZATION AND CALIBRATION FOR THE
MIDDLE EAST AND NORTH AFRICA**

**Muawia Barazangi
Dogan Seber
Eric Sandvol
David Steer
Marisa Vallve
Christine Orgren
Alex Calvert
Graham Brew
Francisco Gomez
Dan Plafcan**

AD-A286 992



**Cornell University
Institute for the Study of the Continents (INSTOC)
Snee Hall
Ithaca, NY 14853 -1504**

24 February 1998

**Final Report
20 June 1995 – 23 December 1997**

APPROVED FOR PUBLIC RELEASE, DISTRIBUTION UNLIMITED.



**DEPARTMENT OF ENERGY
Office of Non-Proliferation and National Security
WASHINGTON, DC 20585**



**AIR FORCE RESEARCH LABORATORY
Space Vehicles Directorate
29 Randolph Road
AIR FORCE MATERIEL COMMAND
HANSCOM AFB, MA 01731-3010**

99000-66


19990507188


SPONSORED BY
Department of Energy
Office of Non-Proliferation and National Security

MONITORED BY
Air Force Research Laboratory
CONTRACT No. F19628-95-C-0092

The views and conclusions contained in this document are those of the authors and should not be interpreted as representing the official policies, either express or implied, of the Air Force or U.S. Government.

This technical report has been reviewed and is approved for publication.


KATHARINE KADINSKY-CADE
Contract Manager


CHARLES P. PIKE, Deputy Director
Integration and Operations Division

This report has been reviewed by the ESD Public Affairs Office (PA) and is releasable to the National Technical Information Service (NTIS).

Qualified requestors may obtain copies from the Defense Technical Information Center. All others should apply to the National Technical Information Service.

If your address has changed, or you wish to be removed from the mailing list, or if the addressee is no longer employed by your organization, please notify AFRL/VSOS-IM, 29 Randolph Road, Hanscom AFB, MA 01731-3010. This will assist us in maintaining a current mailing list.

Do not return copies of the report unless contractual obligations or notices on a specific document requires that it be returned.

REPORT DOCUMENTATION PAGE			Form Approved OMB No. 0704-0188	
Public reporting burden for this collection of information is estimated to average 1 hour per response, including the time for reviewing instructions, searching existing data sources, gathering and maintaining the data needed, and completing and reviewing the collection of information. Send comments regarding this burden estimate or any other aspect of this collection of information, including suggestions for reducing this burden, to Washington Headquarters Services, Directorate for Information Operations and Reports, 1215 Jefferson Davis Highway, Suite 1204, Arlington, VA 22202-4302, and to the Office of Management and Budget, Paperwork Reduction Project (0704-0188), Washington, DC 20503.				
1. AGENCY USE ONLY (Leave blank)	2. REPORT DATE 24 February 1998	3. REPORT TYPE AND DATES COVERED Final Report (20 June 1995 - 23 December 1997)		
4. TITLE AND SUBTITLE Digital Database Development and Seismic Characterization and Calibration for the Middle East and North Africa		5. FUNDING NUMBERS Contract F19628-95-C-0092 PE 69120H PR DENN TA GM WU AB		
6. AUTHOR(S) Muawia Barazangi, Dogan Seber, Eric Sandvol, David Steer, Marisa Vallve, Christine Orgren Alex Calvert, Graham Brew, Francisco Gomez, Dan Plafcan				
7. PERFORMING ORGANIZATION NAME(S) AND ADDRESS(ES) Cornell University Institute for the Study of the Continents (INSTOC) Snee Hall Ithaca, NY 14853-1504		8. PERFORMING ORGANIZATION REPORT NUMBER		
9. SPONSORING / MONITORING AGENCY NAME(S) AND ADDRESS(ES) Air Force Research Laboratory 29 Randolph Road Hanscom AFB, MA 01731-3010 Contract Manager: Katharine Kadinsky-Cade/VSBS		10. SPONSORING / MONITORING AGENCY REPORT NUMBER AFRL-VS-HA-TR-98-0041		
11. SUPPLEMENTARY NOTES This research was sponsored by the Department of Energy, Office of Non-Proliferation & National Security, Washington, DC 20585				
12a. DISTRIBUTION / AVAILABILITY STATEMENT Approved for public release; distribution unlimited.		12b. DISTRIBUTION CODE		
13. ABSTRACT (Maximum 200 words) It is essential for the CTBT monitoring efforts that multidisciplinary information on any given region be readily available and accessible in a digital, on-line format via electronic networks for use by concerned researchers and decision makers. We collected and organized available seismological, geophysical, and geological data sets for the Middle East and North Africa into a comprehensive Geographic Information System (GIS). In addition, we produced original results, such as crustal structure beneath available broadband seismic stations in the Middle East and North Africa region, and basement depth values in the northern Arabian plate. In addition to the GIS databases and tools, we developed a special World Wide Web (WWW) site to allow restricted access to our databases. All the data sets in our GIS system were documented with a standard metadata format in order to explain the source and nature of the data, their resolution, and their accuracy. The developed system and its efficiency in using and analyzing information will help CTBT researchers and decision makers to fuse and integrate the results of the four established monitoring technologies to reach a conclusion in a very short time. The system also significantly contributes to the better location and calibration of suspect events for any given region. This system will also help in On Site Inspection efforts. Our World Wide Web address for information distribution is http://atlas.geo.cornell.edu .				
14. SUBJECT TERMS Middle East Moho Geographic Information System WWW North Africa 2D models Geology Satellite Imagery Crustal Structure Seismology Geophysics			15. NUMBER OF PAGES	
			16. PRICE CODE	
17. SECURITY CLASSIFICATION OF REPORT Unclassified	18. SECURITY CLASSIFICATION OF THIS PAGE Unclassified	19. SECURITY CLASSIFICATION OF ABSTRACT Unclassified	20. LIMITATION OF ABSTRACT SAR	

TABLE OF CONTENTS

INTRODUCTION.....	1
PART I: DEVELOPING A COMPREHENSIVE GIS DATABASE SYSTEM (GEOID – GEOSCIENCE INTERACTIVE DATABASES).....	2
1. Installing GEOID	3
2. Running GEOID	3
2.1. Menu Driven Access	3
2.1.1. Map Controls.....	4
2.1.1.1. Set Maplimits.....	4
2.1.1.2. Set Map Projection	5
2.1.1.3. Lat/Long Grid	5
2.1.1.4. Add Legend	6
2.1.1.5. Zoom in, Zoom out, and Previous zoom	6
2.1.2. Data Sets	6
2.1.2.1. Geographic Data	8
2.1.2.2. Geophysical Data	12
Earthquake Catalogs	12
ISC Phase Data Selection and Analysis Tools.....	14
Focal Mechanisms	16
Middle East Crustal Profiles	17
Seismic Station Locations.....	19
International Monitoring Station Locations.....	20
Turkish GPS vectors	20
2.1.2.3. Geological Data Sets	22
Tectonic Map of the Middle East and North Africa	22
Mine Locations	23
World Stress Map	23
Holocene Volcanoes	25
World Geology Map	25
2.1.2.4 Images/Grids	25
Topography	27
Eurasia Basement Map	29
Eurasia Moho Map.....	29
Cornell basement	29
Cornell Moho	30
University of Colorado Basement.....	30
Lg Coda Q Values.....	31
Pn Velocity.....	31
Bouguer Gravity Data	31
TM Images	35
The Profile Maker	35
2.1.3. Tools and Utilities in GEOID	36
Run Arc Plot Command.....	38
Redraw Map.....	38

Symbol Sets	38
Enter Points.....	39
Measure Distance.....	39
Measure Area.....	39
Save Algorithm/Load Algorithm	39
Hardcopy.....	40
Reset All Variables	40
PART II: DIGITAL DATABASES FOR USE IN REGIONAL DISCRIMINATION OF EARTHQUAKES AND MINE-RELATED EXPLOSIONS IN NORTH AFRICA: A JOINT EFFORT WITH THE LLNL.....	41
1. Monitoring Mining Activity Using Remote Sensing	41
2. Discrimination of Explosions from Earthquakes.....	41
PART III. MIDDLE EAST AND NORTH AFRICA LOCAL COUNTRY SEISMIC BULLETINS.....	46
1. Earthquake Catalogs	46
Phase Data.....	46
Station Data.....	46
Hardcopy Catalogs.....	46
PART IV: METADATA.....	48
PART V: RESULTS OF ORIGINAL SEISMOLOGICAL RESEARCH IN SUPPORT OF CTBT	50
A. CRUSTAL STRUCTURE IN THE MIDDLE EAST AND AFRICA: GRID SEARCH INVERSION OF RECEIVER FUNCTIONS	50
Abstract.....	50
Introduction.....	50
Data	54
Inversion Method	58
Resolution and Error Analysis	64
Results and Interpretations.....	68
Conclusions.....	75
References.....	81
B. LITHOSPHERIC VELOCITY DISCONTINUITIES BENEATH THE ARABIAN SHIELD.....	84
Abstract.....	84
Introduction.....	84
Data and Inversion Method	85
Results	88
Interpretations and Conclusions	89
References.....	93

C. BASEMENT DEPTH AND SEDIMENTARY VELOCITY STRUCTURE IN THE NORTHERN ARABIAN PLATFORM, EASTERN SYRIA	95
Abstract.....	95
Introduction And Geologic Background.....	95
Basement Rocks in Syria	99
Data Analysis	99
Data Acquisition	99
Data Interpretation	102
The Final Velocity Model.....	107
Discussion.....	107
Cenozoic and Mesozoic	110
Paleozoic	110
Precambrian	118
Conclusions	120
References	120
D. AN INTEGRATED GEOPHYSICAL INVESTIGATION OF RECENT SEISMICITY IN THE AL-HOCEIMA REGION OF NORTH MOROCCO .	124
Abstract.....	124
Introduction	124
Tectonic Summary	125
Seismological Observations	128
Examination of location errors	132
Seismicity of the Al-Hoceima region	134
Analysis of Marine Seismic Reflection Profiles	138
Discussion.....	139
Conclusions	147
References	147
E. REGIONAL DISCRIMINATION OF CHEMICAL EXPLOSIONS AND EARTHQUAKES: A CASE STUDY IN MOROCCO.....	152
Abstract.....	152
Introduction	152
Crustal Structure of Northwest Morocco	156
Data.....	156
Processing Methods.....	158
Analysis and Results	163
Discussion.....	167
Conclusions	171
References	172
APENDIX I: COLLECTED REFERENCES ON THE GEOLOGY/GEOPHYSICS OF THE MIDDLE EAST AND NORTH AFRICA.....	174
1. References for the Middle East.....	174
2. References for North Africa.....	207

INTRODUCTION

With the signing of a multilateral comprehensive nuclear test ban treaty, it is essential for monitoring efforts that multidisciplinary "reference" information on any given region be readily available and accessible in a digital, on-line format via electronic networks or on host computers used by concerned researchers and decision makers. We have designed and built a digital geophysical and geological information system to help in these efforts. Several essential data sets can be accessed and analyzed with ease and speed within this system. The data sets are complete with "metadata" information allowing users to be familiar with the source, resolution, accuracy, and limitations of the databases. Data access tools are also an important part of the whole system, since it would be very cumbersome to access a specific data set among all types of databases that are kept on the system. This developed system allows a user to search, manipulate, and interact with the databases easily and efficiently. Our GIS system and scientific results are of direct relevance to US efforts in enhancing regional seismic monitoring and discrimination capabilities and to the implementation and operation of the US NDC and monitoring efforts.

The amount of information available for the Middle East and North Africa region is comparatively limited. In order to enrich the content of our database and provide more detailed data sets, we also conducted several seismological studies. It is well known that variations in crustal and lithospheric structure as well as major topographic relief are crucial information for regional event location, understanding seismic wave excitation and the propagation of high-frequency regional seismic phases, verification, and yield estimation of nuclear and chemical explosions. Our research was focused on obtaining this type of information in the Middle East and North Africa region. We obtained crustal depth and velocities beneath broadband seismic stations using receiver function analysis, estimated basement depth in the northern Arabian plate, studied recordings of earthquake and chemical explosion characteristics in Morocco, and relocated some of the earthquakes along the northern Moroccan coast. In addition, we digitized all available crustal scale profiles in the Middle East region. By using these interpretations we produced more detailed and accurate Moho and basement maps which can be used in modeling efforts. We also developed the first digital tectonic map of the Middle East and North Africa region. Finally, we collected significant number of relevant references related to geology and geophysics of the Middle East and North Africa region.

PART I: DEVELOPING A COMPREHENSIVE GIS DATABASE SYSTEM (GEOID – GEOscience Interactive Databases)

GEOID is a Geographic Information System (GIS) with extensive internal data sets as well as data manipulation, analysis, search, and plotting tools. It includes data sets in four different categories: geographic, geophysical, geological, and imagery/grids. The system has been developed over three years, and it continues to grow in size. The target scale of the internal data sets varies, but an average scale of 1:1,000,000 is preserved throughout the entire system. GEOID provides users a unique opportunity to study, search, and analyze several kinds of geophysical, geological, remote sensing and topography data simultaneously. The efficiency and the speed of the system make it more valuable for users who need to access critical information very quickly. The Comprehensive Test Ban community will benefit significantly from this system. Some of the benefits of the GEOID are: better event location, as it provides the most accurate crustal and velocity information on specific regions, providing "ground truth" for better calibration efforts, better understanding of regional seismic phase propagation by providing easy to use tools to extract crustal scale profiles between two arbitrary points, and the ability to interact with any data in the system. GEOID goes far beyond just map making, helping researchers and decision makers obtain considerable information about the geology and geophysics of a region, and helping in efforts before and after an On Site Inspection by providing comprehensive geographical, geological, and imagery information about that region.

GEOID runs on top of a commercially available Arc/Info GIS software. Before installing GEOID, Arc/Info software must be present in the system. Currently, the system is operational only on a UNIX platform. However, the system dependence is quite minimal and with little effort GEOID can run on any platform running Arc/Info software. Its menu-driven interfaces eliminate the need to know Arc/Info prior to using this system, making it easy to use and attractive to all users at all levels. Almost all the programming in GEOID has been done using Arc/Info's internal Arc Macro Language (AML).

Although the background data sets (i.e., geographic data) in GEOID are global, the geological and geophysical data sets are focused on the Middle East and North Africa region. There are a few global data sets such as seismicity, focal mechanisms of larger events, and a global geology map.

The database format is Arc/Info's coverage and table format. Each data set forms a layer, and it is linked with other data sets either through geographic extent and/or with feature items located in each data set.

1. Installing GEOID

GEOID requires about 6 Gbytes of disk space to install. In the distribution tape there is a README file which details the installation process step by step. You need write access to Arc/Info's home directory, as you need to copy some files there.

2. Running GEOID

Accessing the entire database is done through a series of customized menus. The main control menu is shown in Figure 1. In order to start the program, you need to start Arc/Info and at the Arc: prompt type "GEOID". A global map with oceans highlighted will be plotted and the main menu will be activated (Figure 1). This is the default setting.

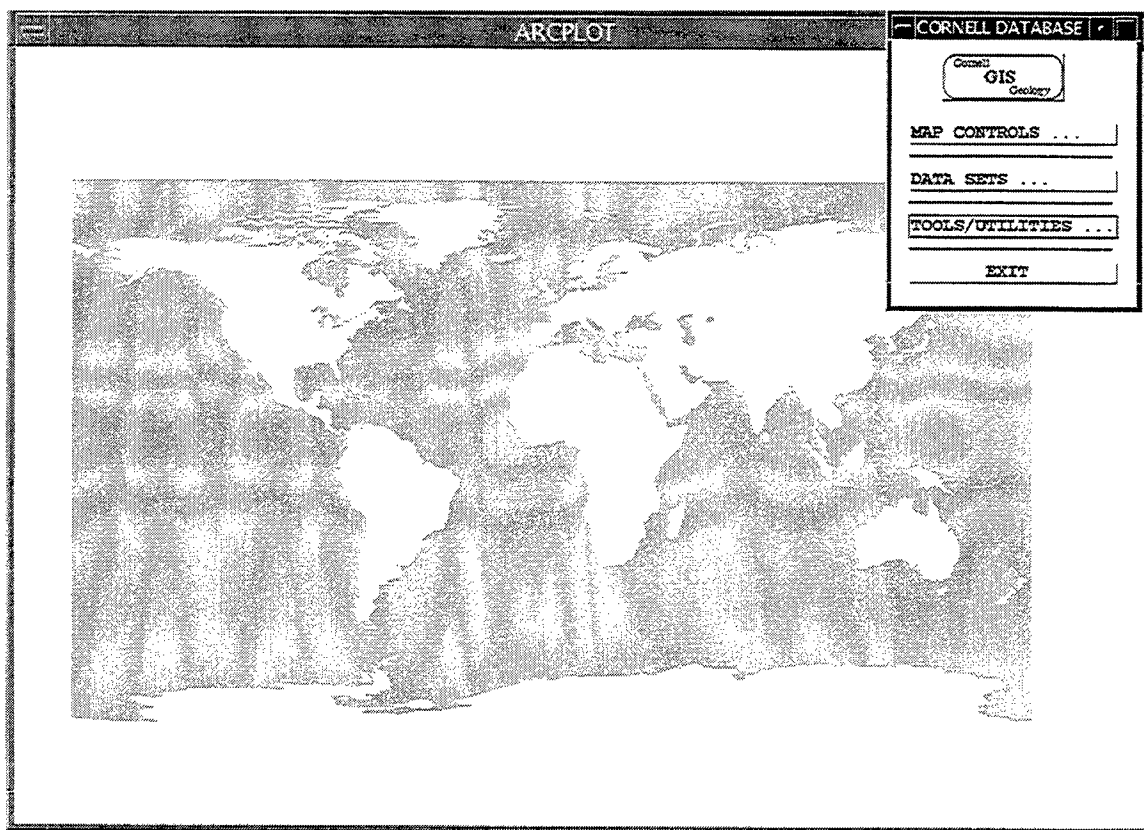


Figure 1. GEOID starts with a main menu and a global map.

2.1. Menu Driven Access

There are two types of buttons used in the menus: check buttons and regular buttons. Check buttons are usually used in displaying any individual data sets and are activated as soon as they are checked. The regular menu buttons are used either for an action or to start up a new sub menu. The main menu includes four buttons, three of which initiate a

sub menu, and one, the exit button, quits the entire program. Buttons which start up additional sub menus are indicated by three dots at the end of the function names.

2.1.1. Map Controls

The “Map Controls” menu can be accessed using the button in Figure 1. This button will start up a new sub menu which allows setting the desired map limits and map projection, adding a latitude and longitude grid, adding a legend, and zoom options (Figure 2).

2.1.1.1. Set Maplimits

The set map limits button is used to set up a region of interest. One can choose an already defined region, such as the Middle East and North Africa or North America, or type in latitudes and longitudes bounding the area of interest (Figure 3).

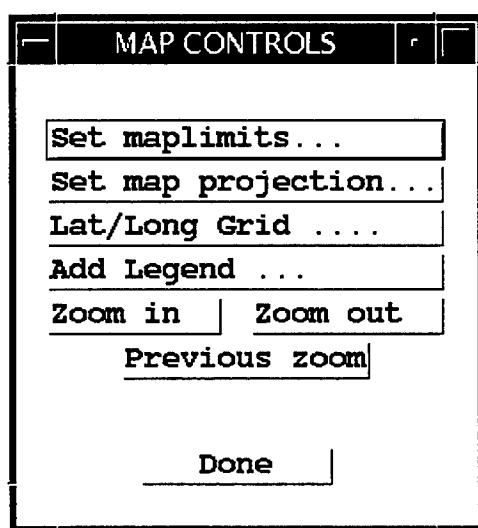


Figure 2. Map controls menu allows users to set essential mapping parameters.

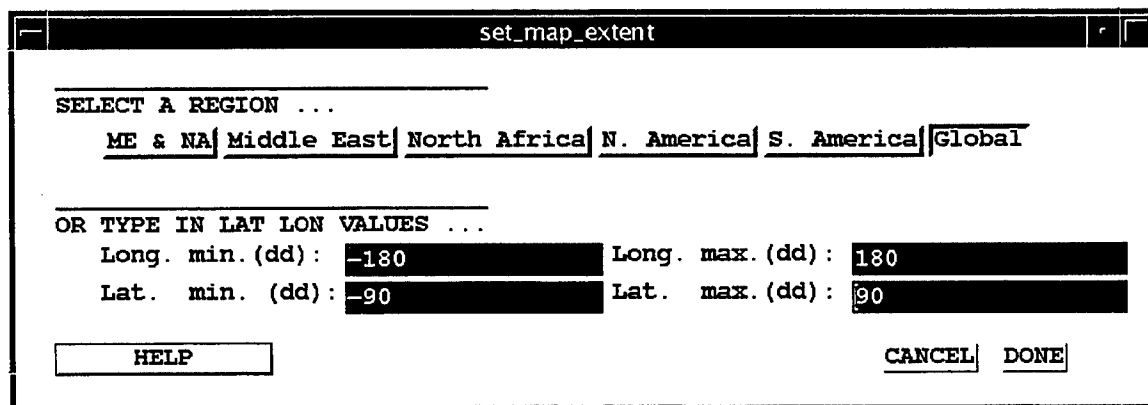


Figure 3. Set map limits menu allows users to set a region of interest either by clicking on a previously defined region or by typing latitude and longitude values bounding a region.

2.1.1.2. Set Map Projection

Map projections in GEOID are done on the fly for all line, polygon, and point type data sets. The grids and images are kept in Equirectangular projection, as projecting any grid will take too long to accomplish on the fly. Using this menu users can set one of the available projections and define the projection's parameters (Figure 4). After this point, until it is changed again, all mapping will use this specified projection. It is possible to change the projection at any time during a session. The default projection is Equirectangular. A warning message will be displayed if a user attempts to display an image file when a different projection is active. In this release there is no option of using other projections. This will be added to the system in future releases.

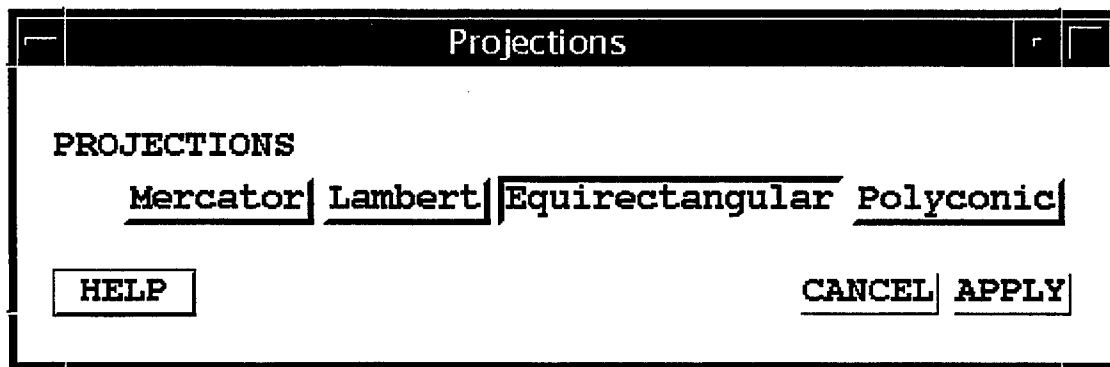


Figure 4. Available map projections in GEOID. In each projection user defined projection parameters can be entered into the system.

2.1.1.3. Lat/Long Grid

This button is used to add a latitude-longitude grid and grid labels to the map. A sub menu allowing a user to choose grid interval, label interval, and their locations appears on the screen (Figure 5). After typing in the desired numbers and checking the "On" button, the grid is displayed once the "Done" button is pressed. It is also possible to set the label format with this menu. Grid label formats are DD, DDM, and DMS representing Decimal Degree, Decimal Degrees - Minutes, and Decimal Degrees - Minutes - Seconds, respectively. Both line and tic (cross) styles are supported in latitude and longitude grids. Labels can be placed on top, bottom, left, or right by highlighting the appropriate button.

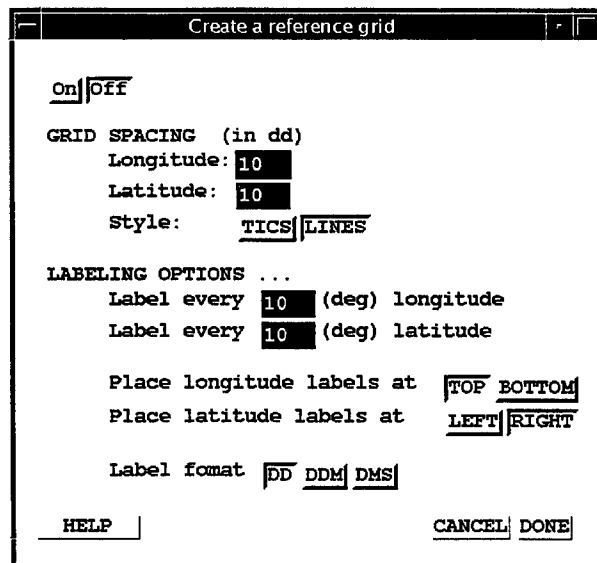


Figure 5. Menu to set up a latitude and longitude grid. Grid interval and label interval must be defined separately as different numbers can be set for each.

2.1.1.4. Add Legend

This button is used to add a legend for the map. GEOID automatically detects which data sets have been activated and generates a legend. The legend's scale (i.e., its size) can be changed by entering a scale factor (Figure 6). The majority of data sets will produce a legend if they are displayed. However, not all data sets can be seen in the legend. It is possible to have items like tectonic units, mine locations, and crustal profile locations, but items like coast lines and country borders will not appear in the legend box. The default legend will appear at the lower right corner of the map. However, it can be moved anywhere on the page by clicking the Move legend button. Once this button is clicked, you need to define the new position and mark the lower left corner on the screen. By clicking the Cancel legend button the legend can be removed from the map.

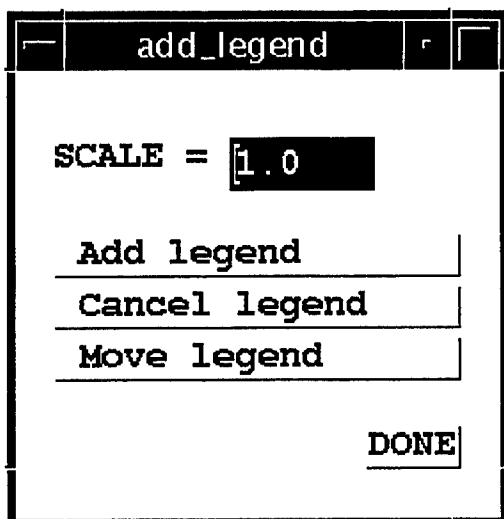


Figure 6. Menu used to place a legend on the map.

2.1.1.5. Zoom in, Zoom out, and Previous zoom

These three buttons are used to set a zoom level. Instead of using the Set map limits option described above, one can use the zoom in button to zoom in on a region of interest directly from the screen. Once the Zoom in button is pressed, two corners of the area of interest must be marked on the screen. You can mark the corners in any order. The new map area will be redrawn when two points are marked in the screen. The Zoom out button

zooms back to initial map limits. The Previous zoom option allows going back one step in zoom level.

2.1.2. Data Sets

The data sets menu button (see Figure 1 inset) is the button through which all the data in the system can be accessed. Clicking on this button will activate the "Datasets" menu with four options representing our four categories of data classes: Geographic, geophysical, geological, and images/grids (Figure 7). For data sources and quality refer to the Metadata section. The following sections highlight all the data sets and related access tools.

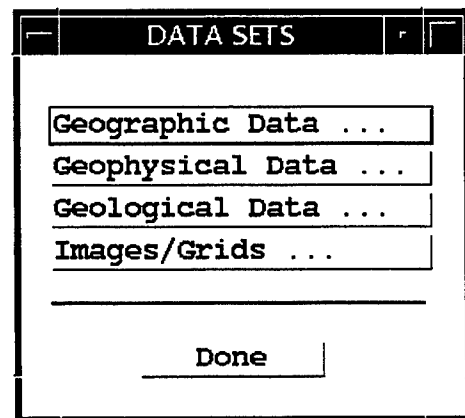


Figure 7. The Data sets menu allows the access to all data sets in GBASE.

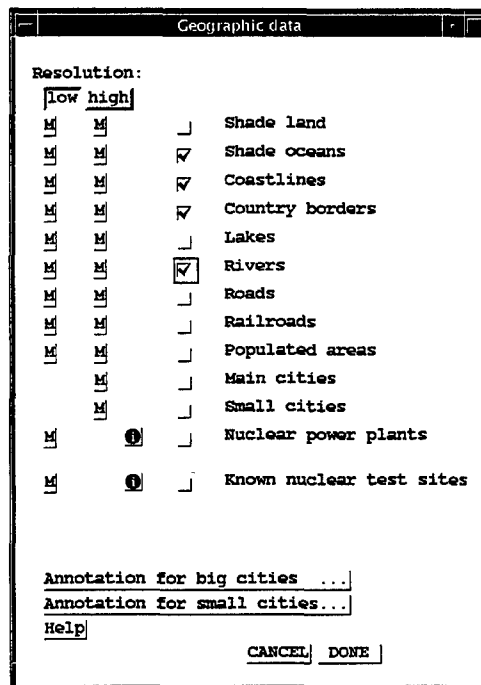


Figure 8. Menu with available geographic data sets. In addition, global data sets of nuclear power plant locations and known nuclear test sites can also be accessed via this menu.

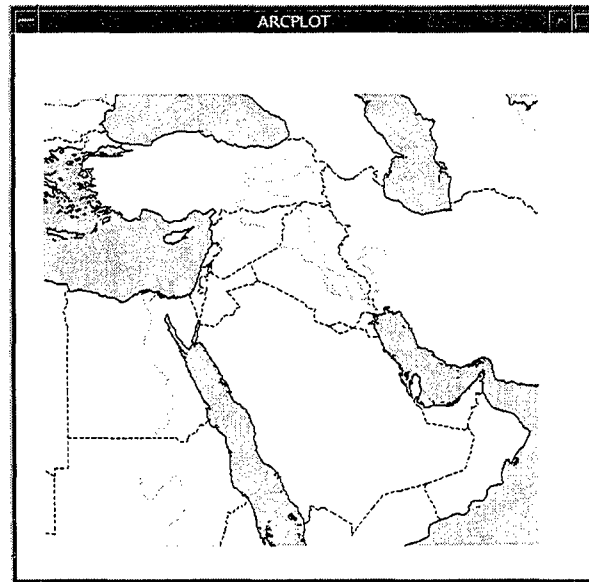


Figure 9. Map obtained after the selection in Figure 8 is made.

2.1.2.1. Geographic Data

Geographic data sets are kept and accessed through this button. All essential geographic information such as coastlines, country borders, city locations, etc., are available. All available data sets can be viewed once this button is checked (Figure 8). All geographic data were extracted from the Digital Chart of the World. The original data sources are maps of 1,000,000 scale. Hence, this represents the resolution level at which these data

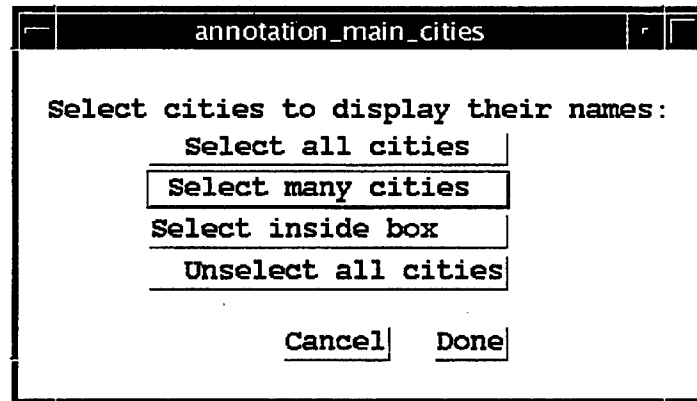


Figure 10a. Menu to label the city names.

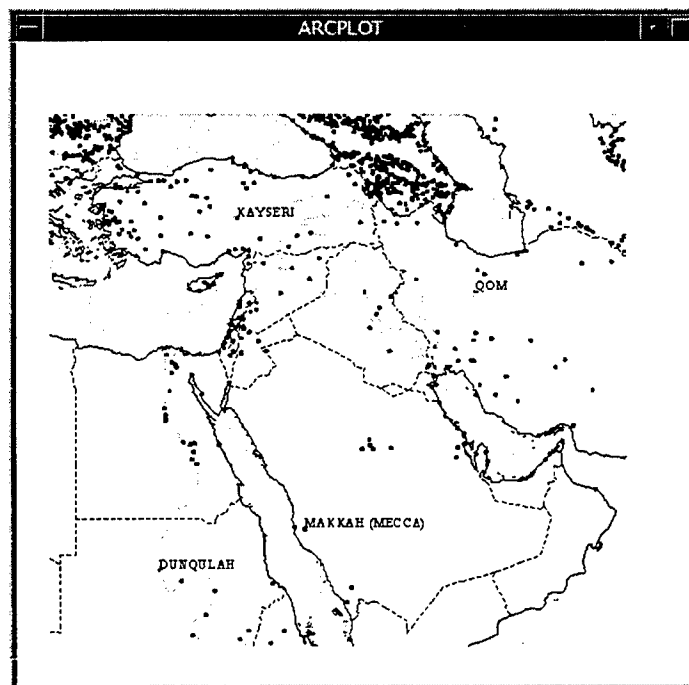


Figure 10b. Map showing the main city location data set. Four cities selected and labeled using the menu shown in Figure 10a.

sets should be used. In order to speed up the plotting process when much smaller scale maps are requested, a resampled low resolution data set is plotted. The low resolution

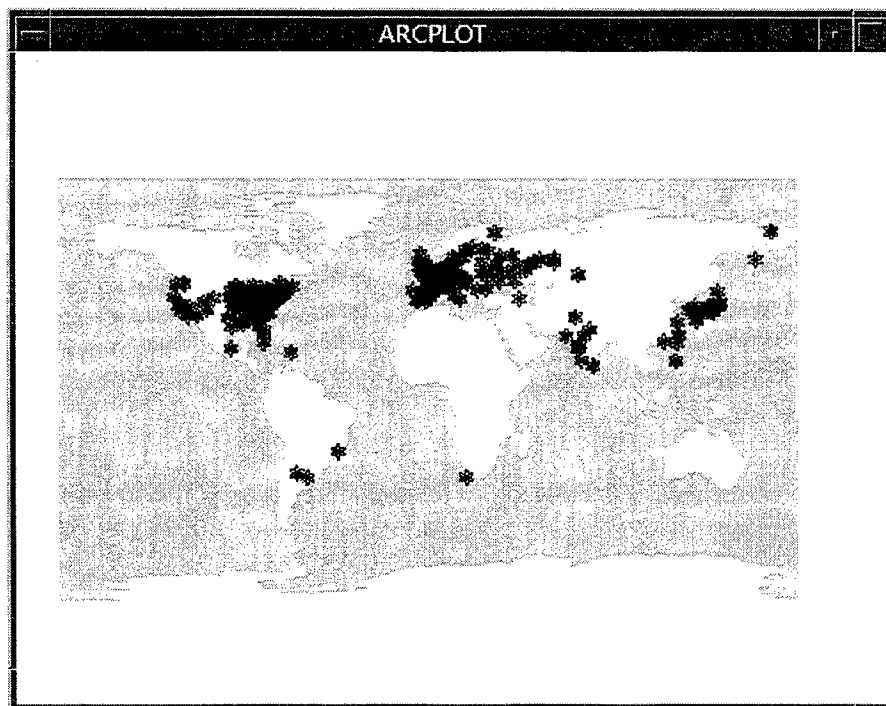


Figure 11. Nuclear power plant locations in the world.

data are the default. The selection criterion above the geographic data sets menu labeled as “low” and “high” must be changed to high, if the user wishes to have the high resolution data sets.

All geographic data can be accessed through check buttons next to their names. As soon as any data set is checked, it is plotted. Figure 9 shows an example of output with selections shown in Figure 8 after zooming on the Middle East region.

The two buttons at the end of the menu (“Annotation for big cities” and “Annotation for small cities”) are used to label cities. An example is shown in Figures 10a and 10b. It is possible either to choose all the cities and label them or choose a few cities and just label the chosen ones. Selecting all the cities usually gives overlapping labels due to the large number of cities being selected. In order to prevent this problem, it is better to select a few cities using the “Select many cities” button and mark the city locations that need to be labeled. As many cities as necessary can be selected. Once the selection is made, the 9 key on the keyboard stops the selection process and the selected cities are labeled. The same selection criteria can also be applied to smaller cities. In order to remove the city labels, the “Unselect all cities” button must be clicked. This removes all of the selections from the selection file.

Other data sets that are kept within the geographic data sets menu are nuclear power plant locations and nuclear test sites. Both of these data sets are global. Figures 11 and 12 show these data sets.

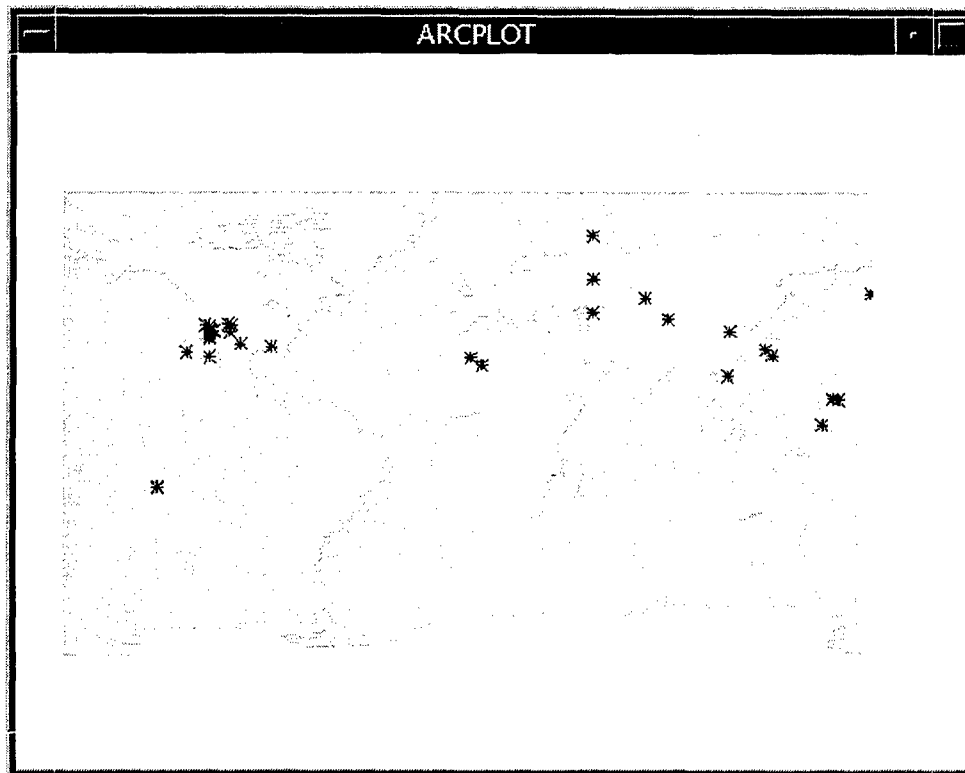


Figure 12. Map showing known nuclear test site locations.

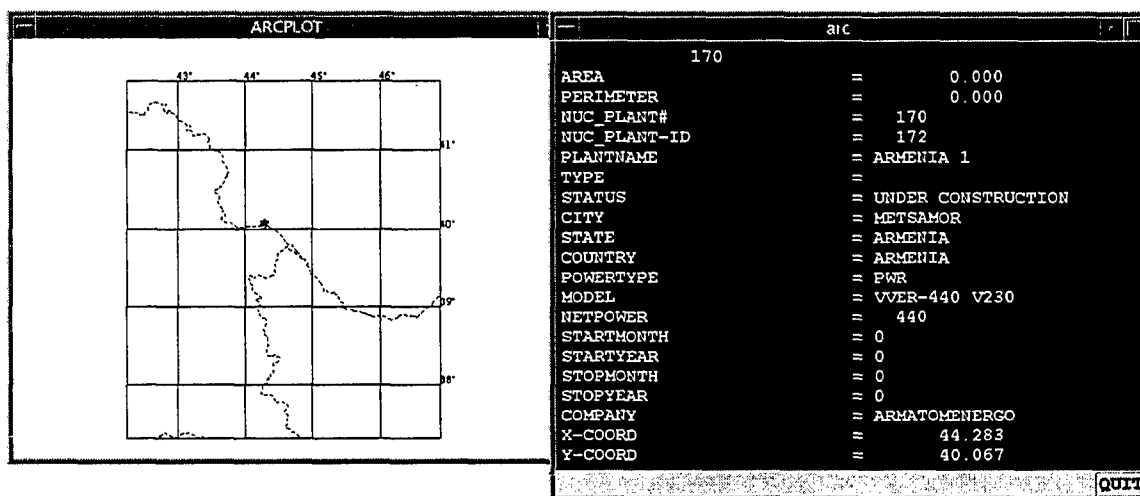


Figure 13. Map showing the Turkish and Armenian border and the nuclear power plant in the region (left). Once the identify button is clicked, the "i" button in Figure 8, and this power plant is selected from the screen, information regarding the power plant is displayed in an adjacent new window.

In the geographic data sets menu as well as in all other data set menus there are icons named "i". These icons indicate that features in these data sets can be identified, and all the items assigned to each feature can be viewed from the screen. For example, in order to identify one of the power plants in the Middle East, after zooming in on that region, one needs to click on the icon "i" next to this data set. This will initiate an interactive search. Going to the map and clicking on any of these nuclear power plants will give information and attributes about the selected feature. An example is shown in Figures 13. After zooming on the Turkish – Armenian border, selecting the "i" next to the nuclear power plants data set, and clicking on the nuclear power plant symbol on the map, a new window will pop up on the screen showing all the attributes available for that data point. This option is quite useful throughout the GEOID environment. It makes maps dynamic, and allows users to obtain information about any data point on the screen.

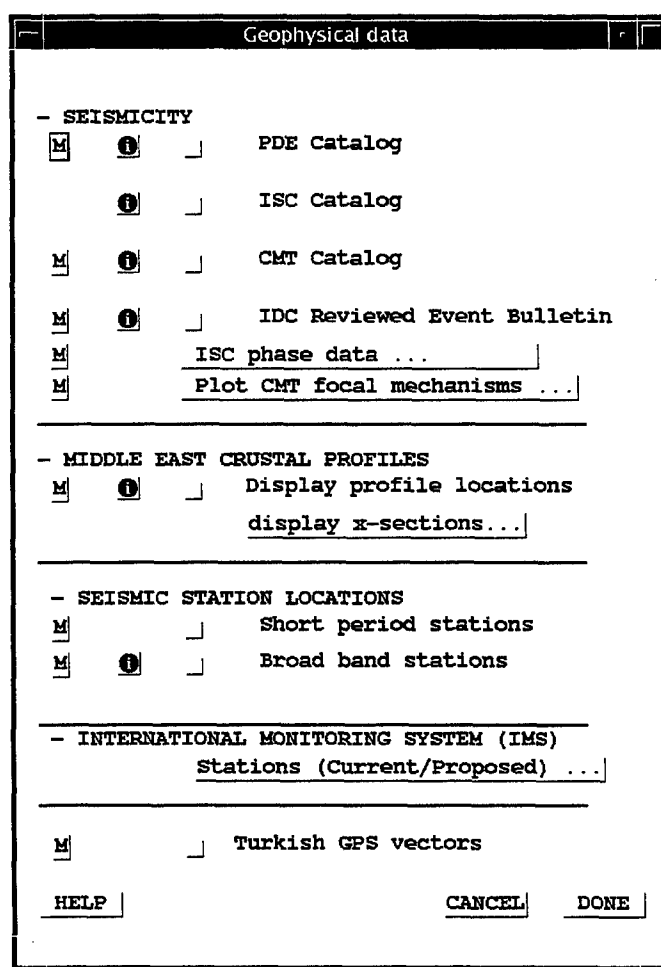


Figure 14. Geophysical data sets menu. Remaining geophysical data sets are included in the Grids/Images menu.

The buttons labeled "M" in this menu as well as in the others represent the metadata access tools. Each data set contains metadata which provides information about the resolution, accuracy, source, and attributes about the data set. In a later chapter the

metadata will be discussed in more detail.

2.1.2.2. Geophysical Data

Although some of the geophysical data sets are placed under the images/Grids menu option, all non-grid type data sets are accessed through this menu button. Figure 14 shows the content of the “Geophysical Data” menu. The data sets include: Seismicity catalogs, focal mechanisms, crustal scale refraction and gravity profile locations and their interpreted depth sections in the Middle East region, local seismic station locations in the Middle East and North Africa, broadband station locations in the Middle East and North Africa, International Monitoring System station locations, and displacement vectors obtained by GPS in the eastern Mediterranean.

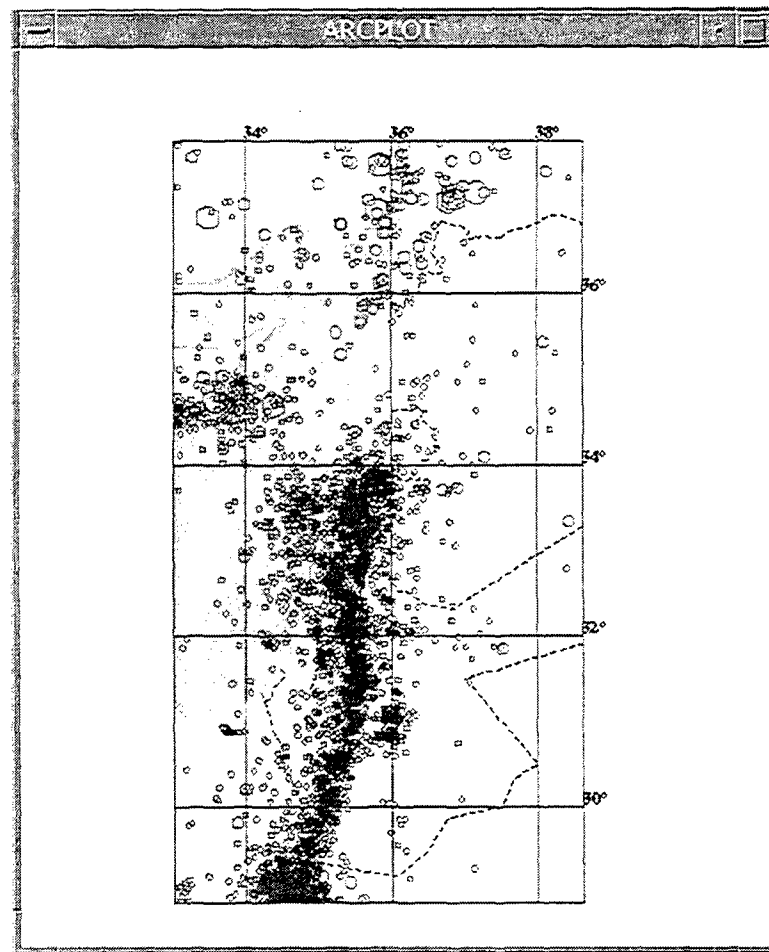


Figure 15. Seismicity along the Dead Sea fault system from the ISC catalog. This map is obtained by first zooming in on this region and then checking the ISC check button in the geophysical data sets menu.

Earthquake Catalogs

We collected all available and reliable seismic catalogs and placed them in GEOID.

These data catalogs include: the USGS, the International Seismological Centre (ISC), Centroid Moment Tensor locations and solutions from Harvard University, and the International Data Centre's reviewed event bulletins. Among these catalogs, only the ISC's catalog is global and is complete with all related phase data. The other catalogs include only the locations and primary information such as magnitude, depth, and origin time.

The USGS catalog covers the period from 1964 to 1992. This data set is only for the Middle East and North Africa region. The ISC catalog covers the period from 1964 to 1994. It is global in nature and complete with all the phase information. The CMT catalog is global, and most useful when events with focal mechanisms need to be analyzed. The catalog covers a time period of 1977 to 1996. The magnitudes of the earthquakes in this catalog are 5.5 or higher. All the events are complete with their attributes as provided by the Harvard group. The IDC catalog covers a much shorter time period (1996 - Sept, 1997), as the IDC is a new organization. The IDC events include magnitude, depth and origin time information.

Figure 15 shows earthquakes from the ISC catalog along the Dead Sea fault system in the Middle East. This map can be obtained by zooming in on the region using the "Zoom in" button, then checking the ISC catalog check button in this menu. The events are plotted with varying symbol sizes related to their magnitudes.

isc_catalog

☒ ⓘ Show Stations

☒ ⓘ Show Earthquakes

Show events recorded by a station

Select station/s from screen ...

Select rectangular area coordinates ...

Select by entering station name ...

Show stations which recorded an event

Select event/s from screen ...

Select rectangular area coordinates ...

CANCEL

Figure 16. ISC phase data selection tool. Either station or event based searches can be conducted.

ISC Phase Data Selection and Analysis Tools

The "ISC phase data" button can be used to start up new tools for further analysis and selection of the ISC phase data (Figure 16). One can search the ISC data set by either station or event attributes. In either case, the search can be done for a single station/event or a group of stations/events located in an area defined by a box. Selecting a single station can be done either by station name or by simply clicking on any station on screen. One can also click on an event to select it from the screen. There are further selection criteria based on date, depth of event, and azimuth of arrival. For example, if one decides to select all events recorded (and reported to the ISC) by station TAB in Iran, he/she first clicks the "select by entering station name" button. This will initiate a secondary menu shown in Figure 17. In this menu, the station name "TAB" is entered in the text input area on top. Then any other selection criteria such as event depth, date, distance range of events, and azimuths can be entered. In this example, if we select a distance range of 0 to 10 degrees we need to modify the default distance variables, then click on the "Start search" button. This search will return all the events in the range of 0–10 degrees from the station "TAB" between the years 1964 - 1994. The output on the screen is shown in Figure 18a. A further step would be either to export the selection as an ascii file or to view the travel time plots of the selected data. If one would like to see

The screenshot shows a window titled "isc_select" with the following content:

Enter Station name:

OPTIONS: _____

Distance (degrees):	Date (m/d/year):
From: <input type="text" value="0"/>	From: <input type="text" value="01/01/1964"/>
To: <input type="text" value="10."/>	To: <input type="text" value="12/31/1994"/>

Depth (km):	Azimuth:
From: <input type="text" value="0.0"/>	From: <input type="text" value="0"/>
To: <input type="text" value="800.0"/>	To: <input type="text" value="360"/>

**** Search Database ****

- ☐ Show selected stations
- ☐ Show selected events

Calculate Great Circle Paths

- ☐ Show great circle paths

View Travel-Time Plot ...

Generate an ascii file of selected data sets

Remove selection and redraw

QUIT

Figure 17. One of the sub menus used in selecting ISC phases by station name.

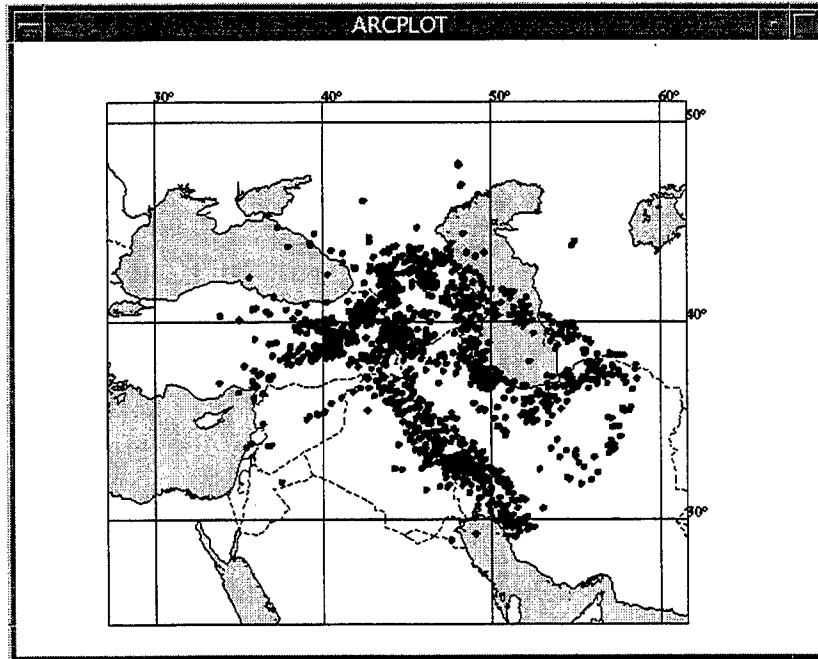


Figure 18a. Station TAB in Iran and recorded earthquakes between 0 and 10 degrees from the station.

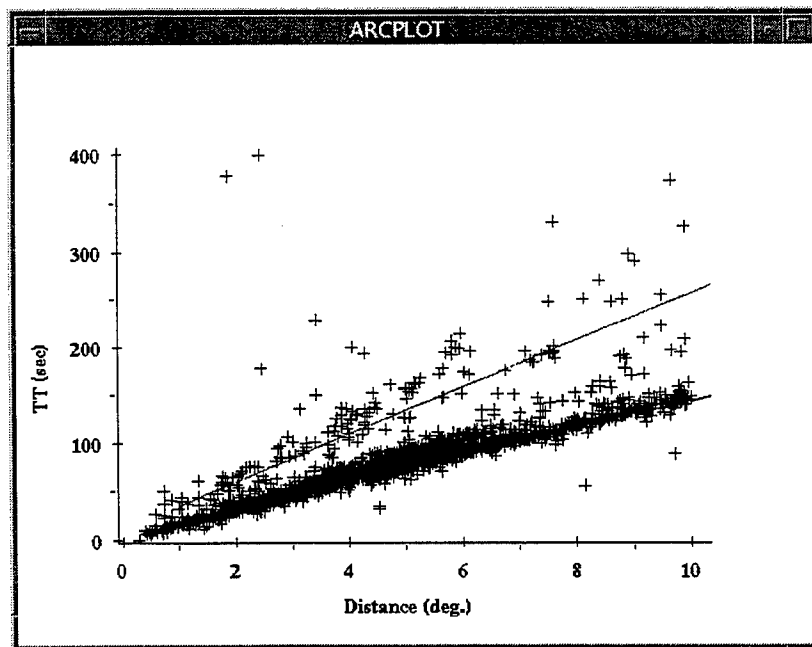


Figure 18b. Travel time plot of selected events in Figure 18a. Theoretical Pn and Sn curves are also plotted as lines.

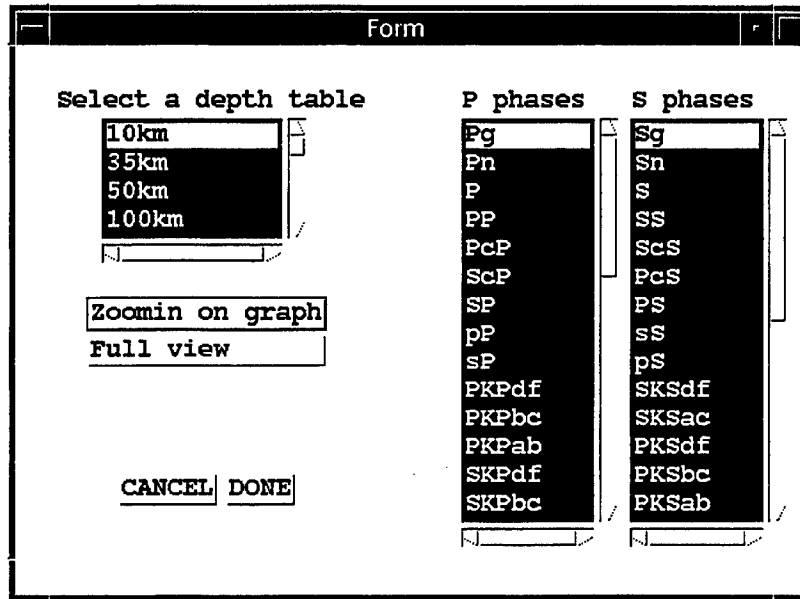


Figure 19. IASPEI-91 travel times are included in GEOID, and theoretical travel times of each of the available phases can be plotted with the selected ISC phases.

the travel time data, a click on the “View Travel-Time Curve” button will initiate a new sub menu (Figure 19) and the travel time plot will be displayed on the screen. In this menu there are options as well. GEOID includes IASPEI-91 travel-time tables. Certain phases from this travel-time table can be plotted on top of the observed phase arrivals. First a depth range needs to be selected. The default value is 10km. This value can be changed by simply clicking on the appropriate depth value. Then, any desired phase can be selected from the list in the window. Figure 18b shows the phase readings and theoretical Pn and Sn phase arrivals. It is also possible to zoom in on a region in the travel-time plot using the zoom in button.

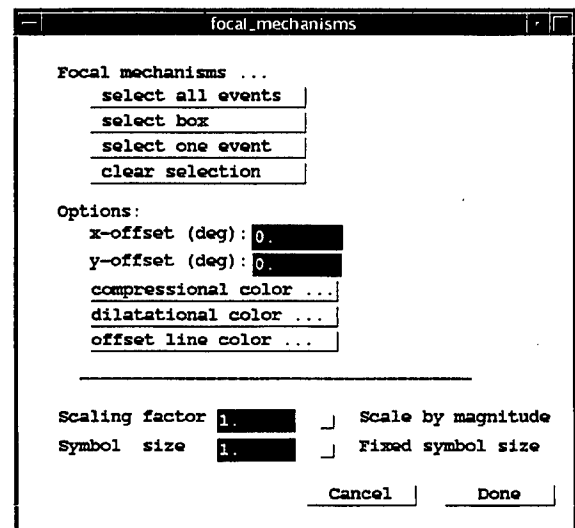


Figure 20. Focal mechanism plotting menu. Events can be plotted after a selection is made, and one of the check buttons is checked.

Focal Mechanisms

Harvard Centroid Moment Tensor (CMT) solutions are included in GEOID. In order to display the focal mechanisms, the “Plot CMT Focal Mechanisms” button needs to be

clicked (Figure 14). This initiates a new window with several options (Figure 20). In this menu one can select all the events or select a single event from screen or events located in a region. A linear offset can be applied to selected focal mechanisms. Focal mechanisms can be plotted with varying sizes relative to their magnitudes or they can be plotted at a fixed size. Once the selection is done, clicking on one of the checkboxes at the bottom of the window plots the focal mechanisms. Figure 21 shows an example plot showing earthquake locations and a few focal mechanisms in Eastern Turkey. The focal mechanism data set is global. Hence, a similar map can be done on any region on earth.

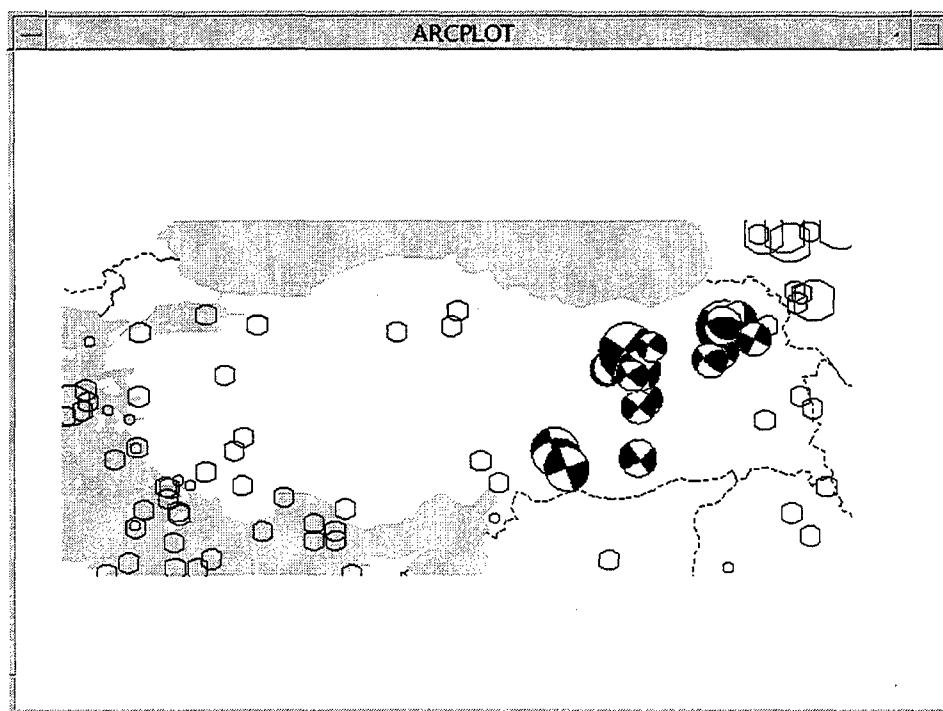


Figure 21. Focal Mechanisms of a few selected events in eastern Turkey. The focal mechanism data set is global.

Middle East Crustal Profiles

We have collected from the literature over 60 crustal scale cross sections in the Middle East region. All profile locations as well as their interpretations have been digitized and added into GEOID. Figure 22a shows the locations of these profiles. A similar map can be obtained by simply checking the data set labeled "Display profile locations" (Figure 14). In order to see the interpreted sections, a new menu is initiated by clicking on the "Display x-sections" button. This will erase the current screen and plot a map of the Middle East region with all available profile locations in the upper left corner of the screen. The remaining area is used to draw the cross sections (Figure 22b). Up to three profiles can be displayed on the screen at a time. In order to display one of the profiles, one of the "select profile" buttons need to be pressed and the desired profile must be selected from the map on the screen by clicking on the profile. Once a profile is selected, it will be displayed in the reserved area on the screen. The interpreted basement is drawn in red and the Moho is in blue. These values were used in obtaining the Cornell

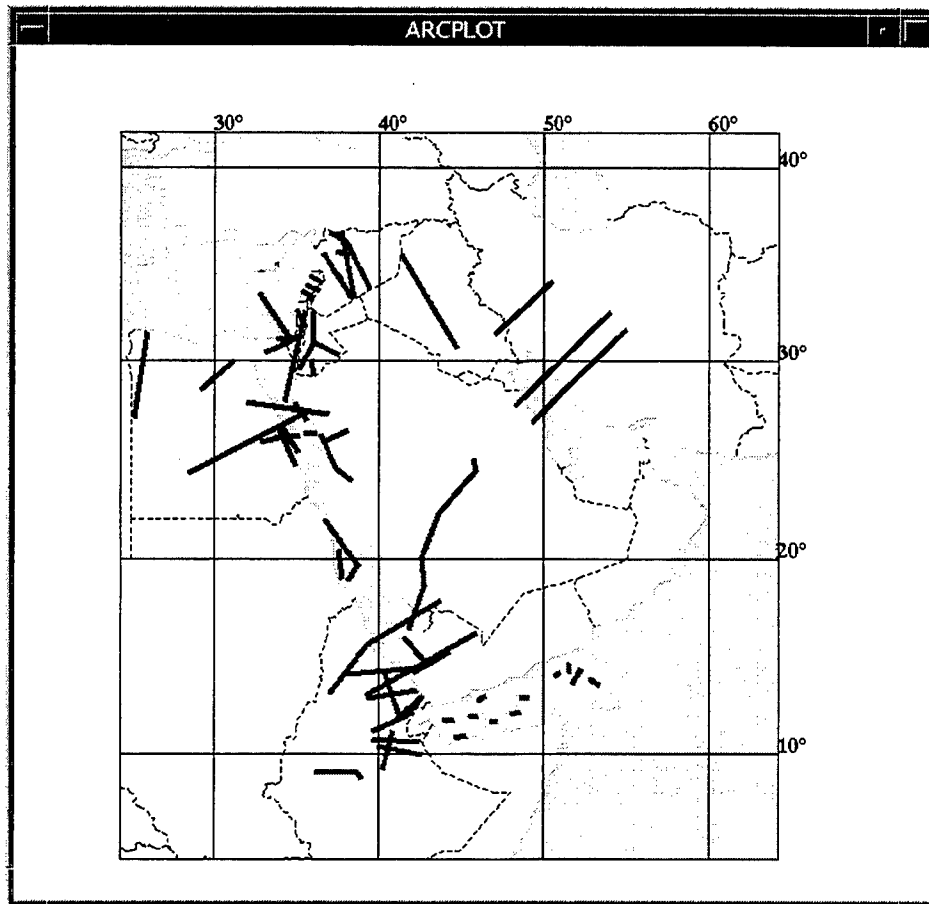


Figure 22a. Locations of collected crustal scale profile locations (thick gray lines).

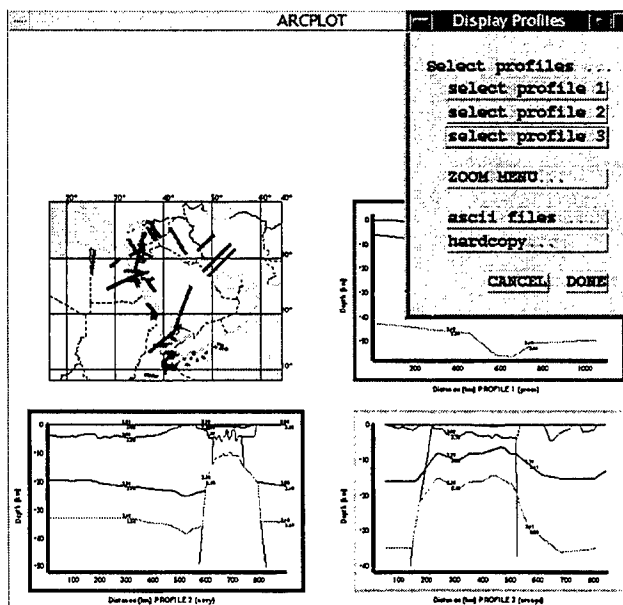


Figure 22b. Up to three cross sections can be displayed on the screen. The menu shown in the upper right corner allows selecting the profiles from the map shown in the upper left corner.

basement and Cornell Moho data sets discussed later in this report. Information about each profile can be downloaded into an ascii file by clicking the "ascii files" menu button. This opens up a new window. A directory path and a file name for each profile must be entered. Once the "Done" button is clicked, an ascii file containing all relevant information, such as publication information, type of data set, etc., is written. Using the zoom menu button, any segment of the map or profiles can be zoomed in, once they are displayed on the screen. In order to create a hardcopy map of the location map and/or profiles, the "hardcopy" button is pressed and file names are typed. An output format can be selected by choosing one of three options: Postscript, Illustrator, and CGM.

Seismic Station Locations

Data for all broadband stations and for short period stations from some of the countries of the Middle East were collected and entered into the GEOID system. The broadband stations are complete with attribute information such as the operating agency of the station, operation period, and instrument type. The short period station locations are not complete for the Middle East and North Africa region. However, the station locations under the ISC phase data coverage are more complete and can be used to replace these station locations.

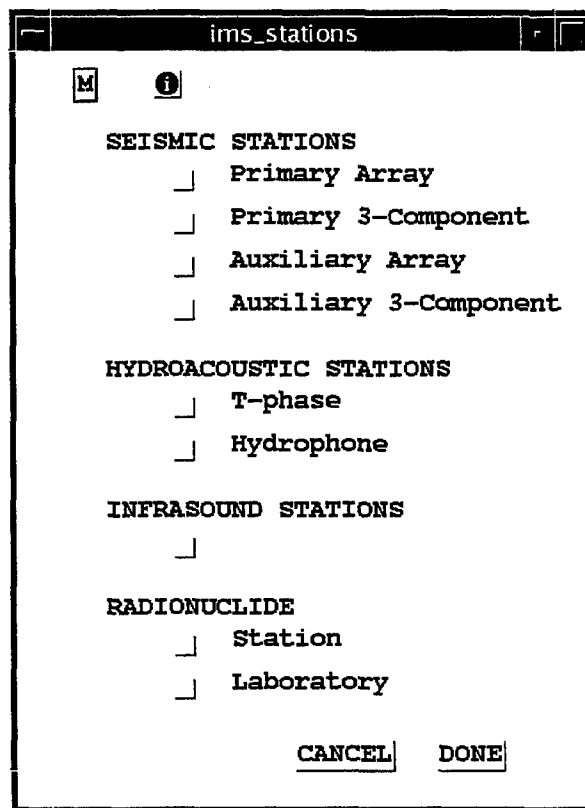


Figure 23a. Menu to display the IMS stations.

International Monitoring Station Locations

We entered all the International Monitoring System (IMS) locations into the GEOID system. A menu to access these data sets can be initialized by clicking on the "International Monitoring System" stations menu (Figure 23a). The locations of the stations were taken from the signed Comprehensive Test Ban Treaty agreement. The stations are divided into four different categories: Seismic, hydroacoustic, infrasound, and radionuclide. A map of these stations can be obtained by marking the check mark areas. Using the "i" button located on top of the window, more information about each site can be obtained. First clicking on the "i" button and then on the desired station location would give the station attributes in a popup window. Figure 23b shows all the stations located in the Middle East and North Africa region.

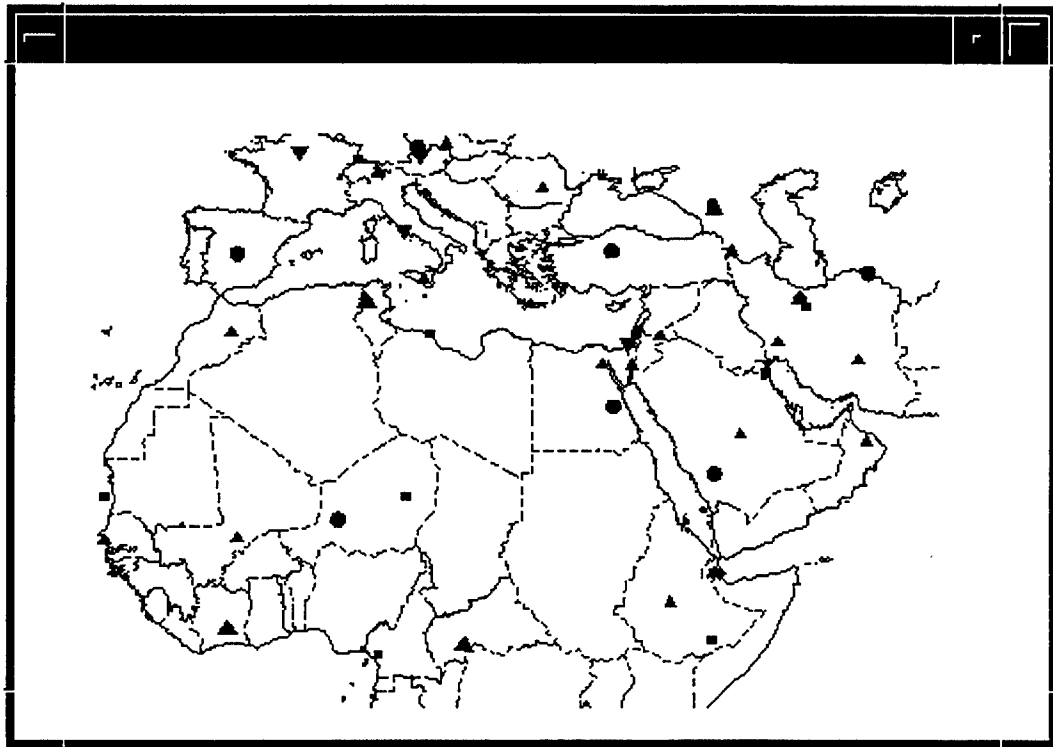


Figure 23b. IMS Stations in the Middle East and North Africa region. Circles and upright triangles are seismic stations; squares and upside-down triangles are radionuclide stations; diamonds are infrasound stations.

Turkish GPS vectors

These continental motion vectors show relative surface motion in the Eastern Mediterranean region, mainly in Turkey. Figure 24 shows available vector locations and their motions relative to Eurasia.

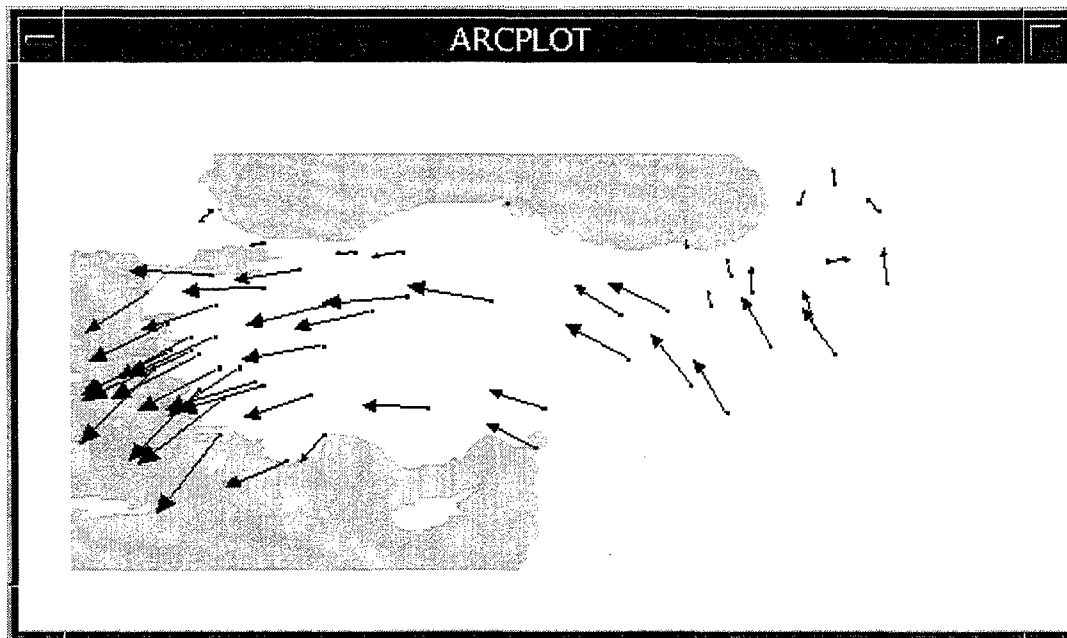


Figure 24. GPS vectors in the Eastern Mediterranean region.

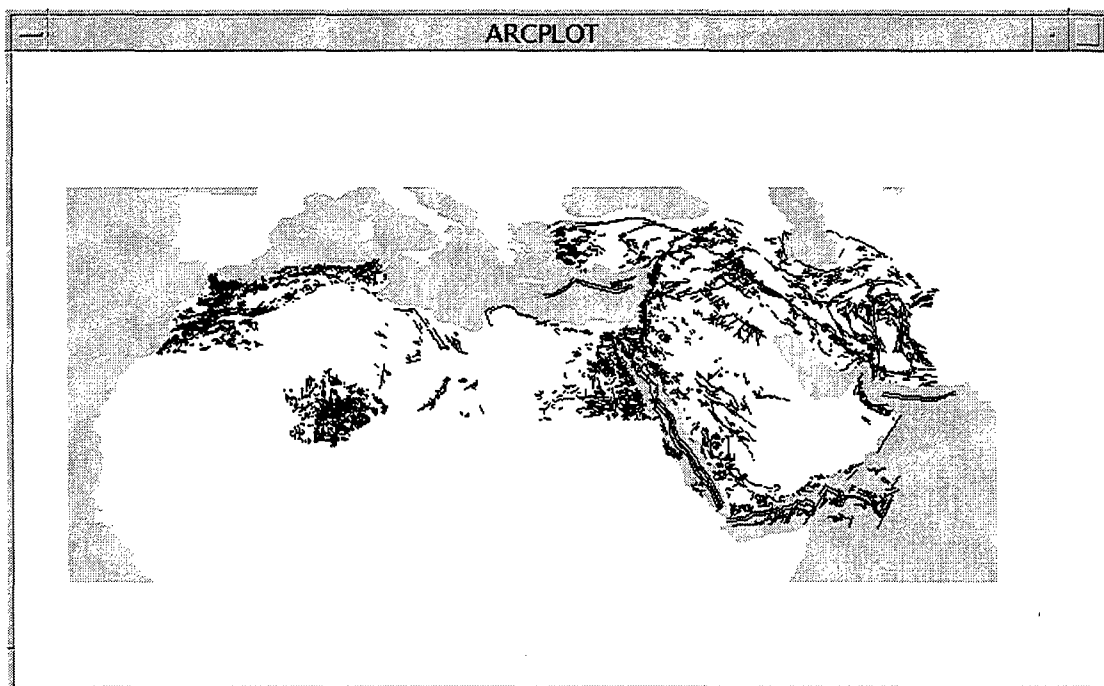


Figure 25. Digitized faults of the Middle East and North Africa region. These faults are parts of the Middle East and North Africa tectonic map that is available in GEOID.

2.1.2.3. Geological Data Sets

Several geological data sets have been included in the GEOID environment. These data sets include a new tectonic map of the Middle East and North Africa region, a low resolution global geology map, a detailed geology map of the United States, and additional data sets such as mine locations in the Middle Eastern and North African countries, world stress map, and historically active volcanoes of the world.

middle_east_tectonics_map

TECTONIC MAP OF THE MIDDLE EAST
AND NORTH AFRICA

Select features:

<u>M</u>	<u>M</u>	<u>i</u>	<input checked="" type="checkbox"/>	Faults
<u>M</u>	<u>M</u>	<u>i</u>	<input type="checkbox"/>	Volcanics Neogene/Quaternary
<u>M</u>		<u>i</u>	<input type="checkbox"/>	Volcanics Paleogene
<u>M</u>		<u>i</u>	<input type="checkbox"/>	Ophiolites
<u>M</u>		<u>i</u>	<input type="checkbox"/>	Volcanoes Active
<u>M</u>		<u>i</u>	<input type="checkbox"/>	Volcanoes
<u>M</u>	<u>M</u>	<u>i</u>	<input type="checkbox"/>	Basement outcrops
<u>M</u>		<u>i</u>	<input type="checkbox"/>	Basement contours
<u>M</u>		<u>i</u>	<input type="checkbox"/>	Depressions

Note: features with more than one
metadata button use data from more
than one coverage.

CANCEL DONE

Figure 26. Menu designed for the Middle East and North Africa tectonic map.

Tectonic Map of the Middle East and North Africa

Several tectonic and geology maps in the Middle East and North Africa have been digitized and merged to create a uniform scale tectonic map of this region. This data set includes features like faults, volcanics, basement outcrops, and ophiolites. Most features in the tectonic map have also been supplemented with related information, such as the

activity of faults, detailed age information, etc. Figure 25 shows all the faults in the region. These data sets can be accessed through the "Tectonic Maps" button under the "Geological Data Sets", and then under the "Middle East and North Africa Tectonic Map" button (Figure 26). Using this menu, any of the tectonic features can be selected and displayed, and features in the map can be identified.

Mine Locations

Mine locations in most of the Middle East and North African countries have been entered into the system (Figure 27). The data are organized by country and can be accessed through the menu button available in the "Geological Data Sets" menu. Detailed information exists for Algeria, Egypt, Iran, Iraq, Israel, Jordan, Libya, Syria, Tunisia, Turkey, and Morocco mines. In addition, less detailed mine locations from the USGS, DCW, and US Bureau of Mines sources have been added. Figure 28 shows the producing mine locations in the Middle East and North Africa region. Each of the locations are complete with attributes such as commodity, mine type, activity, etc.

mine_locations

HELP

- Global Mines
 - GLOBAL MINE LOCATIONS, DCW
 - EURASIAN MINE LOCATIONS, USGS
 - EURASIAN MINE LOCATIONS, USBM
- Regional Mines
 - Canada
- Middle East and North Africa Mines

	Producing	Prospect, etc.
Algeria	J	J
Egypt	J	J
Iran	J	J
Iraq	J	J
Israel	J	J
Jordan	J	J
Libya	J	J
Syria	J	J
Tunisia	J	J
Turkey	J	J
Morocco	J	

CANCEL DONE

Figure 27. Mine locations for most countries in the Middle East and North Africa have been entered and added into the database system.

World Stress Map

World stress data compiled by several organizations have recently been made available. We copied these data and placed them in GEOID with all their attributes. This data set

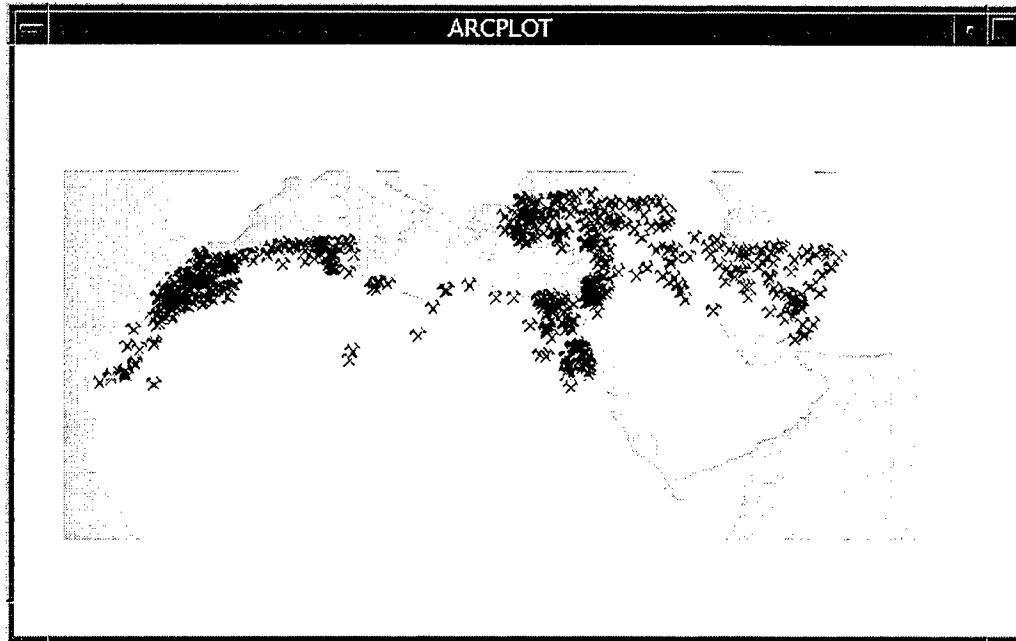


Figure 28. Producing mine locations in the Middle East and North Africa region.

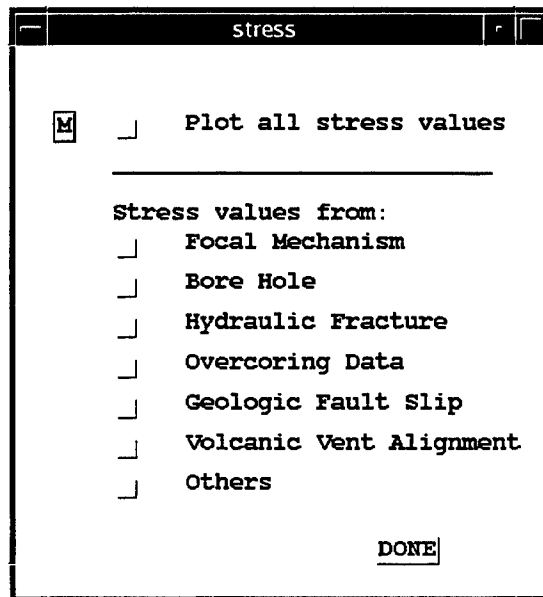


Figure 29. World Stress map menu available under the geological data sets.

includes stress direction estimated from earthquake focal mechanisms, borehole measurements, and field data. This data set is available through the “World Stress Map” button under the geology data sets (Figure 29). A small region near the southern Dead Sea fault is shown with available stress measurements in Figure 30.

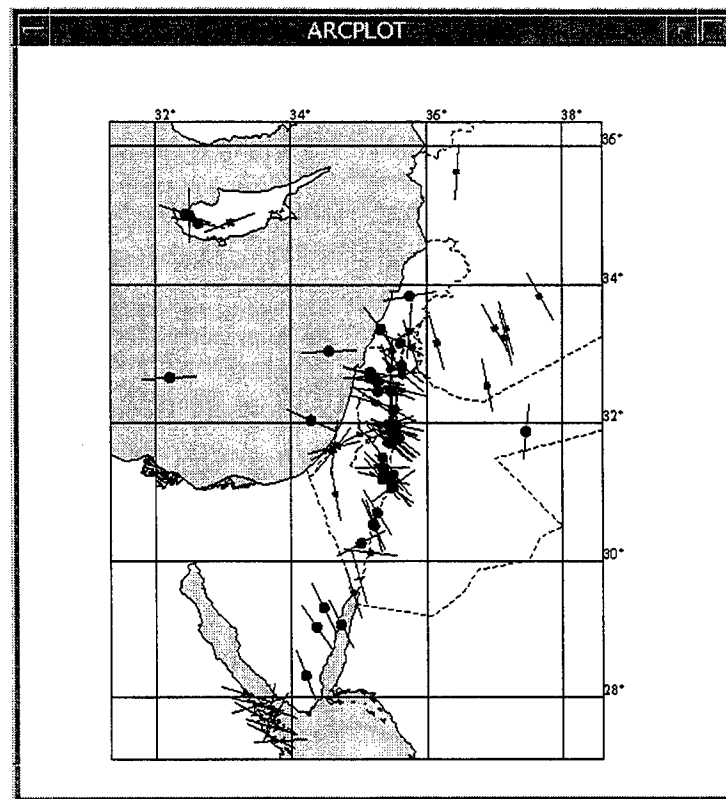


Figure 30. Stress directions in the southern Dead Sea fault region

Holocene Volcanoes

Holocene volcano locations are a comprehensive list of historically active volcano locations (Figure 31). This data set is available for the entire world. The volcanoes data set can be accessed through the "Holocene Volcano Locations" button. There are four different categories: Erupted between 1900 – 1993, Erupted 1 – 1900, Erupted B.C. and/or undated, and thermal activity/uncertain.

World Geology Map

In addition to the data sets mentioned above, there is a global geology map of the world. This map has lower resolution information, and it should be used with regional or continental scale applications. Figure 32 shows this data set in the Middle East and North Africa region.

2.1.2.4 Images/Grids

The grids and images comprise a significant volume of the data sets within the GEOID environment. Several of these data sets were collected as images. Others were gridded for easier use. The cell size in each data set was determined by either data point density or final disk space usage. All the data sets in this category are projected. Projecting them

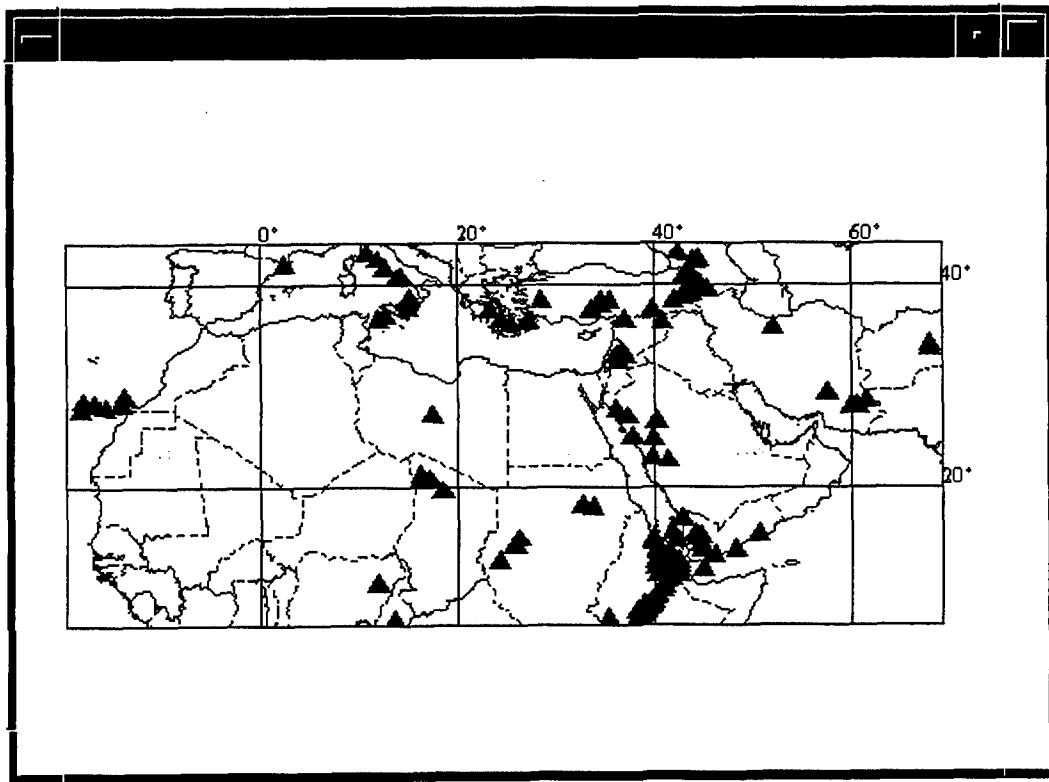


Figure 31. Holocene volcano locations in the Middle East and North Africa.

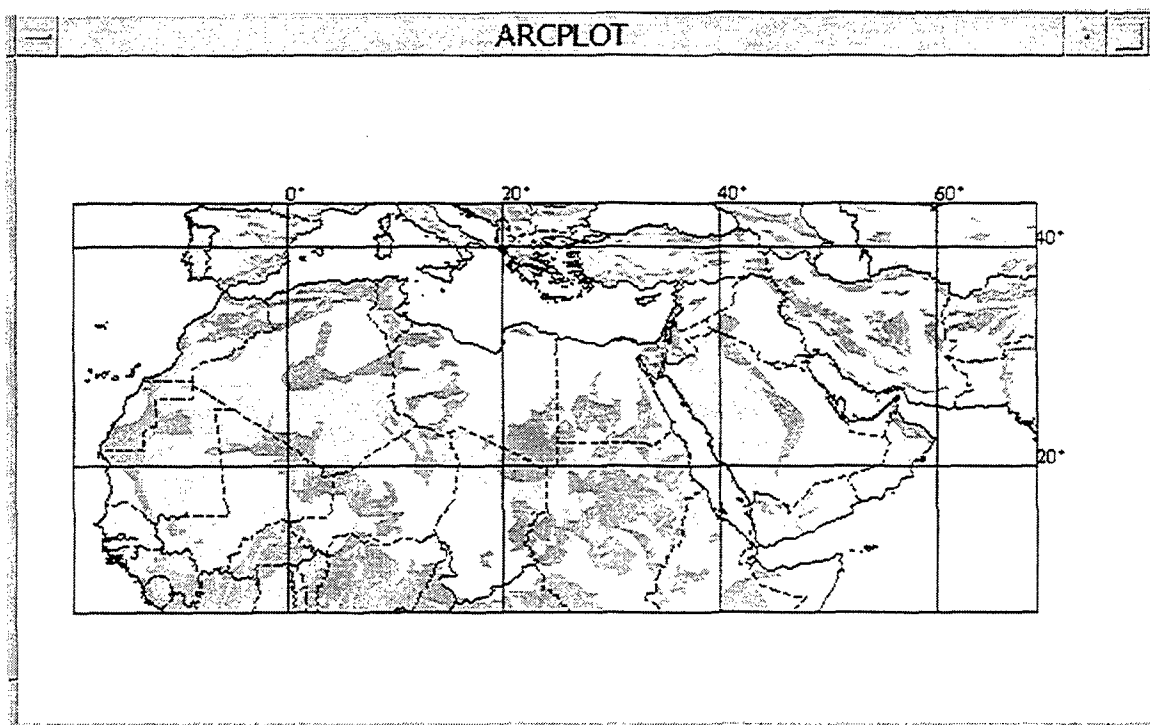


Figure 32. Geology map of the Middle East and North Africa. This is a global data set.

on the fly would take too long to display. The selected projection is Equirectangular, which is also the default projection in GEOID. The data sets can be accessed from the main menu by pressing the "Images/Grids" button. The projection is set to Equirectangular automatically; if it has been set to some other projection by the user, a warning message is displayed. Figure 33 shows the Images/Grids menu.

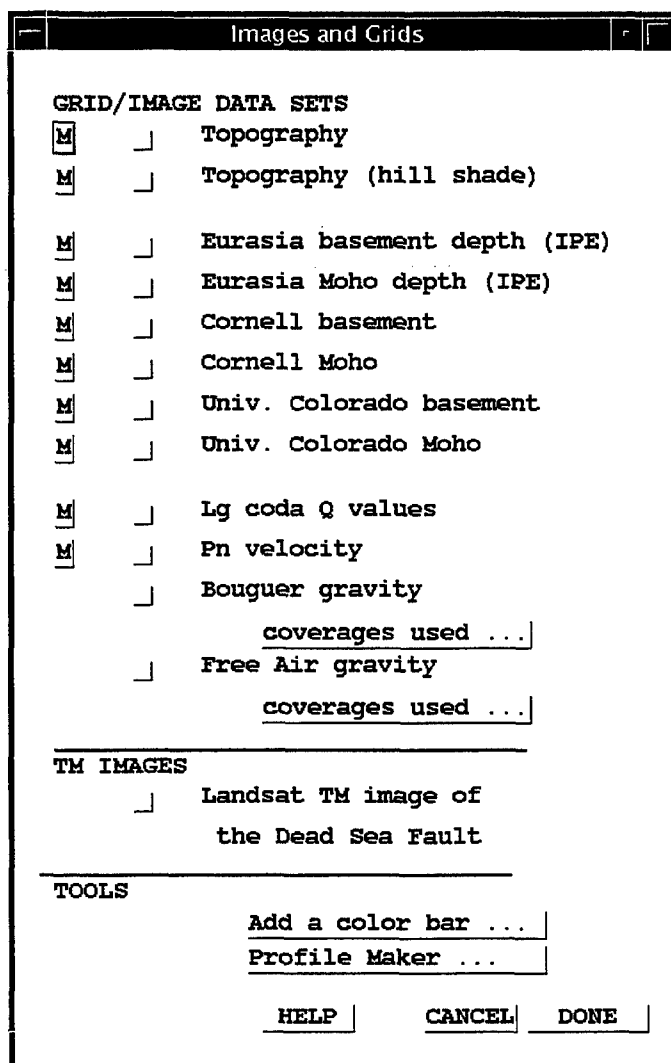


Figure 33. Images/Grids menu and available data sets

Topography

At the top of the list are the topography data, which include submarine bathymetry as well. The cell size of this data set is 2 km. However, the original topography data had a resolution of 1 km. The bathymetry data came from two different data sets, one with about 3 km cell size beneath most of the oceans, and the other with 10 km cell size covering the polar regions. We merged all these data sets and generated a 2 km cell sized data set, hence subsampling the land areas and over sampling the bathymetry. Figure

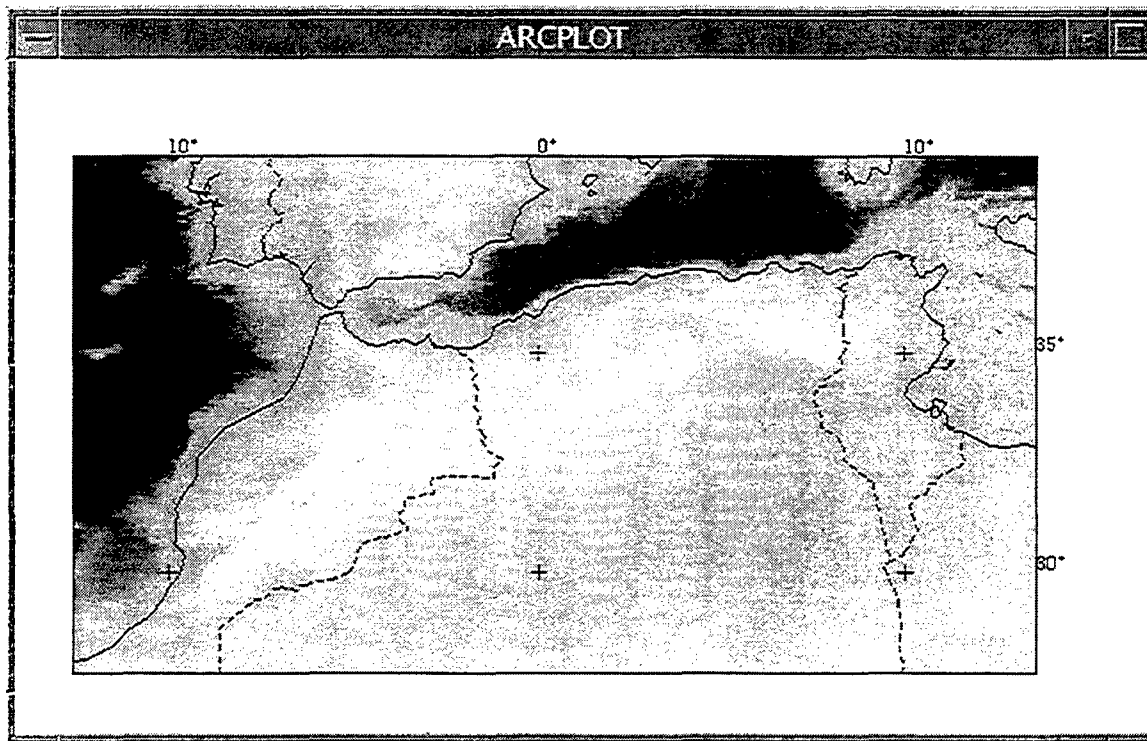


Figure 34a. Topography and bathymetry data of the Atlas mountains in northwestern Africa.

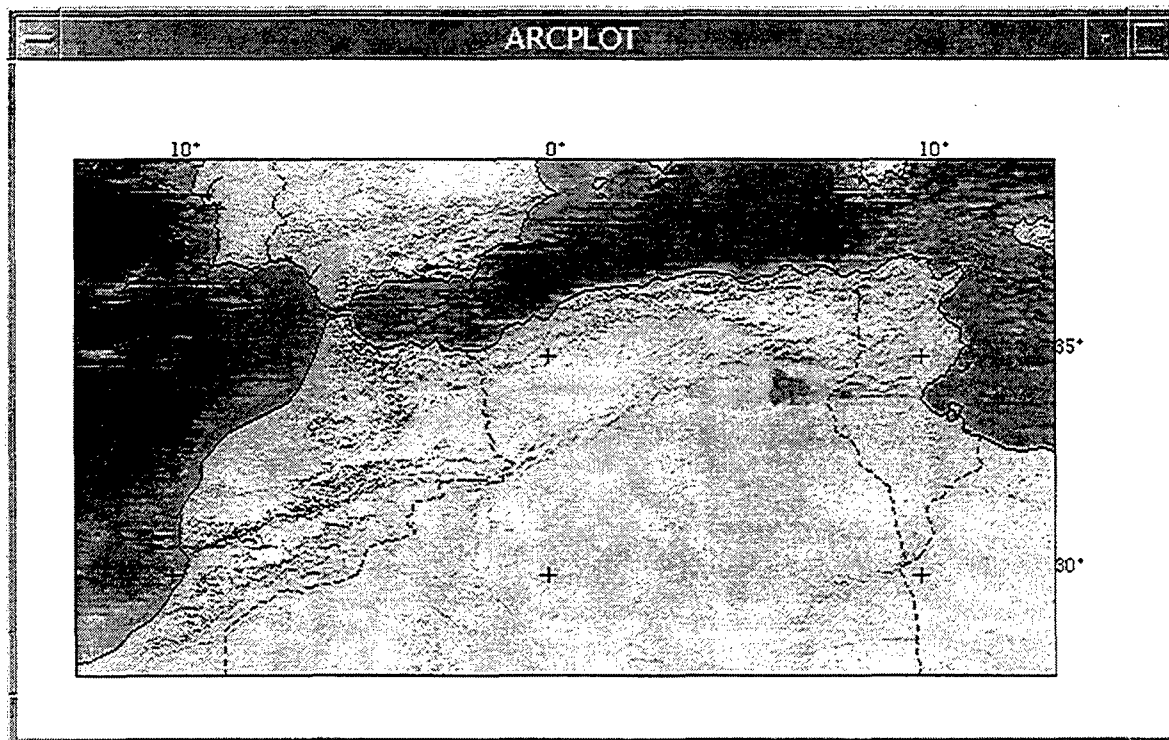


Figure 34b. Hill shaded topography of the same area shown in Figure 34a.

34a shows part of this data set in the Atlas mountains in North Africa. We also created a hill-shaded representation of the topography. This representation allows the relief to be highlighted, and it is convenient for display purposes. Figure 34b shows the same area as Figure 34a with shaded relief option.

Eurasia Basement Map

The Eurasia basement map covers, as its name implies, most of Eurasia. It is taken from the former Soviet Union's IPE (Institute for the Physics of the Earth) maps. The data were gridded to a cell size of 10km. Figure 35 shows part of this data set in the Middle East and North Africa region.

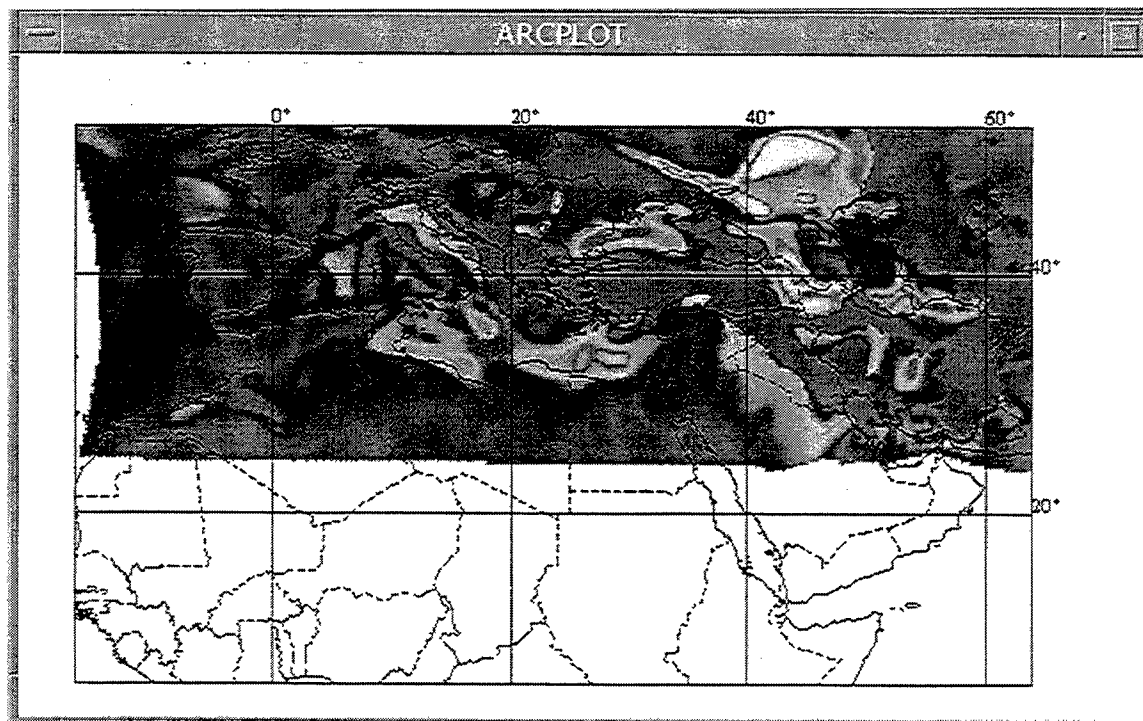


Figure 35. The Eurasia basement map covers parts of the Middle East and North Africa.

Eurasia Moho Map

The Eurasia Moho map is similar to the Eurasia basement map in its source, spatial extent and cell size. Both the basement and Moho maps can be used for continental scale applications. Using them in regional and local studies may be misleading due to their nature. They are averaged and simplified and there is not an independent way of checking the quality of the reported values. Figure 36 shows the Moho values in the Middle East and North Africa region.

Cornell basement

This data set was developed entirely at Cornell for the Middle East region. Results from

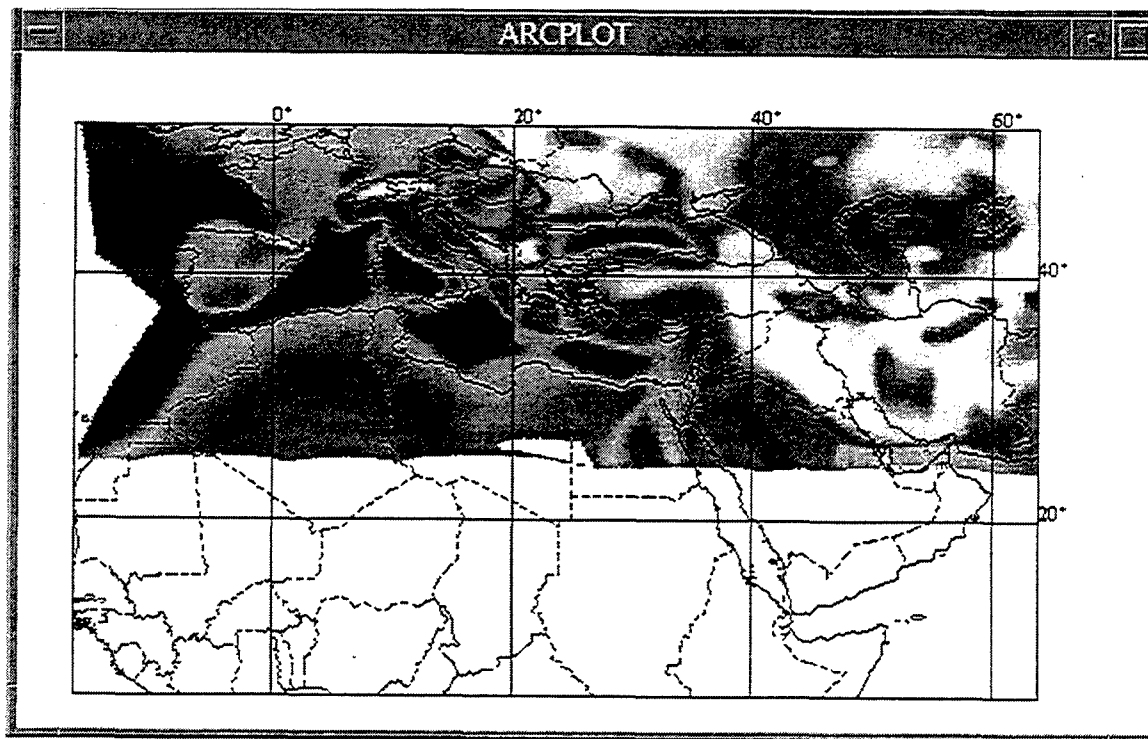


Figure 36. Eurasia Moho map covers parts of the Middle East and North Africa.

several published studies as well as original work in Syria were used in generating this data set. The refraction and gravity profiles taken from the literature are shown in Figure 22a. Figure 37 shows the basement values and geographic extent of the data set.

Cornell Moho

The Cornell Moho data set is also entirely developed at Cornell using several data sets including the profiles shown in Figure 22a, gravity maps, surface wave tomography results, and receiver function studies. Figure 38 shows the Moho values and the geographic extent of the data set. This is the most reliable Moho map in this region. The values can be confirmed with published data sets and other studies.

University of Colorado Basement

This data set was obtained from surface wave tomography studies by the University of Colorado group. The data set covers much of Asia including parts of the Middle East. Figure 39 shows this data set and its geographic extent.

University of Colorado Moho

This is also a data set obtained from surface wave tomography by the University of Colorado group. The data set also covers an area in Asia with some Middle Eastern coverage. Figure 40 shows this data set.

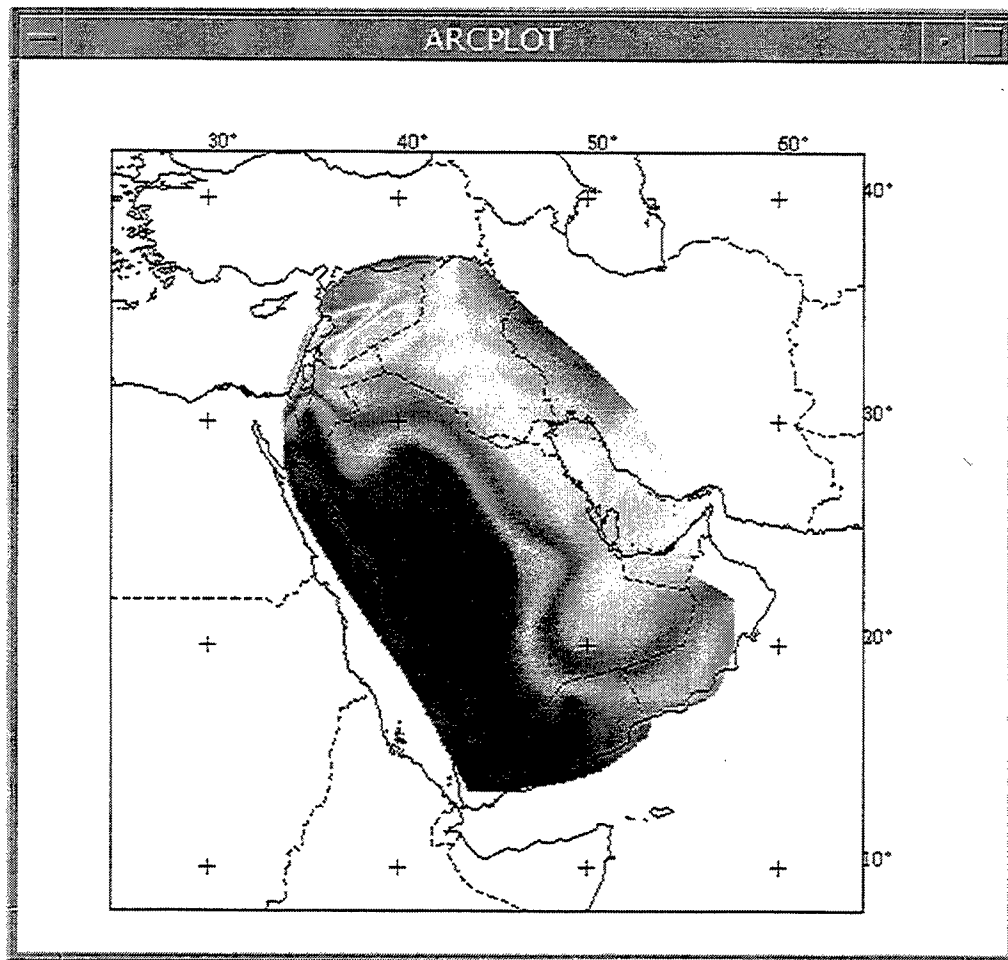


Figure 37. Cornell basement map of the Middle East.

Lg Coda Q Values.

Lg coda Q values were computed for Eurasia by the St. Louis University research group. The values were obtained from a tomographic inversion. The coda Q values represent the efficiency of Lg wave propagation in the crust. Figure 41 shows the Lg coda Q values in the Middle East region.

Pn Velocity

Seismic Pn phase velocities were obtained from the New Mexico State University research group. The data set was obtained using a Pn tomography technique in the Middle East region. The values represent variations from a base velocity of 8.0 km/s. Figure 42 shows the data set and its geographic extent.

Bouguer Gravity Data

These Bouguer gravity data were obtained by gridding the point data provided to us by the Defense Mapping Agency. We are not at liberty to disclose the locations that were used in gridding. However, a secondary data set is provided under the Metadata section to

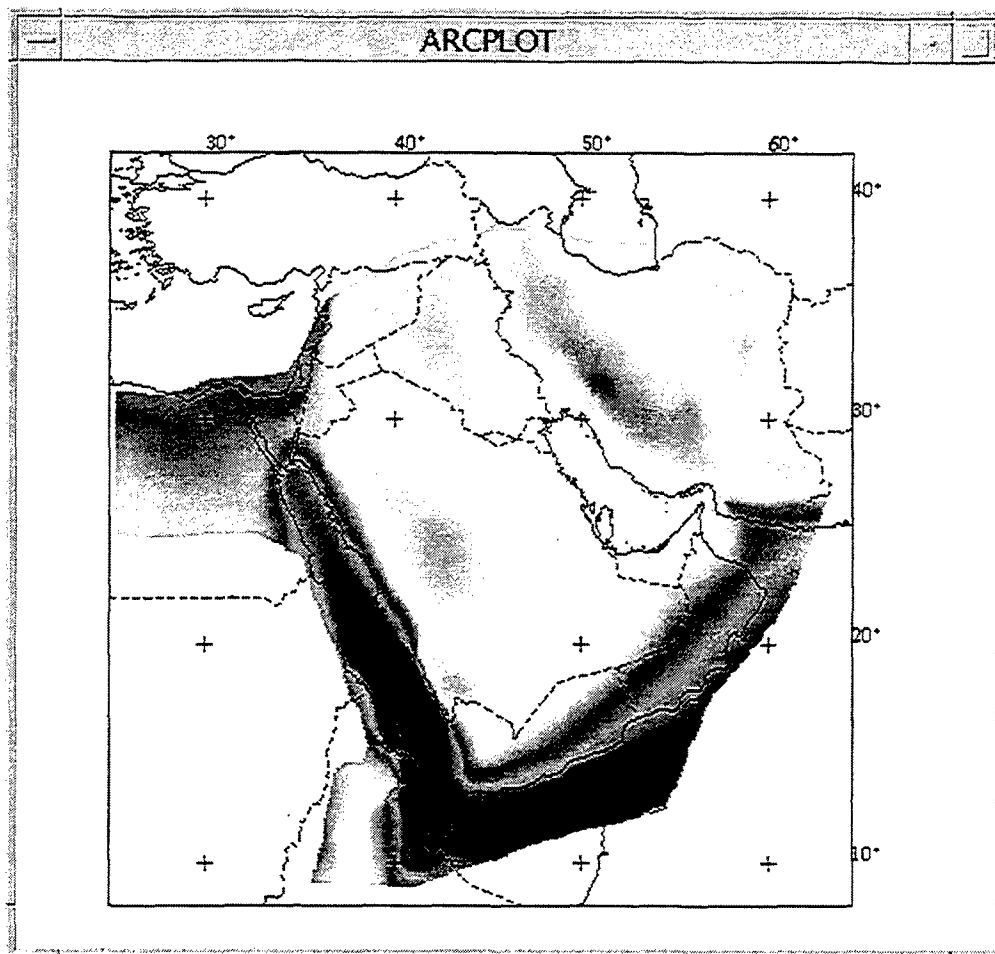


Figure 38. Cornell Moho map of the Middle East

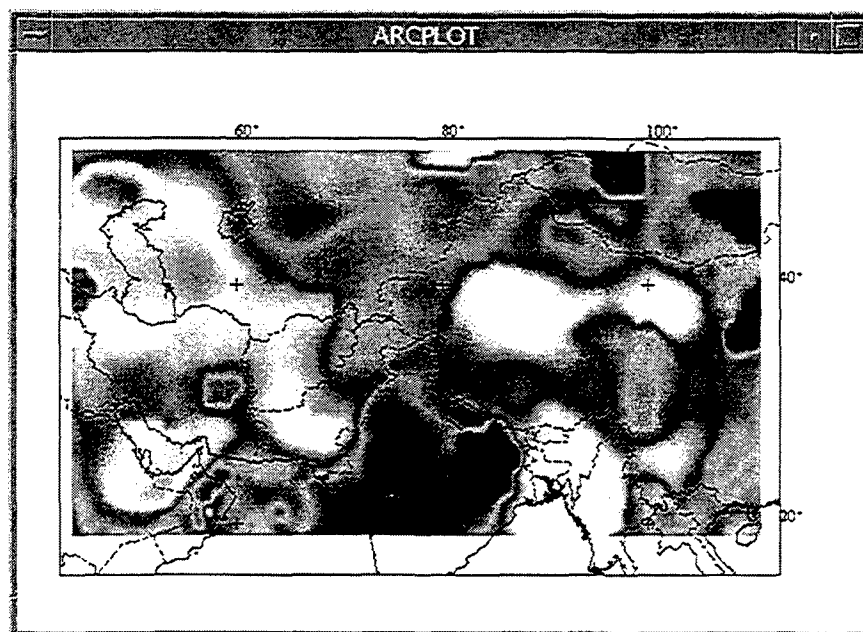


Figure 39. University of Colorado Basement map.

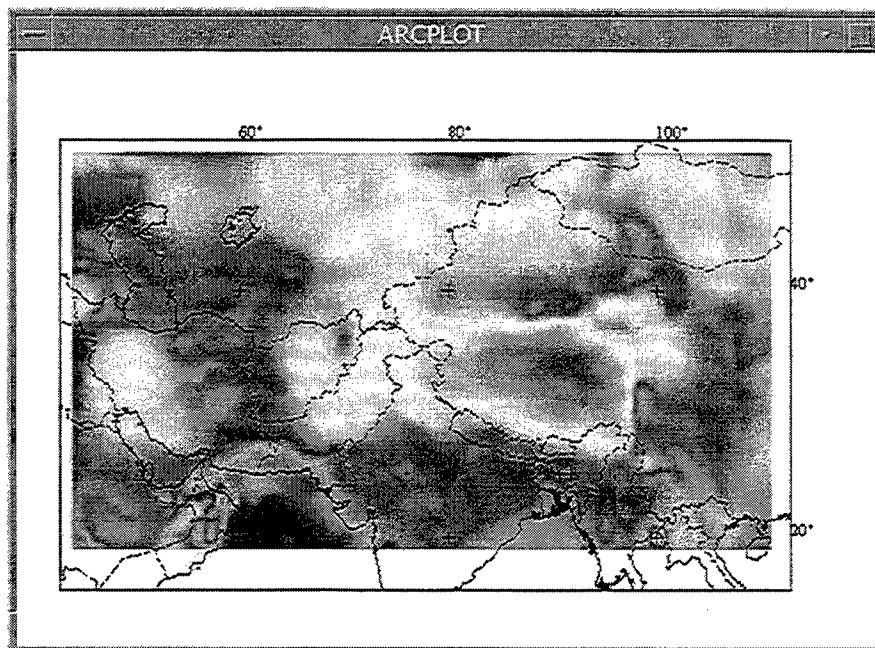


Figure 40. University of Colorado Moho map.

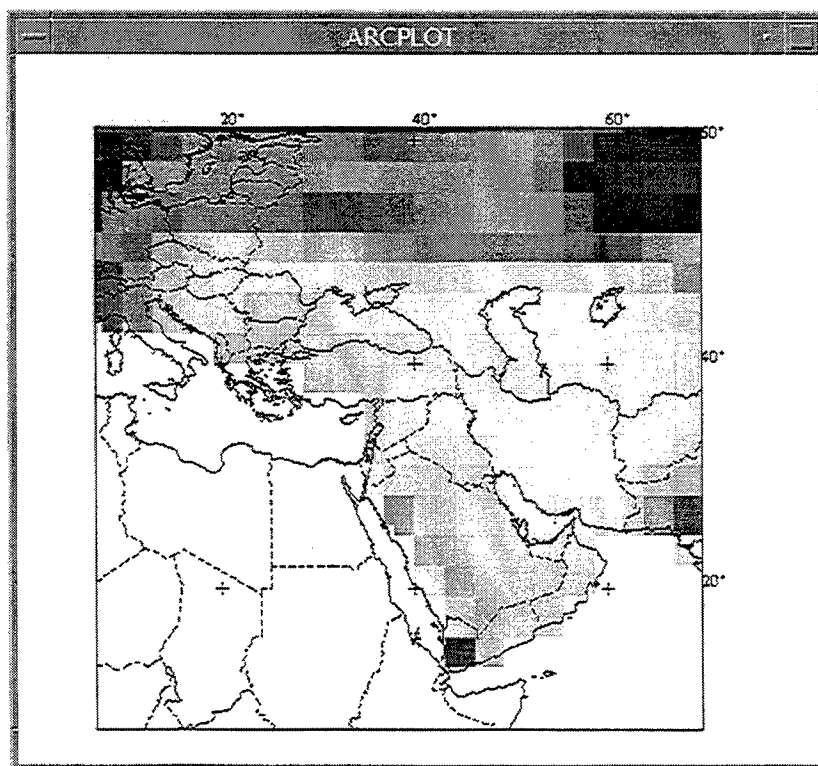


Figure 41. Lg Coda Q values obtained from St. Louis University.

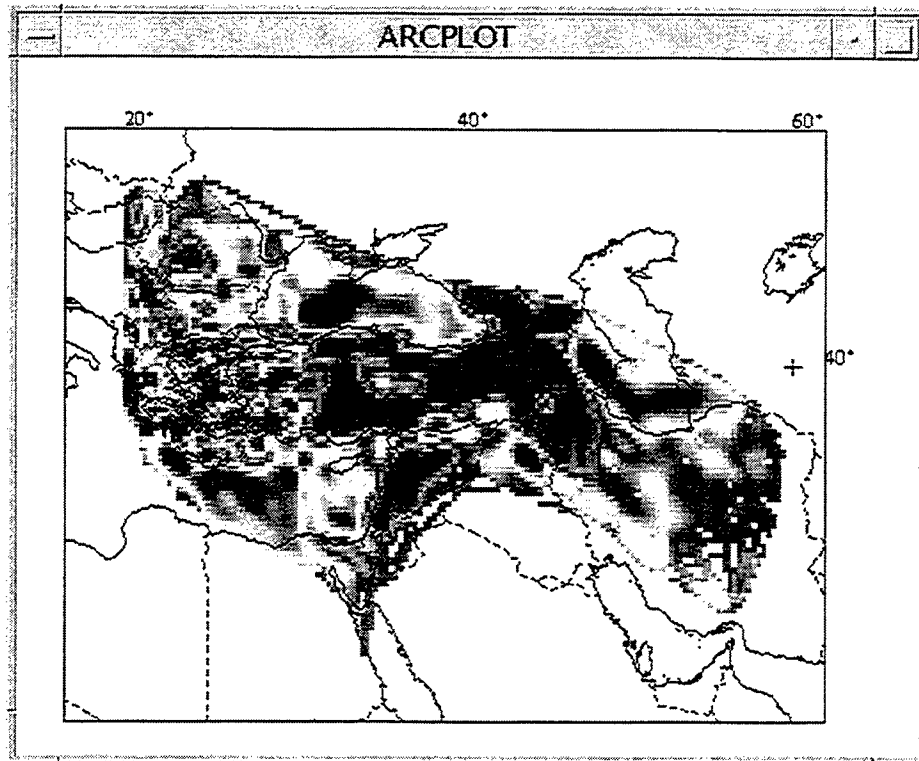


Figure 42. Pn velocity variations in the Middle East obtained from the New Mexico State University group.

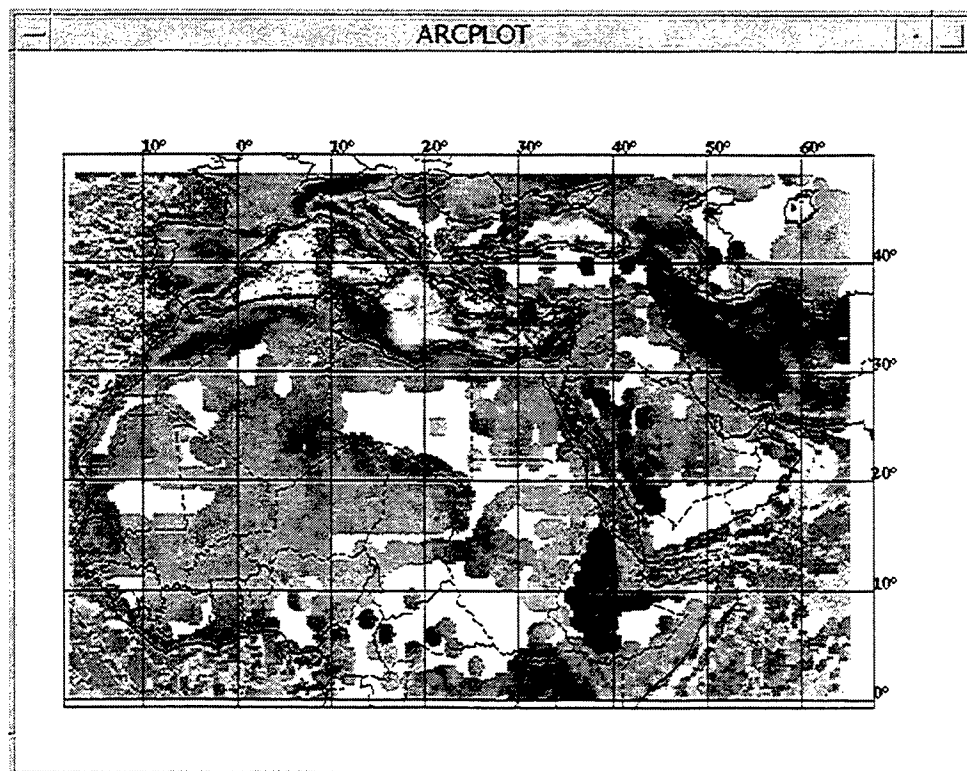


Figure 43. Bouguer gravity data in the Middle East and North Africa.

represent the variance of the grid provided. Figure 43 shows the Bouguer gravity map.

TM Images

We currently hold a data set of about 100 TM scenes in the Middle East and North Africa region. A selection of these scenes is now available in GEOID. The original TM scenes are about 30 m resolution. The data sets in GEOID are subsampled versions of these data sets. The new cell size is 285 m. The scenes were registered and a mosaic was formed. The scenes cover two regions: one in the Atlas mountains of North Africa, and the other in the Northern Arabian plate. Figure 44 shows the mosaic over the Middle East region. The other scenes are being processed and registered.

There are two other "tools" that are provided at the bottom of the "Images/Grids" menu. One of these is used to add a scale bar for the grids, and the other one is used in profile making. The Profile Maker will be discussed in the next section.

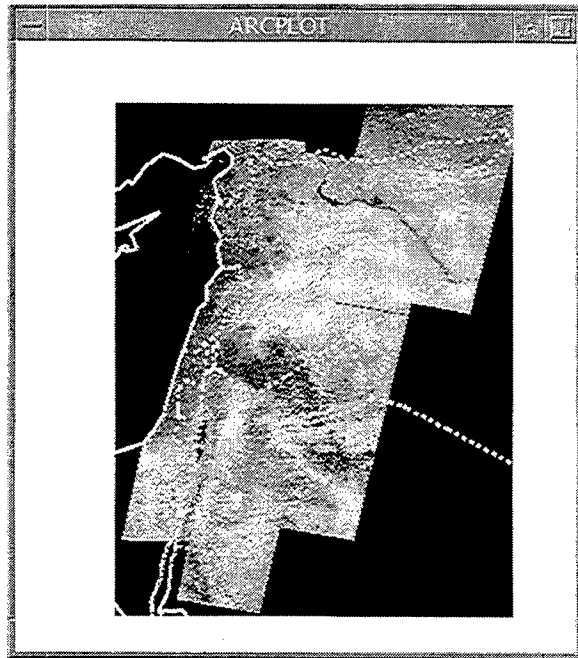


Figure 44. TM mosaic of the Northern Arabian plate.

The Profile Maker

The profile maker is a tool developed at Cornell to extract profiles or cross sections from the gridded data sets. The profile maker can be used to extract cell values along a transect, or it can be used to construct crustal scale cross sections including topography, basement, and Moho values. Clicking on the "Profile Maker" button initiates a new sub menu and redraws the screen. The screen is divided into two sections: one to plot the map and the other to view the profile (or cross section) values. In the Profile Maker menu first the grids need to be selected from the "Select the grids" menu (Figure 45). Then two point locations representing the beginning and end points of the profile need to be entered. This can be done by either entering the values in the text entry locations or by selecting the "Select 2 points from the screen" button and marking two points on the screen. Following this, pressing on the "apply" button would extract the requested profile or cross section. Figure 46 shows a sample output of a cross section obtained using topography, basement, and Moho values. A great circle path approximation is applied, so that the distance along the profile is the minimal distance between the end points. The extracted profile can be saved in an ascii file or plots of the map and the cross section can be made using the hardcopy button.

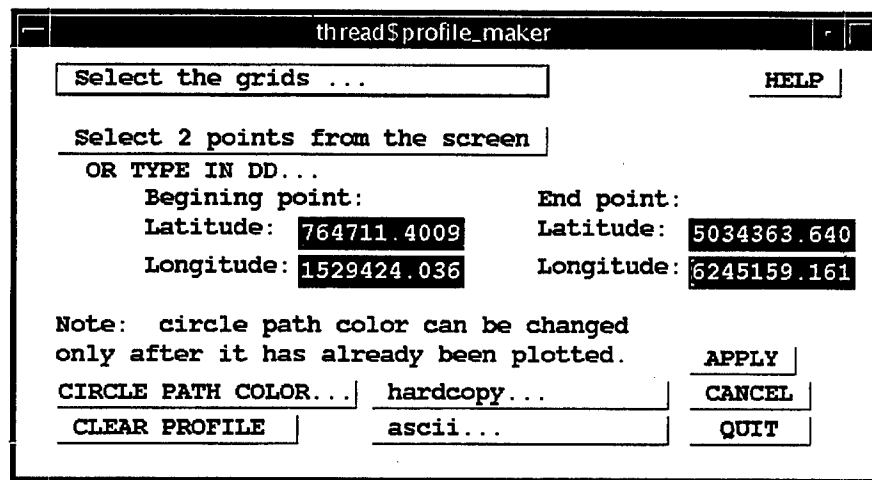


Figure 45. The Profile Maker menu. First the grids need to be selected. Then marking two points on the map or just entering the transect's end coordinate values enables the profile to be extracted by selecting the apply button.

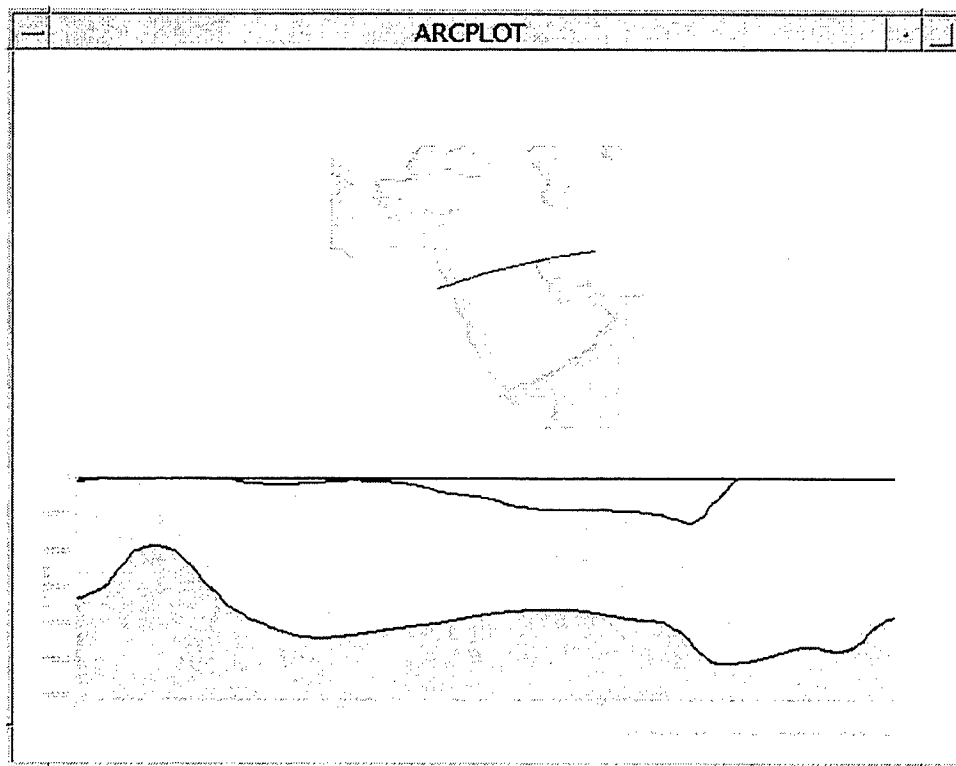


Figure 46. An output from the Profile Maker. Three grids are selected for this cross section: Topography, basement, and Moho.

2.1.3. Tools and Utilities in GEOID

GEOID is developed with certain tools and utilities. As discussed in section 2.1.1 some of the map creation tools are kept under that section. However, we developed several

other tools that can help users in their data analysis and mapping. In the next section we will explain other available tools shown in Figure 47.

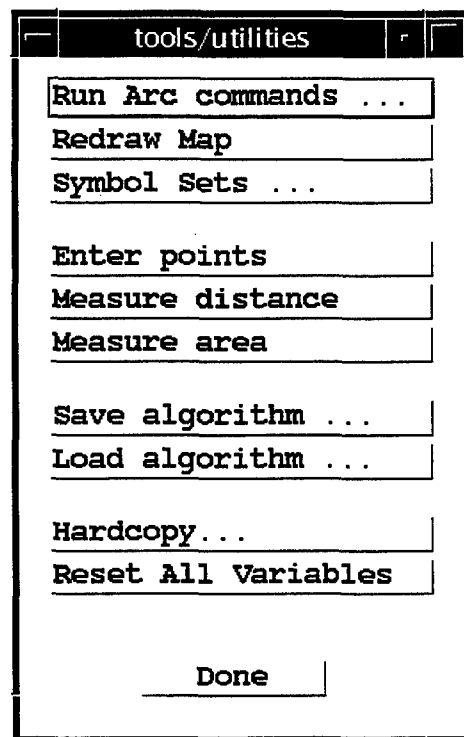


Figure 47. Tools and Utilities menu.

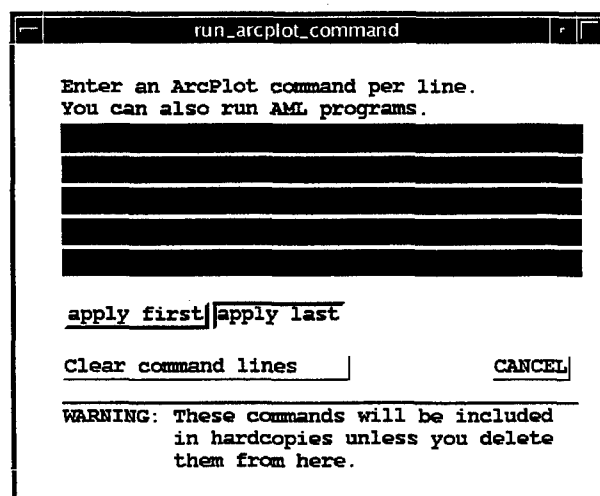


Figure 48. Arc/Info commands can be entered through this menu. This allows users to add their own data sets as external inputs to GEOID. The external data sets become part of the GEOID environment and all the projection, hardcopy, and other options are applied to them directly as if they were internal data sets.

Run Arc Plot Command

This Arc/Info command access tool (Figure 48) is developed for users who are familiar with Arc/Info. Using this tool one can extract information from the system or plot one's own external data and make it part of the GEOID system. For example, if a user has his/her own data set that he/she would like to display with the data sets in GEOID, all the user has to do is type the regular Arc/Info commands that would plot the ArcInfo coverage in one of the five entry lines given in the Arc Plot Command menu. This would make the new data set an external part of the GEOID system. All the zoom, map projections and printing option would work with this external data set. This makes the GEOID system quite powerful for expansion. Similarly, if the user has multiple data or they require selection and definitions, then the user can create an AML program and run it from these command lines. This is quite a useful tool for those who wish to add their data into GEOID and take advantage of GEOID's structure.

Redraw Map

The Redraw Map button is used when some of the mapping parameters are changed. In order to erase the screen and redraw the modified selections this button needs to be pressed. It will redisplay all the selected items in the right order (i.e., polygons would not overlay point or line data sets).

Symbol Sets

Each data set in GEOID is plotted with a default symbol type and color. However, using the symbol sets menu, one can overwrite the default parameters. The "Symbol Sets"

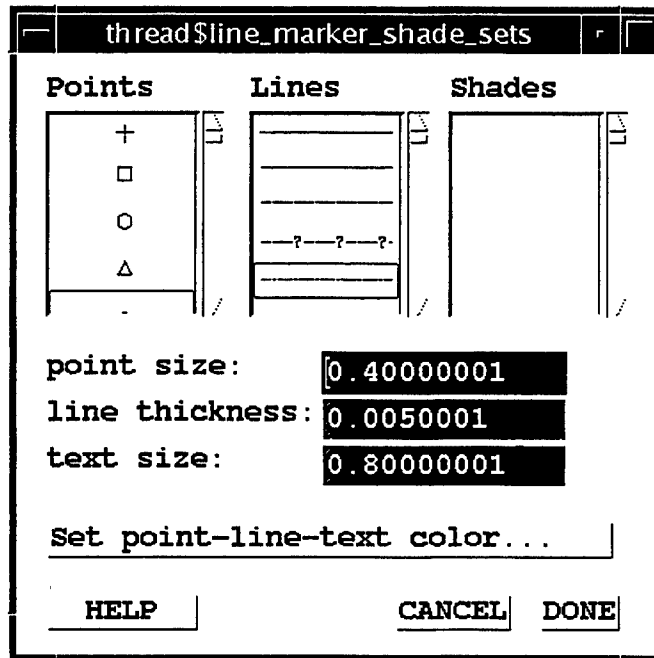


Figure 49. Symbol Sets menu allows changing default symbol types for each data set.

menu (Figure 49) allows one to change line, marker and shade colors as well as size of the symbols. For example, earthquakes are plotted with circles as default. If one wants

to plot them as pluses, the plus symbol from the "Symbol Sets" menu needs to be selected. Following that step, the earthquake data set must be re-checked in order for the change to take effect. Once changed the new symbol stays changed until the session is closed. Similarly, all the line and shade types can be changed. The "Set point-line-textcolor" button allows the user to a new color for these items.

Enter Points

This is also a window for user input. If the user has a few points (lat, long pairs) that he/she wishes to display in GEOID with its data sets without creating Arc/Info files, this menu provides an easy solution (Figure 50). Typing longitude and latitude pairs in the text area in this menu would display them in GEOID. The typed values remain there until they are cleared by pressing the "clear all values" button in this menu.

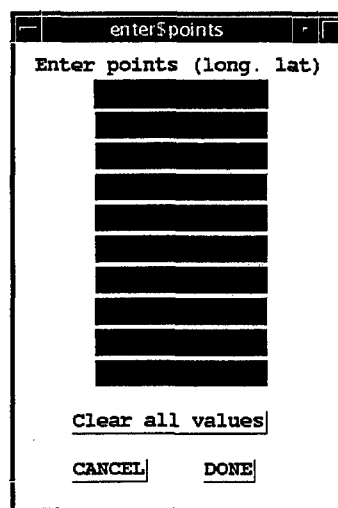


Figure 50. The "Enter Points" menu allows users to define points manually. These points are plotted on the map.

Measure Distance

The Measure Distance button is a simple tool to measure a line distance between two or more points. Once this button is clicked, the user must mark points on the map. A minimum of two points is required. However, as many number of points as necessary can be entered. The entry should end by hitting the "9" key from the keyboard. This will produce an output in the terminal window giving the distance obtained by connecting the points in inches and in map units (usually in meters).

Measure Area

Measuring area is very similar to the "Measure Distance" tool. The only difference is that a minimum of three points is needed to define an area. When the selection of the area on the screen is done, the "9" key will quit the area definition and the output will be written in the terminal window.

Save Algorithm/Load Algorithm

These two tools allow users to save the environment that they are in (such as the map extent area, displayed data sets, symbols, etc.) and restores back to that environment upon loading the algorithm. Within a session, all changed symbol sets or selected data sets will be saved and restored. Once the session is exited, all this information is lost. These algorithm buttons are used to restore the saved environment quickly.

Hardcopy



This is a tool used in obtaining a hardcopy of the screen output (Figure 51). The user can set a map scale, a page size, page layout, and an output file format. The default output format is postscript. An extension is added to the output file name.

Create a Hardcopy

Scale: 1: 33487467.01578

Hardcopy size (inches) ...
☐ Page size: 7 x 9

x: 7
y: 6

Page layout ...
☒  ☐ 

Hardcopy format ...
☒ Postscript ☐ GIF ☐ Illustrator ☐ CGM

output directory: /tmp

output file name:

CANCEL DONE

Figure 51. Hard copy menu allows users to create a hardcopy of the map on screen.

Reset All Variables

This button resets all the variables already changed and returns to the beginning environment.

PART II: DIGITAL DATABASES FOR USE IN REGIONAL DISCRIMINATION OF EARTHQUAKES AND MINE-RELATED EXPLOSIONS IN NORTH AFRICA: A JOINT EFFORT WITH THE LLNL

Ground truth information was provided to the Lawrence Livermore National Laboratory for experimental discrimination of mine-related explosions from earthquakes. Remotely sensed data, knowledge of regional geology and tectonics, and other data sets were provided for two distinct projects at LLNL: (1) Detection of recent strip-mining activity using satellite remote sensing by Dr. William Pickles, and (2) Discrimination of mine-related explosions from earthquakes using regional waveform data by Dr. David Harris and Dr. William Walter. The primary contact person at Cornell for this activity was Francisco Gomez, a graduate student whose studies focus on the regional geology and tectonics of Morocco. Two visits were made to LLNL by Francisco Gomez during Winter 1996 and Winter 1997, as well as one visit to Cornell by Dave Harris during the Summer of 1997.

As part of this work, several data products were produced for use of the researchers at LLNL. All of these have already been delivered to LLNL. A summary of these data is given in Table 1.

1. Monitoring Mining Activity Using Remote Sensing

One of the largest mining operations in Morocco is the phosphate mining area near Khouribga and Oued Zem (Figure 1). At these locations, phosphate is mined from extensive sedimentary layers through strip-mining. As a result, mines and piles of tailings are clearly visible in satellite imagery and aerial photographs. Documentation of each mine blast is kept by the Moroccan authorities, and this information has been made available to researchers at Cornell. Digital Landsat Thematic Mapper (TM) imagery (ca. 1984) of the region was provided to LLNL for Dr. Pickles' research, along with stereo aerial photographs acquired from the Division of Cartography in the Moroccan Ministry of Agriculture. Published topographic and geologic maps were also provided.

Additional digital Landsat Thematic Mapper (TM) data were provided to LLNL as needed, along with data processing algorithms for viewing with ERmapper digital image processing software. Data were provided for several regions of northern Morocco and one area of southern Tunisia. TM data have a spatial resolution of 28.5 meters and provide spectral resolution in the visible, near infrared and mid infrared. The semi-arid to arid climate of much of North Africa is ideal for distinguishing lithological and soil variations using these images.

2. Discrimination of Explosions from Earthquakes

Other efforts were made at LLNL to identify mines based on seismic cluster analysis, and once again, we provided supporting information to LLNL researchers. These areas were in the region of Gafsa, Tunisia (Figure 2), and the Prerif and Khouribga/Oued Zem areas of Morocco (Figure 1). Landsat TM imagery (ca. 1986 and 1984, respectively) was provided, along with digital image processing algorithms developed at Cornell for use with ERmapper image processing software.

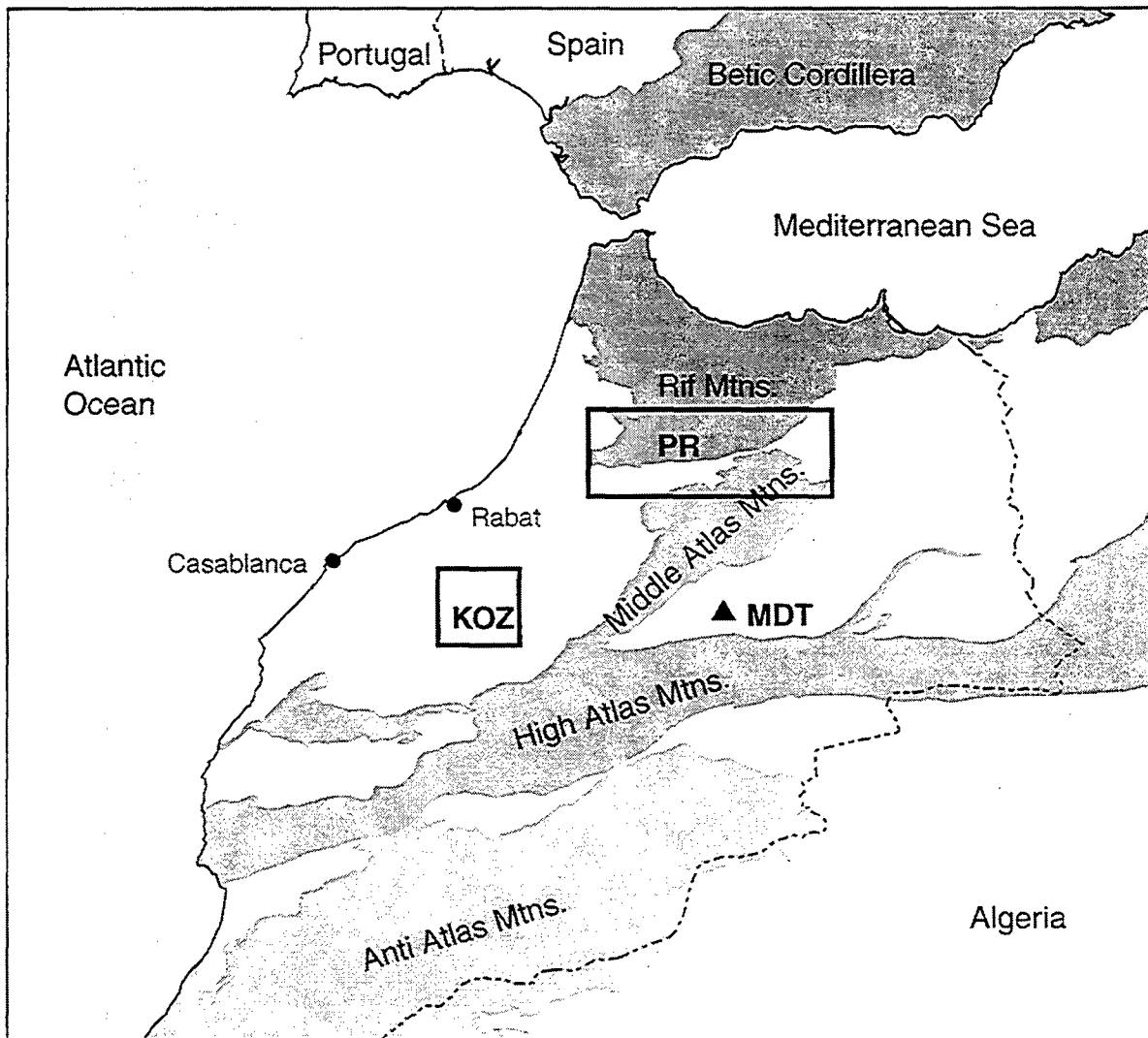


Figure 1. Map showing the regions of interest for seismic activity and mine correlation study. KOZ= Khouribga/Oued Zem mining areas; PR= Pre-Rif; MDT= Broadband seismic station.

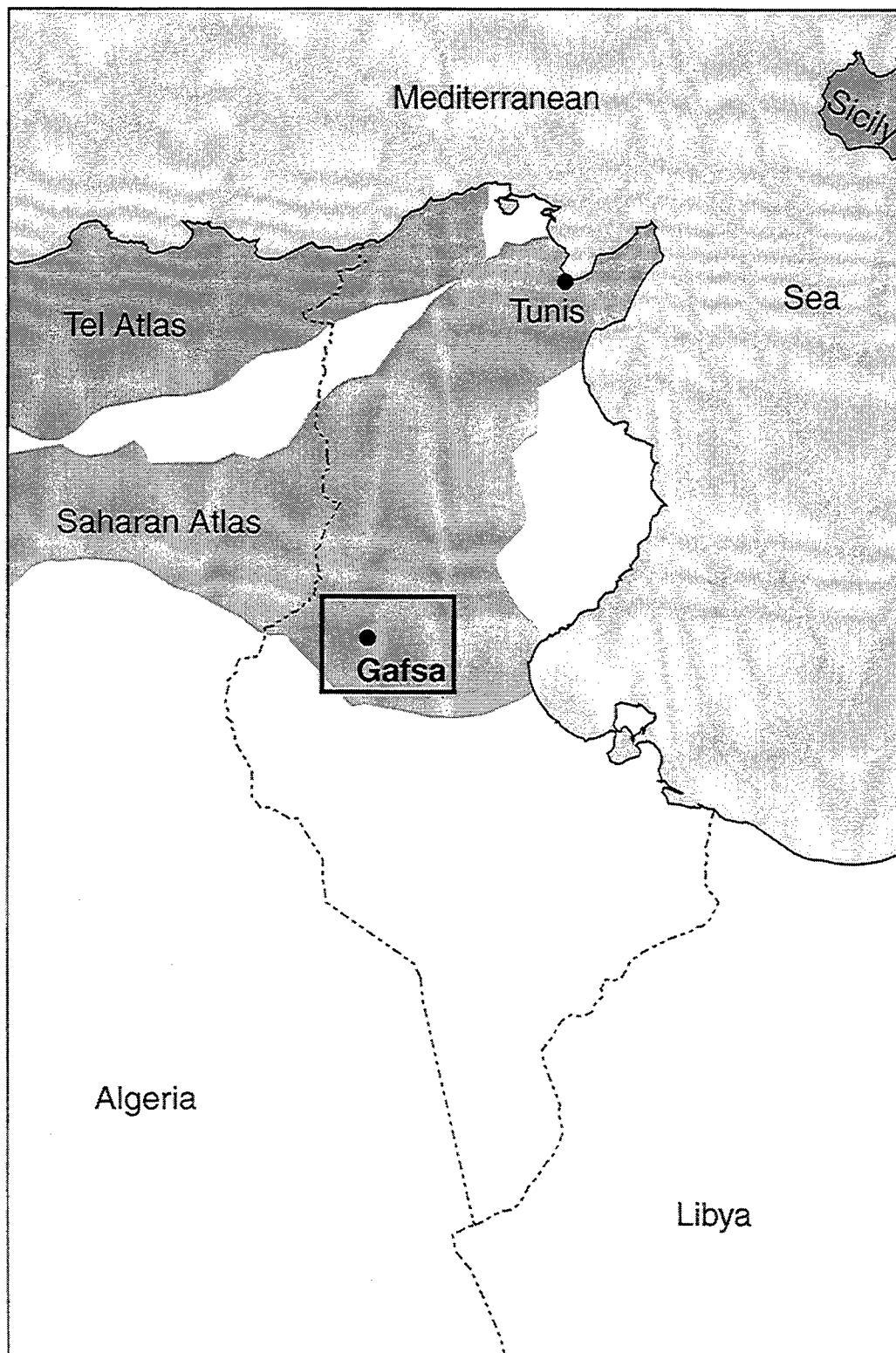


Figure 2. Map showing the location of the area of study in Tunisia.

One of the key products was a digital database of mines in Morocco. This was produced from information provided by the Moroccan Ministry of Energy and Mines listing all of the mines for metallic and non-metallic resources in the country. This database also includes information about the minerals being mined, the type of deposit, morphology, age, rock type, and mineralogical associations. All of this information was entered into GEOID system for use with other data sets. Locations of each mine are given to the nearest minute. The mines are described in more detail in *Panorama de L'Industrie Miniere (Overview of the Mineral Industry)* published by the ministry in 1990. The database does not contain information about periods of activity of the mines, but it is presumed that most in the list were active at the time of publication. This database is also included on the tape with the rest of the database package.

Another product was a digital image file of the *Carte Miniere et Energetique du Maroc (Mineral and Energy Map of Morocco)*, also published by the ministry in 1982. Although this information is dated, it is the only published map available and provides information about mine production. The GIS database is more up-to-date than this map.

Identifying phosphate strip mines corresponding to suspected explosions was successful with the satellite imagery due to the surface effects and the distinct spectral signature of phosphate mine tailings. The suspected events in the Pre-Rif region of Morocco, however, were not successfully correlated with mines or mine-like features in the satellite imagery. (It should be noted that the imagery is approximately 5 years older than the data used in the cluster analysis.) These regions involve mining that may employ different techniques.

This effort is ongoing, and we will continue to provide assistance as needed. Dr. Harris and Dr. Walter plan to process more data in Morocco that overlaps with the operation of the Moroccan regional seismic network. This should provide additional constraints on event locations.

Table 1. Table showing data provided to LLNL under this segment of the contract.

Data Product	Date	Source	Format	Notes
Moroccan Mine Database	1990	compiled from data provided by Ministry of Energy & Mines	ARC/INFO, ASCII	
Mineral & Energy Map of Morocco	1982	Ministry of Energy & Mines	scanned from 1:2,000,000 map, in TIFF & BIL formats (w/ Ermapper header files)	
Topographic maps of Khouribga- Oued Zem region	1950s	Division of Cartography, Ministry of Agriculture	1:100,000; paper; scanned at LLNL	
Geologic Map of Khouribga- Oued-Zem	1970s	Ministry of Energy & Mines	1:100,000; paper; scanned at LLNL	
Landsat Thematic Mapper (TM) image data	1984 (Morocco) 1986 (Tunisia)	EROS Data Center (USGS)	BIL files with Ermapper header files	
Aerial photographs of Khouribga-Oued Zem	1990	Division of Cartography, Ministry of Agriculture	1:40,000; paper	

PART III. MIDDLE EAST AND NORTH AFRICA LOCAL COUNTRY SEISMIC BULLETINS

We have organized all of the available earthquake locations, station locations, and phase data from local bulletins from the Middle East and North Africa region. In all cases, except for one, the formats are the same: fixed column, Fortran style ascii formats containing all of the data that we were able to extract from these files. Unfortunately, due to differences in the methods of location from country to country, we left out some of the parameters which are unique to that country's particular network and are not in our estimation vital information. We have, however, provided the original data that we have started from, so users can go back to the original data to extract these attributes. These data are provided in the attached digital tape. It is also important to note that we have finished putting 31 years of ISC phase, event, and station data (totalling some 25 million phase readings) into ARC/INFO format as well as having incorporated it into our GIS menu system. This database contains an even more comprehensive database than the regional one we are providing here. We have also included phase readings from the Lebanese station BHL. This data file has not been reformatted because Lebanon does not currently produce earthquake location bulletins and hence we were not able to associate the phase picks with earthquakes using a local catalog.

1. Earthquake Catalogs

The formats for the local/national earthquake catalogs for the Middle East are generally fairly similar. Unfortunately most countries provide very little information concerning error analysis. The format we have used for these ascii flat files is uniform except for Turkey. We have a catalog which has been compiled from a variety of networks in Turkey since 1985. This is a very large catalog because it includes seismicity in western Turkey, a very active region.

Phase Data

We have phase data for three countries: Syria, Morocco, and Saudi Arabia. The data files with the format below have been created by extracting phase data only when the event coordinates were given. In the original phase files there are a large number of phase readings for unspecified and unassociated teleseismic and regional events. We have also included phase data from Lebanon; however, the phase picks have not been associated with corresponding seismic events since Lebanon does not produce a national catalog.

Station Data

Along with each of the phase data files we have given corresponding station files. All stations referenced in the phase data files are present in these files. All of the station names are unique, that is, if a station changed location we have changed the name of that station name in the phase and station data files.

Hardcopy Catalogs

Cornell also has a large number of hardcopies of local earthquake catalogs and phase readings. Within this database we have phase reading and earthquake location data for

Israel from the period 1982 to 1991. We also have earthquake locations and phase data from Jordan for the years 1983 through 1991 in hardcopy form. For Yemen we also have phase readings and local earthquake locations for the year 1996. We have phase readings as well as earthquake locations from the Kandilli Observatory seismic network in Turkey. Upon request we would be happy to provide hardcopies of some of these bulletins.

PART IV: METADATA

It is important that data be accompanied by written documentation to enable accurate assessment of their reliability. Metadata, or "data about data", describe the content, quality, condition, source, history, and other characteristics of a dataset. Without metadata, this information is known only to those who acquired or modified the data and the data lose value as the information is lost. With metadata, prospective users can determine what data exist, the fitness of these data for their applications, and the conditions for accessing these data.

To provide consistency for users with datasets from other sources, the Federal Geographic Data Committee (FGDC) Content Standard for Digital Geospatial Metadata was applied. Metadata standards facilitate data sharing through time and space. The standard specifies the information content of metadata for a set of digital geospatial data; its purpose is to provide a common set of terminology and definitions for documentation related to these metadata. The standard establishes the names of data elements and groups of data elements, the definitions of these data elements and groups, and information about the values that are to be provided for the data elements.

The FGDC data elements are as follows:

Identification Information - basic information about the data set. Examples include the title, the geographic area covered, currentness, and rules for acquiring or using the data.

Data Quality Information - an assessment of the quality of the data set. Examples include the positional and attribute accuracy, completeness, consistency, the sources of information, and methods used to produce the data.

Spatial Data Organization Information - the mechanism used to represent spatial information in the data set. Examples include the method used to represent spatial positions directly (such as raster or vector) and the number of spatial objects in the data set.

Spatial Reference Information - description of the reference frame for, and means of encoding, coordinates in the data set. Examples include the name of and parameters for map projections or grid coordinate systems, horizontal and vertical datums, and the coordinate system resolution.

Entity and Attribute Information - information about the content of the data set, including the entities types and their attributes and the domains from which attribute values may be assigned. Examples include the names and definitions of features, attributes, and attribute values.

Distribution Information - information about obtaining the data set. Examples include a contact for the distributor, available formats, information about how to obtain data sets online or on physical media (such as cartridge tape or CD-ROM), and fees for the data.

Metadata Reference Information - information on the currentness of the metadata information and the responsible party. Examples include currentness and information about the organization that provided the metadata.

(Metadata overview is from the FGDC website at <http://www.fgdc.gov/Metadata/metav1-0.html> and <http://www.fgdc.gov/Communications/Metadata/Metabroc.html>)

The complete Metadata for data sets mentioned in the previous sections are included in the attached CD-ROM.

PART V: RESULTS OF ORIGINAL SEISMOLOGICAL RESEARCH IN SUPPORT OF CTBT

A. CRUSTAL STRUCTURE IN THE MIDDLE EAST AND AFRICA: GRID SEARCH INVERSION OF RECEIVER FUNCTIONS

Abstract

A grid search inversion is used to estimate average crustal thickness and shear wave velocity structure beneath 12 three-component broadband seismic stations in the Middle East, North Africa, and nearby regions. The crustal thickness in these regions is found to vary from a minimum of 8 ± 2 km in East Africa (Afar region) to a maximum of 60 ± 5 km in the lesser Caucasus. Stations located within the stable African platform indicate a crustal thickness of about 40 km. Teleseismic waveform data are used to create receiver function stacks for each station. Using a grid search inversion scheme, we have inverted for the optimal and most simple shear-velocity models beneath each station. The grid search inversion method guarantees that we solve for the global minimum within our defined model parameter space. Using the grid search, we also qualitatively estimate the least number of layers required to model the observed receiver functions' major seismic phases (e.g., PS_{Moho}). A jackknife error estimation method is used to test the stability of our receiver function inversions for all 12 stations in the region that have recorded a sufficient number of high quality broadband teleseismic waveforms. The 12 estimates of crustal thicknesses are consistent with known crustal variations and tectonic settings in these regions.

Introduction

In the Middle East and Africa there is only very sparse coverage of three-component broadband seismic stations (Figure 1). In order to improve knowledge of the crustal seismic velocity structure in the regions we have used receiver functions for all broadband stations located in the Middle East and North Africa. By inverting these receiver functions we place constraints on Moho depth and average shear wave velocities in regions where few geophysical measurements have been made. We have opted to determine first-order features of the crust and uppermost mantle; therefore, we have only interpreted the first 20 seconds of the teleseismic P-wave coda.

Receiver function inversion, both quantitative and qualitative, has become a widely used seismological technique to obtain shear wave velocity structure beneath single, three-component seismic stations [e.g., *Phinney*, 1964; *Burdick and Langston*, 1977; *Langston*, 1979; *Owens et al.*, 1988]. The receiver function technique has the advantage of eliminating many of the components of a seismogram that complicate interpreting teleseismic body waves (Figure 2). Figure 2 shows the idealized case for receiver function interpretation. Inverting the PS_{Moho} phase in a receiver function has become a very common way to interpret crustal thickness as this phase is generally observed globally. More recently the non-uniqueness and the relative lack of stability of the receiver function inversion have also been well documented [e.g., *Ammon et al.* 1990; *Sheehan et al.* 1995; *Baker and Gurrola*, 1996]. In order to address these problems, other methods, including algorithms such as simulated annealing and the genetic algorithm,

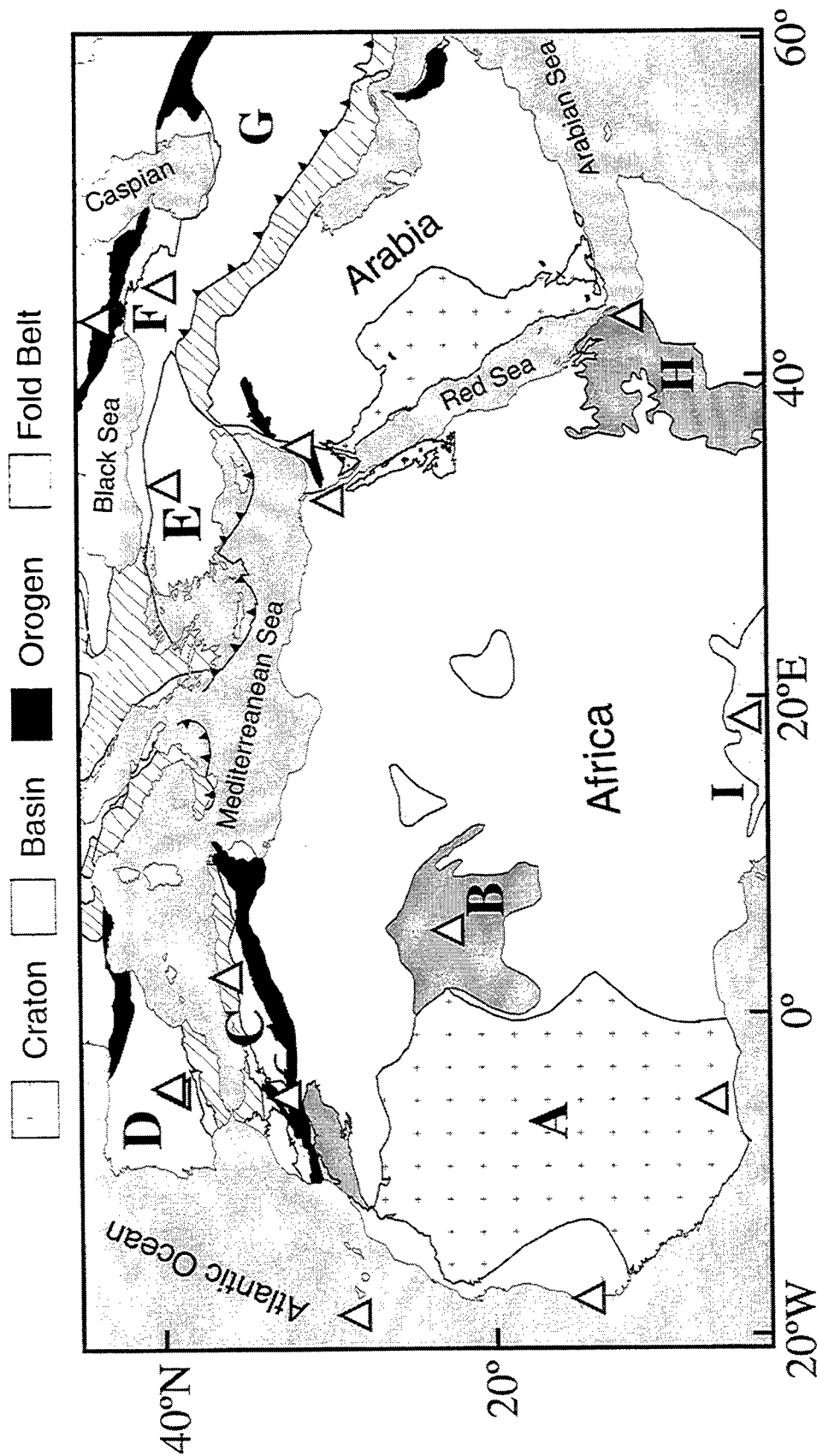


Figure 1. A simplified tectonic map of the Middle East and North, Central, and Western Africa. The tectonic units shown are primarily those in which we have a broadband station. Broadband stations are shown as white triangles. (A) West African Craton, (B) Hoggar hot spot, (C) Atlas mountain belt system including the High, Middle, and Tel Atlas Mountains, (D) Iberian Meseta, (E) Anatolian block, (F) Anatolian Plateau, Lesser Caucasus and Greater Caucasus (shown in black), (G) Iranian Plateau, (H) East African Rift System, and (I) Congo Basin and craton.

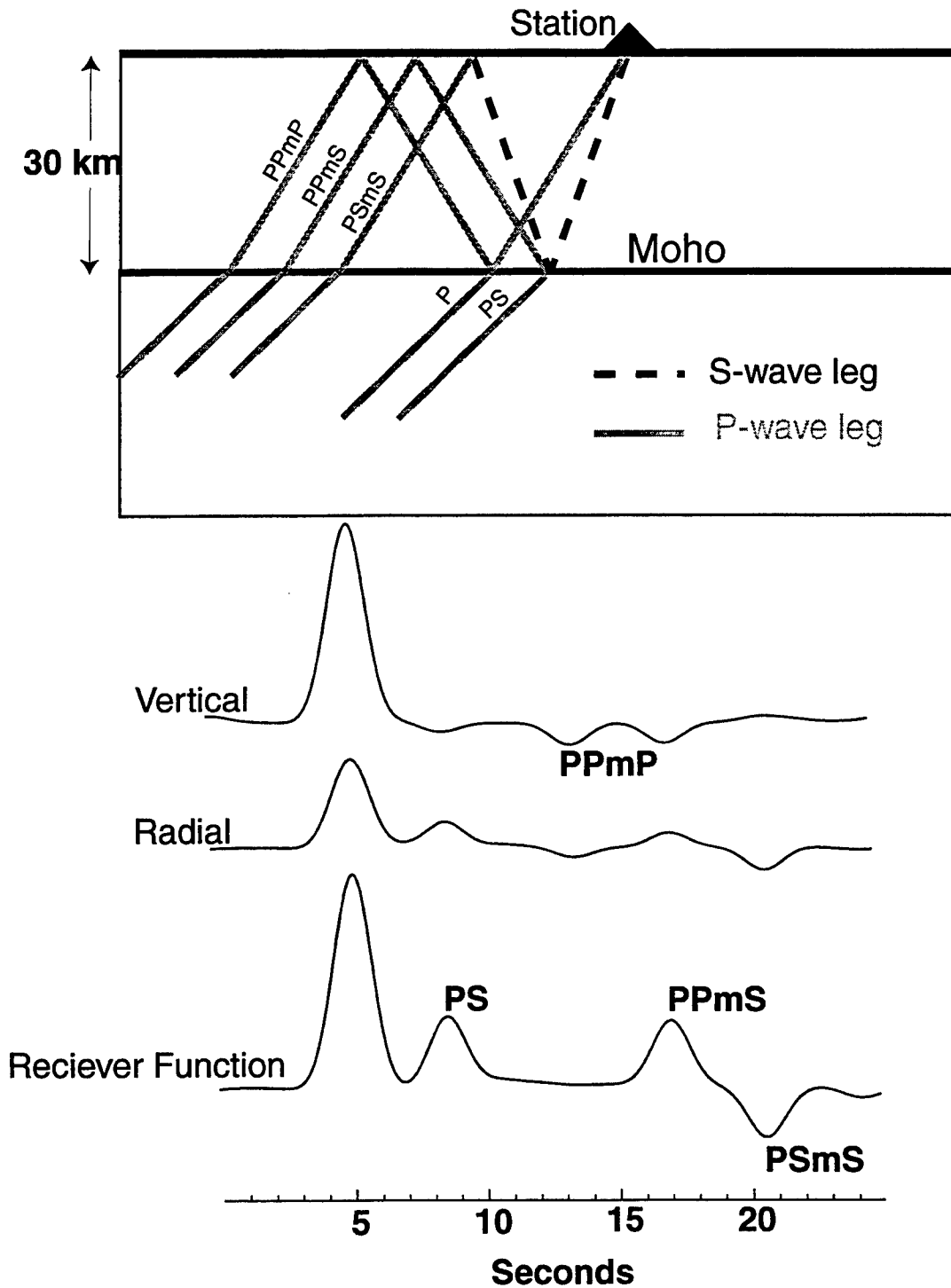


Figure 2. A schematic ray tracing diagram for a hypothetical teleseismic p-wave incident on a 30 km thick crust. The light gray rays correspond to a P-wave leg while the dashed black rays are S-waves. The radial and vertical component synthetics were created with the reflectivity synthetic seismogram algorithm. Note that the P-multiples have divided out of the radial receiver function.

have been employed to improve the initial model dependence resulting from the non-uniqueness of the inversion [Zhao and Frohlich, 1995]. However, even with these techniques there is no guarantee that one will obtain the true global minimum due to the non-linearity of the receiver function inversion.

Further studies have demonstrated that the receiver function inversions lack stability; that is, the receiver function inversion is extremely sensitive to small amounts of noise in the data [Baker and Gurrola, 1996]. Methods have been designed to overcome this lack of stability by avoiding the deconvolution process and directly modeling the teleseismic P-wave coda [Zhao and Frohlich, 1995]. This technique has the disadvantage of not completely accounting for source-side structure. We have used deconvolution in order to be able to stack our receiver functions, as is essential for bringing out coherent portions of the receiver function waveform. In order to account for the large number of local minima we have used a grid search technique which guarantees that we will solve for the global minimum. Furthermore, in order to estimate how robust this minimum is, we utilize a jackknife inversion scheme to estimate a confidence region for each of the model parameters.

The Middle East and Africa are excellent regions in which to employ a grid search technique to estimate crustal structure and thickness because there have been only a few regional-scale geophysical observations. Combining the grid search with our stability test we were able to make estimates of crustal structure along with quantitative estimates of the resolution of our inversion. In the Middle East there have been a number of refraction studies that provide estimates of basement and crustal thicknesses [e.g., Ginzburg and Folkman, 1980; Ginzburg *et al.*, 1981; Yuval and Rotstein, 1987; El-Isa *et al.*, 1989]. We are able to test the grid search technique by comparing our model and error estimates with these independent measurements of crustal structure. However, in North Africa the number of regional-scale geophysical measurements is very limited. In Egypt and Morocco there have been a few measurements of crustal thickness from refraction experiments [Makris *et al.*, 1982; Wigger *et al.*, 1984] that can be compared to our results.

There are numerous and diverse tectonic regimes in the Middle East and Africa (Figure 1); hence, it is critical to our understanding of these regions to have some knowledge of crustal thickness. In the Middle East, the Dead Sea fault system is thought to be a transtensional feature associated with regional crustal thinning. Continental collision is also taking place along the Bitlis suture, which has led to the subsequent escape of the Anatolian block and the uplift of the Iranian-Anatolian Plateau. Because little is known about the crustal structure in this region, even single station models are important. In Africa the tectonic setting is dominated by the African craton. However, there is a large intra-continental zone of deformation in the Atlas system in North Africa. The question of whether or not a crustal root exists in this intra-continental mountain belt is critical to determining the compensation mechanism for the Atlas system.

Data

We have collected over 600 Megabytes of broadband, three-component teleseismic waveform data, for the years 1988 through 1995, produced by 15 Federation of Digital Seismic Networks (FDSN), Global Seismographic Network (GSN), Mediterranean Network (MEDNET), GEOSCOPE, and GEOFON permanent broadband stations in the Middle East and Africa (Figures 1 and 4a). We have used waveforms from events located at distances between 35 and 85 degrees in order to avoid problems with regional and core phases. We have examined all available records and eliminated those with signal-to-noise ratios of less than approximately 4 to 1, where we define noise as the seismic energy preceding the direct P-arrival after deconvolution. We have also attempted to eliminate the effects of large scale lateral velocity heterogeneity by calculating the radial direction using the three-component teleseismic P waveform. We have minimized the tangential component energy and then rotated the horizontal components into this corrected radial and tangential directions. Although this procedure will not remove the effect of smaller scale crustal and upper mantle velocity heterogeneity, we have found that it does remove the effect of teleseismic ray bending resulting from large scale mantle heterogeneity.

We have employed the commonly used “water level” spectral division technique [e.g., *Langston, 1979; Ammon et al., 1990*] to calculate each of the receiver functions used in this study (Figure 3). In order to solve for receiver functions that are sensitive primarily to first-order features, we have used a gaussian filter with an $\alpha = 1.5$. Station GNI contained a large amount of 1 Hz noise, so we used an even longer period low-pass (gaussian) filter ($\alpha = 1.0$). The gaussian filter produced fairly coherent receiver functions that contained data with frequencies of 0.5 Hz. This filter limits, to a certain degree, the resolution of the shape and slope of the discontinuities within our velocity models. However, we are primarily interested in the first-order depth to these discontinuities, and hence are willing to lose resolution of crustal structure in order to minimize the effects of small-scale “non-one-dimensional” structures beneath the receivers. Seismic data from 15 stations have been used to calculate high quality receiver function waveforms (Figures 4b, 4c, 4d). We have chosen not to use 3 of the fifteen stations (MBO, TBT, and MEB) shown in Figures 4b, 4c, and 4d because we were not able to model the waveforms with a reasonable 1-D earth model.

Our data selection is not restricted to deep earthquakes. P-wave teleseisms with relatively simple vertical responses, whether from deep or shallow earthquakes, have been selected. Simple P-wave vertical waveforms should correspond to simple source-time functions. Receiver functions from small shallow events, taken from seismograms with simple first motions, showed strong coherence with receiver function waveforms from deep events. Receiver function stacks, shown in Figure 4, were created for data originating from several available azimuths in order to attempt to obtain the average, with respect to azimuth, shear wave velocity model (Figure 5). We have also tested for the effects of lateral heterogeneity. We have stacked for only one distance (± 10 degrees) in order to avoid problems caused by move-out of the PS phases due to differences in angles of incidence (i.e., differences in the ray parameter).

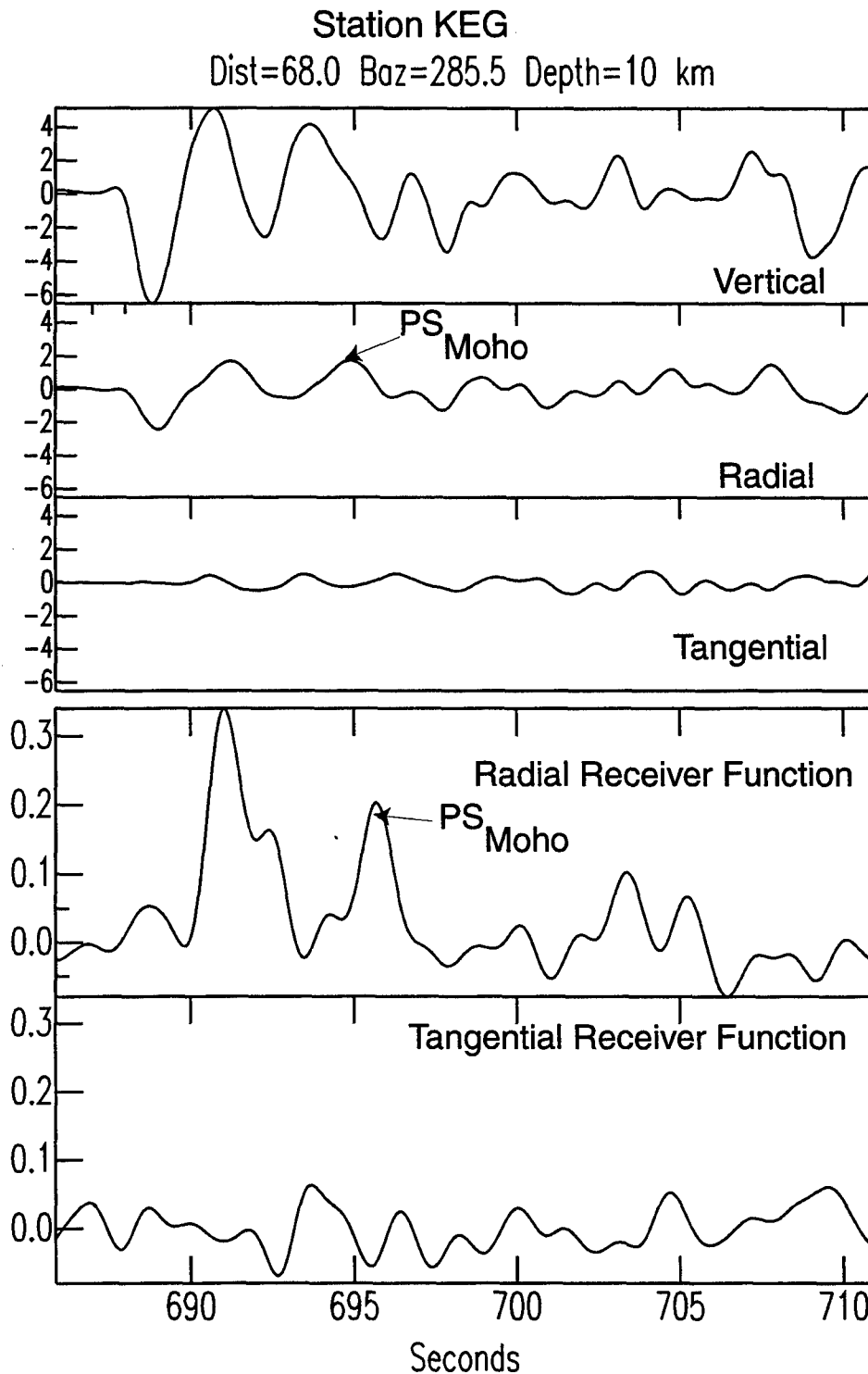


Figure 3. A plot showing a three-component broadband teleseismic P-wave recording at an example station KEG; the earthquake was located in the central portion the Atlantic mid oceanic ridge. After doing the spectral division to create radial and tangential receiver functions, the PSMoho phase is identified on both seismograms and radial receiver functions. Note that even though this event is at a relatively shallow hypocentral depth, the vertical response is fairly simple.

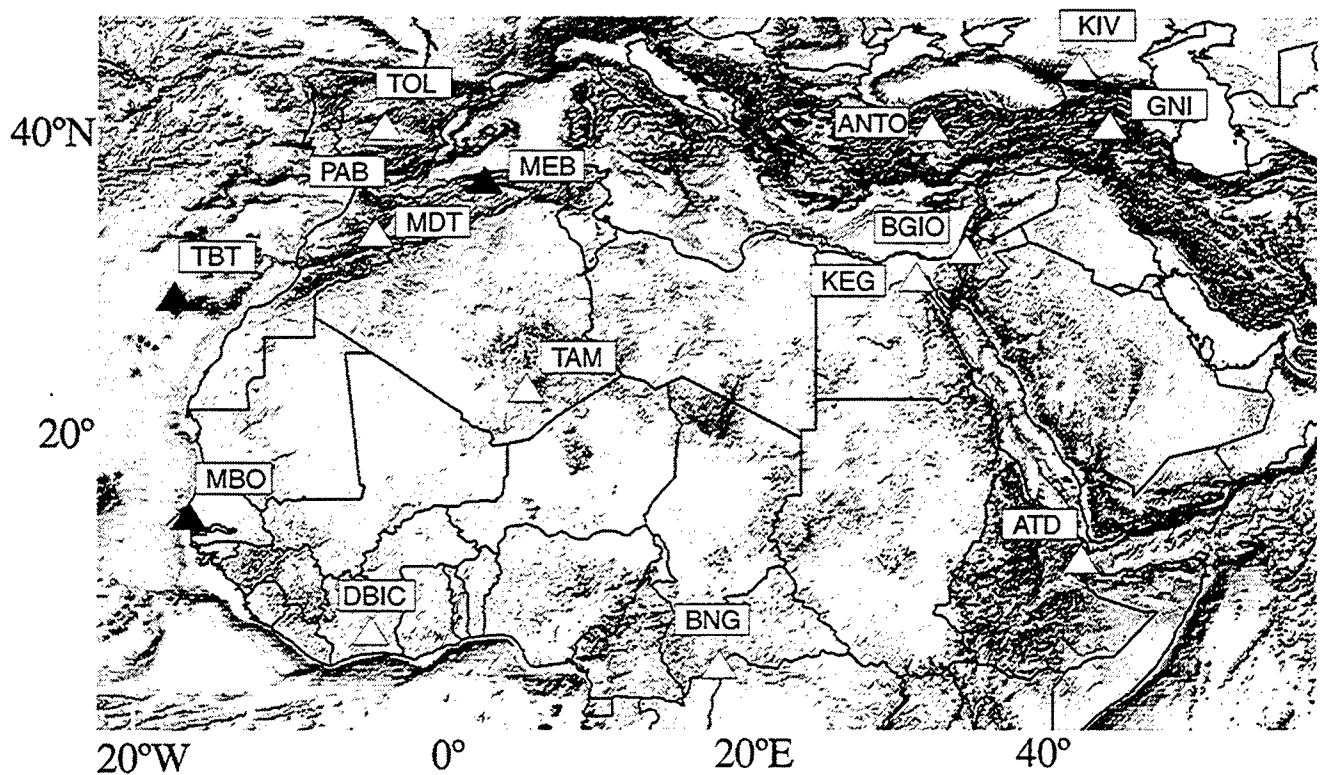


Figure 4. Map showing all stations for which a receiver function stack was computed. Only 12 of these stations (white) were used to invert for a shear wave velocity model. The three that were not inverted were stations MBO, MEB, and TBT (black). All stacked radial and tangential receiver functions that have been computed for the Middle East and north, central, and western Africa are shown in figures 4b, 4c, and 4d. Station names are shown on the left of the radial receiver function. The top trace, for each station, corresponds to the radial receiver function while the bottom trace is the tangential receiver function. Several of these receiver functions were determined to contain waveforms that could not be modeled with a reasonable 1-dimensional model and hence are not addressed in this paper. The extremely large PSbasement at station MBO has made it very difficult to model with a one-dimensional velocity model. Stations TBT and MEB both had very noisy and incoherent waveforms.

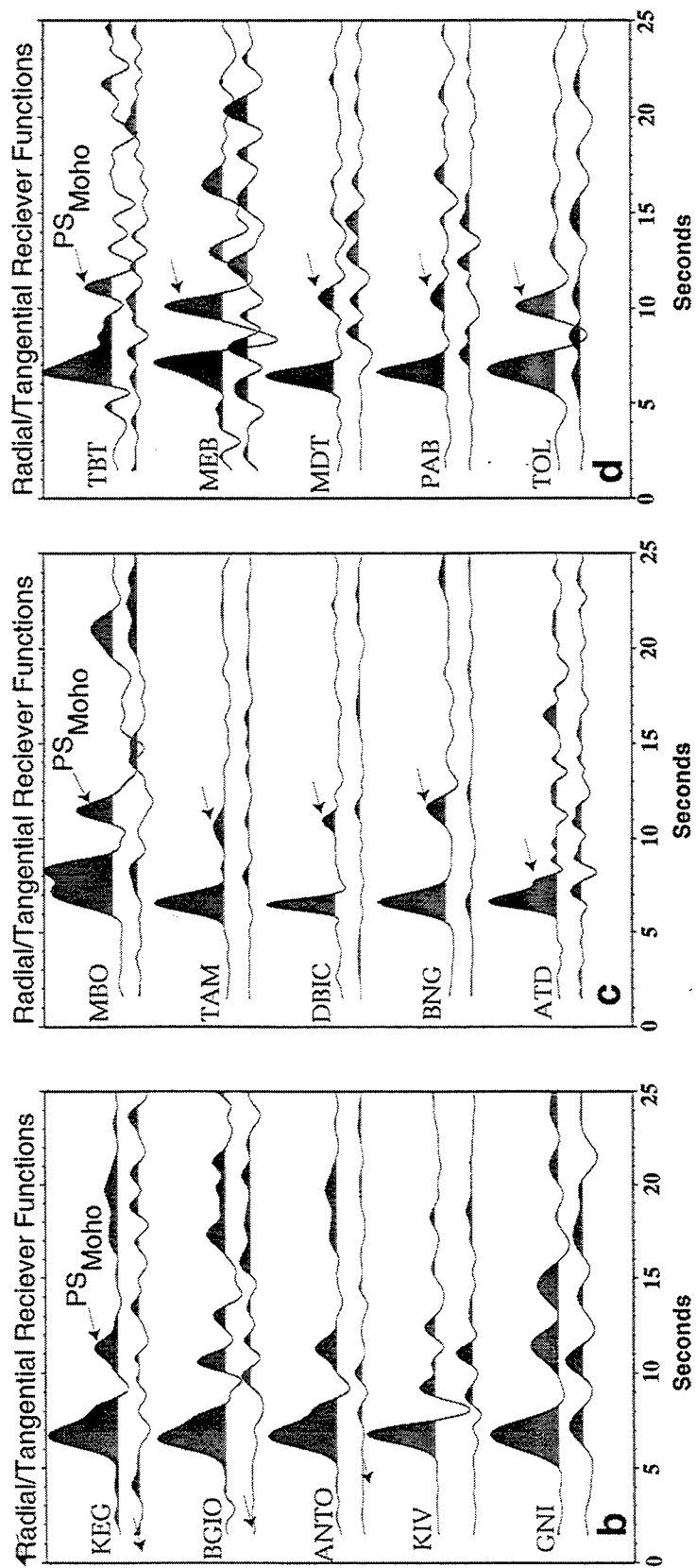


Figure 4 (cont.)

Inversion Method

In order to invert the observed receiver function stacks for the crustal shear wave velocity structure we apply a two-iteration grid search method combined with a jackknife error estimation technique (Figure 6). A reflectivity synthetic seismogram algorithm, initially developed by *Kennett* [1984], is used to create our synthetic receiver functions. To invert the receiver function data reliably for crustal and uppermost mantle shear wave velocity structure we employ a grid search scheme using a maximum of six layers in our model. It should be noted here that the half-space (mantle shear wave velocity) is constrained only by the amplitude of the direct P wave and the amplitude of the PSMoho phase; hence it is much less reliable. We have chosen a maximum of six layers since it is unlikely that we will be able to uniquely resolve a higher number of layers because of the number of phases that can usually be identified within a receiver function waveform. For simple receiver functions, a one-layer crustal model was found to match the observed data reasonably well (see stations BNG and DBIC in Figure 4). Using an assumed maximum and minimum possible thickness and shear wave velocity for each layer, the least squares difference between the observed and synthetic receiver functions is minimized. We also experimented with the absolute value of the difference between the observed and synthetic (L1 norm), but found little difference in the results. The advantage of our grid search scheme is the guarantee that within the limitations of our grid spacing, we will solve only for the global minimum. The grid spacing for the shear wave velocity is 0.1 km/s and 2 km for layer thickness and in some cases 1 km for the first layer (basement thickness, see Table 1). This parameterization corresponds to a much finer grid search of the velocity-space than of the thickness-space. This tends to make velocity appear more sensitive to noise than to layer thickness (Figure 7). This can be demonstrated with the slope of the depth-velocity trade-off: for shallow discontinuities this slope is more sensitive to the velocity than to the layer thickness.

Table 1. Beginning and ending values and the grid spacing for each model parameter used in each station's grid search receiver function inversion. V_S and D represents shear velocity and layer thickness, respectively.

Layer #	ΔV_S (km/s)	ΔD (km)	Min V_S (km/s)	Max. V_S (km/s)	Min D (km)	Max. D (km)
Station ANTO						
1	0.1	2	2.70	3.50	7	13
2	0.1	2	3.04	3.84	14	22
3	0.1	2	3.14	3.84	4	10
4	0.1	2	3.54	4.24	1	5
5	0.1	1	4.54	4.64	5	5
Station ATD						
1	0.1	1	2.80	3.70	1	6
2	0.1	2	3.00	3.60	2	8

3	0.1	2	3.20	3.90	2	8
4	0.1	2	3.44	4.34	2	8
5	0.1	1	4.34	4.64	5	5
Station BGIO						
1	0.1	2	2.74	3.44	1	7
2	0.1	2	3.24	4.04	8	18
3	0.1	2	3.34	4.24	8	20
4	0.1	2	4.04	4.54	14	20
5	0.1	2	4.54	4.64	5	5
Station BNG						
1	0.1	1	2.90	4.50	28	55
2	0.1	2	4.34	4.74	2	8
3	0.1	2	4.54	4.84	4	4
4	0.1	2	4.54	4.84	4	4
5	0.1	1	4.54	4.84	5	5
Station DBIC						
1	0.1	1	2.50	4.20	20	50
2	0.1	2	4.54	4.84	2	2
3	0.1	2	4.54	4.84	2	2
4	0.1	2	4.54	4.84	2	2
5	0.1	1	4.54	4.84	5	5

poisson's ratio: 0.22 to 0.30 0.01 grid interval

Station GNI						
1	0.1	2	3.04	3.94	26	46
2	0.1	2	3.34	4.24	6	12
3	0.1	2	3.84	4.44	2	10
4	0.1	2	3.94	4.54	12	20
5	0.1	1	4.54	4.74	5	5
6	0.1	1	4.64	4.74	5	5
Station KEG						
1	0.1	2	2.90	3.30	2	8
2	0.1	2	3.40	4.05	4	12
3	0.1	2	3.40	4.15	10	22
4	0.1	2	3.74	4.44	6	14
5	0.1	1	4.54	4.74	5	5
Station KIV						
1	0.2	2	3.30	4.14	6	14
2	0.2	2	2.84	3.74	4	10
3	0.2	2	2.84	3.84	4	12
4	0.2	2	3.64	4.44	16	30
5	0.2	1	4.54	4.74	5	5
Station MDT						
1	0.1	2	3.70	3.90	2	8
2	0.1	2	3.30	3.90	4	8
3	0.1	2	3.44	4.34	10	16

4	0.1	2	3.64	4.44	6	22
5	0.1	1	4.44	4.74	4	4
6	0.1	1	4.64	4.74	4	4
Station PAB						
1	0.1	2	3.10	3.80	4	12
2	0.1	2	3.20	3.90	4	10
3	0.1	2	3.44	4.34	4	10
4	0.1	2	3.74	4.54	4	10
5	0.1	1	4.34	4.84	5	5
Station TAM						
1	0.1	1	2.80	3.30	1	5
2	0.1	2	3.00	3.90	8	18
3	0.1	2	3.20	4.10	8	20
4	0.1	2	3.44	4.44	4	14
5	0.1	1	4.54	4.74	5	5
Station TOL						
1	0.1	2	3.10	3.80	4	12
2	0.1	2	3.20	3.90	4	10
3	0.1	2	3.44	4.34	4	10
4	0.1	2	3.74	4.54	4	10
5	0.1	1	4.34	4.84	5	5

In order to further reduce the computation time of the grid search inversion, we decimated the stacked receiver functions down to 5 samples per second. Since the receiver functions are filtered to 1.5 Hz and below, this did not cause any aliasing problems or differences in bandwidth between the synthetics and the observed receiver functions. This decimation, along with several other minor optimizations to the synthetic receiver function generator, enabled the calculation of approximately 150 synthetics per second on a SPARC Ultra 2 workstation.

Only 9 to 11 model parameters are used in the inversion (4 to 5 layers where the layer thickness, shear wave velocity and a half space velocity are modeled), so the receiver function inversion's non-uniqueness problem is reduced. The longer period receiver functions are fit reasonably well by a 5 layer model. Bulk Poisson's ratios for stations DBIC and BNG are also included in the grid search inversion. A grid search spacing of 0.01 with a maximum and minimum of .030 and .022, respectively, was used. The sensitivity of receiver functions to Poisson's ratio has been well established [e.g., *Zandt and Ammon, 1995*]. We have found an optimal bulk Poisson's ratio of 0.25 for these two stations.

The grid search scheme allows us to map the RMS error surface (Figure 7). This allows us to examine, qualitatively, the error surface for multiple or local minima (i.e., to test for non-uniqueness). Figure 7 is a portion of the 9-dimensional error surface for station KEG in which we do not see evidence of large local minima that are located far from the global minima. The progressive broadening of the minima with increasing layer depth is an indication that errors are propagating from the upper layers to the lower one. However, this is only a portion of the error surface from the grid search inversion. The difficulty in

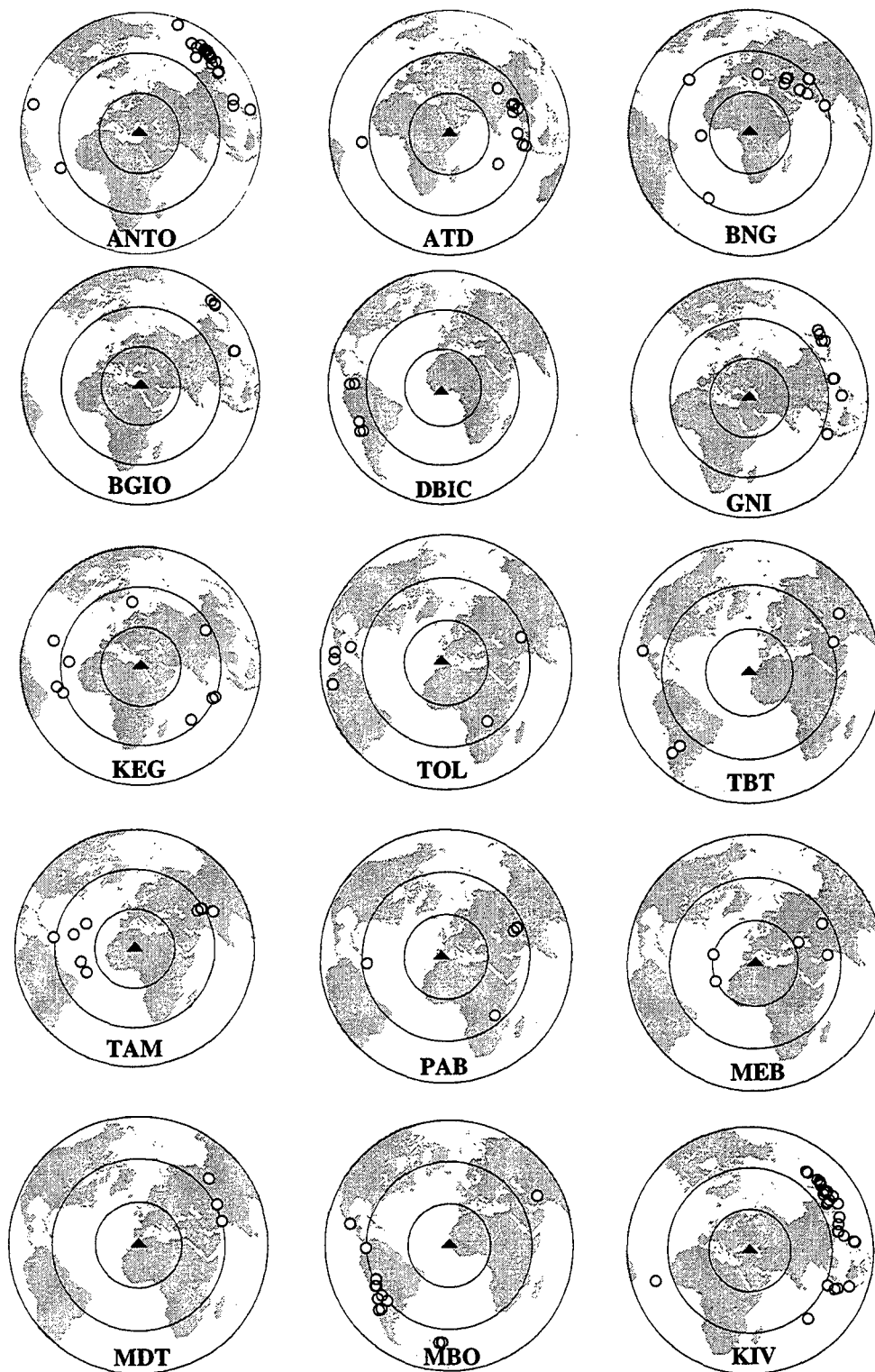


Figure 5. A plot of all events used in each stack for all 15 stations shown in Figure 4. The concentric circles represent 30 degree increments centered on each station shown. We have restricted our event-stations distances to between 35 and 85 degrees but only stacked within 10° .

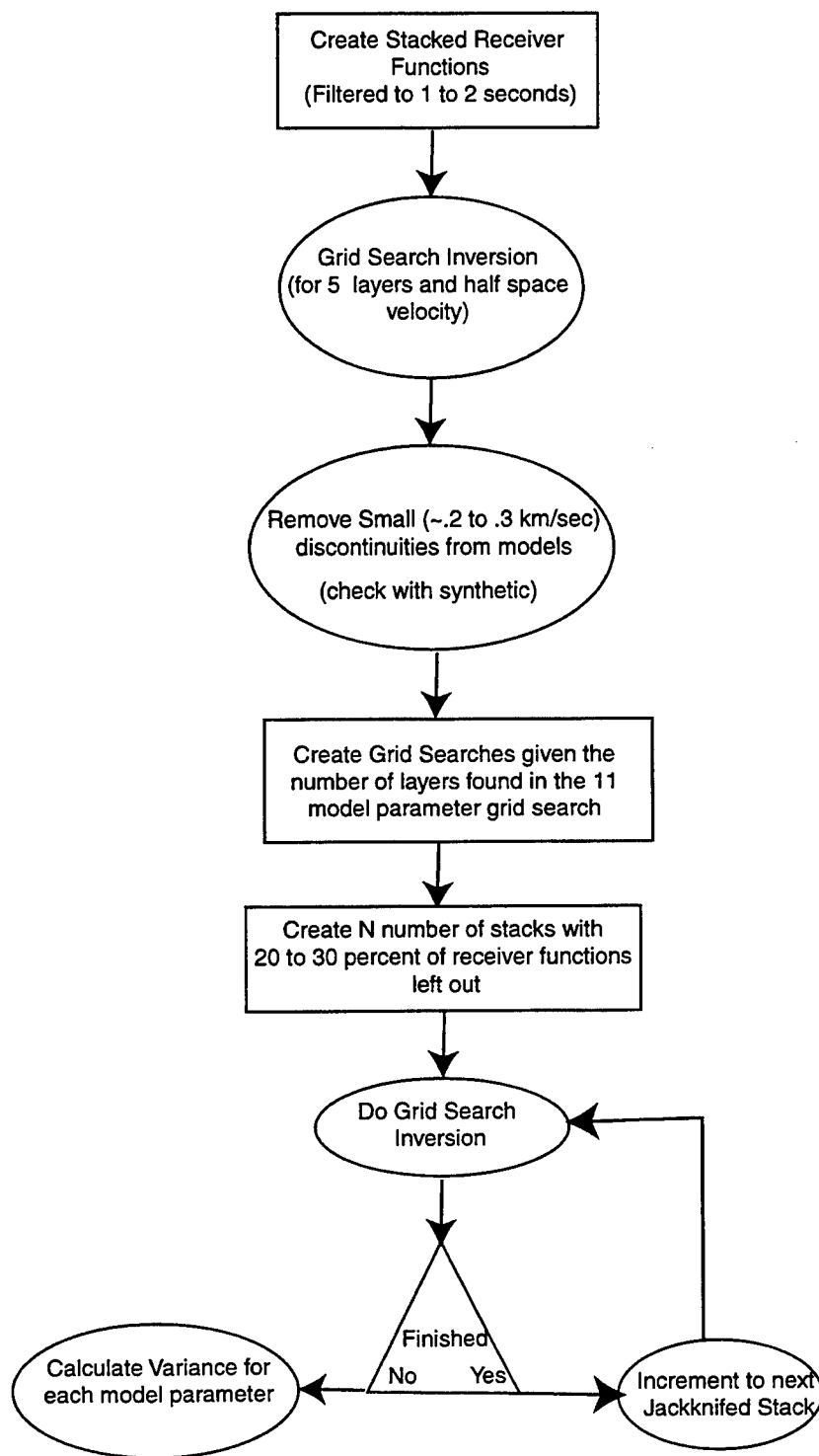
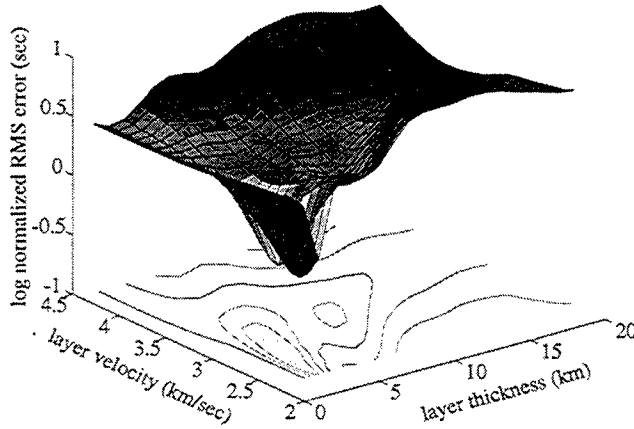
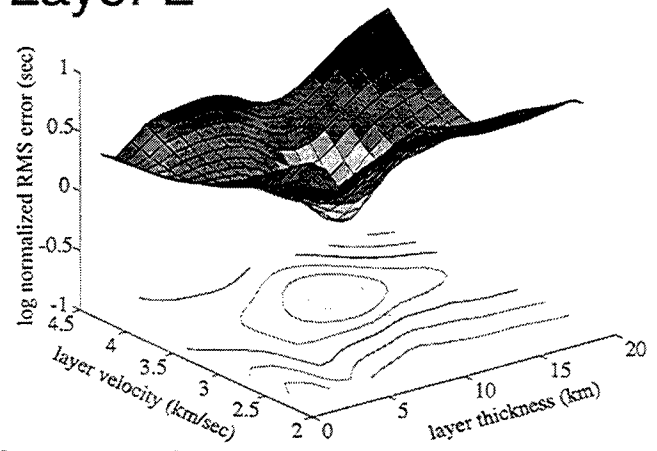


Figure 6. Flowchart showing the generalized procedure used in inverting and estimating the errors associated with each of the optimal shear wave velocity models. This approach is a systematic and generalized method to infer first-order crustal structure from teleseismic P-wave coda.

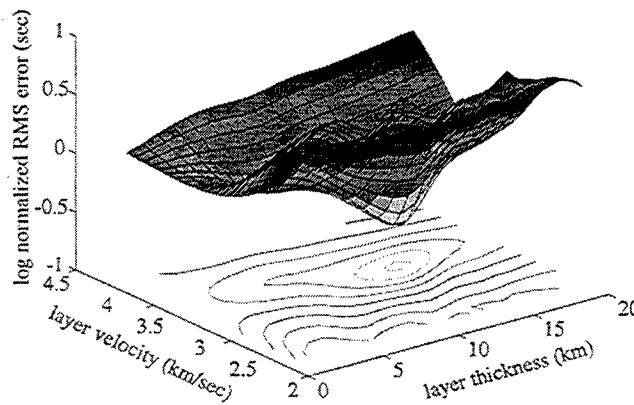
Layer 1



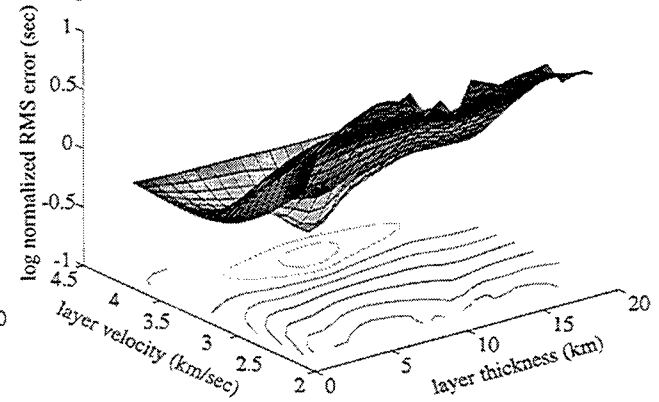
Layer 2



Layer 3



Layer 4



Station KEG

Figure 7. Plots showing an example of RMS error surfaces for the stacked receiver function from station KEG. The layer error surfaces were obtained by holding the other eight model parameters constant, at the final model, while the layer shear wave velocity and thickness were allowed to vary. Note that in layer one the minimum's slope is biased toward the velocity axis; this is a result of a finer grid spacing for the velocity than the thickness model parameter.

using the error surface in determining a confidence region is the need to quantitatively estimate the correlated noise contained within the receiver function time series. This becomes a rather difficult problem because neither the tangential receiver function nor the noise preceding the deconvolved radial and vertical seismograms provide a reasonable estimate of the correlated noise time series. Therefore, we have avoided using the error surface to estimate our confidence limits.

We have found that comparisons between the grid search technique and the linearized least squares (LLS) method yield significantly different results if one does not consider the non uniqueness of the LLS technique. For those receiver functions that are relatively simple in nature (i.e., only a PSMoho phase), the results are similar given a starting model that is close to the final solution. We have employed the *Ammon et al.* [1990] method of using multiple starting models in order to make our comparison. We found significant differences for many of the resulting models obtained for stations KEG and BGIO (Figure 8). The mean of the LLS models for station KEG agreed with our grid search results; however, the results from the LLS inversions for station BGIO tended to be biased toward a thicker crust than that of our grid search results. It should be noted that many of the LLS solutions did agree with our grid search model; however, five of the models yielded crustal thicknesses of more than 35 km. We have also found that the smoothing constraint often used with the LLS inversions can potentially cause significantly different velocity models, as seen in the final models for station BGIO. We did try a number of different smoothing parameters and LLS model perturbations in order to test when the LLS method diverged from the grid search solution. We have found significant differences between the grid search solution and the LLS solution for all solutions which did not have initial models near the solution. Inversion techniques, such as simulated annealing and genetic algorithms, should improve this performance.

Resolution and Error Analysis

After obtaining the results from our grid search we qualitatively analyzed, for each station's best model, each layer as to whether or not the layer contributed a significant amount of energy to the synthetic (Figure 4). We have performed this exercise for all 12 stations. Stations BNG and DBIC were initially modeled using a 4 layer crust, but we found that the grid search procedure effectively chose a one-layer crust; therefore we could effectively model the crust with only two parameters (i.e., shear velocity and thickness). Only the data recorded by station BGIO fit the data significantly better by including more than four layers in the grid search. Owing to computational limitations with our jackknife error technique, we used the best fit for four layers beneath BGIO (Figure 9). The limitation of the number of model parameters in the waveform inversion has allowed us also to employ either a bootstrap or a jackknife resampling error estimation scheme, and we will see later in the paper that the resolution at this station is such that it is unlikely that we can resolve a multi-layer velocity model.

When estimating errors of our inversion results, we normally require an estimate of the noise contained within the receiver function stacks. Estimating an accurate and robust "noise time-series" from the receiver function data is usually not possible [*Paulssen and Visser*, 1993]. The difficulty in estimating the true noise contained within the stacked

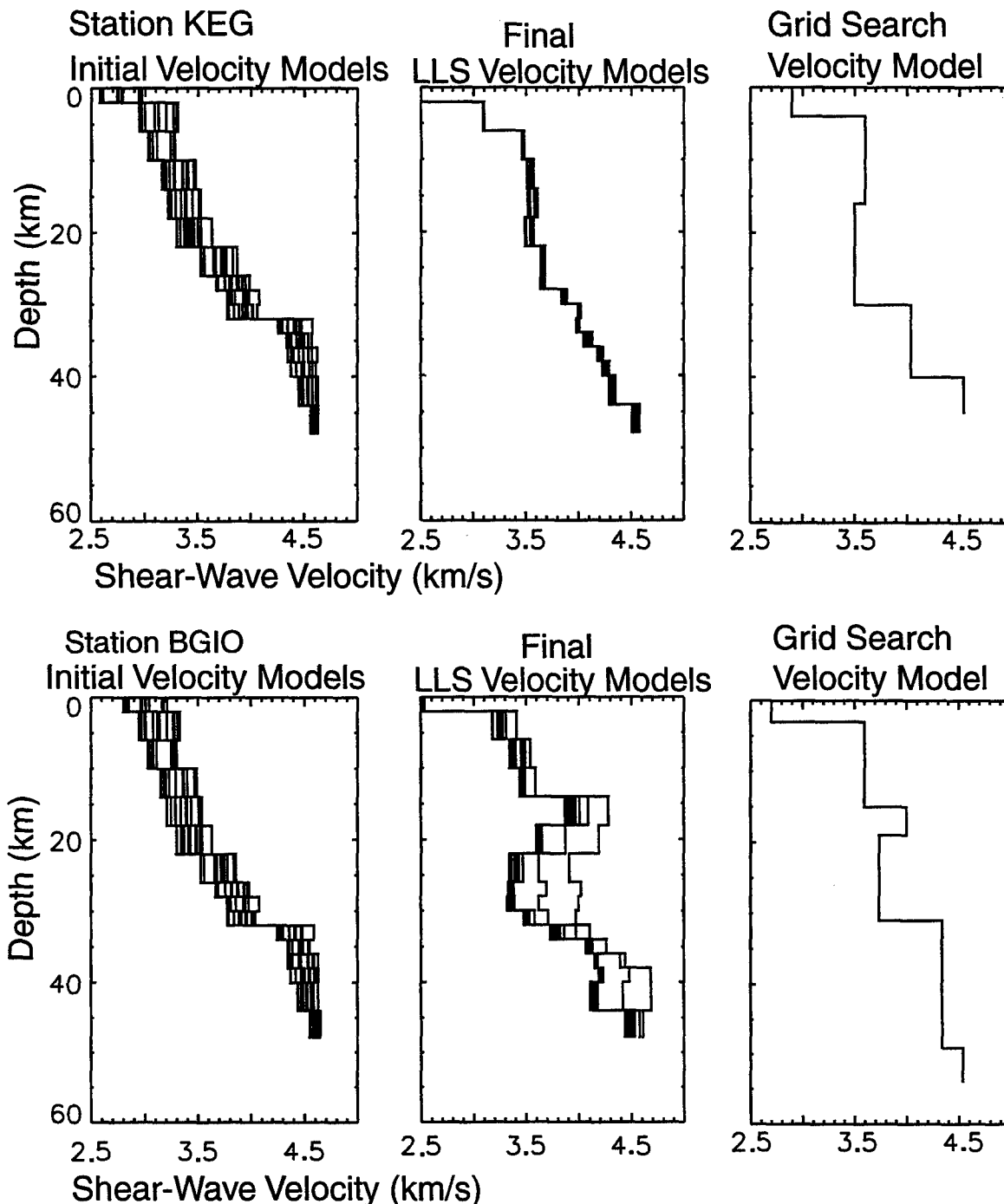


Figure 8. A comparison of the linearized least squares (LLS) and grid search inversions for two stations, KEG and BGIO, in the Middle East (see Figure 4). We have used a smoothing parameter of 0.1 and a damping parameter of 0.01 for the LLS inversion. We have also used the Ammon et al. [1990] method of using an initial velocity model suite in order to measure the non-uniqueness of the inversion. The LLS inversion also utilized 25 layers with fixed layer thicknesses of 2 km. Our grid search inversion used a 5 layer over half space model. Note that the differences between station KEG's grid search and LLS final model(s) can be attributed to the smoothing constraint used. Station BGIO's grid search final model is considerably different from many of the final models obtained from the LLS technique.

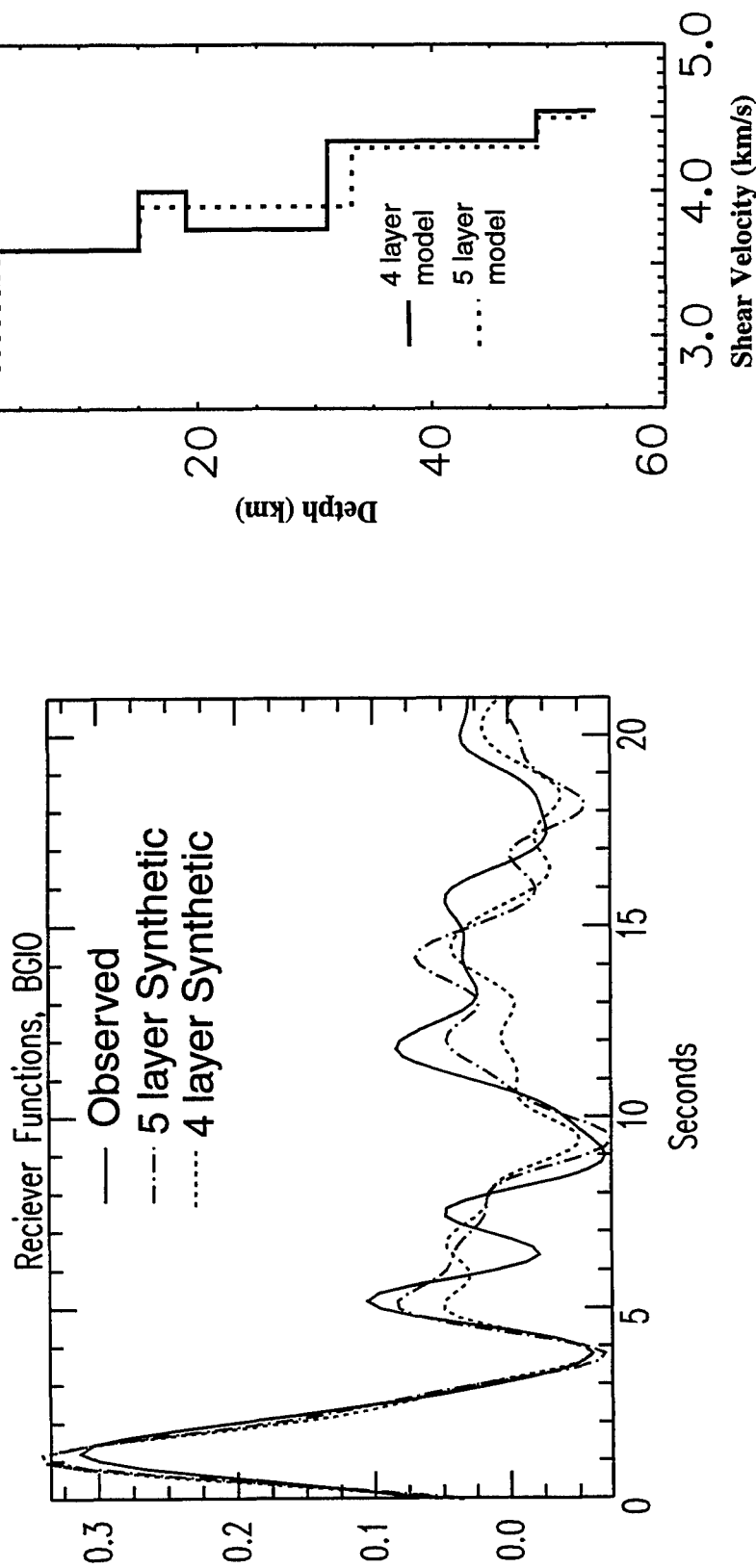


Figure 9. A comparison of 4 and 5 layer grid search solutions for station BGIO. The left panel shows the synthetic waveforms corresponding to a shear velocity model obtained from a grid search using 11 model parameters (5-layer crust over a mantle half space), a 9 model parameter grid search inversion (4-layer crust over a mantle half space), and the observed stacked receiver function. The right panel shows the velocity models obtained from both inversion schemes.. Teleseismic waveforms from station BGIO are the most complex of the 15 stations that we examined; hence we had the most difficulty modeling the BGIO receiver functions with a 4-layer model. Station BGIO is the only station where we observed a significantly better fit, between the observed and computed waveforms, for a five-layer model than a four-layer model.

receiver functions has led us to avoid estimating confidence regions from either (1) constructing confidence regions from the error surface, or (2) bootstrap error estimation via an estimated noise time series or randomized residuals, because the definition of a correlated residual time series is not obvious.

A jackknife data resampling technique has the advantage of not requiring the estimation of a noise vector or time series, and these techniques have been proven to yield unbiased and robust error estimates for both linear and non-linear inversions [Efron, 1982; Wu, 1986; Tichelaar and Ruff, 1989]. Therefore, we have chosen this resampling method to estimate the stability and errors of our shear wave velocity model inversions. An example of this method applied to the receiver function inversion for station KEG is shown in Figure 10. The drawback of this technique is that it will not account for systematic errors in the data. Recently, *Gurrola and Baker* [1996] have suggested that such systematic errors exist within receiver function waveforms. This would then lead to systematic offsets in the estimated velocity models that would not be accounted for in either a bootstrap or jackknife resampling method. We have been able to test for effects of such systematic errors for stations where Moho depths have been measured using other geophysical techniques.

Wu [1986] derived an expression for the formal error utilizing a jackknife resampling scheme. We can write, after Wu [1986], the expression for the formal error:

$$\sigma^2_{jackknife} = \frac{k - p + 1}{n - k} \sum_i^N (\omega_i - \bar{\omega})^2 \quad (1)$$

where k is the total number of degrees of freedom (DOF) contained within the jackknife waveform stack, p is the number of model parameters (2 times the number of layers plus one), n is the total DOF summed over each of the receiver functions contained within the stack, ω_i is the estimated model parameter for each jackknife resampled waveform data set and $\bar{\omega}$ is the mean of the given model parameter (thickness or shear-velocity for a given layer). We have estimated the DOF contained within each receiver function using the method of *Silver and Chan* [1991] and *Jenkins and Watts* [1968]:

$$DOF \approx 2\left(\frac{2E^2}{E_4} - 1\right)$$

where

$$E \approx \sum_{j=1}^{N-1} |u^2(j)| + 1/2(|u_0|^2 + |u_N|^2) \quad (3)$$

$$E_4 \approx \sum_{j=1}^{N-1} |u^4(j)| + 1/3(|u_0|^4 + |u_N|^4) \quad (4)$$

where $u(j)$ is the band limited digital time series (i.e., the receiver function waveform). This approximation works well for this case since equation (1) is not very sensitive to the number of DOF because we are taking the ratio of the deleted DOF.

This technique gives an estimate of the receiver function stability, as long as there is a sufficient number of receiver functions that can create a “large” (≥ 50) number of resampled stacks. Note that equation (1) reduces to the calculation of the standard variance for the case where we delete all but one of our data vectors from our stacks. In order to test the robustness of this error estimator we tried a number of different resampling schemes (i.e., delete-1, delete-2, delete $n-1$, etc.) and compared the resulting error estimates. We found that for stations ANTO and KEG the variance of our estimators was about 20%. However, we found that if k is nearly as large as n and thereby causing the normalizing term to be very large, the error estimator is biased upward.

Results and Interpretations

In general, stations with relatively simple waveforms (i.e., simple PSMoho and its corresponding multiples) yield the best constrained results. However, complicated waveforms can also produce well resolved models if tighter constraints can be placed on the shallow structure. We used results from the jackknife error estimation to confirm this idea. We believe that this new grid search scheme provides a good mechanism in which to incorporate constraints from other independent geophysical/geologic measurements.

Crustal thickness in North and Central Africa is found to be generally on the order of 36 to 43 km (Figure 11), except for station ATD which is located on either exposed oceanic crust or very thin continental crust [Mohr, 1989] (Figure 11). We have found a Moho depth of 8.0 ± 1.5 km for station ATD. Our crustal shear-wave velocity model is in agreement with the prior geophysical studies that have found that this region blocks Lg waves [Searle, 1975] as well as having relatively low Pn velocities [Makris and Ginzburg, 1987]. Each of these observations is consistent with a thin and relatively slow crust and uppermost mantle.

In the stable African craton there are three stations at which we have been able to estimate crustal structure. Station TAM, near the Hoggar hot spot, yields the most stable inversion results where 90 jackknife receiver function inversions all resulted in crustal

thickness of 38 km (Figures 12 and 13). This indicates that, ignoring systematic errors, the variance of our estimate of crustal thickness is less than half of the thickness grid search spacing (1 to 2 km). Similar crustal velocities and thicknesses were found for station DBIC; however, we have considerably less data to constrain this model. Consequently, our jackknife error estimates are not as reliable since we were not able to create more than 15 jackknife receiver function stacks. We did find little variance between these 15 jackknife models. It is not surprising that the most reliable data were discovered for broadband stations in the African craton. This is a region where the 1-dimensional earth approximation is most valid. Data from three coastal stations in North and Central Africa (i.e., MBO, TBT, and MEB) contain evidence of very strong lateral heterogeneity and teleseismic P-wave multi-pathing as well as a large amount of noise in the computed receiver functions. At all three of these stations it was impossible to model the observed receiver function waveforms with a suitable one-dimensional shear-velocity model and hence we have not reported inversion results for these stations. In the case of TBT and MEB, the signal-to-noise ratio was very poor; however, at station MBO we had several high quality receiver function waveforms. It is possible that focusing of a PS phase at the sediment-basement contact, caused by 2- or 3-dimensional velocity structure, is causing the large amplitude PS phases that we observe at this station.

In Egypt, at station KEG, we have found a crustal thickness of 33 km. *Makris et al.* [1982] found crustal thicknesses on the order of 30 km (30 to 32 km) in northern Egypt, from refraction data, which are consistent with our analysis at station KEG. At station BGIO our estimates seem thicker (33 km) than many of those from seismic refraction work. *Yuval and Rotstein*, [1987] give crustal thicknesses of 31 km near BGIO and *Ginzburg et al.* [1982] estimated 29 to 30 km thick near BGIO. We may be seeing crustal thicknesses farther to the east, since all of the waveforms we have used are arriving from the east-northeast, where the crust appears to thicken [*Ginzburg and Folkman*, 1980]. Basement depths from stations BGIO and KEG are also surprisingly consistent with prior geophysical/geologic observations [*Makris*, 1982]. Jackknife error analyses indicated that these two sediment thicknesses are robust measurements. The error estimates for the sediment thicknesses are actually smaller than those for the depth to Moho errors. This is a good indication that the errors are propagating from the shallow layers to the deeper layers.

For other stations in North Africa we have found that the crust is usually on the order of 40 km thick. Only near the Moroccan Atlas Mountains, at station MDT, do we find a crustal thickness less than 40 km. In North Africa we have obtained a crustal thickness of 36 km on the eastern edge of the Middle Atlas Mountains, the Missouri Basin. This result is consistent with refraction experiments across the Middle Atlas [*Wigger et al.*, 1992] that also estimated a crustal thickness of 36 to 37 km beneath MDT.

In Spain, there are two broadband stations within 50 km of one another (stations TOL and PAB) which are both located within the Iberian Meseta. Inversion results from station PAB are fairly stable while results from TOL are very unstable (see Figures 12 and 13). The PAB and TOL optimal shear wave velocity models are relatively consistent in Moho depth (see Table 2). Most other features in each of the two stations' velocity models are

not consistent with one another; however, our error estimates indicate that these features cannot be reliably interpreted. Our poor waveform fits for station TOL also demonstrate that, within our grid search upper and lower bounds, there is no one-dimensional velocity model which fits the observed receiver function waveforms (Figure 14). Our waveform fits for station PAB (Figure 14) are far superior to those for TOL, which is also consistent with our jackknife error estimates (Figure 11). These error estimates, along with the waveform fits, demonstrate that the PAB velocity model is more reliable than the model for station TOL.

Table 2. Our best measurements of crustal thickness using our stacked receiver functions. The error has been calculated from the variance of the jackknife model parameters. The number of jackknife resampled data sets that are used are also given. Those stations with fewer than 50 jackknife iterations are statistically undersampled, therefore these error estimates are not as reliable.

Name	Latitude (degrees)	Longitude (degrees)	Crustal Thickness (km)	Jackknife Iterations
ATD	11.53	42.85	8.0 ± 1.5	165
ANTO	39.86	32.79	37.0 ± 1.3	90
BGIO	31.72	35.09	33.0 ± 3.3	10
BNG	4.44	18.55	43.0 ± 2.1	90
DBIC	6.68	-4.86	40.0 ± 2.3	6
GNI	40.05	44.72	64.0 ± 4.8	15
KEG	29.93	31.83	33.0 ± 4.1	84
KIV	43.96	42.69	43.0 ± 5.0	90
MDT	32.82	-4.61	36.0 ± 1.3	6
PAB	39.55	-4.35	34.0 ± 2.7	20
TAM	22.79	5.53	$38.0 \pm 0.0 (< 1.0 \text{ km})$	91
TOL	39.88	-4.05	34.0 ± 4.1	10

We have also found evidence of a pronounced mid-crustal low velocity zone in the Greater Caucasus, beneath station KIV (Figure 11). Although low velocity zones imaged using receiver functions must be viewed with a great deal of suspicion because of the potential for distortion of the waveform from the deconvolution, this observation appears to be very robust. First, we observe a very large amplitude, negative polarity PS phase, arriving 1.2 seconds after the P-wave. There is very little azimuthal variance of the large negative PS phase, indicating that this low-velocity zone is not a small isolated pocket of slow material. Also, our jackknife error estimates indicate that this is a robust feature

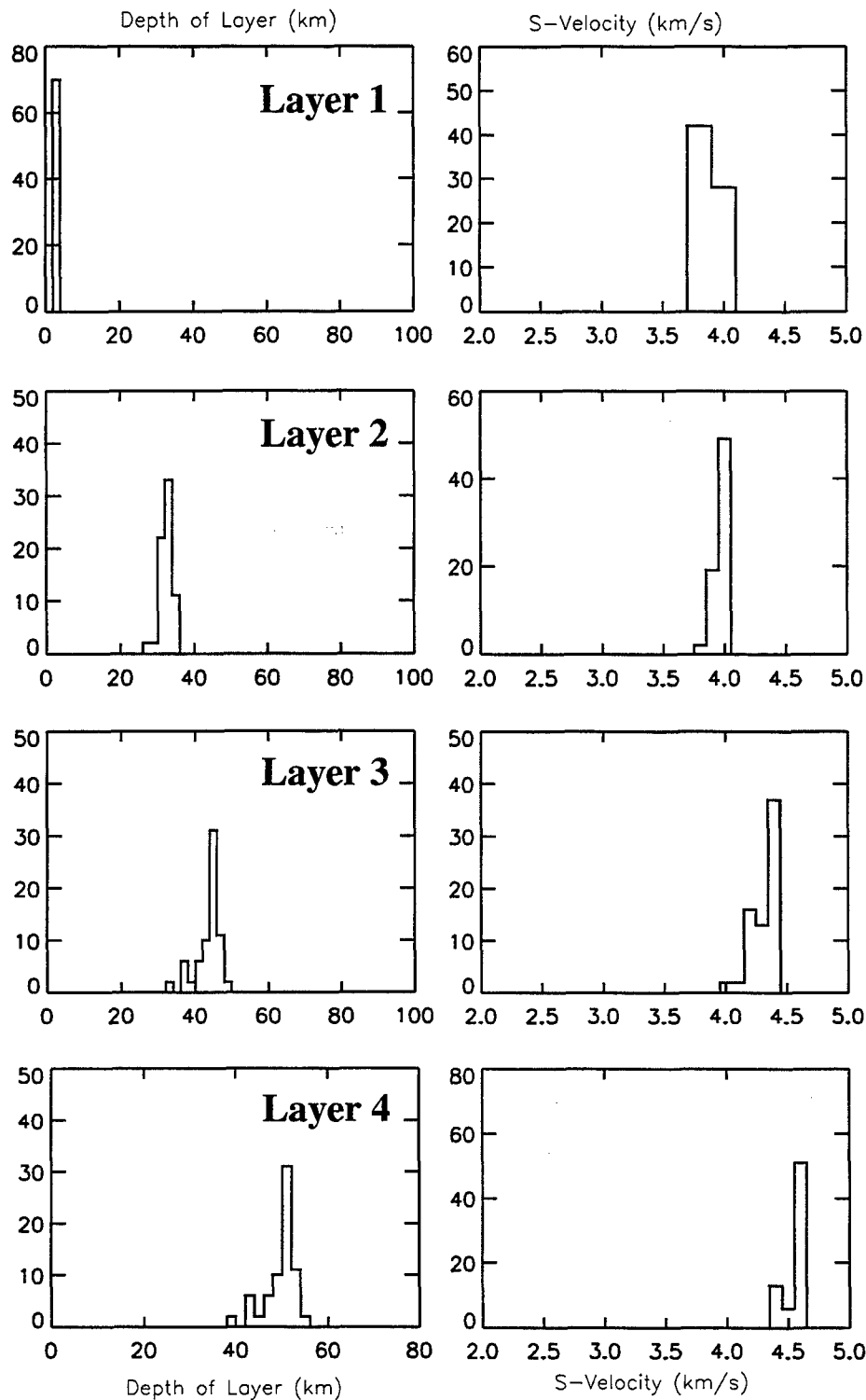


Figure 10. A set of histograms corresponding to 8 model parameters used in the KEG station grid search inversion. We obtained these histograms by inverting 121 jackknife receiver function stacks. We used a delete-3 jackknife resampling scheme to produce these receiver function stacks. The large variance in the data indicates either a strong azimuthal variation in the data or a relatively unstable inversion result (i.e., large variance in the data). We examined the data for evidence of azimuthal effects and found little evidence in our data.

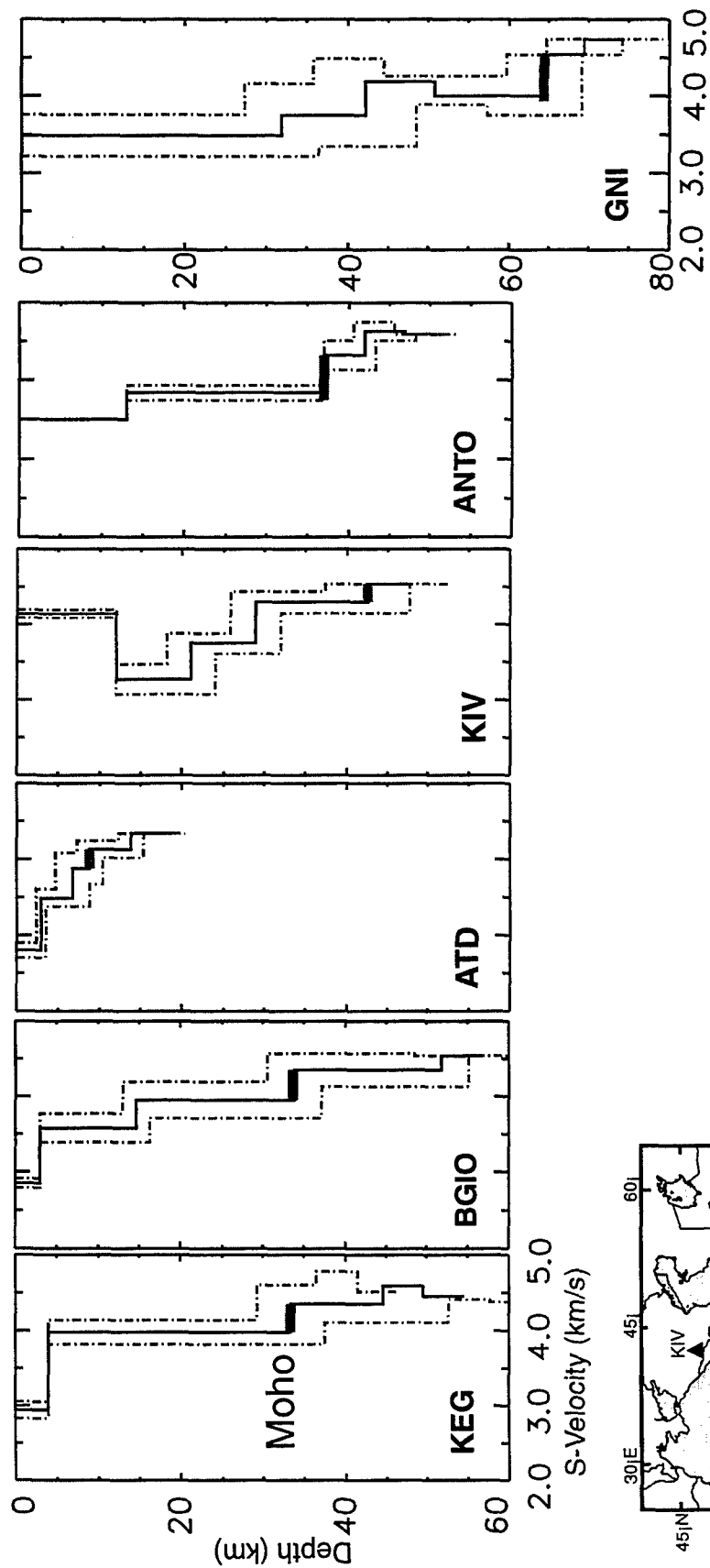
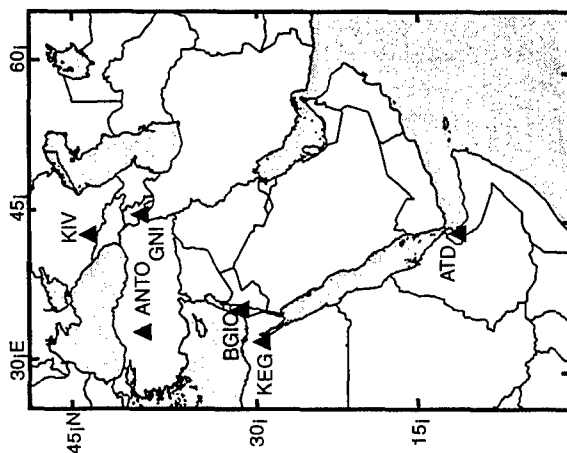


Figure 11. The final shear wave crustal velocity models and the location of the interpreted Moho for 12 stations in the Middle East (Figure 11a) and Africa (Figure 11b). Locations are shown of broadband stations from which sufficient data were available to compute a reasonably high quality stacked receiver function. Our interpreted Moho discontinuity is shown as a thick gray line on each model. The maximum and minimum models, obtained from the jackknife error estimations, are shown as dashed lines. Several models (e.g., models for stations KEG and BGIO) have larger velocity errors than layer thickness error estimates for shallow layers. This is a result of a coarser grid spacing for layer thickness than the velocity grid spacing. The receiver function synthetics are less sensitive to shear velocity than depth to the discontinuity for the shallow layers as well. This can also be seen in the slope of the minimum shown in Figure 7.



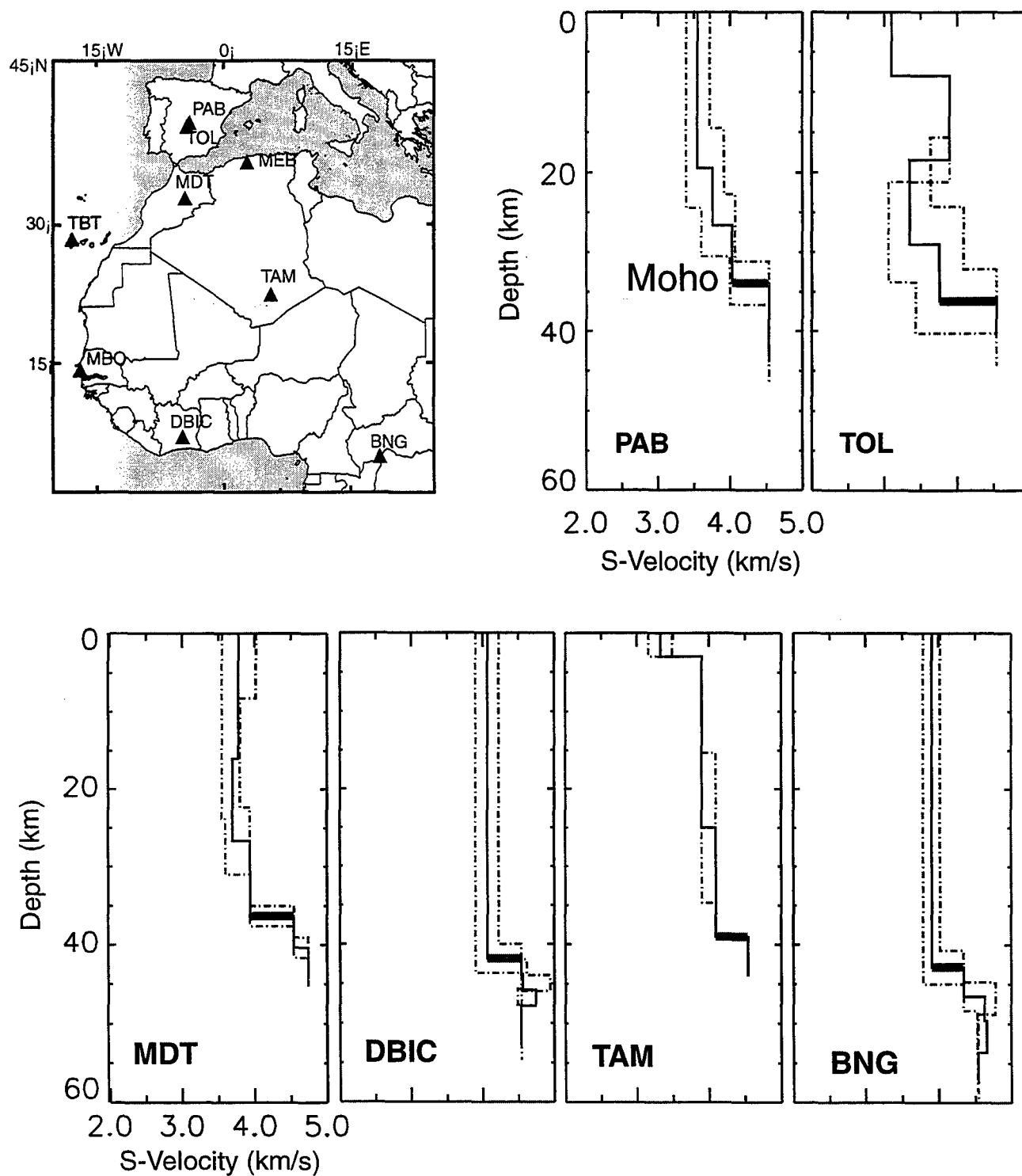


Figure 11b

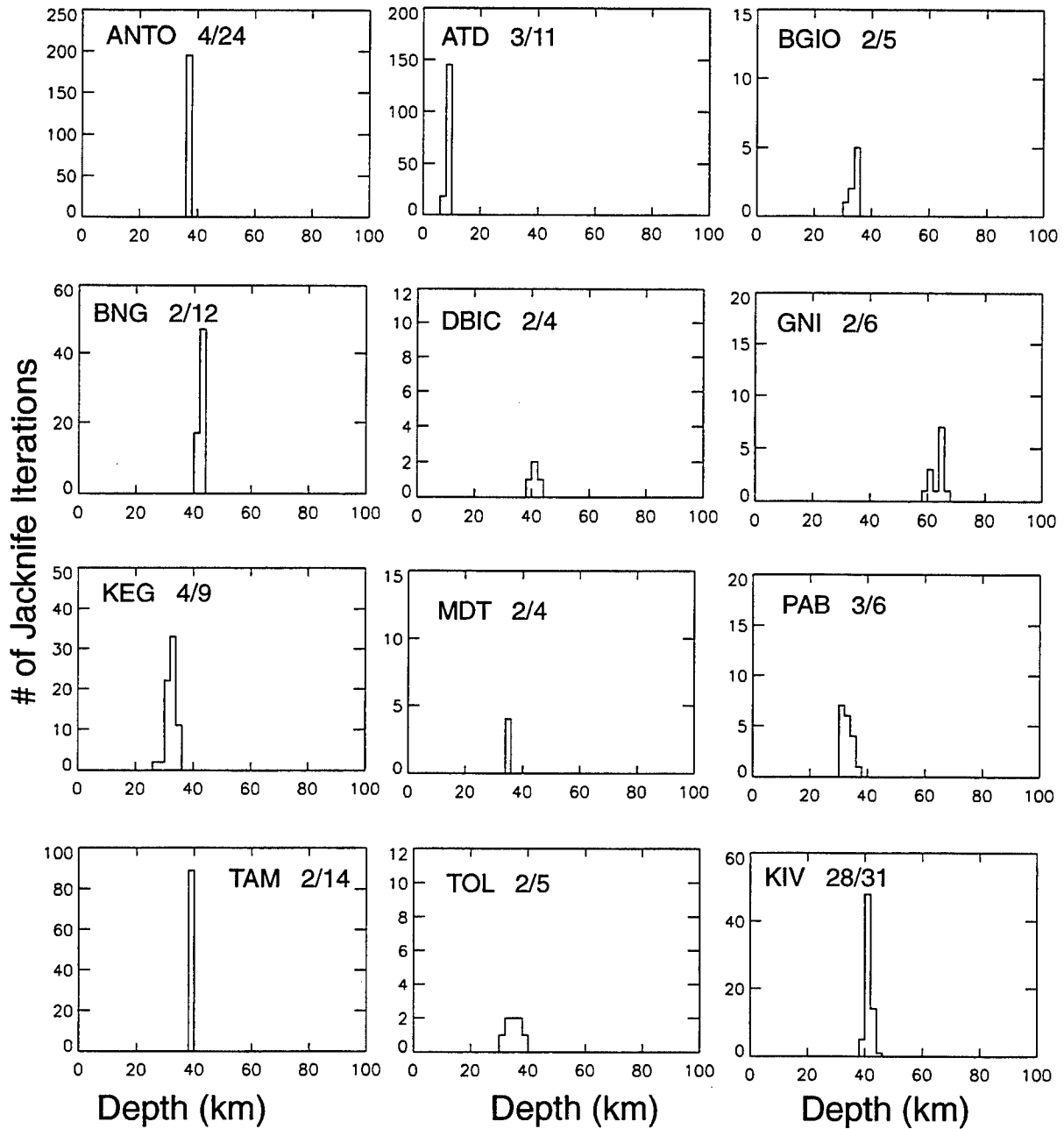


Figure 12. Jackknife histograms of the crustal thicknesses for all 12 stations analyzed in this study. We have determined the number of layers needed to fit the waveforms and then looked at the stability of the depth to the base of the lowest crustal layer using jackknife resampling to obtain each histogram shown. The two numbers to the right of the station name are the number of receiver functions deleted to create each jackknife stack and the total number of receiver functions added into the stack, respectively. Note the large variance in the total number of jackknifed data sets used. This is a function of the number of individual receiver function waveforms that were available to resample from.

(Figures 12 and 13). This is the only low velocity zone we have imaged, within our error estimates, out of the 12 stations we analyzed.

We observed two large, azimuthally coherent PS phases at station GNI (Figure 4b). The first phase corresponds to a discontinuity at approximately 40 km while the later phase corresponds to a 60 km discontinuity. Data at station GNI were observed to be of relatively low quality and contain a large amount of noise within the stacked receiver function. The jackknife error estimates also indicated a relatively unstable solution (Figures 11 and 14); therefore which shear wave velocity discontinuity corresponded to the Moho was not clear. Given the high topography, one might expect to observe a crustal root in this region, so we have interpreted the second boundary to be the Moho discontinuity. Receiver functions also contained a large amount of coherent and azimuthally dependent energy that appears on the tangential receiver functions. This may be an indication of a dipping Moho. It is also possible that crustal polarization anisotropy could be causing the PS_{Moho} phases to change polarization direction, thereby leading to the observed SH energy.

Within the center of the Anatolian block, analysis of receiver functions recorded at station ANTO yielded a relatively simple velocity model with a crustal thickness of 37 km. There have been very few reliable estimates of crustal thickness in this region; however, a crustal thickness of 37 km in this region is not unreasonable given that this region has a fairly stable continental crust.

Conclusions

Our study shows that the grid search waveform inversion provides a robust and efficient method for determining depth to first-order crustal discontinuities. Using this method, we have inverted for optimal and most simple shear-wave velocity models as well as corresponding error estimates in the Middle East and Africa (Figure 15) where no prior results exist. The method presented here has several advantages over prior receiver function techniques: (1) The grid search inversion has no dependence on an initial model, (2) the grid search inversion guarantees that we will solve for the global minimum within the chosen parameters limits, (3) the jackknife error estimation gives a measure of the stability of the inversion and finally, (4) these methods allow for constraints from other independent studies (e.g., on shear wave velocity or depth to a discontinuity) to further add to the robustness of our results. The crustal thickness measurements we have made using these methods provide important constraints for future studies of the geodynamic and tectonic processes taking place in the Middle East and Africa.

In western and central Africa we have found that the crust is consistently about 40 km thick. We have found slightly thicker crust at station BNG, in central Africa. We have also determined that the crust appears fairly thick (~40 km) very close to the African coast at station DBIC. Station ATD, located in the Afar region of eastern Africa, is the exception to these observations. Velocity models for this station indicate that Djibouti is situated on either oceanic or very stretched continental crust. This is consistent with previous tectonic and geologic observations in the Afar [e.g., *Mohr, 1989*].

In the northern portion of the Middle East, our velocity models vary widely from very thick crust to approximately the global average crustal thickness. In the Lesser Caucasus beneath station GNI, we have found somewhat ambiguous evidence for a large crustal root, although this model has a very large uncertainty (± 4.5 km) associated with the depth to Moho. This is an indication that the Lesser Caucasus are isostatically supported. In the Greater Caucasus, near station KIV, there is a relatively young volcano, which erupted around 2.8 Ma [Gizas *et al.*, 1991], and associated calc-alkaline lava [Zonenshain *et al.*, 1990]. This may imply the existence of a partially molten or highly-heated mid-crustal pluton related to recent subduction in the Greater Caucasus. The existence of a high heat flow anomaly in the Greater Caucasus [Cermak and Rybach, 1987] and the very large velocity contrast at this boundary (Figure 11a) are consistent with the existence of a magma chamber. Alternatively, a large nappe root is thought to underlie the Greater Caucasus; the top of this root, at the contact of the pre-Jurassic basement and the Jurassic slates and shales would produce a negative impedance contrast. Studies of the structural geology in the Greater Caucasus have indicated that the nappe root may extend to 15 km, the depth of the discontinuity that we have imaged [Dotduyev, 1986]. Furthermore, independent observations of this nappe structure have been observed in the Greater Caucasus by both geologic and geophysical studies [Tagiyev, 1985; Sholpo, 1993].

Near the Dead Sea fault, at station BGIO, we have not found convincing evidence of any crustal thinning. However, we do observe a fairly large variance (± 4 km) for this receiver function inversion model. The BGIO and KEG shear-velocity models are consistent with the refraction models in the region [Ginzburg *et al.*, 1981; Makris *et al.*, 1982; Yuval and Rotstein, 1987]. It is surprising that even our inversion results that are not very stable (i.e., models for stations BGIO and KEG) agree well with other independent estimates of crustal structure. All prior estimates of crustal thickness in this region fall well within our jackknife error estimates, implying that systematic noise does not have a large effect in these stations' inversion results. This is a good indication that basement depths can in many cases be resolved from receiver function inversions. There is a trade-off in resolution between the measurement of basement thickness and measurement of crustal thickness. Receiver function with large PS_{basement} phases tend to have distorted and less coherent PS_{Moho} phases. We have also found, using our jackknife error analysis, a tendency of the errors in depth-to-basement to propagate to the depth to Moho measurements.

Our crustal structure measurements in the Middle Atlas, at station MDT, are important confirmation of prior work which has indicated that there is not a significant crustal root beneath the Middle or High Atlas mountains. Station MDT is only in the vicinity of these two mountain ranges, but Wigger *et al.* [1992] profiles cross these two mountain ranges as well as coming to within 10 km of station MDT. The receiver function model agrees very well with Wigger *et al.* velocity models beneath the Missouri basin, on the flanks of the Middle and High Atlas. Therefore, this is circumstantial evidence that Wigger's *et al.* image of a flat Moho beneath the Middle Atlas is correct. Beneath station TAM, located near the Hoggar hot spot, we have observed very well constrained crustal thicknesses that are not significantly thinner than the crustal thickness measurements we

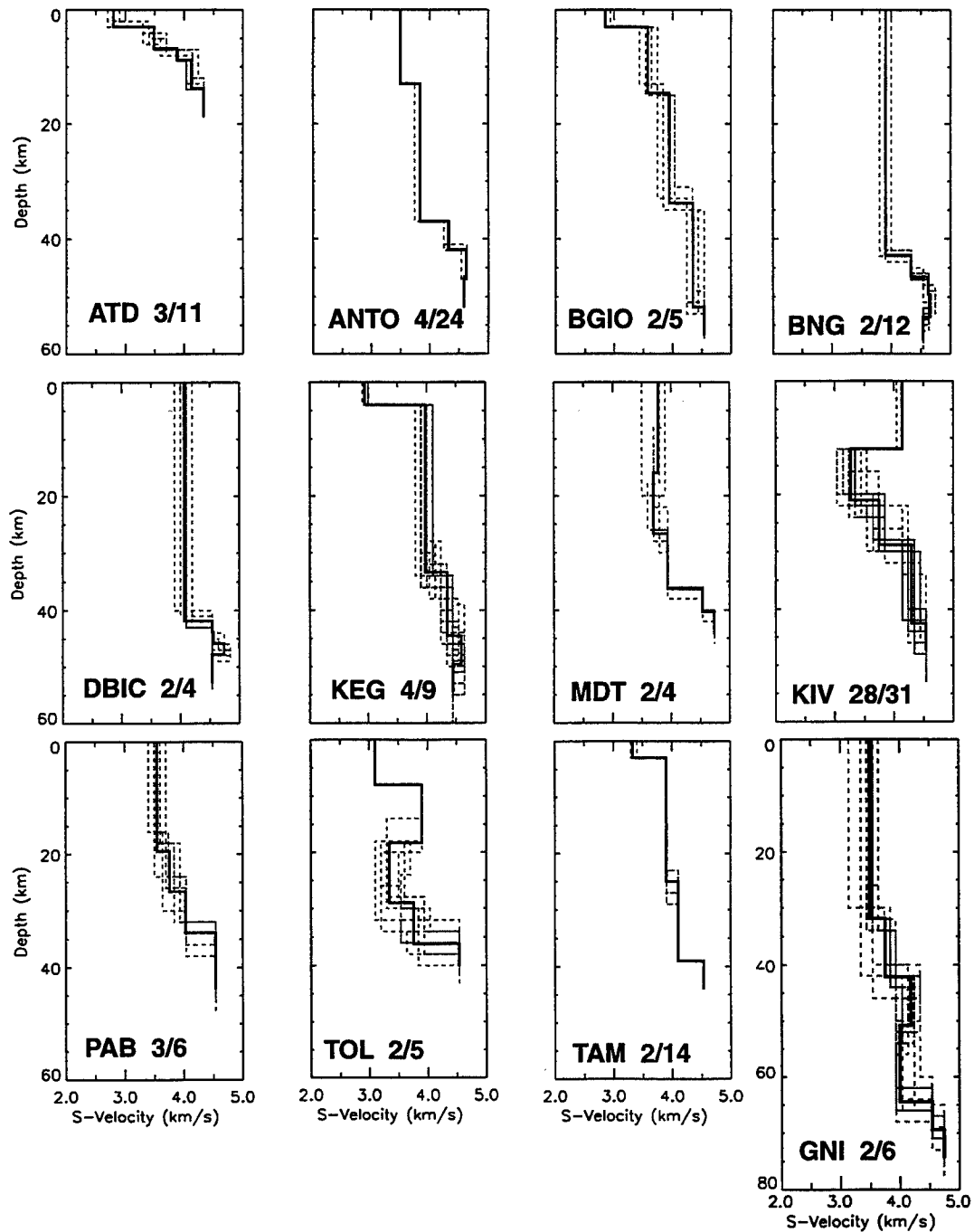


Figure 13. Jackknife shear velocity models for all 12 stations used in this study. These velocity models correspond to models obtained from the resampled receiver function stacks (shown as dashed gray lines). The solid line indicates the mean model. The two numbers to the right of the station name are the number of receiver functions deleted to create each jackknife stack and the total number of receiver functions added into the stack, respectively. The variance of the jackknife shear wave velocity models indicate how stable each receiver function inversion is.

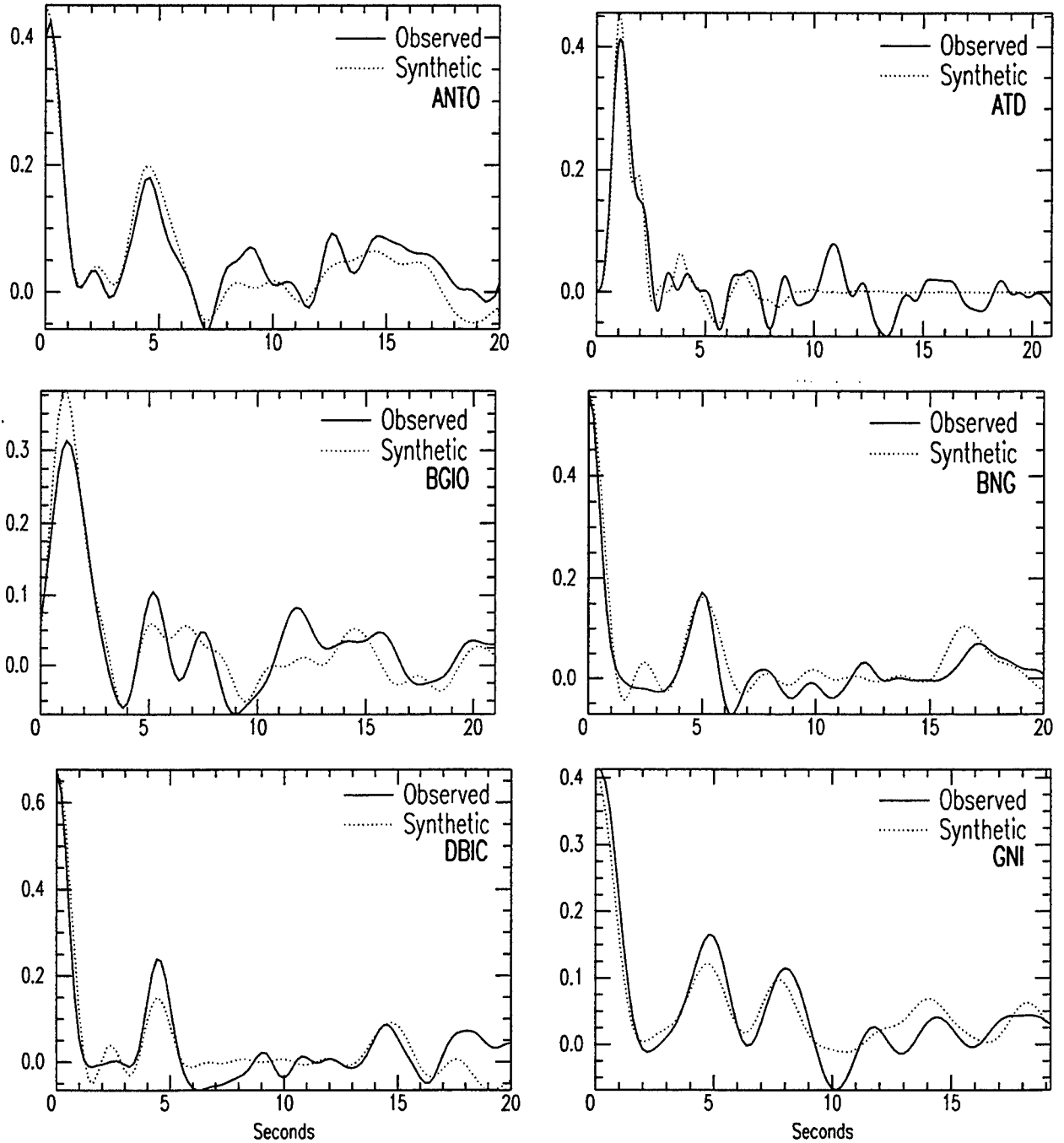


Figure 14. The resulting waveform fits from the 12 receiver function inversions we have performed. The dark-dashed lines are the synthetics while the light-solid lines are the observed stacked receiver function waveforms. We are able to obtain relatively good fits between the observed and synthetic receiver functions when using models with four or fewer layers in the grid search inversions.

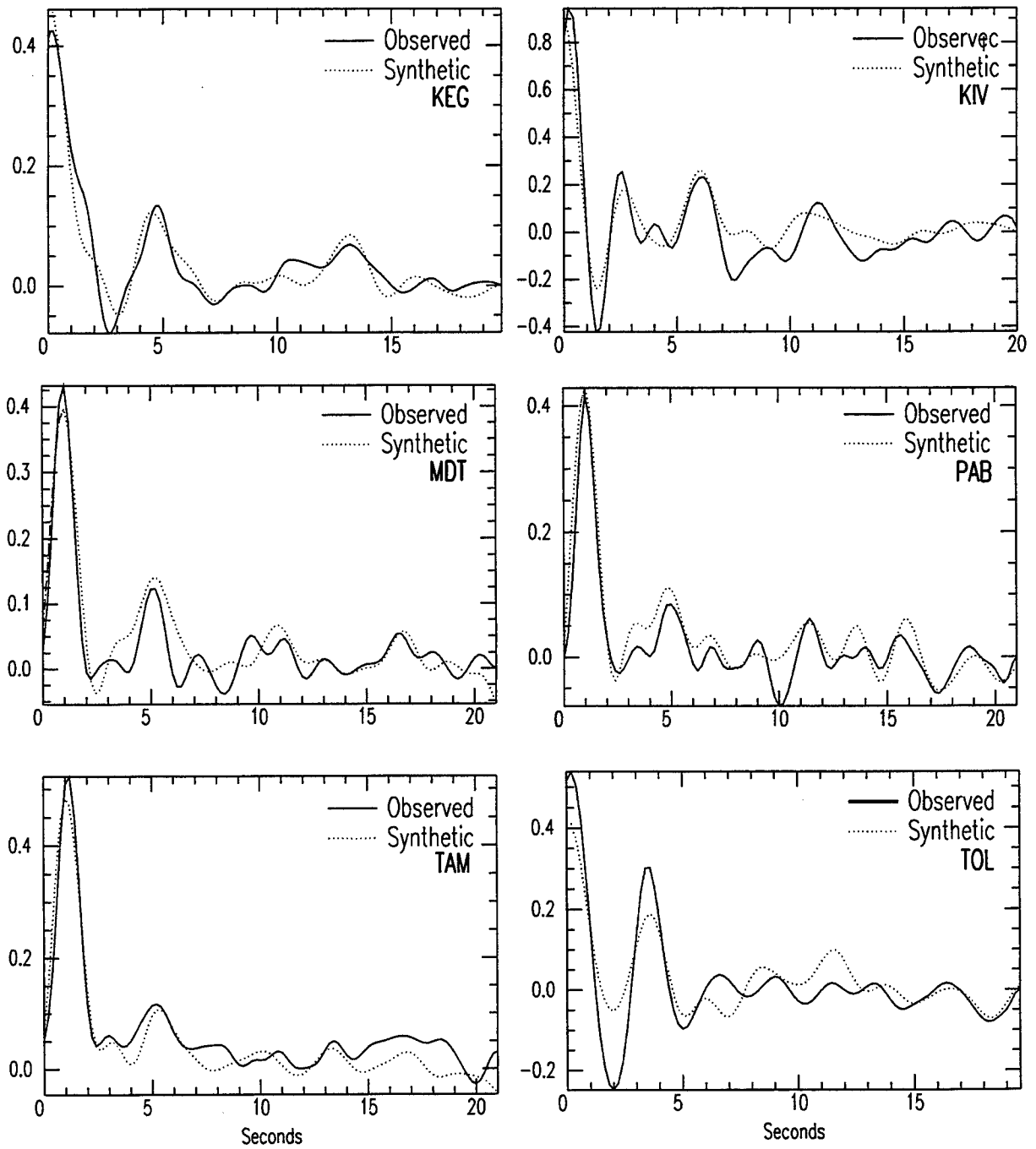


Figure 14b.

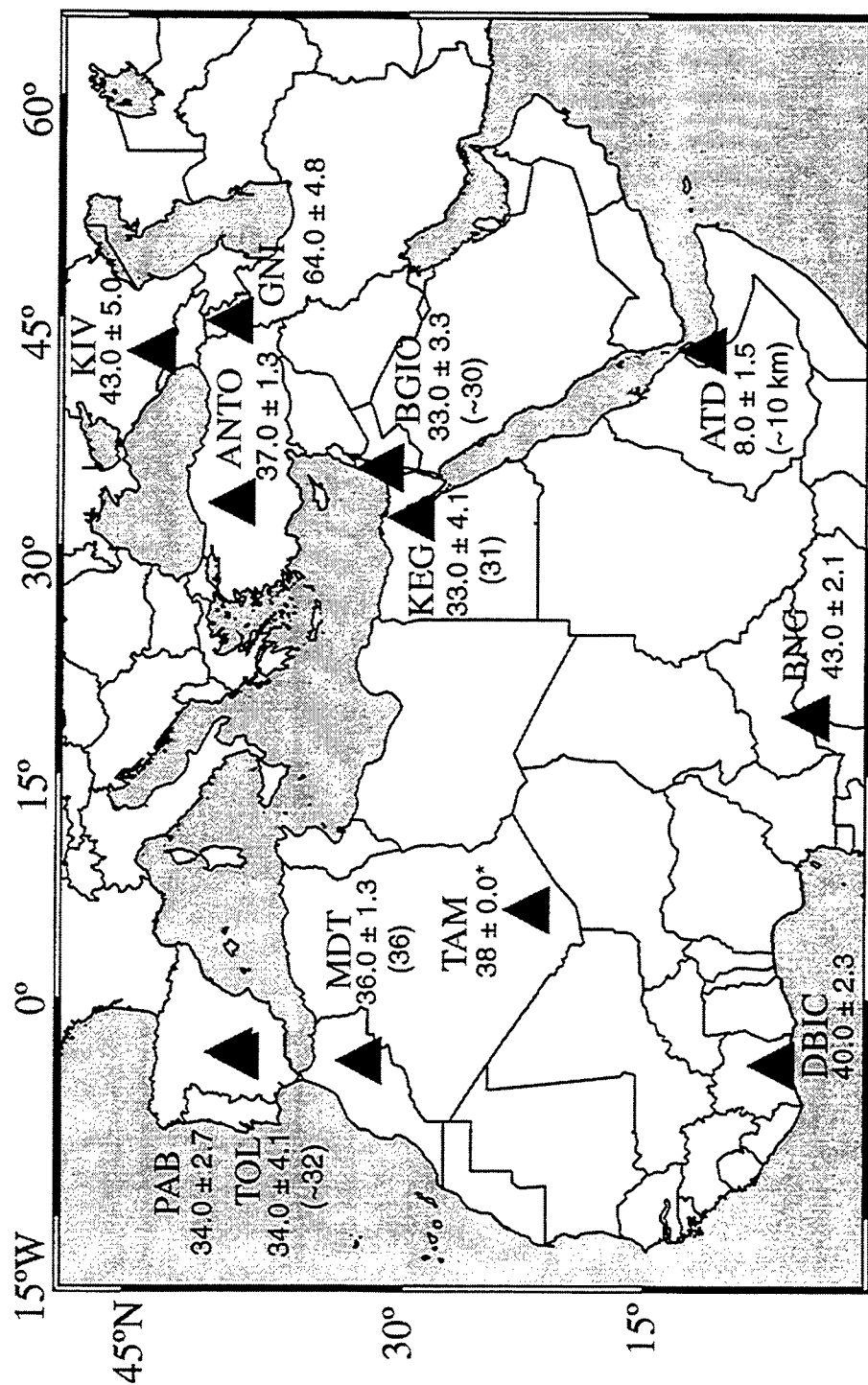


Figure 15. A map showing the grid search and prior, if available, estimates of crustal thickness, and jackknife error estimates in the Middle East and Africa. In all cases that we have examined, the grid search inversion crustal thicknesses agree, within the jackknife error estimates, with previous studies' estimates.

have made in the other regions of the African craton (stations BNG and DBIC). This is an indication that the mantle plume beneath TAM has not significantly altered the crustal structure. Stations BNG, DBIC, and TAM are separated by approximately 500 km, yet receiver function velocity models for these are all consistent with one another. Each of these stations has a fairly simple crust, with no evidence of major velocity discontinuities within the crust. These models also all have approximately 40 km thick crust. This may be an indication that the African craton is fairly uniform in crustal thickness and structure. However, since the data in the African craton is highly spatially aliased (3 stations) we cannot make any firm conclusions concerning crustal structure throughout this region.

The grid search inversion scheme presented in this paper is a general and systematic method for determining first-order crustal seismic velocity features from receiver function waveforms. Furthermore, the jackknife error estimation is a new method that, when combined with the grid search inversion scheme, will yield relatively unbiased estimation of waveform inversion stability. Owing to noise sensitivity of most waveform inversions, stability estimation is essential in determining the reliability of the final models. The jackknife resampling method offers a relatively unbiased and robust estimate of the stability when enough data are available to construct 50 or more jackknifed resampled data sets. Our estimations of variance appear consistent with qualitative observations of data quality and azimuthal variance. When sufficient data are present the jackknife algorithm can be used to estimate uncertainty as a function of azimuth. In summary, we have demonstrated that the grid search inversion method along with the jackknife stability test yield reliable one-dimensional large scale, first order crustal structure. The grid search method is the only way to guarantee an optimal and simple solution for the receiver function waveform inversion. We have found significant differences in models obtained from the grid search and the linearized least squares method for station KEG and BGIO. This observation argues that there are instances when it is important to use a more general approach for inverting receiver function waveforms for crustal shear wave velocity structure.

Acknowledgments: We thank the people who run the IRIS, MEDNET, GEOSCOPE, and GEOFON broadband networks for providing us with the high quality broadband data required for this study. We also thank Tom Hearn (New Mexico State University), Ali Hadi (Cornell University) and Eli Baker (Maxwell Technologies) for very useful discussions on inversion and error estimation procedures. We especially thank Jim Ni (New Mexico State University) for his help and the additional use of his computer resources. This research was sponsored and supported by the US Department of Energy Contract F19628-95-C-0092, issued by Phillips Laboratory.

References

Ammon, C. J., Randall, G.E., and Zandt, G., On the nonuniqueness of receiver function inversion, *J. Geophys. Res.*, **95**, 15,303-15,318, 1990.

- Baker, G.E., Minster, J.B., Zandt, G., and Gurrola, H., Constraints on crustal structure and complex Moho topography beneath Pinon Flat, California from teleseismic receiver functions, *Bull Seism. Soc. Am.*, in press, 1997.
- Bates, D.M. and D.G. Watts, *Nonlinear Regression Analysis and Its Applications*, John Wiley, New York, 1988.
- Burdick, L.J., and Langston, C.J., Modeling crustal structure through the use of converted phases in teleseismic body-wave forms, *Bull. Seism. Soc. Am.*, **67**, 677-691, 1977.
- Cermak, V. and Rybach, L., *Terrestrial Heat Flow and the Lithosphere*, Springer Verlag, New York, 1987.
- Dotduyev, S.I., The nappe structure of the Great Caucasus (in Russian), *Geotektonika*, **5**, 94-105, 1986.
- Efron, B., *The Jackknife, Bootstrap, and Other Resampling Plans*, Society of Industrial and Applied Mechanics Review, Philadelphia, 1982.
- Gazis, C., Lanphere, M., Taylor, H., and Gurbanov, A., $^{40}\text{Ar}/^{39}\text{Ar}$ and $^{18}\text{O}/^{16}\text{O}$ studies of the Chegem ash-flow caldera and the Eldjurt granite: Cooling of two late Pliocene igneous bodies in the Greater Caucasus Mountains, Russia, *Earth Planet. Sci. Lett.*, **134**, 377-391, 1995.
- Ginzburg, A. and Folkman, Y., The crustal structure between the Dead Sea Rift and the Mediterranean Sea, *Earth Planet. Sci. Lett.*, **51**, 181-188, 1980.
- Ginzburg, A., Makris, J., Fuchs, K., and Prodehl, C., The structure of the crust and upper mantle in the Dead Sea Rift, *Tectonophysics*, **80**, 109-119, 1981.
- Gurrola, H., Baker, E., and Minster, B., Resolution of Receiver Function waveforms and resulting limitations in the modeling of earth structure, *EOS, Transactions, AGU*, **77**, 460, 1996.
- Kennett, B., *Seismic Wave Propagation in Stratified Media*, Cambridge University Press, London England, 1984.
- Langston, C.A., The effect of planar dipping structure on source and receiver responses for constant ray parameter, *Bull. Seism. Soc. Am.*, **67**, 1,029-1,050, 1977.
- Langston, C.A., Structure under Mount Rainier, Washington inferred from teleseismic body waves, *J. Geophys. Res.*, **84**, 4749-4762, 1979.
- Makris, J. and Ginzburg, A., The Afar depression: transition between continental rifting and sea-floor spreading, *Tectonophysics*, **141**, 199-241, 1987.
- Marzouk, I.A., Study of crustal structure of Egypt deduced from deep seismic and gravity data, Ph.D. Thesis, University of Hamburg, 1988.
- Mohr, P., Nature of the crust under Afar: New igneous, not thinned continental, *Tectonophysics*, **46**, 369-406, 1989.
- Owens, T.J., Crosson, R.S., and M.A. Hendrickson, Constraints on the subduction geometry beneath western Washington from broadband teleseismic waveform modeling, *Bull. Seism. Soc. Am.*, **78**, 1219-1234, 1988.
- Paulssen, H. and J. Visser, The crustal structure in Iberia from P-wave coda, *Tectonophysics*, **221**, 111-123, 1993.
- Phinney, R.A., Structure of the Earth's crust from spectral behavior of long-period body waves, *J. Geophys. Res.*, **69**, 2997-3017, 1964.
- Sandvol, E. A., and Hearn, T., Bootstrapping shear wave splitting errors, *Bull. Seism. Soc. Am.*, **84**, 1971-1977, 1994.

- Searle, R.C., The dispersion of surface waves across the Afar. In: A. Pilgerand and A. Roesler (Editors), Afar Depression of Ethiopia. Schweizerbart, Stuttgart, 113-120, 1975.
- Sheehan, A., Abers, G., Jones, C.H., and Lerner-Lam, A., Crustal thickness variations across the Rocky Mountain front from teleseismic receiver functions, *J. Geophys Res.*, **100**, 20,391-20,404, 1995.
- Sholpo, V.N., Structure of inversion anticlinoria in the core of the Greater Caucasus; an advection hypothesis, *Geotectonics*, **27**, 245-251, 1993.
- Silver, P. and W. Chan, Shear wave splitting and mantle deformation, *J. Geophys Res.*, **96**, 16,429-16,454, 1991.
- Tagiyev, R.E., New data on the structure of the Kura Basin and the southeasterly plunge of the Greater Caucasus, *Geotectonics*, **18**, 444-447, 1985.
- Tichelaar, B., and Ruff, L., How good are our best models? jackknifing, bootstrapping, and earthquake depth, *EOS, Transactions, AGU*, **70**, 605-606, 1989.
- Wigger, P., Asch, G., Giese, P., Heinsohn, W.D., El Alami, S.O., and Ramdani, F., Crustal structure along a traverse across the Middle and High Atlas mountains derived from seismic refraction studies, *Geologische Rundschau*, **81**, 237-248, 1992.
- Wu, C.J.F., Jackknife, bootstrap and other resampling methods in regression analysis, *Annal. Stat.*, **14**, 1261-1295, 1986.
- Yuval, Z., and Rotstein, Y., Deep crustal reflection survey in central Israel, *Journal of Geodynamics*, **8**, 17-31, 1987.
- Zandt, G. and Ammon, C., Continental crust composition constrained by measurements of crustal poisson's ratio, *Nature*, **374**, 152-155, 1995.
- Zhao, L., and Frohlich, C., Teleseismic body-waveforms and receiver structures beneath seismic stations, *Geophys. J. Int.*, **146**, 355-370, 1995.
- Zonenshain, L.P., Kuzmin, M.I., and Natapov, L.M., Geology of the USSR: A plate tectonic synthesis, *Geodynamic Series*, American Geophysical Union, Washington D.C., **21**, p.171-175, 1990.

B. LITHOSPHERIC VELOCITY DISCONTINUITIES BENEATH THE ARABIAN SHIELD

Abstract.

We have determined lithospheric mantle and crustal velocity structure beneath the Arabian Shield through the modeling of teleseismic P waves recorded by the 9 station temporary broadband array in western Saudi Arabia. The receiver function deconvolution technique was used to isolate the receiver-side PS mode conversions. A grid search method, which should yield an unbiased global minimum, was used to solve for both optimal and simplest multi-layered shear-wave velocity models. Results from this analysis show that the crustal thickness in the Shield area varies from 35 to 40 km in the west, adjacent to the Red Sea, to 45 km in central Arabia. Stability tests of each inversion indicate that the models are relatively well constrained. We have also observed evidence for a large positive velocity contrast at sub-Moho depths at four stations at depths of 80 to 100 km. This discontinuity may represent a change in rheology in the lower part of the lithosphere or remnant structure from the formation of the Arabian Shield.

Introduction

Saudi Arabia consists primarily of a continental Shield and is bounded by young rifting and sea floor spreading to the west and the Zagros fold and thrust belt system to the east. The Arabian Shield is comprised of a series of accreted Proterozoic island arc terranes which were possibly formed during several subduction episodes [Greenwood *et al.*, 1980]. The northern and eastern portions of the Arabian Shield include the Afif terrane which is composed of granites (640-580 Ma), volcanic rocks, and meta-sediments (660-600 Ma) which overlie a crystalline basement [Husseini, 1988]. The volcanic fields in particular are very young; 21 eruptions are known to have occurred in the last 1500 years [Camp *et al.*, 1987]. On the western margin of Saudi Arabia, geophysical studies indicate that the Red Sea is an active spreading center [Cochran *et al.*, 1991]. To the east the Shield is bounded by the Mesozoic sedimentary rocks of the Arabian Platform which dip gently eastward and overlap the Shield unconformably [Powers *et al.*, 1966].

There have been a number of geophysical studies of the crustal and upper mantle structure of the Arabian Shield [e.g., Niazi, 1968; Mooney *et al.*, 1985; Mechie *et al.*, 1986; Ghalib, 1992; Mohktar, 1995]. In particular, a large reversed refraction profile was shot in 1978 across the Saudi Arabian Shield [Mooney *et al.*, 1985]. The profile location is shown in Figure 1. Crustal thickness was found to increase gradually toward the center of the Saudi Arabian Platform and thin very rapidly near the coast of the Red Sea. Sub-Moho velocity discontinuities were also found beneath the Moho at approximately 60 to 70 km depth [Mooney *et al.*, 1985]. Studies of surface wave dispersion and attenuation beneath the Arabian Peninsula found an average crustal thickness of approximately 45 km in the eastern part of Arabia and high attenuation ($Q=60$ to 150) beneath all of the Arabian Platform [Seber and Mitchell, 1992; Mohktar, 1995]. Badri [1991] found very high attenuation in the upper crust of the Arabian platform ($Q_p=165$) and very low in parts of the Arabian Shield upper crust ($Q_p=1560$).

Data and Inversion Method

From November 1995 to March 1997, nine temporary broadband three-component stations were deployed across the Saudi Arabian Shield (Figure 1). These stations consisted of STS-2 seismometers recorded at 40 sps on a REFTEK data acquisition system. All nine station sites proved to be exceptionally quiet and recorded very high quality data that we used to create receiver function stacks from a minimum of six receiver function waveforms (Table 1). Station BISH, however, recorded very little data before being damaged early in the experiment. We used the spectral deconvolution method to create the receiver function stacks. The majority of earthquakes that were used to create our receiver function stacks were located to the northeast of our stations. Therefore the teleseismic P-waves are sampling crustal and mantle structure just to the northeast of each of the stations used in this study. The time domain receiver function method was used to test for possible waveform distortion from the spectral division technique. We found very little difference between the spectral division technique and the time-domain deconvolution.

A grid search technique was used to invert the receiver function stacks for the shear-wave velocity structure. In order to invert the observed receiver function stacks for the crustal shear wave velocity structure, we applied a two-iteration grid search method combined with a jackknife error estimation technique [Sandvol *et al.*, submitted 1998]. A reflectivity synthetic seismogram algorithm, initially developed by Kennett [1984], was used to create our synthetic receiver functions. To invert the receiver function data we employed a grid search scheme using a maximum of six layers in our model. It should be noted that the half-space (upper mantle shear wave velocity) is constrained only by the amplitude of the direct P wave and the amplitude of the PSMoho phase; hence it is somewhat unreliable. We used results from surface wave studies [Seber and Mitchell, 1992; Mohktar, 1995] to provide constraints on the upper mantle velocities beneath the Arabian Shield. The search interval was chosen to be 0.1 km/sec for the shear wave

Table 1. Best measurements of crustal thickness using the stacked receiver functions. The error has been calculated from the variance of the jackknife model parameters. The number of jackknife resampled data sets used is also given. Stations with fewer than 50 jackknife iterations are statistically undersampled therefore those error estimates are not as reliable and are indicated by asterisks.

Station Name	Latitude (degrees)	Longitude (degrees)	Crustal Thickness (km)	# of events in stack	Jackknife Iterations
SODA	18.29	42.37	38.0 ± 1.0	12	67
TAIF	21.28	40.34	$40.5 \pm 2.5^*$	6	20
RANI	21.31	42.77	$35.0 \pm 2.5^*$	7	35
HALM	22.84	44.31	40.0 ± 1.0	21	100
AFIF	23.93	43.04	39.0 ± 1.0	18	90
RAYN	23.52	45.50	$44.0 \pm 2.5^*$	6	20
RIYD	24.72	46.64	45.0 ± 2.0	10	50
UQSK	25.79	42.36	37.0 ± 1.5	12	70

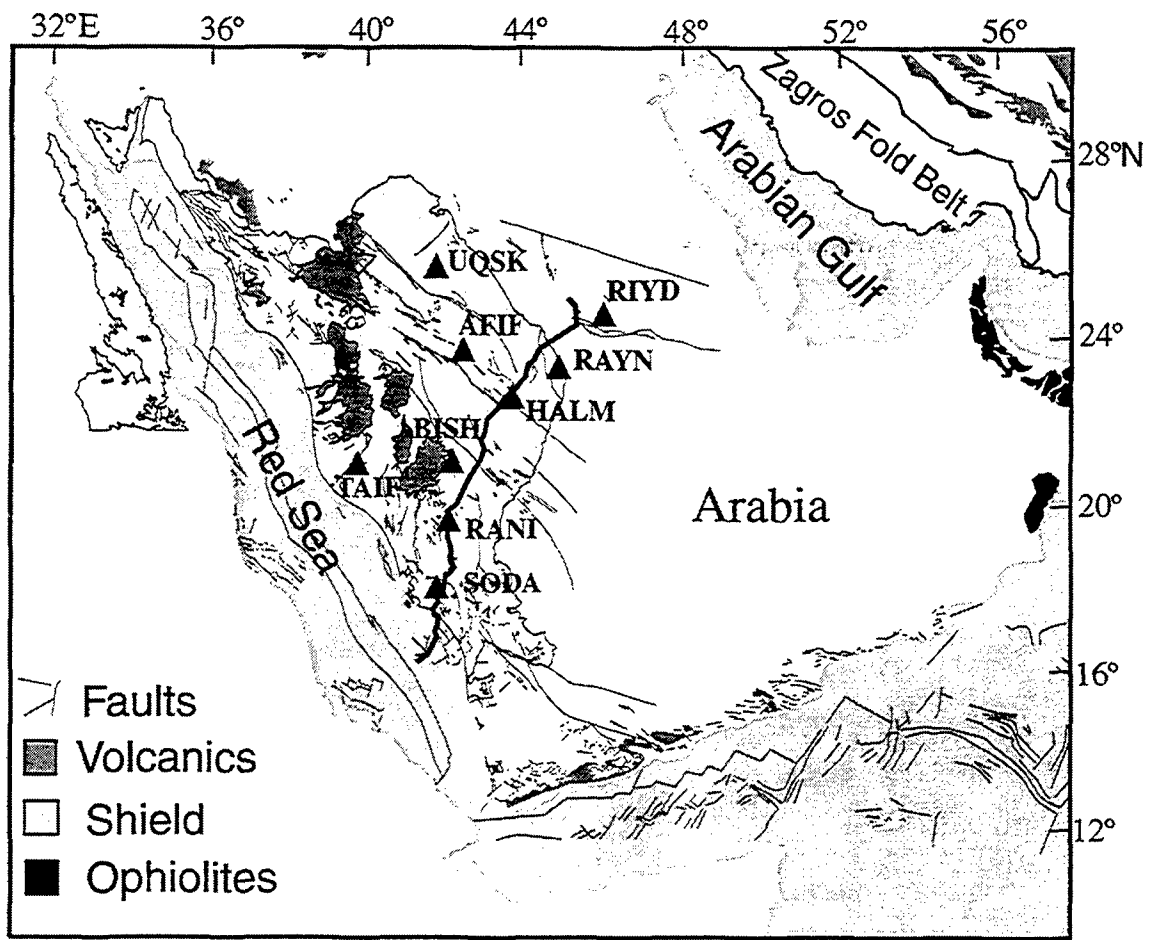


Figure 1. Simplified tectonic map of the Arabian peninsula. Also shown are all of the broadband stations (solid triangles) as well as the 1978 refraction profile line. Station BISH is the only station which has not been used in our study due to a lack of data.

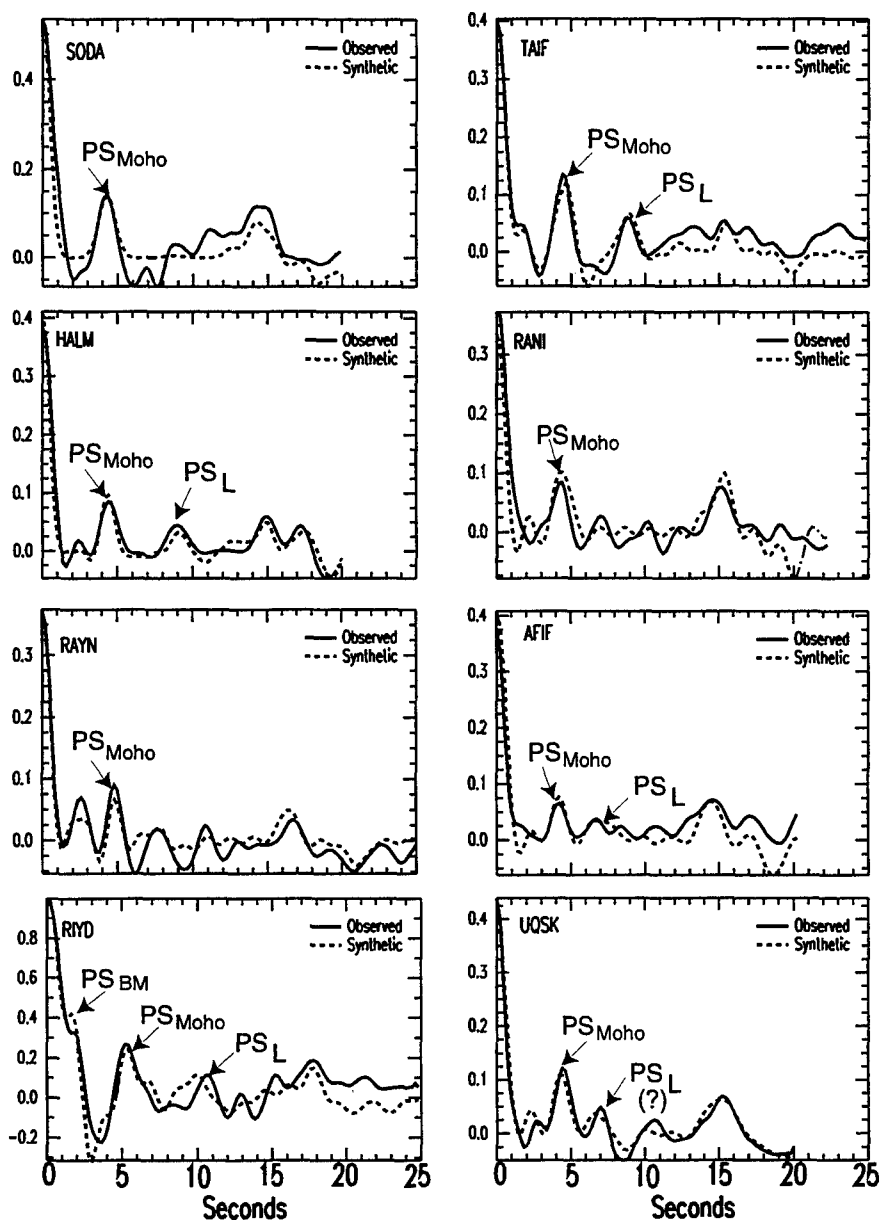


Figure 2. Stacked and optimal synthetic receiver function comparisons for all eight stations used in this study. Using at most a three-layer crust to model these waveforms we have obtained reasonably good fit for all eight stations. At station RANI we also allowed the Poisson's ratio to vary along with the shear-velocity and layer thickness in order to obtain a good fit. Also identified are the P-to-S (PS) conversion at the basement (PSBM), Moho (PSMoho), and a mantle velocity discontinuity (PSL). In addition to these phases we have also fit the absolute amplitudes of the receiver functions, except for station RIYD. At station RIYD an error occurred with the gain of the vertical component, therefore we have normalized this receiver function.

velocity and 2 km for layer thickness and in some cases 1 km for the first layer (Table 1). After obtaining the results from our grid search we qualitatively analyzed each layer as to whether or not the layer contributed a significant amount of energy to the synthetic. We performed this exercise for all 9 stations. The limited number of model parameters in the waveform inversion has allowed us also to employ either a bootstrap or a jackknife resampling error estimation scheme.

A jackknife data resampling technique has the advantage of not requiring the estimation of a noise vector or time series, and these techniques have been proven to yield unbiased and robust error estimates for non-linear inversions [Efron, 1982; Tichelaar and Ruff, 1989]. Therefore, we have chosen this resampling method to estimate the stability of our shear wave velocity model inversions. The drawback of this technique is that it will not measure errors in our velocity models caused by systematic errors in the data. We have been able to test for effects of such systematic errors for stations where Moho depths have been measured using other geophysical studies.

This technique gives a reliable estimate of the receiver function stability, as long as there is a sufficient number of receiver functions that can create a "large" (≥ 50) number of resampled stacks. In order to test the robustness of this error estimator we tried a number of different re-sampling schemes (i.e., delete-1, delete n-1, etc.) and compared the resulting error estimates. We have found that our error estimates vary by no more than 20% depending upon which resampling method one uses. We use the largest error estimates from the different jackknife resampling schemes.

Results

We have found crustal thicknesses on the order of 40 km throughout the Arabian Shield. There are however, some slight variations (± 5 km). Near the southern Arabian coast the crust appears thinner at stations SODA and RANI, where we have found good waveform matches for crustal thicknesses of 38 and 35 km, respectively (Figure 2). Results from stations SODA and TAIF indicate that the crust appears to gradually thicken northward (Figure 3). This is consistent with the observation that the Red Sea rift is opening progressively faster towards the south. Also, the 40 km Moho depth indicates that the transition from oceanic to continental crust is extremely abrupt. Beneath station RANI, the crust is relatively thin (35.0 ± 2.5 km). At this station it was necessary to vary the V_p - V_s ratio in order to fit both the P-to-S conversion as well as the crustal multiples. Using a Poisson's ratio of 0.24, we were able to fit the waveforms reasonably well (Figure 2).

Within the Arabian Shield the crust is consistently thicker than at the coastal stations. We have found Moho depths of 39, 40, and 44 km at stations AFIF, HALM, and RAYN, respectively (Figure 3). Beneath the northernmost station, UQSK, the crust appears to thin to 37 km. At station RAYN we have also observed evidence of a boundary which separates the upper from lower crust. This is the only station at which we needed a major mid-crustal impedance contrast to fit the receiver function waveforms. At station RIYD, located off the Arabian Shield, we found the thickest crust of 45 km. This value is consistent with the body wave and surface wave-inversion studies that have also found a

mean crustal thickness of 45 km beneath the eastern Arabian platform [Al-Amri *et al.*, 1995; Mohktar, 1995].

An additional finding was the depth to basement beneath station RIYD. The depth to the basement-sedimentary cover contact was found to be 3 km. This depth is in good agreement with the depth to basement found from oil exploration wells in the region [Peterson and Wilson, 1986] which also found the basement to be 3 km beneath station RIYD. RIYD is the only station where we have observed what can be reasonably interpreted as the basement-sedimentary cover contact.

We have also observed several sub-Moho phases (Figure 2). These PS conversions provide strong evidence that the Arabian lithospheric mantle velocity structure cannot be described by a continuous velocity gradient. There appears to be at least one fairly discrete velocity boundary beneath four of the stations in the Arabian Shield. This boundary is not observed at stations SODA, RANI, and RAYN. Its absence at station RAYN may be due to destructive interference between the multiple reflections occurring at a mid-crustal velocity discontinuity and the PS conversion at the mantle discontinuity (Figure 3). Assuming we can correlate this feature beneath these stations, we observe a progressive shallowing of the upper mantle discontinuity towards the north beneath stations HALM and AFIF. However, we have found that this discontinuity at station AFIF is poorly constrained (± 7 km). Comparing stations HALM and RIYD, we observe a gradual dip of the boundary toward the east (Figure 3). It is also reasonable to interpret our results as not a continuous velocity discontinuity but as entirely unrelated features in the lithospheric mantle.

We also observe evidence for a large positive velocity discontinuity at 90 km very clearly at station TAIF. This is a very unexpected result since the lithosphere-asthenosphere boundary is thought to be at approximately 100 km along the Red Sea coast [Ghalib, 1992], with a negative velocity contrast. This may be an indication that, like the crust, there is a rapid lateral change in the thickness of the lithosphere from the Arabian Shield to the Red Sea.

Interpretations and Conclusions

The 1978 refraction experiment [Mooney *et al.*, 1985] allows us an excellent opportunity to compare our velocity model results with an entirely independent data set (Figure 4). The refraction experiment measured compressional wave velocities, while receiver function inversions are primarily sensitive to shear-wave velocity. The receiver function inversion crustal thickness estimations are very similar to those obtained by Mooney *et al.* [1985]. Only at station RANI do we observe a significant (> 2 km) difference between the two studies. We do not, however, observe evidence for most of the mid-crustal velocity changes; probably most of the velocity contrasts were not large enough to produce significant S-wave energy in the teleseismic P-wave coda. At station RAYN however, there is a great deal of correlation between the refraction and the receiver function models. Overall we can conclude that these two independent methods have given very similar results, lending validation to both methods.

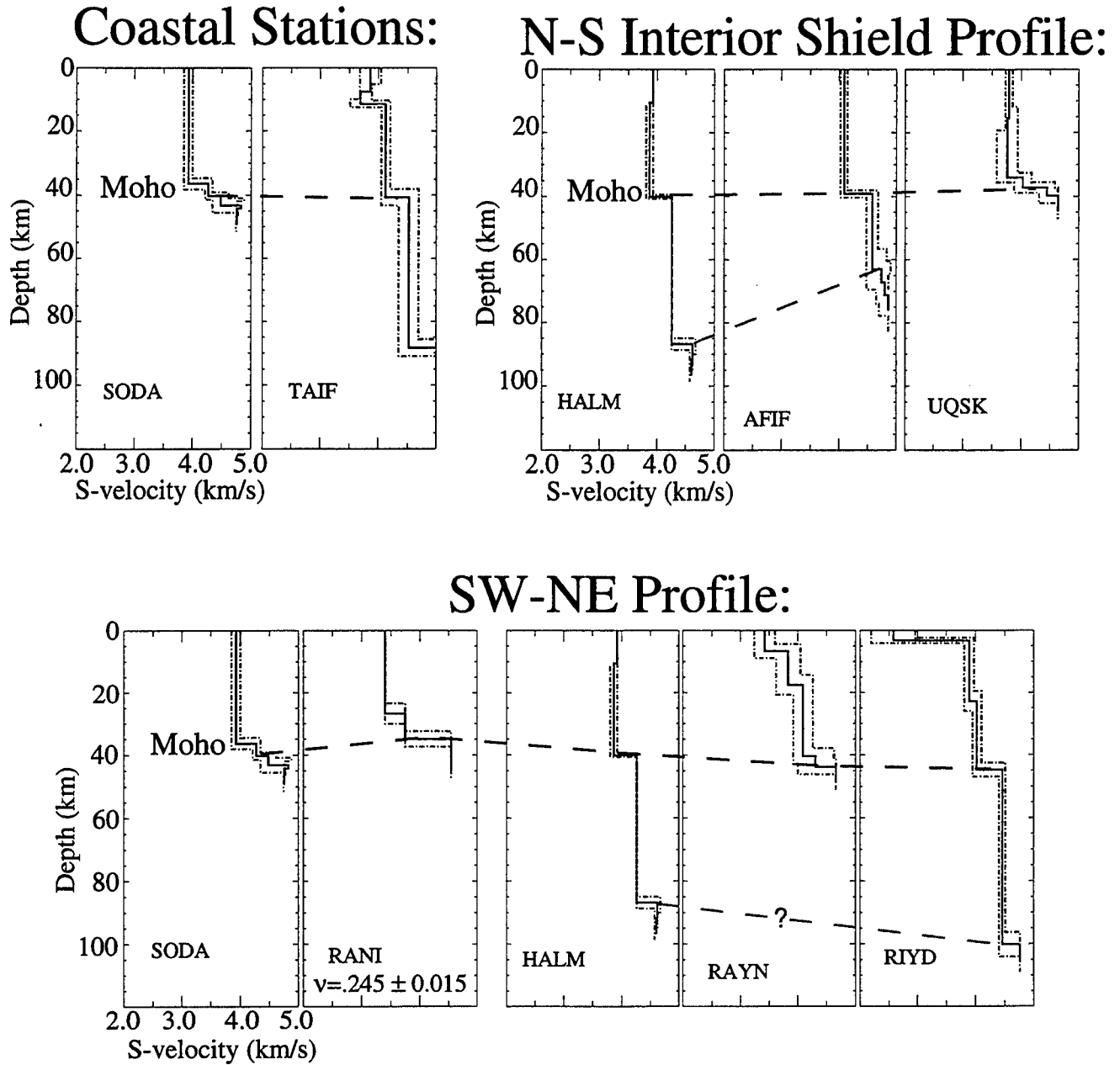


Figure 3. Summary of the shear-wave velocity models obtained in this study. The error bounds for each of velocity models from the jackknife error estimator are also given (dashed lines). For station RANI the Poisson's ratio (?) and jackknife error estimate are also given. Each of the boundaries shown (Moho and mantle discontinuity) are drawn, assuming a linear variation between stations.

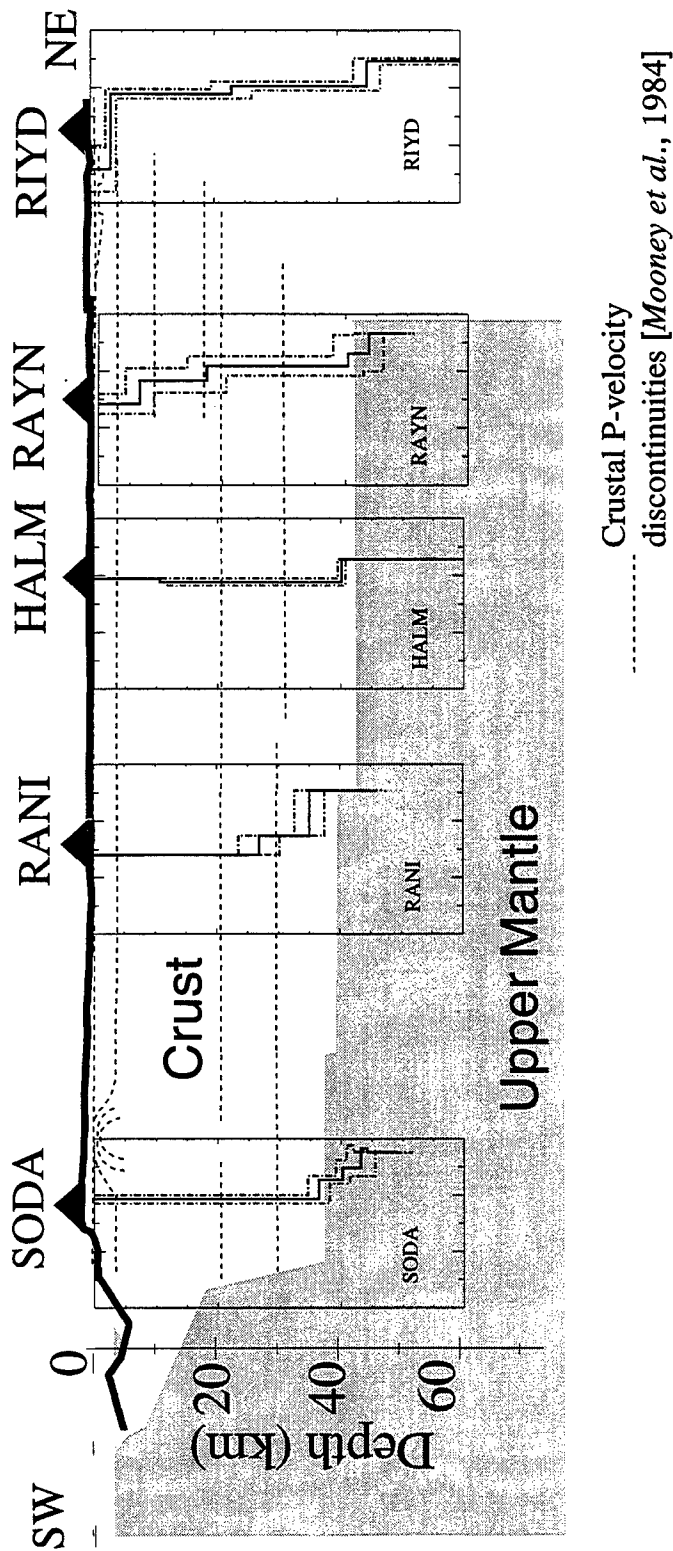


Figure 4. A comparison of our shear-wave velocity models with the model of Mooney et al. [1985] which is based on a refraction profiling study. The shaded/white boundary marks the Moho boundary derived from the 1978 refraction experiment (see Figure 1). The majority of our models compare favorably with this model. Only station RANI disagrees by more than 2 km. Also shown are the major crustal P-wave velocity anomalies (dashed thin lines). For the most part the receiver function inversions are insensitive to these boundaries, however, most of these are very subtle features (< 0.15 km/s P-wave velocity contrast). Only beneath station RAYN does the receiver function inversion detect upper-crustal and mid-crustal velocity discontinuities. These features are also seen on the refraction model and have substantially larger impedance contrasts (~ 0.3 km/s) than those observed in the southwestern portion of the profile.

We have observed a localized zone of relative crustal thinning at stations RANI as well as a small anomaly in the Poisson's ratio at station RANI. It is unclear what type of processes would lead to this localized crustal thinning; however, the amount of thinning is relatively small (< 5 km). There also is significant change in crustal structure between stations HALM and RAYN (Figure 4) which is very similar to that observed by *Mooney et al.* [1985]. This change in upper crustal velocities could be attributed to a change in the grade of metamorphism in the upper crust. Overall we observe a trend of crustal thickening towards the northeast and relatively little change in crustal thickness towards the north-northwest. This may be indicative of shortening of the Arabian plate caused by the collision of Arabia with Eurasia along the Zagros fold and thrust belt.

Our estimation of crustal thickness values does not correlate well with the topography or the major tectonic boundaries. It is possible that in order for the Arabian crust to be in isostatic equilibrium there are systematic density variations in the upper mantle and crust near station SODA and RANI in the south and UQSK in the north. We do not observe systematic changes in the shear-velocity structure to support such an idea, but it should be noted that at all three of these stations we have a fairly high error associated with the mean crustal S-wave velocity.

The origin of the positive upper mantle S-wave velocity discontinuity is not entirely clear. If these velocity contrasts are representative of independent upper mantle structure and not a continuous boundary underlying the Arabian Shield then they could be attributed to individual remnant structures from when the Arabian Shield was formed during the late Proterozoic orogenic events, about 600 Ma. Similarly, these anomalies could represent localized structure originating from the propagation of magma through the lithospheric mantle. Our observations bound a region in which there is evidence for asthenospheric upwelling [*Camp and Roobol*, 1992]. However, the location of our observations does not correlate well with either the paleo-subduction zones or the locations of surficial Neogene and Quaternary volcanics (Figure 4). Furthermore, data indicate that there is a positive velocity contrast in the lithospheric mantle, not a negative one. Another possible explanation would be that we are imaging the bottom portion of the lithosphere which has been altered through metasomatism. This alteration may have caused the seismic velocities to increase significantly. If these velocity discontinuities are at the base of the lithosphere, then it is very interesting to note that the lithosphere does not appear to thin much eastward. Other than the lack of evidence for this anomaly at stations SODA, RANI, and UQSK this would seem to be the most likely explanation given what we know about the lithospheric thickness in this region.

The location of a 90 to 100 km deep positive velocity contrast beneath station TAIF is circumstantial evidence for a thick lithosphere along the Red Sea coast. The existence of both a thick crust and lithosphere along the eastern Red Sea margin, along with other key pieces of geologic evidence [e.g. *McKenzie et al.*, 1970], are consistent with the Red Sea forming via continental splitting. Furthermore, the splitting would need to be fairly rapid in order that the continental lithosphere, flanking the rift, is not significantly thinned.

Acknowledgments: We thank Adam Edelman at IGPP for helping extract the seismic data and Ali Gharib for his help in retrieving the data used in this study. We also thank Alexander Calvert, Francisco Gomez, and Christine Orgren at Cornell for useful discussions and help in editing this paper. This work was funded by a US Department of Energy Contract F19628-95-C-0092.

References

- Al-Amri, A., Necioglu, A., and Gharib, A. A., Crustal structure of the Arabian platform from the spectral analysis of long period body P-wave amplitude ratios, *International Union of Geodesy and Geophysics (abstract)*, **21**, 385-386, 1995.
- Badri, M., and Sinno, Y., Qp crustal structure in central Saudi Arabia, *Journal of African Earth Sciences*, **12**, 561-568, 1991.
- Camp, V.E., The Madinah eruption, Saudi Arabia: magma mixing and simultaneous extrusion of three basaltic chemical types, *Bull. Volcanol.*, **49**, 489-508, 1987.
- Camp, V.E., and Roobol, M. J., Upwelling asthenosphere beneath western Arabia and its regional implications, *J. Geophys. Res.*, **97**, 15,255-15,271, 1992.
- Cochran, J.R., Gaulier, J., and Le Pichon, X., Crustal structure and the mechanism of extension in the northern Red Sea; constraints from gravity anomalies, *Tectonics*, **10**, 1018-1037, 1991.
- Efron, B., The jackknife, bootstrap, and other resampling plans, *Society of Industrial and Applied Mechanics Review*, Philadelphia, 1982.
- Ghalib, H.A.A., *Seismic Velocity Structure and Attenuation of the Arabian Plate*, Ph.D. Thesis, Saint Louis University, 314 pp., 1992.
- Greenwood, W.R., Anderson, R.E., Fleck, R.J., and Roberts, R.J., Precambrian geologic history and plate tectonic evolution of the Arabian Shield. *Saudi Arabian Deputy for Miner. Resources Bull.*, **24**, 35 pp., 1980.
- Husseini, M.I., The Arabian infracambrian extensional system, *Tectonophysics*, **148**, 93-103, 1988.
- Kennett, B., *Seismic Wave Propagation in Stratified Media*, Cambridge University Press, London England, 150 pp., 1984.
- Mechie, J., Prodehl, C., and Koptschalitsch, G., Ray path interpretation of the crustal structure beneath Saudi Arabia, *Tectonophysics*, **131**, 333-352, 1986.
- McKenzie, D.P., Davies, D., and Molanr, P., Plate tectonics of the Red Sea and East Africa, *Nature*, **226**, 243-248, 1970.
- Mohktar, T., Phase velocity of the Arabian Platform and the surface waves attenuation's characteristics by waveform modeling, *Journal of King Abdul Aziz University, Earth Sci.*, **8**, 23-45, 1995.
- Mooney, W.D., Gettings, M.E., Blank, H.R., and Healy, J.H., Saudi Arabian seismic-refraction profile: a travel time interpretation of crustal and upper mantle structure, *Tectonophysics*, **111**, 173-246, 1985.
- Niazi, M., Crustal thickness in the Saudi Arabian Peninsula, *Geophys. J. Astron. Soc.*, **15**, 545-547, 1968.
- Peterson, J.A. and Wilson, J.L., Petroleum stratigraphy of the Northeast Africa-Middle East region. In Hydrocarbon Potential of Intense Thrust Zones, Proc., *OAPEC Seminar*, December 1986, Abu Dhabi, **II**, 227-330, 1986.

- Powers, R.W., Ramiriez, L.F., Redmond, C.D., and Ehlberg, E.L. Jr., Geology of the Arabian Peninsula--Sedimentary geology of Saudi Arabia. U.S. Geol. Surv., Profess. Pap., **560-D**, p. 147, 1966.
- Sandvol E., Seber, D., Calvert, A., and Barazangi, M., Crustal structure in the Middle East and Africa: grid search inversion of receiver functions, submitted to Journ Geophys. Res., 1998.
- Seber, D. and Mitchell, B. Attenuation of surface waves across the Arabian peninsula, *Tectonophysics*, **204**, 137-150, 1992.
- Tichelaar, B., and Ruff, L., How good are our best models? jackknifing, bootstrapping, and earthquake depth, *EOS, Transactions, AGU*, **70**, 605-606, 1989.

C. BASEMENT DEPTH AND SEDIMENTARY VELOCITY STRUCTURE IN THE NORTHERN ARABIAN PLATFORM, EASTERN SYRIA

Abstract

Basement depth in the Arabian plate beneath eastern Syria is found to be much deeper than previously supposed. Deep-seated faulting in the Euphrates fault system is also documented. Data from a detailed, 300 km long, reversed refraction profile, with offsets up to 54 km, are analyzed and interpreted, yielding a velocity model for the upper ~ 9 km of continental crust. The interpretation integrates the refraction data with seismic reflection profiles, well logs and potential field data, such that the results are consistent with all available information. A model of sedimentary thicknesses and seismic velocities throughout the region is established. Basement depth on the north side of the Euphrates is interpreted to be around 6 km, whilst south of the Euphrates basement depth is at least 8.5 km. Consequently, the potentially hydrocarbon-rich pre-Mesozoic section is shown, in places, to be at least 7 km thick. The dramatic difference in basement depth on adjacent sides of the Euphrates graben system may suggest that the Euphrates system is a suture / shear zone, possibly inherited from Late Proterozoic accretion of the Arabian plate. Gravity modeling across the southeast Euphrates system tends to support this hypothesis. Incorporation of previous results allows us to establish the first-order trends in basement depth throughout Syria.

Introduction And Geologic Background

We present an interpretation of seismic refraction data collected along a north-south profile in eastern Syria. The refraction data are interpreted in conjunction with well logs, seismic reflection data, gravity and magnetic data. Hence, previously unknown metamorphic basement depth, and pre-Mesozoic sedimentary thickness, in eastern Syria are established. Along with indications of basement and deep sedimentary structure, this can help to determine the intracontinental tectonic processes that have shaped the region.

The tectonic setting of Syria within the Arabian plate (Figure 1) shows that the country is almost surrounded by active plate boundaries. The western boundary is marked by the left-lateral Dead Sea fault system which extends from the Gulf of Aqaba in the south to the Cyprus subduction zone - Bitlis suture - Dead Sea transform triple junction in the north. The Dead Sea fault marks the boundary between the Arabian plate to the east and the Levantine (east Mediterranean) subplate to the west. To the north of Syria lies the Bitlis suture which represents the collision zone of the Arabian and Eurasian plates. Continuing movement along this boundary is accommodated by thrusting along the Bitlis suture as well as movement on the East Anatolian left-lateral fault, as the Anatolian subplate maneuvers to escape collision. To the east and southeast of Syria the Neogene-Quaternary Zagros fold belt marks the collision zone of the Arabian plate with Iran (e.g. Sengor & Kidd 1979; Sengor & Yilmaz 1981).

It is generally believed that the movement along the surrounding plate boundaries controls the intraplate deformation observed in Syria (e.g. Barazangi *et al.* 1993). The two main structural features of the country are the Palmyride fold and thrust belt of central Syria, and the Euphrates fault system in the east (Figure 2). It has been suggested

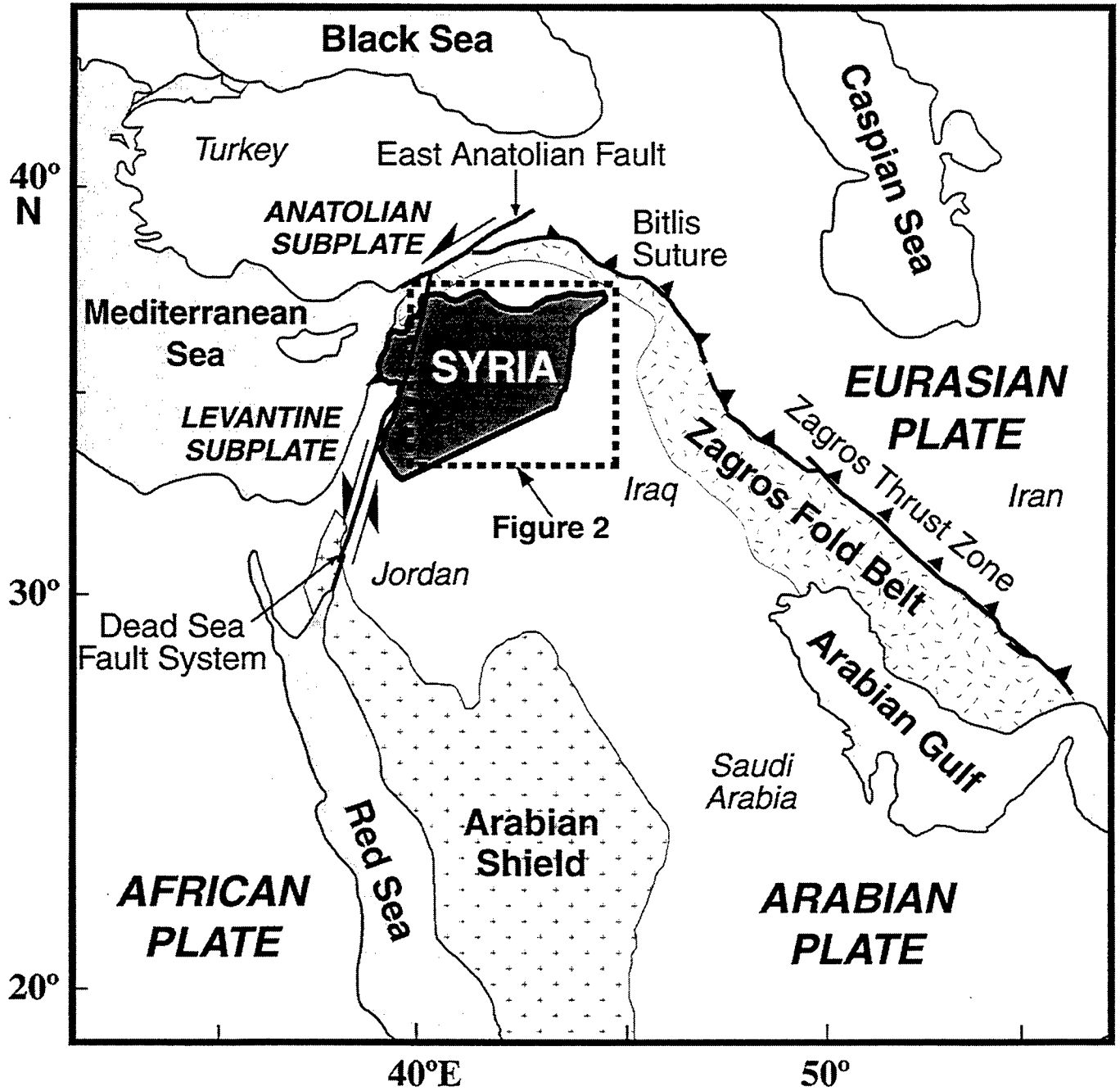


Figure 1. Regional tectonic setting of the northern Arabian platform.

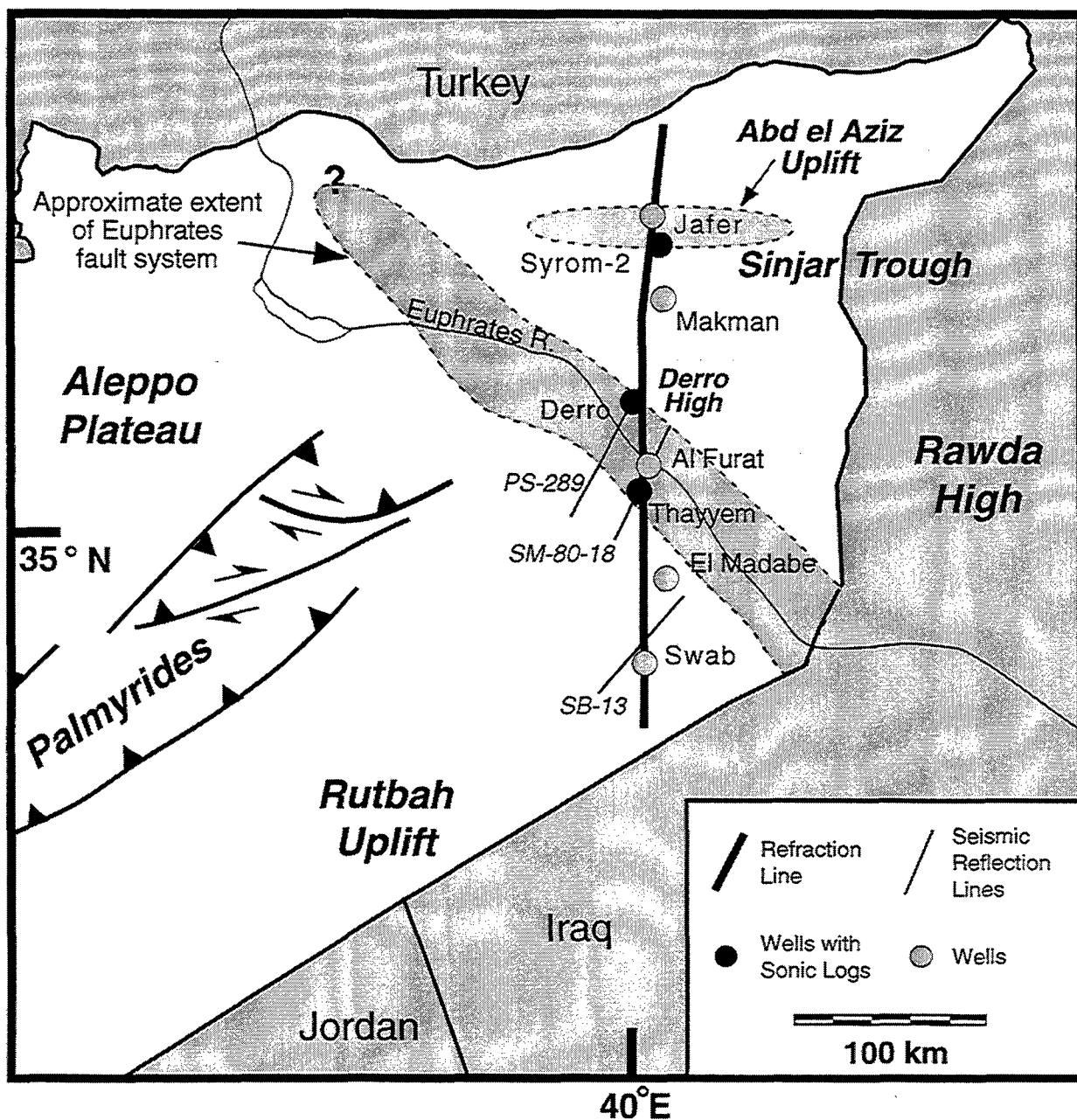


Figure 2. Map of eastern and central Syria showing location of selected data sources. Shaded area represents approximate location of Euphrates fault system. The extent of the faulting to the north and into Turkey is largely unconstrained. Only a small portion of the total number of seismic reflection lines used in this study are shown. Substantial additional well data farther from the refraction line were also available.

(e.g. Best *et al.* 1990) that these structures could be formed by reactivation along zones of weakness in the Arabian plate - weaknesses that have perhaps persisted since the Proterozoic (e.g. Barazangi *et al.* 1993; Litak *et al.* 1996a). However, whilst an appreciable amount of research has been conducted in the Palmyrides (e.g. Chaimov *et al.* 1990; McBride *et al.* 1990; Al-Saad *et al.* 1992; Barazangi *et al.* 1992), relatively little work has focused on eastern Syria. In particular, the Euphrates system has received limited attention in comparison to its geologic and economic importance (e.g. Beydoun 1991; de Ruiter *et al.* 1994). Recent work (Sawaf *et al.* 1993; Alsdorf *et al.* 1995; Litak *et al.* 1996a, 1996b) has increased understanding of the Euphrates system, but detailed assessment of basement structure and depth in this region has, until now, been unavailable. Hence, our results are a valuable contribution to the knowledge and understanding of the regional structure and tectonics of eastern Syria.

The area of eastern Syria focused upon in this study can be roughly divided into four structural zones of intraplate deformation, within which the deformation appears to be controlled by movement on the nearby plate boundaries. From north to south these are the Abd el Aziz structural zone, the Derro high, the Euphrates fault system and the Rutbah uplift (Figure 2).

The Abd el Aziz uplift is an anticlinorium controlled mainly by a major south-dipping reverse fault (e.g. Ponikarov 1967; Lovelock 1984). It is thought that the Abd el Aziz was a sedimentary basin in the Mesozoic which inverted in the Neogene (Sawaf *et al.* 1993), and may have been the northwestern edge of the larger Sinjar trough which existed at that time (Lovelock 1984).

South of Abd el Aziz, and to the north of the Euphrates, is a series of structural highs, controlled by deeply penetrating faults. Most prominent of these is the Derro high which is interpreted to be bounded by north-dipping reverse faults that separate this area from the Abd el Aziz (Sawaf *et al.* 1993). Basaltic outcrops along some of the larger faults around the Derro high could offer further evidence for the deep-seated nature of faulting in this area.

Although largely unexpressed by surface features, the Euphrates fault system represents an aborted rift system, striking roughly NW-SE and extending completely across Syria. The faulting is thought to represent a Late Cretaceous transtensional graben system with minor reactivation in Neogene times (Lovelock 1984). The system can be roughly divided into three parts along its length (Litak *et al.* 1996a): a northwestern segment exhibiting shallow grabens and significant inversion; a central segment where the Euphrates system bounds the Palmyrides and strike-slip movement is apparent; and the southeastern part which is characterized by deep graben features and only very minor inversion (Figure 2). Although Lovelock (1984) suggested that most movement in the system took place on a few major faults, recent work clearly indicates that the deformation is widely distributed (de Ruiter *et al.* 1994; Litak *et al.* 1996a, 1996b). Faulting, for the most part, is nearly vertical in most places, resulting in limited (< 6 km) extension across the system (Litak *et al.* 1996b).

The southernmost section of the refraction profile crosses the eastern edge of the Rutbah uplift, an extensive upwarp which affects large parts of western Iraq, northern Jordan and southern Syria. Doming and extensive erosion of the area is known to have taken place during the Mesozoic and Tertiary (e.g. Lovelock 1984). Very little deformation is found in the strata of the Rutbah Uplift, except along the northeastern edge where it trends into the Euphrates depression.

Basement Rocks in Syria

The lack of current constraints on basement depth in Syria is a consequence of an almost complete absence of basement outcrops, and only one well, in the far northwest of the country, has penetrated the Precambrian (Ponikarov 1967). The few basement exposures that exist are in northwest Syria, Jordan, southern Israel and in southern Turkey, all at extensive distances from the study area, and in different geologic regimes (Ponikarov 1967; Sawaf *et al.* 1993). Leonov *et al.* (1989) constructed a depth to basement map within Syria based on well data and seismic reflection data, thus establishing the broad trends which are still generally accepted. However, the small scale and lack of direct evidence used in the study of Leonov *et al.* (1989) limit its applicability and new results presented here disagree somewhat with this earlier assessment. Best *et al.* (1993) mapped basement for the whole of Syria by using a prominent Mid-Cambrian reflection event as a proxy for basement rocks. However the results presented here show there can be substantial differences between the depth of the Middle Cambrian and basement rocks. Seber *et al.* (1993), using seismic refraction data, established basement depths in central Syria to be around 6 km beneath the Aleppo Plateau, 9-11 km beneath the Palmyrides and at least 8 km in the south of the country. Additionally, Seber *et al.* (1993) found seismic velocities of basement rocks to be around 6 km s⁻¹, in agreement with the findings of refraction surveys in Jordan which interpreted basement velocities of 5.8 - 6.5 km s⁻¹ (Ginzburg *et al.* 1979; El-Isa *et al.* 1987). However, in the absence of previous investigations in eastern Syria, the results presented here offer a unique assessment of basement depth in this region, and hence offer new insight on the deformational history of the northern Arabian platform.

Data Analysis

Data Acquisition

The model of basement depth and deep sedimentary structure that we develop relies on the analysis of several data sources, particularly a 300 km long seismic refraction profile. The refraction data were collected as part of a larger seismic profiling effort spanning all of Syria, conducted by a Soviet/Syrian joint project in 1972-3. Nine refraction lines were shot, totaling 2592 km, providing unique data for the study of deep sedimentary structure.

The original analysis of the seismic refraction data (Ouglanov *et al.* 1974) relied on interpretation techniques that established velocities using simplistic formulae that are now known to be problematic. Additionally, the original interpretation attached stratigraphic significance to some of the velocity contrasts observed in the refraction interpretation. Data from wells drilled since this initial interpretation show these stratigraphic inferences to be incorrect. However, as this old interpretation was never written in final form, and was never published, further results of the 1974 analysis of the

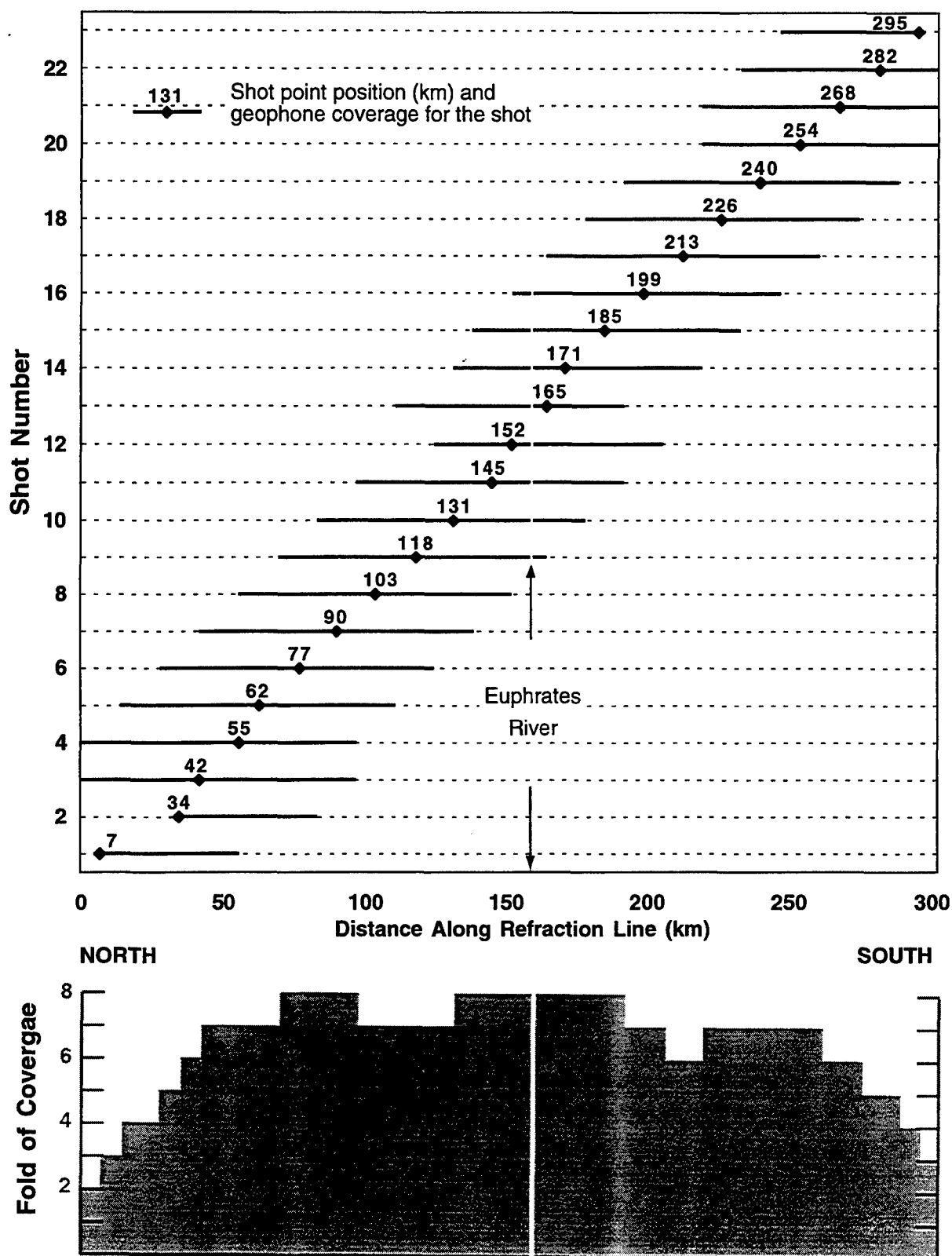


Figure 3. Configuration of shots and geophone spreads used in the refraction interpretation. Cumulative fold of coverage also shown.

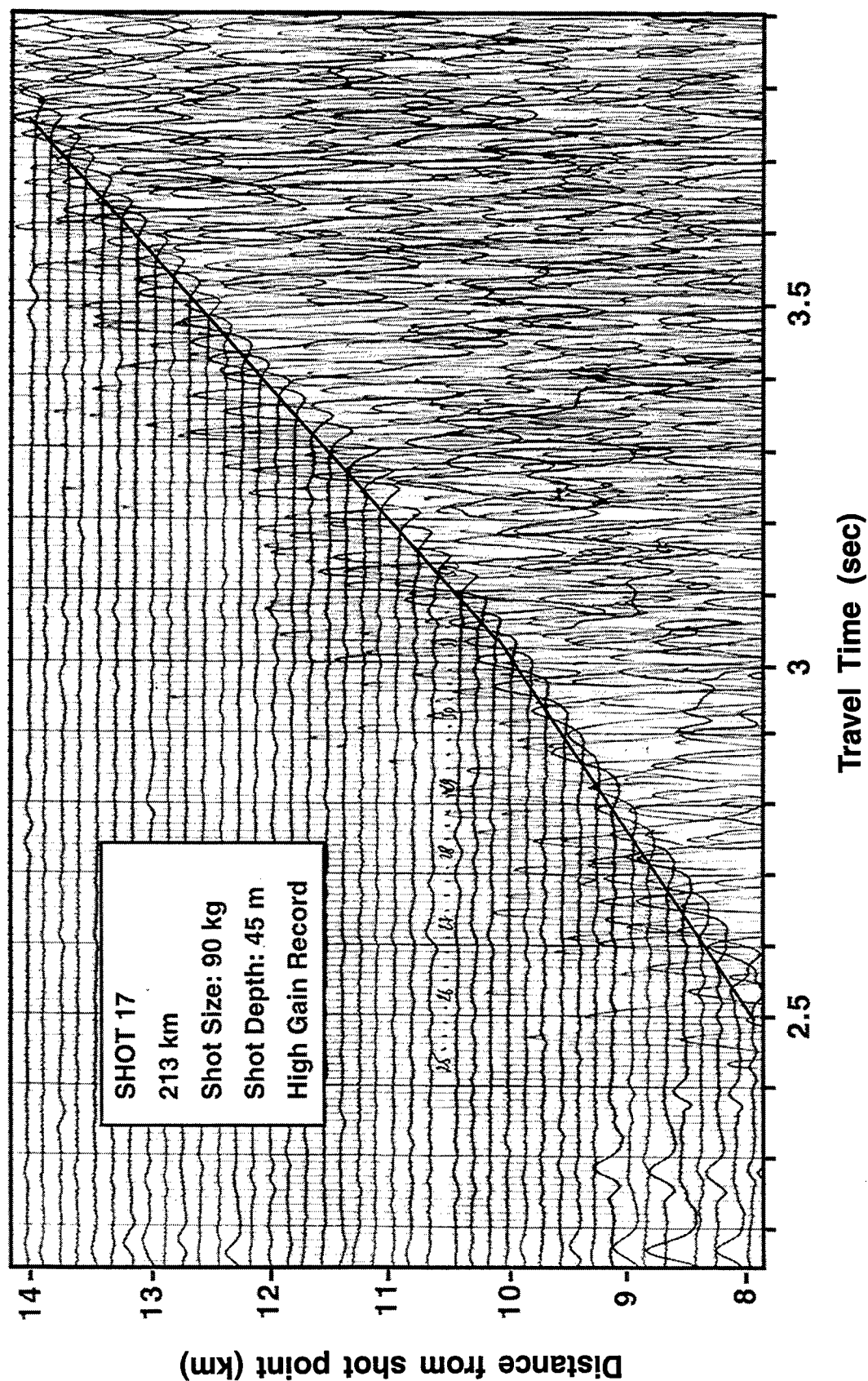


Figure 4. Typical example of original refraction data. Part of reverse spread from shot 17. Note the good quality of first arrivals (highlighted with line added by authors) which were digitized to accomplish a ray-traced interpretation.

data are not discussed here. With the benefit of technological advances in the interpretation of these type of data, and aided by extensive supplementary data sources, we present a new interpretation of the original data showing basement depth to be much greater than originally interpreted.

Figure 2 shows the location of the profile, the seismic reflection lines and the well logs used in this interpretation. The refraction line is 302 km long and oriented north-south. A total of 44 shot points were employed along the profile having a spacing of approximately 7 km. Shot sizes varied between 50 and 1250 kg dependent on geophone offset; data were recorded along forward and reverse geophone spreads for each shot, and geophone spacing was 150 meters. For most shots both a high and low gain analog recording were made. The geophone spreads were of two types: every second shot point had 'short' spreads of 28 km maximum offset and the remaining, 'long', spreads had nominal maximum offsets of 48 km, with the longest spread being 54 km. Since deep sedimentary structure was the primary focus of this investigation, it was decided that the shorter spreads (28 km offsets) contained little data that could not be obtained independently from the longer spreads. Thus, data from 23 shots, each with forward and reverse geophone spreads, are used in our interpretation. This yields a fold of coverage at least 700% in most places (Figure 3), unusually high for a survey of this type.

In analyzing these data the original photographic analog recordings from the survey were used to digitize first and, wherever possible, subsequent arrivals. Recognition of first arrivals was generally unambiguous owing to large shot sizes and relatively quiet recording conditions (Figure 4). Identification of subsequent arrivals, however, was generally precluded by the large amplitudes of the traces and short recording times. A total of approximately 17,000 arrivals were digitized.

Data Interpretation

The refraction data were interpreted using a geometric ray-tracing approach utilizing the software of Luetgert (1992). Preliminary interpretation involved simple refraction modeling; the positions and velocities of various user-defined layers in the software were subtly altered until travel times of calculated rays-paths through the computer model matched those of the digitized arrival times. This preliminary-type interpretation produced a 7-layer model with seismic velocity increasing in each deeper layer. Although naturally in agreement with the refraction data, the velocity interfaces in this model were found to be in disagreement with some velocity boundaries observed in sonic logs and travel times from seismic reflection data. The disagreement was largely a consequence of the limitations in the refraction method, in particular the inability to resolve low-velocity layers that are clearly demonstrated by the sonic logs (Figure 5).

However, the ambiguity of low-velocity layers can be eliminated if velocity information is available from an independent source, or if reflection travel times are known in addition to refraction times (e.g. Kaila, Tewari & Krishna 1981). Therefore, an interpretation strategy was adopted in which the refraction, reflection and well data were used simultaneously in the refinement of the velocity model, thus establishing a model consistent with all available data. This began with the construction of an initial velocity

model constrained at shallow depths (< 4 km) by seismic reflection and well data, with sonic logs from parts of 3 wells (Figure 2) allowing estimates of seismic velocities. The deeper section of the initial model was less constrained and relied on extrapolation from the shallow section and limited reflection data. The ground surface of the model was extracted from digital topographic data, sub-sampled to approximately 1 km horizontal resolution. The initial model was refined through ray-tracing to improve agreement with the various data, in particular the refraction arrival times. The modeling effort, described further below, culminated in what is hereafter referred to as the 'final velocity model' - a model consistent with all the available data.

Due to the high fold of coverage of the refraction data, and the various other constraining data, many iterations were necessary to produce a velocity model in agreement with all the data. The refraction interpretation was done by taking each individual shot in turn, and changing the velocity model to produce the best fit between the observed and the calculated arrivals for that shot. However, due to the higher than 100% fold of coverage, modifications made to the model by examining the fit for one shot obviously changed the fit between the observed and calculated arrivals for other adjacent shots. Thus, after each change to the velocity model, the fit between the calculated and observed arrivals from every shot had to be checked. The final velocity model was determined by obtaining the best overall fit of the arrivals for all the shots. Although this was extremely time-consuming, the process yielded an essentially unique velocity model that is in agreement with all the refraction arrivals.

It was clear from the integrated modeling that some of the velocity interfaces detected by the refraction data coincided with age horizons and associated velocity changes in sonic log data. Figure 5 shows the sonic log and synthetic seismogram from the Derro well, along with velocities from the final velocity model. This shows how the velocities in the final model fit those found in the sonic log, whilst at the same time the depths of the velocity interfaces match the depths of certain age horizons found in the well. Where such correlations were observed the velocity model was modified to fit both the well data and the refraction data as accurately as possible.

Knowing the age of certain velocity interfaces, reflection data were utilized in conjunction with the refraction data. Two-way reflection times derived from the final velocity model and those from seismic reflection data were compared to support the refraction interpretation and add further detail which could not be resolved by the refraction method alone. For example, faults interpreted from seismic reflection data were used to refine the details of the final velocity model (e.g. Figure 6a). Figure 6 shows examples of how two-way times in the final velocity model compare to those from seismic reflection data. Although not all prominent reflections are associated with refractions (e.g. mid-Cambrian reflector, Figure 6b) most of the reflectors are correlated to refracting horizons, indicating a similar physical nature for refracting and reflecting horizons.

Aeromagnetic data (Filatov & Krasnov, 1959) show few anomalies of interest from the study region, with generally long wavelength, low amplitude variations indicating

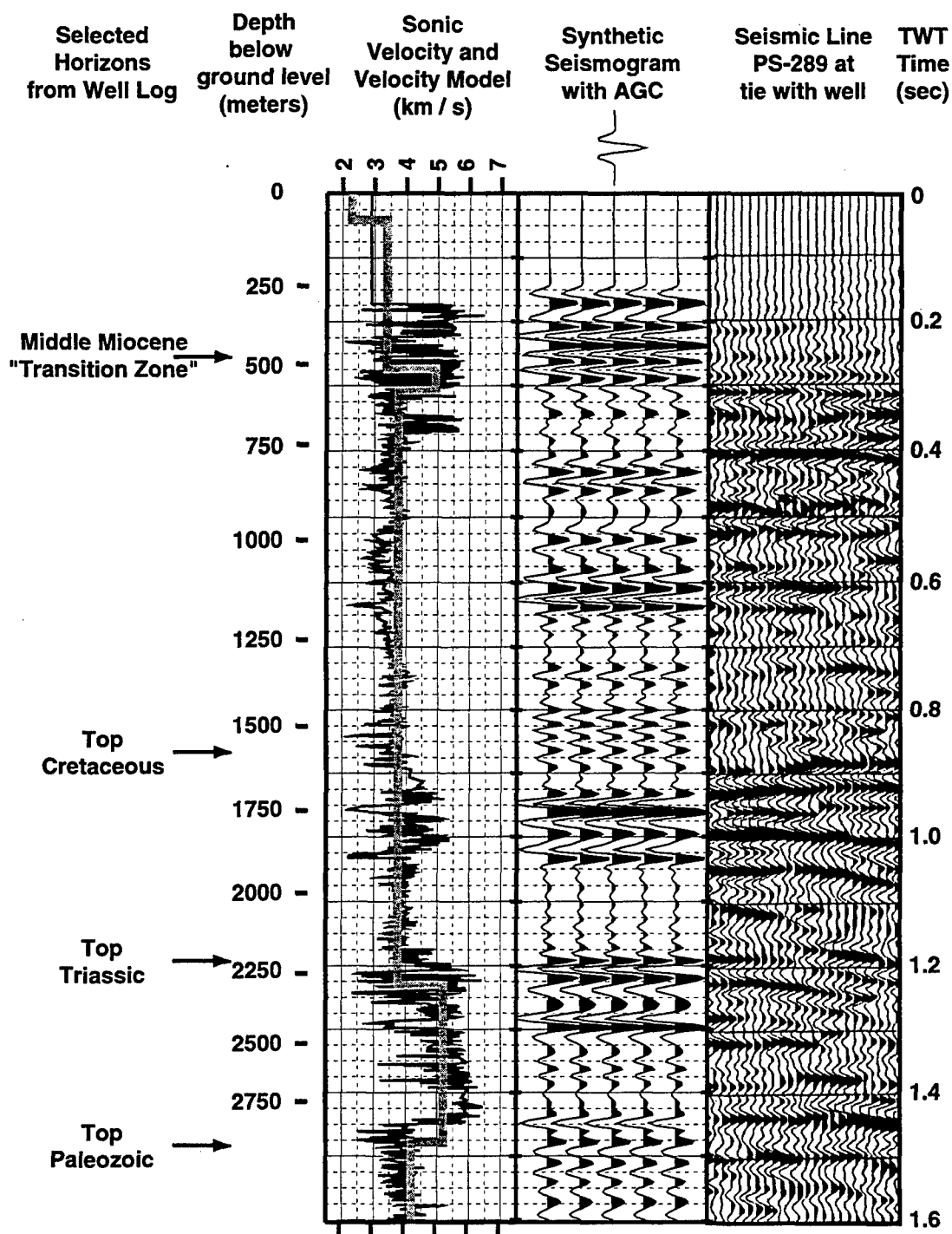


Figure 5. Sonic log and synthetic seismogram from Derro well (see Fig. 2 for location). Velocities from final velocity model shown by heavy gray line on same scale. Sonic logs from this and several other wells were used to constrain the velocity model. Note the low-velocity Upper Paleozoic strata which are undetectable by refraction data alone. Seismic line PS-289 at the tie with the Derro well is shown for comparison to the synthetic seismogram.

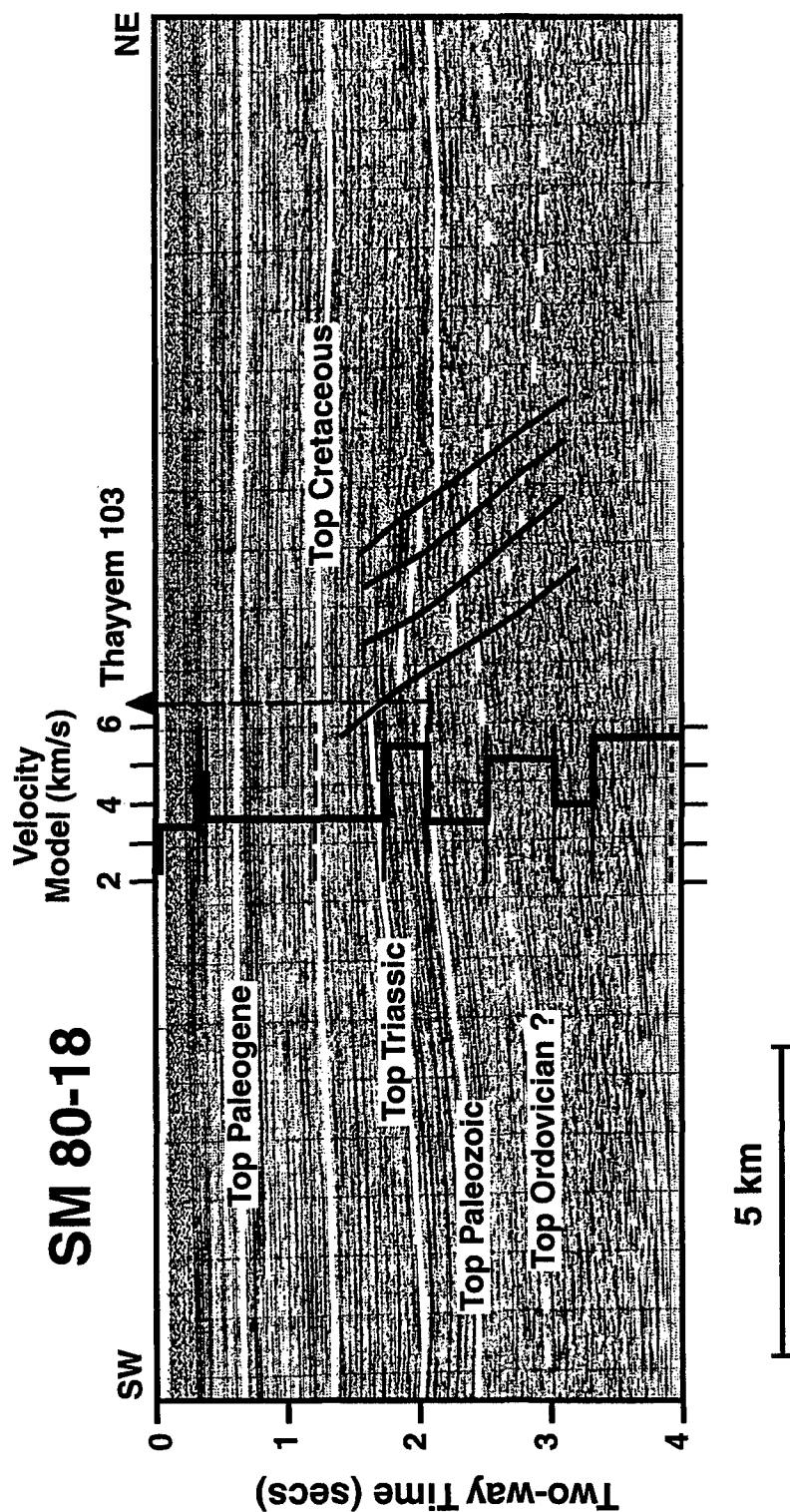


Figure 6 (a, b). Examples of correlations between seismic reflection data and two-way incidence reflection times deduced from the velocity model (see Fig. 2 for location of seismic reflection lines). Interfaces not corresponding to velocity changes are shown as dotted lines on the velocity graph. Uncertain velocity interface positions shown as long dashed lines.

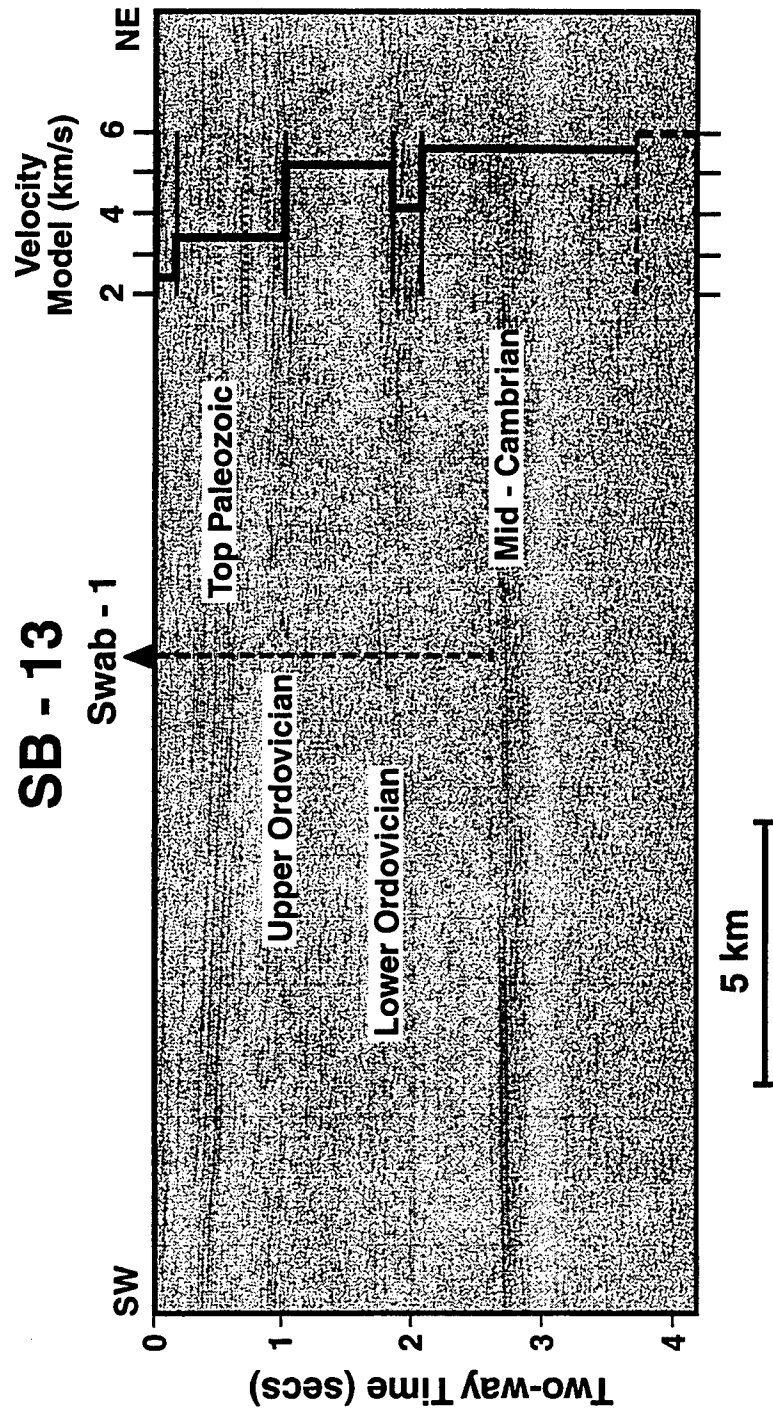


Figure 6b.

sources at significant depths. Assuming the source of the anomalies to be basement rocks then the magnetic data agree with the observations of large basement depths established in the velocity model, with shallower sources in the north. Isolated patches of short wavelength, high amplitude magnetic anomalies correspond with known basaltic outcrops. Additionally, gravity observations along the profile (BEICIP 1975) were compared to the gravity signature of the velocity model, with each velocity layer assigned an appropriate density. In this case also, the calculated and observed observations show overall agreement. More analysis of gravity data is presented in the next section.

The Final Velocity Model

The final velocity model that satisfactorily fits all available data is presented in Figure 7a. The velocities in some of the layers change laterally, but layers have uniform velocities in a vertical direction. Well data along the profile, superimposed on the velocity interfaces and their presumed stratigraphic significance, demonstrate the close semblance between the model and well data (Figure 7b).

However, despite direct evidence for the majority of the model, a few uncertainties remain. For example, no direct evidence exists for parts of some low velocity layers, hence the exact position of these horizons is, in places, uncertain. It is also not possible to obtain exact measures of the velocities of the low-velocity zones in these cases and so parts of the layers have been given velocities that are interpolations between well-determined values. Additionally, the depth to basement in the far south of the model is only thought to be a minimum constraint. No refractions were observed in this part of the refraction profile at velocities considered typical of those for metamorphic basement rocks, either because basement velocities are appreciably slower in this region, or because the geophone spreads employed were too short to sample refractions from the apparently deeper basement in this region. The latter explanation is considered more probable, therefore the depth to basement shown is a minimum (Figure 7). Another uncertainty concerns the interface signified as top of Khanasser (Lower Ordovician) in the north of the model. The interface interpreted based on the refraction data does not correspond exactly with observations from the Jafer well (Figure 7b). Therefore, the refractor in this region is labeled 'Infra-Khanasser'.

Despite these shortcomings, the majority of the final velocity model is based on direct evidence from at least one and, in many cases, several sources. In general, the modeled refraction times show excellent agreement with the observed arrivals from the refraction data. Four examples of this, from various points in the transect, are shown in Figure 8. Each of the other shots, not shown here, demonstrate similar agreement between the velocity model and the observed arrival times. Given reasonable inaccuracies in the fit between observed and calculated refraction arrivals, such as those indicated in Figure 8, the errors in the bulk of the model can be shown to be relatively small, with approximately ± 200 m error in depth to most interfaces and less than ± 0.1 km s⁻¹ in velocities.

Discussion

A model of seismic velocity down to basement in eastern Syria has been constructed

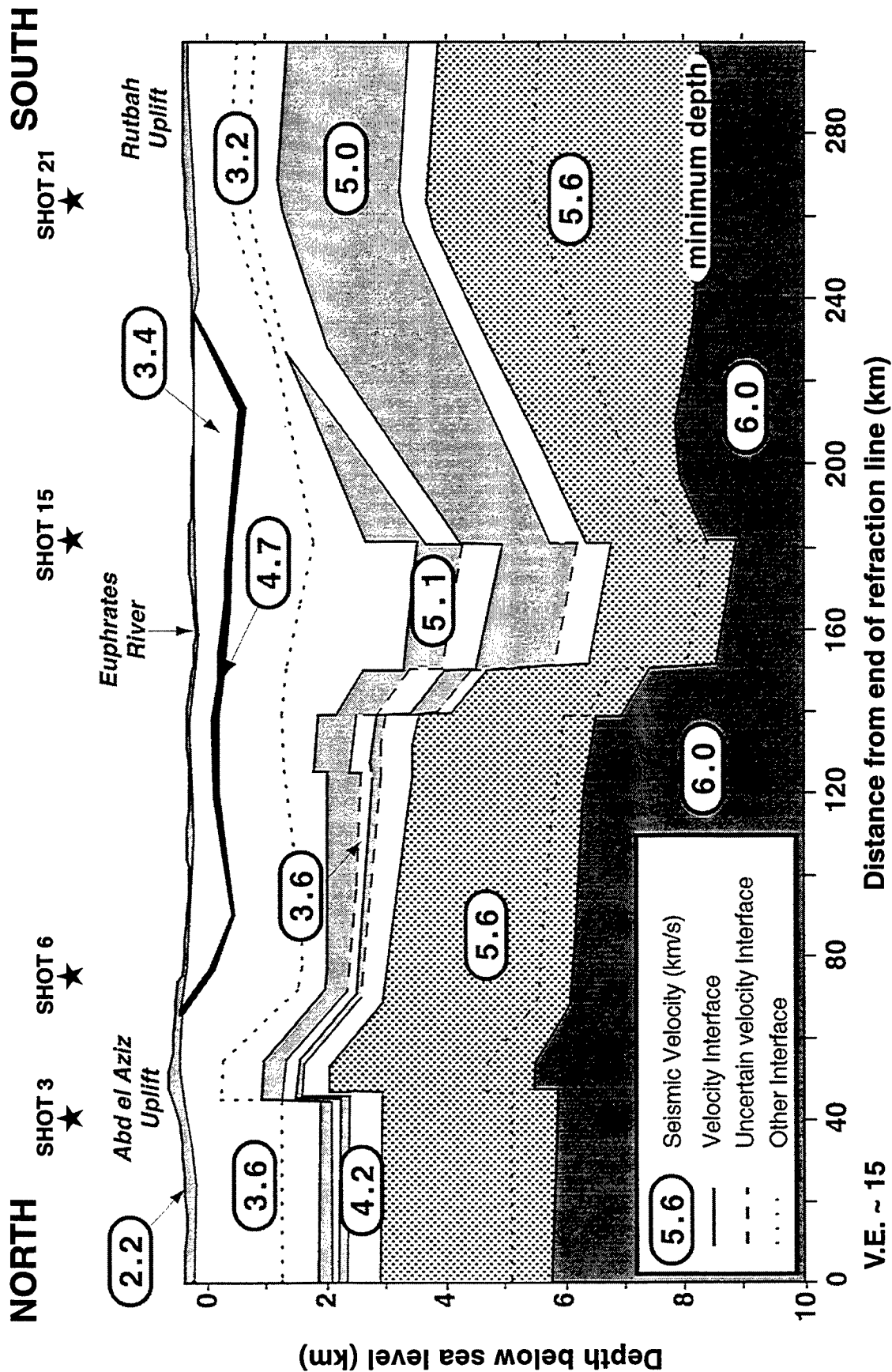


Figure 7. Cross section showing the final velocity model. Model interfaces not corresponding to velocity changes are shown as dotted lines. Uncertain interface positions are shown as long dashed lines. (a) shows seismic velocity model and interface positions. Locations of shots used in Fig. 8 also shown. (b) demonstrates the correlation between the velocity interfaces and age boundaries sampled in wells along the refraction profile.

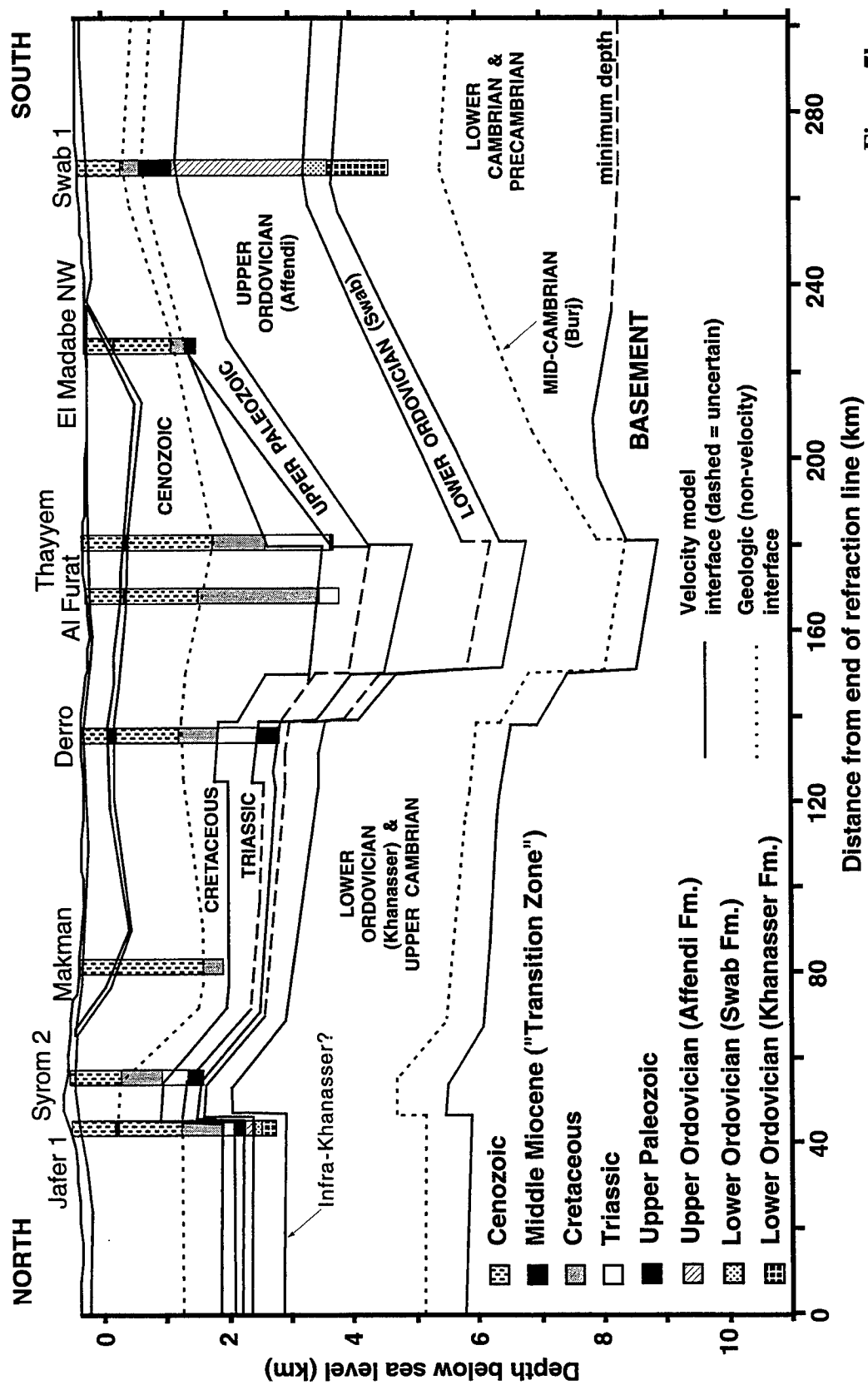


Figure 7b.

from the interpretation of refraction data and additional coincident data sources (Figure 7). The model shows basement-involved tectonics beneath the Euphrates graben system and the Abd el Aziz uplift. The faulting is steeply dipping (even though the model is oblique to the dominant strike of the area), a result supported by the extensive seismic reflection analysis of Litak *et al.* (1996b). In the area where the refraction transect crosses the Euphrates, Litak *et al.* (1996b) reported that the graben morphology in the upper sedimentary section is similar to the 'classic' model of a normally-faulted rift system, more so than elsewhere along the Euphrates. Our model shows this style of faulting persists to basement depth.

The model indicates that whilst increasing formation age generally causes increasing seismic velocity, velocity is also controlled by depth of burial and, more significantly, by lithology. These, and other ideas, are explored below as each of the velocity layers, from shallowest to deepest, is discussed in relation to its stratigraphic significance and relevance to regional tectonics.

Cenozoic and Mesozoic

The uppermost velocity layer (2.2 km s^{-1}), is interpreted as being a superficial covering of weathered and poorly consolidated material underlain by more competent rocks of various ages ($3.2 - 3.6 \text{ km s}^{-1}$). Somewhat deeper is a relatively high velocity (4.7 km s^{-1}) layer extending across the middle portion of the model (Figure 7a). This stratum hindered refraction interpretation by acting as a 'screening layer' (as described by Rosenbaum 1965; Poley and Nooteboom 1966), preventing some seismic energy from reaching deeper interfaces. However, enough energy was returned from deeper horizons to permit meaningful analysis (e.g. Figure 8c). The position of the 4.7 km s^{-1} layer was correlated with well data (Figures 5 and 7b) to a Middle Miocene sequence of anhydrites, gypsum and limestone, known locally as the 'Transition Zone' (Sawaf *et al.* 1993). Slight doming of this horizon, as well as the underlying top of Cretaceous interface, that was not detected as a refractor but which is mapped on the basis of well logs and reflection data, may be due to minor inversion on the north side of the Euphrates graben. This inversion is probably the result of the continued Cenozoic collision between the Arabian and Eurasian plates along the Bitlis suture and Zagros collision zone (Litak *et al.* 1996b).

Below the Cretaceous, the Triassic layer ($5.1 - 5.4 \text{ km/s}$), of predominantly dolomites and anhydrites, produces good refractions of characteristically high seismic velocity. The Triassic strata pinch out in the south whilst thinning slightly away from the graben toward the north (Figure 7b).

Paleozoic

The Upper Paleozoic formations - Permian, Carboniferous, Silurian (Devonian is entirely absent) - are grouped together on the basis of their similar seismic velocities ($3.2 - 3.6 \text{ km s}^{-1}$) (Figure 7a). These mainly shale and sandy shale formations (Table 1) show slight thinning towards the north. The thinning is a result of extensive erosion that took place whilst northern Syria formed an intermittent broad subaerial uplift from Late Silurian to

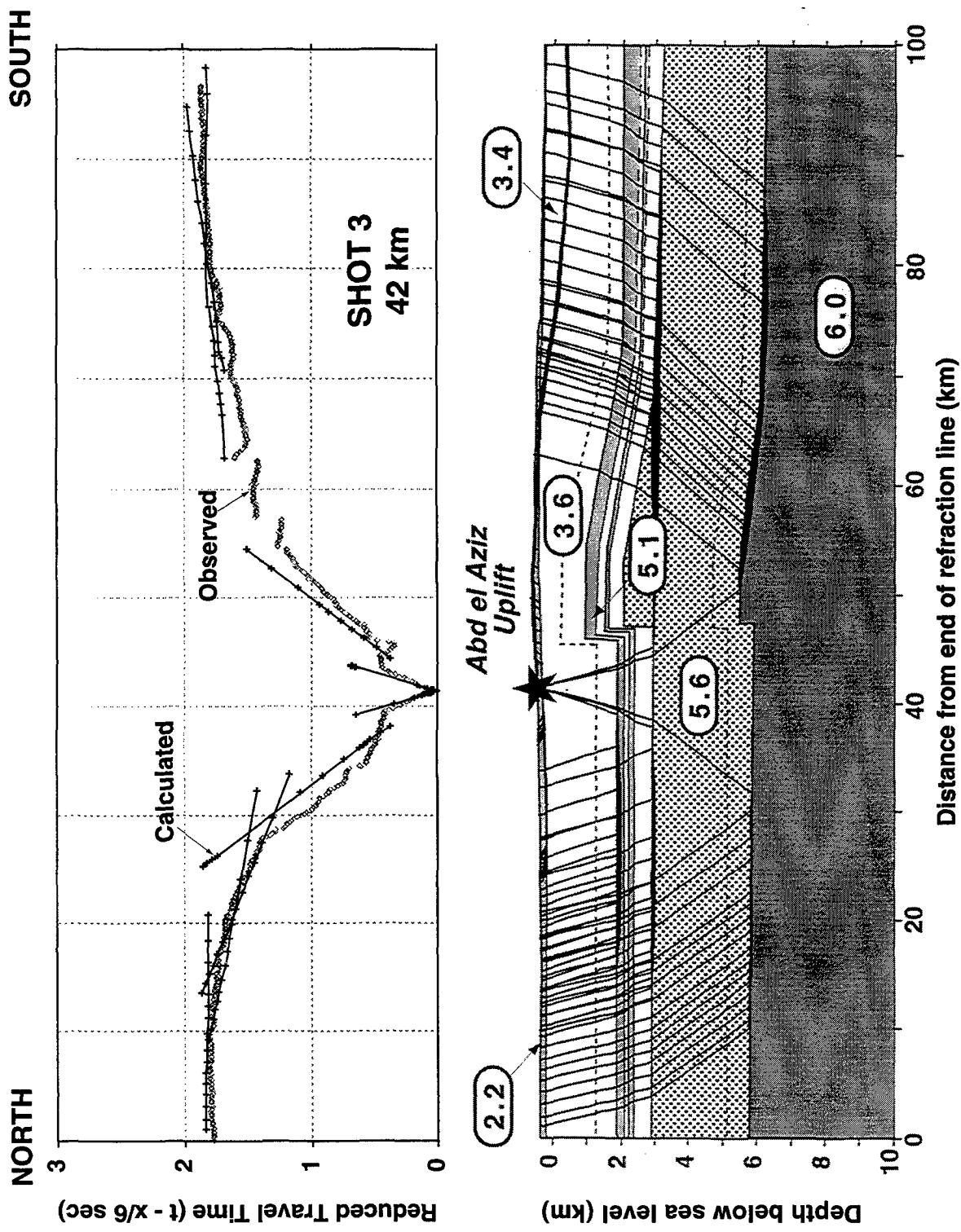


Figure 8 (a-d). Examples of ray-tracings from the final velocity model chosen to represent the full range of structures interpreted along the transect. Numbers represent seismic velocities in km s⁻¹. Note the effect of the near-surface high-velocity layer in (c). Modeled refractions from basement in (d) do not necessarily fit observed arrivals, but are shown to illustrate that basement depth for this part of the model is a minimum.

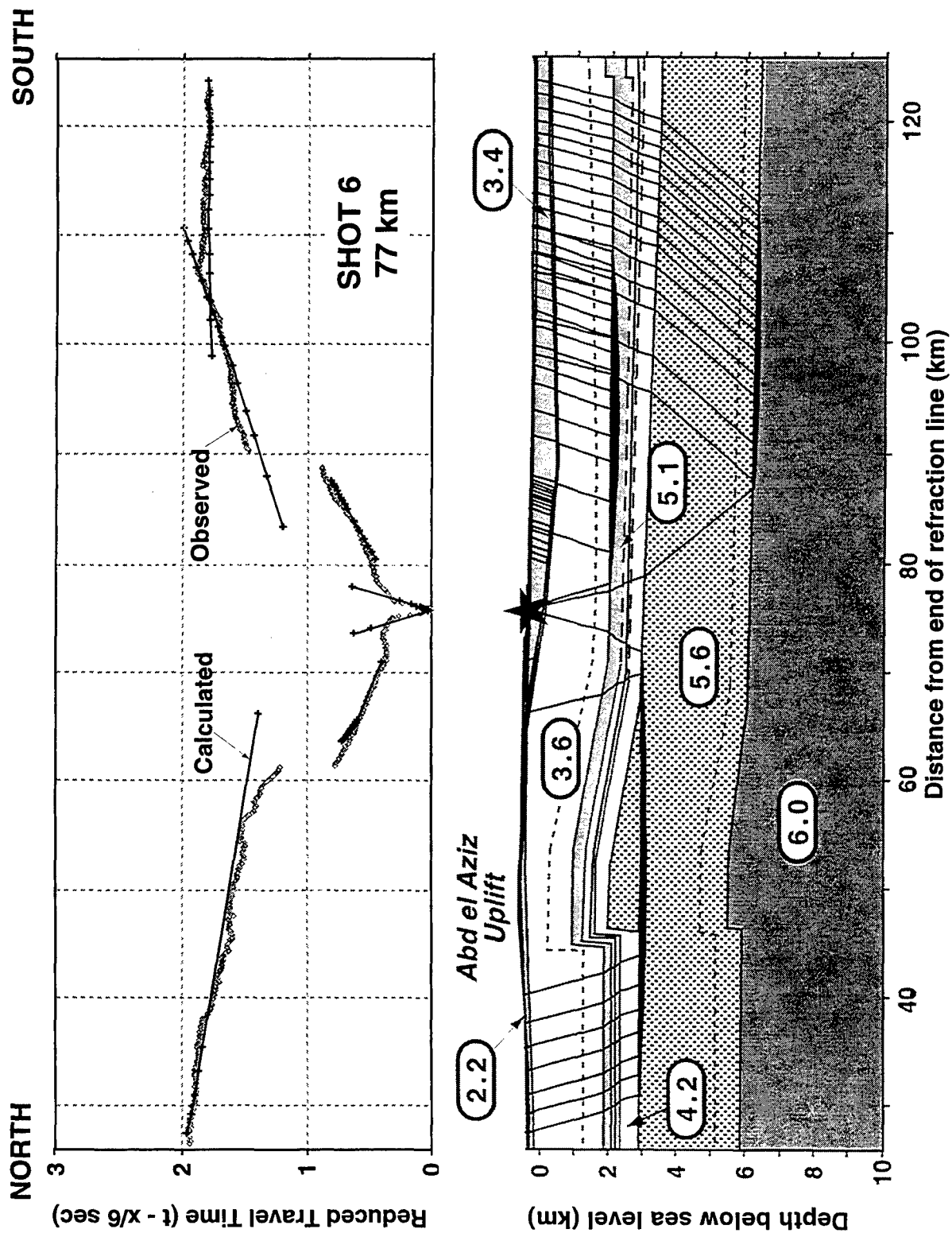


Figure 8b

SOUTH

NORTH

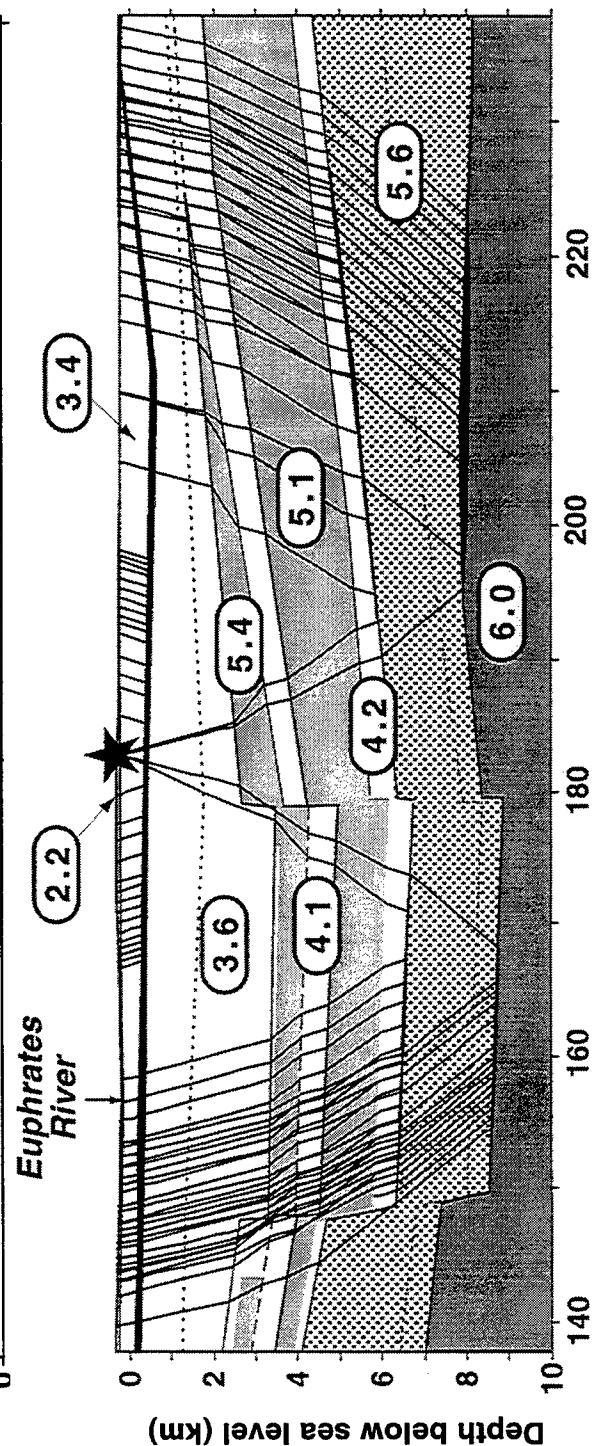
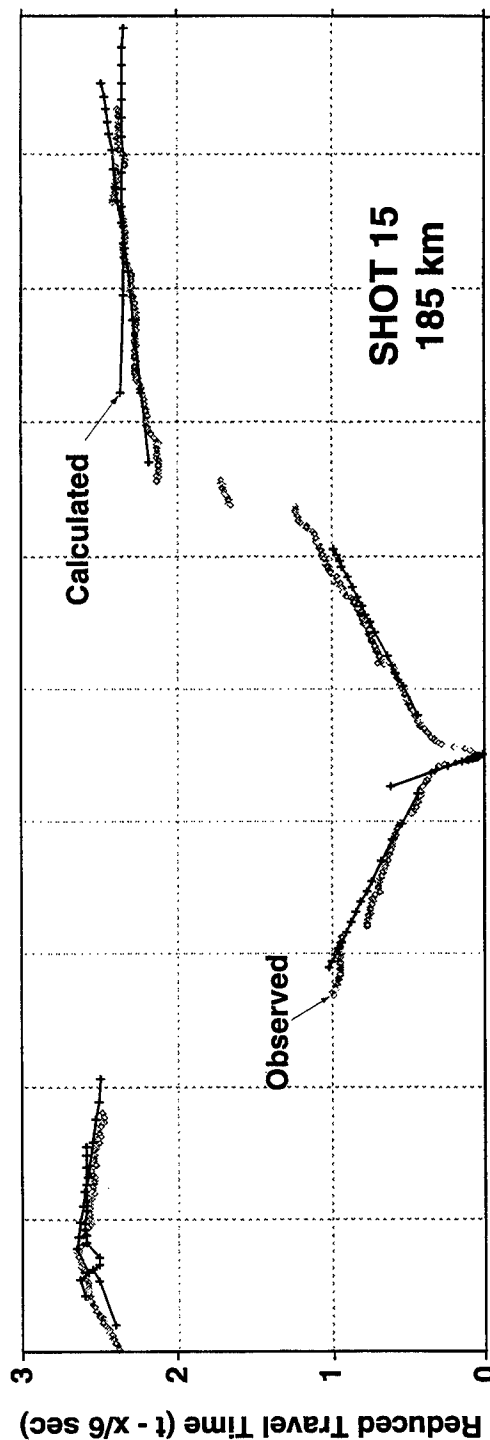


Figure 8c.

NORTH

SOUTH

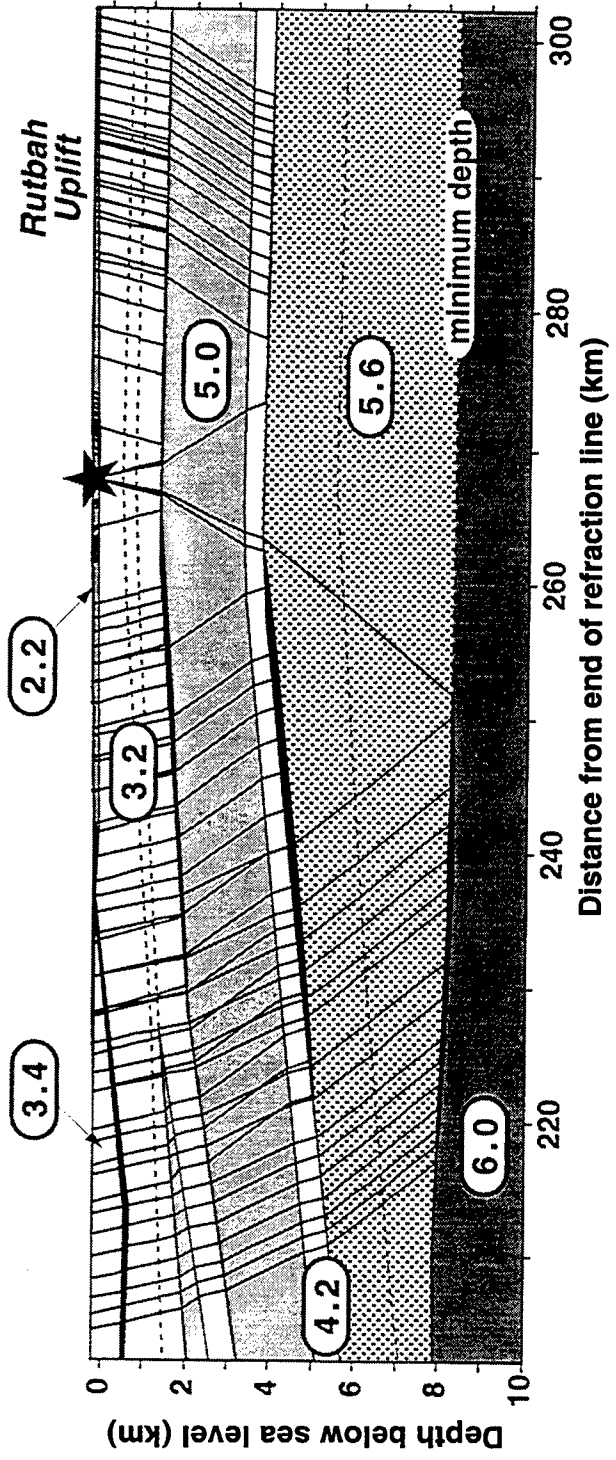
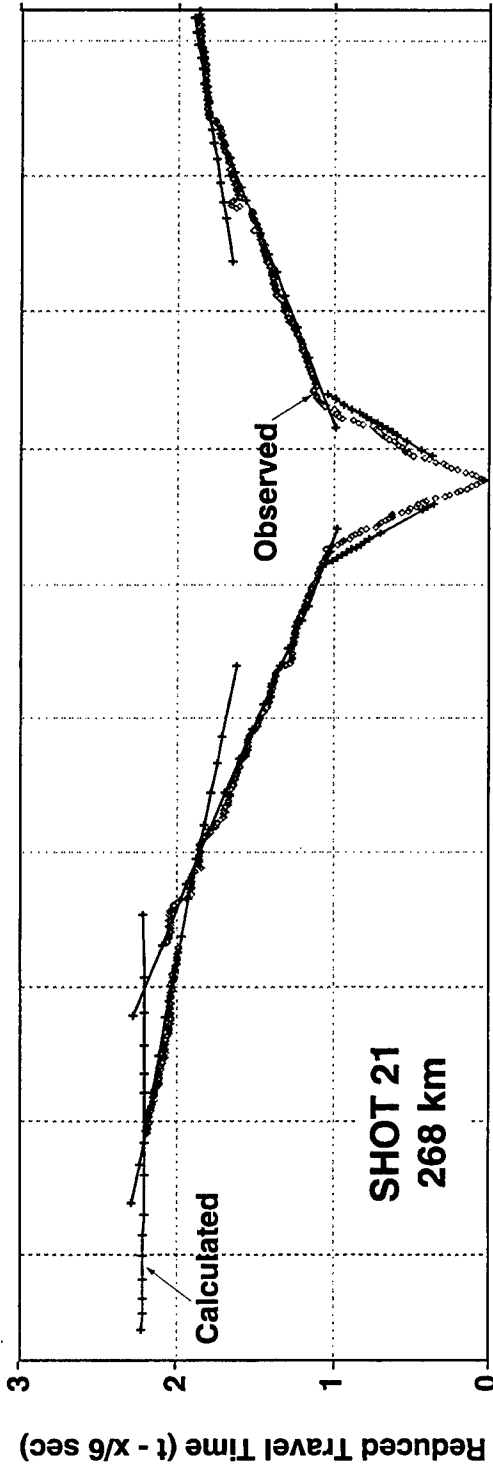


Figure 8d.

Permian time (Sawaf *et al.* 1993). The uppermost Ordovician, the Affendi formation (5.0 - 5.1 km s⁻¹), is clearly of higher velocity than the overlying rocks, presumably due to its predominately sandstone lithology. The Affendi formation shows thinning by around 2 km from south to north, again possibly due to uplift in northern Syria.

Below the Affendi formation is a 4.0 - 4.2 km s⁻¹ layer corresponding to the shaley Swab formation of Early Ordovician age deposited during the Llandeilian regression (Husseini 1990). Beneath the Swab is the lowest Ordovician formation, the Khanasser, a predominately quartzitic sandstone unit with correspondingly high seismic velocity of 5.5 - 5.6 km s⁻¹. The Khanasser formation, combined with the Upper Cambrian sediments, show a thickening of around 1.7 km from south to north. This observation corresponds with the map of Husseini (1989) that shows isopachs of these units following the edge of the Arabian plate, with thickening of the Upper Cambrian/Lower Ordovician sediments away from the center of the Arabian platform towards the Tethys Ocean to the northeast.

Global sea-level rise in the Early to Mid-Cambrian caused the deposition of an extensive carbonate layer, the Mid-Cambrian Burj limestone, throughout Syria. Due to the high impedance contrast with the surrounding clastic rocks, this horizon forms a prominent reflection event which is correlated across much of the country (e.g. Figure 6b). However, perhaps because of the limited thickness of this unit (< 200 meters), no definitive refraction arrivals are observed from the Burj formation. Thus reflection times from seismic data have been combined with the velocity model to give an approximate position of the Burj limestone within the model (Figure 7b).

Thinning of the strata between the Burj limestone and basement rocks by more than 2 km from the south to the north is observed (Figure 7b). This extensive thickness of Lower Cambrian / Precambrian clastics to the south of the Euphrates could be a consequence of pre-Mid-Cambrian rifting and subsidence. It is thought that during the Early Cambrian (600 - 540 Ma) the Arabian plate underwent NW-SE crustal extension (e.g. Husseini 1988, 1989; Cater & Tunbridge 1992). This rifting is evidenced in the extensive evaporite basins of Pakistan, Oman and the Arabian Gulf region, and rifting farther to the northwest is possible.

Seber *et al.* (1993), using similar refraction data, also established a thickened pre-Mid-Cambrian section in south-central Syria, as did the gravity interpretation of Best *et al.* (1990) which showed the likelihood of thickened Lower Paleozoic / Precambrian sediments to the south of the Palmyrides. These observations could show that the Early Cambrian rifting was extensive across southern Syria whilst the north of the country remained structurally high.

An alternative, better supported, explanation for the thickened pre-Mid-Cambrian section in the south, could be that the Euphrates trend formed a suture / shear zone caused by the Proterozoic accretion of the Arabian plate. This idea is expanded upon in the Precambrian discussion below.

Overall, the thickness of the pre-Mesozoic sedimentary section demonstrated here is

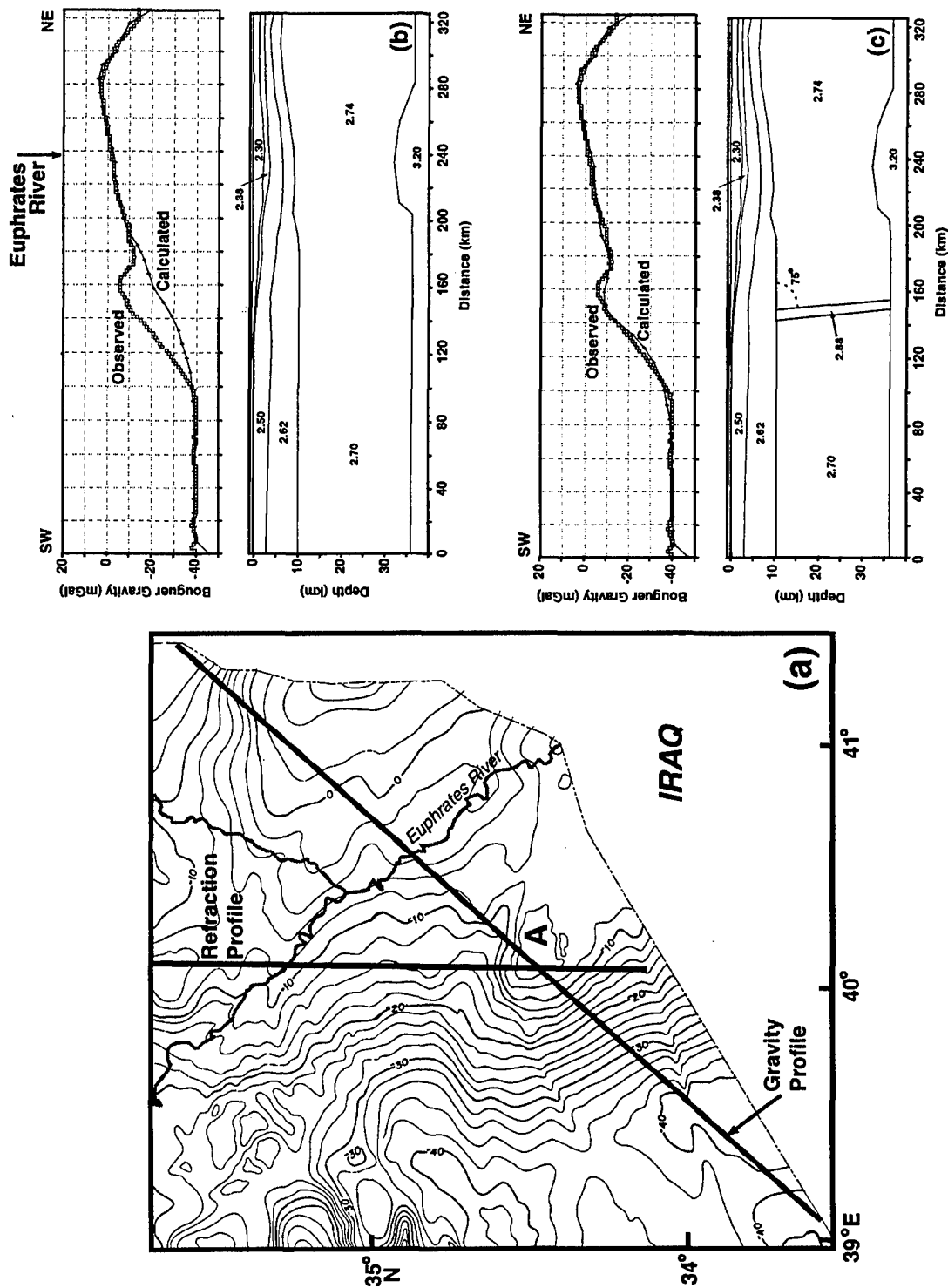


Figure 9. (a) Map showing Bouguer gravity anomalies in southeastern Syria across the Euphrates graben system. Bouguer reduction density = 2.53 kg m⁻³. Contour interval 2 mGal. (b) Gravity model to explain gross trends in gravity anomalies. Gravity high to NE of Euphrates modeled using shallower basement and a reduction in crustal / upper mantle density contrast. (c) Refinement of the model in which gravity high 'A' in (a) is modeled with dipping high-density body in crust.

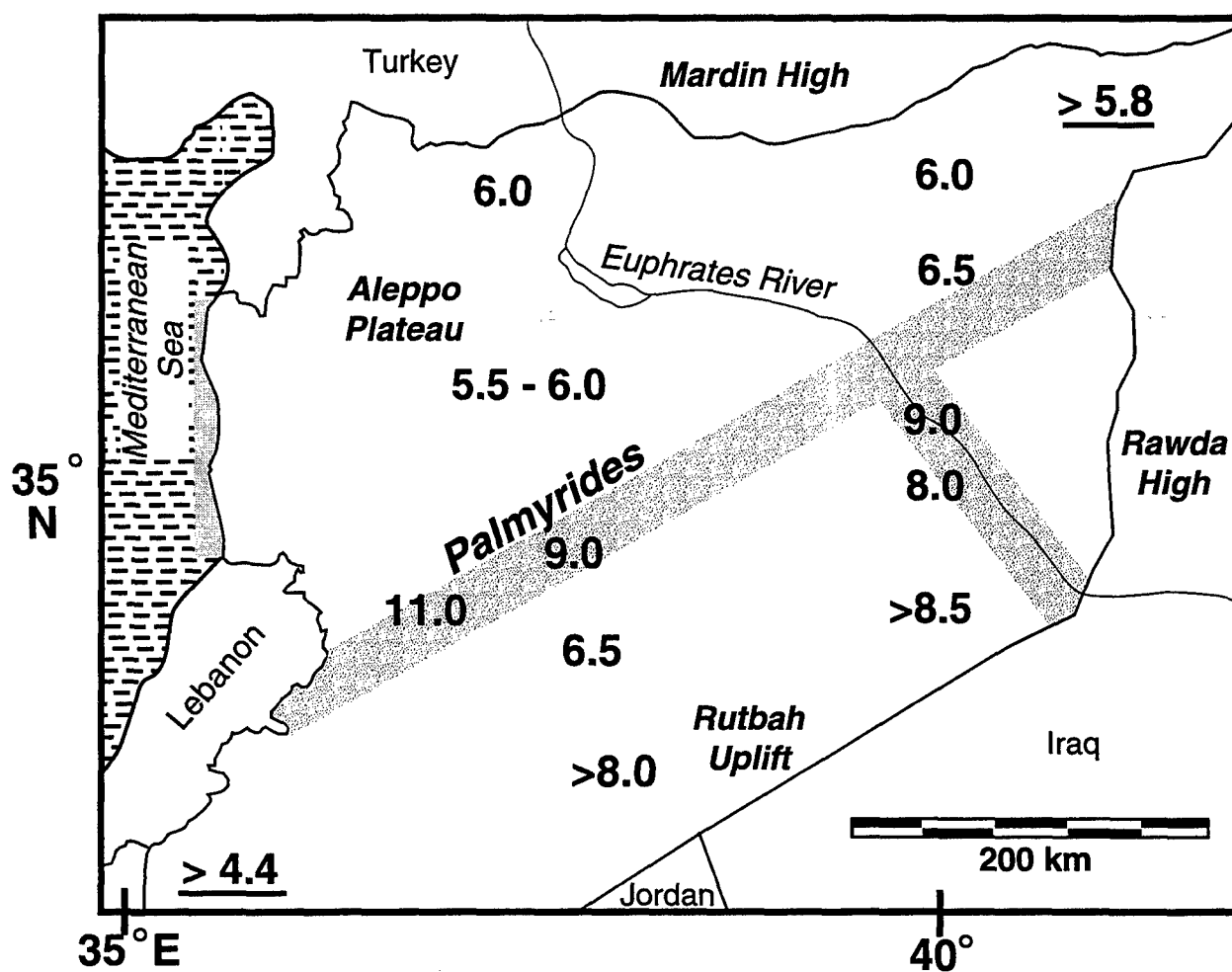


Figure 10. Map showing basement depths in Syria in kilometers below surface. Results from this study and previous refraction interpretation of Seber et al. (1993). Underlined data points are from selected deep well data. Shading represents locations of possible suture / shear zones.

significantly greater, by more than 3 km in places, than any previous estimates. These observations have important economic implications since extensive Paleozoic clastic reservoir rocks and source rocks are known to exist in eastern Syria and elsewhere in the Middle East (e.g. Hussein 1990). As emphasized in the regional summary of Beydoun (1991), Paleozoic plays are likely to be a significant factor in future Middle East hydrocarbon production.

Precambrian

Although no wells penetrate basement rocks in Syria and basement has not been unambiguously identified on seismic reflection sections, previous refraction studies (Ginzburg *et al.* 1979; El-Isa *et al.* 1987; Seber *et al.* 1993) have established basement velocities to be around 6 km s⁻¹. Therefore, we assume the velocity layer of 6 km s⁻¹ in the velocity model represents basement (Figure 7a). Across the Rutbah uplift in the far south of the profile, basement depth is at least 8.5 km. Along the southern margin of the Euphrates fault system we have definitive refraction arrivals that put the basement at 8 km below surface. North of this region, the basement deepens through faulting into the deepest part of the Euphrates graben system, where basement depth is around 9 km. To the north of the Euphrates basement depth is around 6 km.

Although previous investigations are consistent with these general trends in basement depth (Lovelock 1984; Leonov *et al.* 1989; Best *et al.* 1993), our interpretation generally puts basement somewhat deeper than the earlier suggestions. This is particularly true in the Rutbah uplift where the estimates of both Lovelock (1984) and Leonov *et al.* (1989) suggest basement depth at least 3 km shallower than the new results.

The obvious difference in basement depth on either side of the Euphrates graben system could be evidence of a terrane boundary along the Euphrates trend. The Arabian shield (Figure 1) accreted from discrete crustal blocks during the Late Proterozoic (e.g. Fleck *et al.* 1980; Pallister *et al.* 1987; Stoesser & Camp 1985; Vail 1985) and it is thought that similar processes might have formed the northern Arabian platform. Zones of weakness inherited from the accretion might control regional tectonics in the platform (e.g. Barazangi *et al.* 1993; Best *et al.* 1993, Litak *et al.* 1996a), but thick sedimentary cover across the region makes such ideas difficult to prove. The stark difference in basement depth across the Euphrates could be an indication of two different crustal blocks accreting somewhat to the southwest of what is now the Euphrates graben system. This accretion could have been in the form of a suture zone, a shear zone, or some combination of the two - current data do not allow the definition of the precise mechanism. The possible accretion event in Syria would have to be Proterozoic, or very early Phanerozoic, in age since seismic reflections from the Mid-Cambrian Burj limestone (e.g. Figure 6b) are continuous across most of Syria (e.g. Best *et al.* 1993).

This accretionary hypothesis, previously implied by Best *et al.* (1993) and Sawaf *et al.* (1993), is also consistent with gravity investigations. Bouguer gravity observations (BEICIP 1975) show a clear difference across the Euphrates with generally high gravity values to the northeast, and lower values to the southwest of the graben system (Figure 9a). We model a profile across these observations, constraining the upper structure of the

model in accordance with seismic reflection interpretation, and changing the deep crustal structure to obtain the best fit with the gravity values. Densities are constrained in the upper section by well logs from the El Madabe and Thayyem wells (Figure 2).

Figure 9(b) shows a geological model that accounts for the gross trends in the gravity observations. The difference in gravity values on either side of the Euphrates is modeled by invoking differences in the density of basement and lower crustal rocks, and by differences in basement depth (as derived from our refraction modeling). Even though maximum basement depth to the southwest is largely unconstrained, modeling the large scale gravity anomaly with variations in basement depth alone is not plausible, and a crustal density contrast is required. In this model (Figure 9b) the difference in crustal density and basement depth on opposite sides of the Euphrates supports the suture / shear zone hypothesis. Previous gravity models (e.g. Best, Wilburt & Watkins 1973; Gibb & Thomas 1976) show that, in a wide variety of settings, crustal density contrasts are a common feature of suture zones. The Euphrates graben is in isostatic equilibrium, compensated by an elevated Moho. It is interesting to note that the gravity observations also tend to refute the Early Cambrian / Late Proterozoic rifting hypothesis discussed in the previous section. The gravity observations do not support a thinning of the crust to the south, which one would expect in a rifted area.

Further gravity modeling (Figure 9c) attempts to explain the local gravity high on the southwest margin of the Euphrates (labeled 'A' in Figure 9a), which extends a considerable distance into Iraq to the southeast (not shown). Although a basement high is thought to exist in this area (based on seismic reflections from the Mid-Cambrian Burj reflector), no reasonable uplift of the basement could account for this significant gravity anomaly. The high could be explained by a dipping, high-density mafic body extending to Moho depth (Figure 9c). The location of this gravity high also appears to correspond with a magnetic anomaly from a deep source, perhaps further evidence for a mafic or ultramafic body at depth within the crust. The dip of the body shown in Figure 9c is fairly arbitrary, and many variations of this shape could be made to fit the observations. A similar high-density body was modeled by Hutchinson, Grow & Klitgord (1983) as part of their gravity interpretation of the Piedmont gravity gradient along a possible Appalachian suture zone.

Obviously, the gravity models presented here are highly non-unique (e.g. Hutchinson *et al.* 1983). Constant ambiguity exists between density and structure, for example, basement depth versus crustal density contrast. However, our gravity modeling appears to show that the hypothetical suture / shear zone across the Euphrates shares many features in common with other sutures documented elsewhere. Such a zone along the trend of the Euphrates graben could offer a unified explanation for various tectonic and geophysical observations in the area. The accretionary hypothesis lends considerable support to the ideas of Best *et al.* (1990, 1993) which were expanded upon by Litak *et al.* (1996a). These authors implied a regional NW-SE trend of weak zones beneath the northern Arabian platform, inherited from Proterozoic / Earliest Phanerozoic tectonics, amongst which is the Euphrates trend.

Incorporation of our results with those from other workers leads to a regional picture of basement depth and trends across much of Syria. Figure 10 shows our results, along with basement depths derived using similar data by Seber *et al.* (1993), and selected deep well data. We see a clear trend of deeper basement to the south of the Palmyrides and to the southwest of the Euphrates, and shallower basement to the north. The deepest basement is located actually beneath the Euphrates and Palmyride structures. The locations of possible suture / shear zones (modified from Best *et al.* 1993) are also shown. Whilst the suture / shear zones along the Euphrates and Palmyride trends have now been documented with gravity and refraction data, the zone to the northeast remains untested and is largely hypothetical.

Conclusions

Basement depth and the location of several deep sedimentary interfaces are mapped from the interpretation of seismic refraction data incorporated with seismic reflection data, well logs and potential field data. Thus, basement depth beneath eastern Syria is found to be greater, by between 1 and 3 km, than previously supposed. Across the Rutbah uplift the basement is at least 8.5 km deep, in the Euphrates depression it is around 9 km, and to the north of the Euphrates basement is between 5.5 and 6.5 km in depth (Figure 7). Hence, extensive thicknesses of pre-Mesozoic rocks are documented. Deeply penetrating faults are identified in the Euphrates graben system demonstrating the thick-skinned tectonic style of this region. Incorporation of results from previous research allows gross trends in basement depth across Syria to be presented (Figure 10).

Clearly different basement depths on the northern and southern sides of the Euphrates graben could be evidence for the Late Proterozoic accretion of the northern Arabian platform with the Euphrates fault system as a suture / shear zone. This idea is supported by gravity observations that suggest higher density crust to the northeast of the Euphrates trend - a common feature of other suture zones. This leads support to the speculation of a system of weak zones beneath the northern Arabian platform, inherited from Late Proterozoic / Early Cambrian accretion, which continue to control regional tectonics.

Acknowledgments. The data for this study were provided by the Syrian Petroleum Company. This research was supported by Arco, Exxon, Mobil and Unocal. Partial support was also sponsored by the U.S. Department of Energy Contract #F19628-95-C-0092. We thank A. Calvert, F. Gomez, E. Sandvol and W. Beauchamp, all of Cornell University, for their useful comments and suggestions.

References

- Al-Saad, D., Sawaf, T., Gebran, A., Barazangi, M., Best, J. & Chaimov, T., 1992. Crustal structure of central Syria: the intracontinental Palmyride Mountain belt, *Tectonophysics*, **207**, 345-358.

- Alsdorf, D., Barazangi, M., Litak, R., Seber, D., Sawaf, T. & Al-Saad, D., 1995. The intraplate Euphrates depression-Palmyrides mountain belt junction and relationship to Arabian plate boundary tectonics, *Annali Di Geofisica*, **38**, 385-397.
- Barazangi, M., Seber, D., Al-Saad, D. & Sawaf, T., 1992. Structure of the intracontinental Palmyride mountain belt in Syria and its relationship to nearby Arabian plate boundaries, *Bulletin of Earth Sciences, Cukurova University, Adana, Turkey*, **20**, 111-118.
- Barazangi, M., Seber, D., Chaimov, T., Best, J., Litak, R., Al-Saad, D. & Sawaf, T., 1993. Tectonic evolution of the northern Arabian plate in western Syria. In *Recent evolution and Seismicity of the Mediterranean Region*, edited by E. Boschi *et al*, 117-140. Netherlands: Kluwer Academic Publishers.
- BEICIP, 1975. *Gravity maps of Syria: Damascus (Syria)*, Bur. Etud. Ind. Coop. Inst. Fr. Pet., Hauts de Seine, 96 pp.
- Best, J. A., Barazangi, M., Al-Saad, D., Sawaf, T. & Gebran, A., 1990. Bouguer gravity trends and crustal structure of the Palmyride Mountain belt and surrounding northern Arabian platform in Syria, *Geology*, **18**, 1235-1239.
- Best, J. A., Barazangi, M., Al-Saad, D., Sawaf, T. & Gebran, A., 1993. Continental margin evolution of the northern Arabian platform in Syria, *Am. Assoc. Petrol. Geol. Bull.*, **77**, 173-193.
- Beydoun, Z. R., 1991. Arabian plate hydrocarbon geology and potential – a plate tectonic approach. In *Studies in Geology*, **77**. Tulsa, Oklahoma, USA: American Association of Petroleum Geologists.
- Cater, J. M. L. & Tunbridge, I. P., 1992. Paleozoic tectonic history of SE Turkey, *J. Petrol. Geol.*, **15**, 35-50.
- Chaimov, T., Barazangi, M., Al-Saad, D., Sawaf, T. & Gebran, A., 1990. Crustal shortening in the Palmyride fold belt, Syria, and implications for movement along the Dead Sea fault system, *Tectonics*, **9**, 1369-1386.
- de Ruiter, R. S. C., Lovelock, P. E. R. & Nabulsi, N., 1994. The Euphrates graben, Eastern Syria: A new petroleum province in the northern Middle East. In *Geo '94, Middle East Petroleum Geosciences*, edited by Moujahed Al-Husseini, 357-368. Manama, Bahrain: Gulf PetroLink.
- El-Isa, Z., Mechie, J., Prodehl, C., Makris, J. & Rihm, R., 1987. A crustal structure study of Jordan derived from seismic refraction data, *Tectonophysics*, **138**, 235-253.
- Filatov, V. & Krasnov, A., 1959. *On aeromagnetic surveys carried out over the Syrian territory, the United Arab Republic during 1958-1959*, (Unpublished), Technoexport, Damascus, 33 pp.
- Fleck, R. J., Greenwood, W. R., Hadley, D. G., Anderson, R. E. & Schmidt, D. L., 1980. Rubidium-Strontium geochronology and plate-tectonic evolution of the southern part of the Arabian shield, *US Geol. Sur. Professional Paper*, **1131**, 38 pp.
- Gibb, R. A. & Thomas, M. D., 1976. Gravity signature of fossil plate boundaries in the Canadian shield, *Nature*, **262**, 199-200.
- Ginzburg, A., Markris, J., Fuchs, K., Prodehl, C., Kaminski, W., & Amitai, U., 1979. A seismic study of the crust and upper mantle of the Jordan-Dead Sea rift and their transition toward the Mediterranean Sea, *J. geophys. Res.*, **84**, 1569-1582.
- Hutchinson, D. R., Grow, J. A. & Klitgord, K. D., 1983. Crustal structure beneath the southern Appalachians: nonuniqueness of gravity modeling. *Geology*, **11**, 611-615.

- Husseini, M., 1988. The Arabian Infracambrian extensional system, *Tectonophysics*, **148**, 93-103.
- Husseini, M. I., 1989. Tectonic and deposition model of late Precambrian-Cambrian Arabian and adjoining plates, *Am. Assoc. Petrol. Geol. Bull.*, **73**, 1117-1131.
- Husseini, M. I., 1990. The Cambro-Ordovician Arabian and adjoining plates: A glacio-eustatic model, *J. Petrol. Geol.*, **13**, 276-288.
- Kaila, K. L., Tewari, H. C. & Krishna, 1981. An indirect method for determining the thickness of a low-velocity layer underlying a high velocity layer, *Geophysics*, **46**, 1003-1008.
- Leonov, Y. G., Sigachev, S. P., Otri, M., Yusef, A., Zaza, T. & Sawaf, T., 1989. New data on the Paleozoic complex of the platform cover of Syria, *Geotectonics*, **23**, 538-542.
- Litak, R. K., Barazangi, M., Beauchamp, W., Seber, D., Brew, G., Sawaf, T. & Al-Youssef, W., 1996a. Mesozoic-Cenozoic Evolution of the Euphrates Fault System, Syria: Implications for Regional Kinematics, *Geol. Soc. Lon. J.*, **154**, 653-666, 1997
- Litak, R. K., Barazangi, M., Brew, G., Sawaf, T., Al-Imam, A. & Al-Youssef, W., 1996b. Structure and Evolution of the Petroliferous Euphrates Graben System, Southeast Syria, *Am. Assoc. Petrol. Geol. Bull.*, **82**, 1173-1190, 1998
- Lovelock, P. E. R., 1984. A review of the tectonics of the northern Middle East region, *Geol. Mag.*, **121**, 577-587.
- Luetgert, J. H., 1992. Interactive two-dimensional seismic ray-tracing for the Macintosh™, *US Geol. Sur., Open File Report 92-356*, Menlo Park, California
- McBride, J. H., Barazangi, M., Best, J., Al-Saad, D., Sawaf, T., Al-Otri, M. & Gebran, A., 1990. Seismic reflection structure of intracratonic Palmyride fold-thrust belt and surrounding Arabian platform, Syria, *Am. Assoc. Petrol. Geol. Bull.*, **74**, 238-259.
- Ouglanov, V., Tatlybayev, M. & Nutrobkin, V., 1974. *Report on seismic profiling in the Syrian Arab Republic*, (Unpublished, obtained privately from the Syrian Petroleum Company), General Petroleum Company Report, Aleppo, Syria, 73 pp.
- Pallister, J. S., Stacey, J. S., Fischer, L. B. & Premo, W. R., 1987. Arabian shield ophiolites and late Proterozoic microplate accretion, *Geology*, **15**, 320-323.
- Poley, J. Ph. & Nooteboom, 1966. Seismic refraction and screening by thin high-velocity layers (A scale model study). *Geophys. Prosp.*, **XIV**, 184-203.
- Ponikarov, V. P., 1967. *The geology of Syria: explanatory notes on the geological map of Syria, scale 1:500,000 part I: stratigraphy, igneous rocks and tectonics*, Damascus, Syrian Arab Republic, Ministry of Industry.
- Rosenbaum, J. H., 1965, Refraction arrivals through thin high-velocity layers. *Geophysics*, **30**, 204-212
- Sawaf, T., Al-Saad, D., Gebran, A., Barazangi, M., Best, J. A. & Chaimov, T., 1993. Structure and stratigraphy of eastern Syria across the Euphrates depression, *Tectonophysics*, **220**, 267-281.
- Seber, D., Barazangi, M., Chaimov, T., Al-Saad, D., Sawaf, T. & Khaddour, M., 1993. Upper crustal velocity structure and basement morphology beneath the intracontinental Palmyride fold-thrust belt and north Arabian platform in Syria, *Geophys. J. Int.*, **113**, 752-766.

- Sengor, A. M. C. & Kidd, W. S. F., 1979. Post-collisional tectonics of the Turkish-Iranian plateau and a comparison with Tibet, *Tectonophysics*, **55**, 361-376.
- Sengor, A. M. C. & Yilmaz, Y., 1981. Tethyan evolution of Turkey: A Plate tectonic approach, *Tectonophysics*, **75**, 181-241.
- Stoesser, D. B. & Camp, V. E., 1985. Pan-African microplate accretion of the Arabian shield, *Geol. Soc. Am. Bull.*, **96**, 817-826.
- Vail, J. R., 1985. Pan-African (late Precambrian) tectonic terrains and the reconstruction of the Arabian-Nubian Shield, *Geology*, **13**, 839-842.

D. AN INTEGRATED GEOPHYSICAL INVESTIGATION OF RECENT SEISMICITY IN THE AL-HOCEIMA REGION OF NORTH MOROCCO

Abstract

Data produced by the Moroccan national seismological network and marine seismic reflection profiles are used to investigate the most seismically active region in Morocco, located on the Mediterranean coast at the intersection of the Rif mountain belt and the submarine Alboran Ridge. This region, in the vicinity of the city of Al-Hoceima, marks an east-west transition in the marine and land deformation styles of the distributed plate boundary between Africa and Iberia, and was the site of a $M_w=6.0$ earthquake on May 26, 1994.

The epicenter of the Al-Hoceima earthquake is relocated onshore, refining the initial submarine location close to the Alboran Ridge. The spatial distribution of foreshocks and aftershocks shows a NE-SW trend that continues partly offshore and is subparallel to the earlier, yet still prominent, Miocene geologic structural trend. The predominantly strike-slip focal mechanism for the Al-Hoceima event is characteristic of earthquakes in the region. Marine seismic reflection profiles, which intersect the offshore region of seismicity, image active high angle faults with possible strike-slip components. The seismicity trend is not directly related to the submarine Alboran Ridge or the geomorphologically prominent Nekor fault. Deformation appears to be occurring on a number of subsidiary strike-slip faults that together compose a NE-SW zone of distributed shear.

The distributed strike-slip and documented normal faulting taking place in the eastern Rif mountains, although characteristic of the Rif region, are in contrast to the thrusting style of deformation that occurs farther to the east in the Algerian Tell Atlas. This may be related to the reported lateral variations and evolution of the convergent plate boundary in these regions during the Neogene and Quaternary times.

Introduction

The northerly expansion of the Moroccan National Seismological Network in 1993 and the subsequent $M_w = 6.0$ earthquake on May 26, 1994 in the vicinity of the city of Al-Hoceima (Figure 1) (hereafter referred to as the Al-Hoceima earthquake) provides the first opportunity for a detailed study of large-scale seismic deformation occurring in the Moroccan portion of the diffuse plate boundary between Iberia and west Africa. The Al-Hoceima region, situated on the Moroccan coast near the eastern termination of the Rif mountain belt and the western termination of the submarine Alboran Ridge, is acknowledged to be the most seismically active region in Morocco (e.g., Cherkaoui, 1991) and has been identified as key to the understanding of the Moroccan margin (Tesson *et al.*, 1987).

In this paper, we give a brief summary of the evolution of this enigmatic, complex plate boundary and the structure and possible evolution of the Al-Hoceima region, and we interpret the results of the relocation of the recent earthquakes using digital data collected by the Moroccan seismological network in both a local and regional context. The distribution of seismicity and its relationship to potentially seismogenic structures is

examined, and seismic reflection profiles collected over the marine extensions of these structures are used to study the geometry of faults at depth. A kinematic model is proposed for the development of the Al-Hoceima region. The similarities and differences between the Al-Hoceima earthquake and other large events that have occurred on the North African margin are discussed as well as the relationship of these observations to the geodynamic models that have been proposed for the Alboran region.

Tectonic Summary

The Alboran region, consisting of the Alboran Sea and the bounding Rif and Betic mountain belts, represents the westernmost limit of the Alpine orogenic belt. The region has experienced a complex deformation history, and the recent diffuse seismicity (e.g., see Figure 1b; Medina and Cherkaoui, 1992; Seber *et al.*, 1996) testifies to its continuation today. Attempts to explain the striking topographic (Fig. 1a), geological and geophysical N-S symmetry of the region (e.g., Seber *et al.*, 1996) and apparent synchronous subsidence of the Alboran Sea basin and uplift of the Betic and Rif mountain belts during the Miocene have led to the proposal of diverse geodynamic models, including trapped microplates (Andrieux *et al.*, 1971), retreating subduction zones (Royden, 1993), mantle diapirs (Loomis, 1975), and delamination/collapse (Platt and Vissers, 1989; Watts *et al.*, 1993; Docherty and Banda, 1995; Seber *et al.*, 1996).

The Alboran basin is floored by thinned continental crust (e.g., Hsü and Ryan, 1973; Comas *et al.*, 1995) with a thickness of ~17 km and is underlain by anomalous uppermost mantle (W.G.D.S.S.A.S., 1978). The western section has undergone significant amounts of subsidence with Neogene stratigraphic thicknesses reaching 7 km (Comas *et al.*, 1992) but exhibits only limited faulting, and has the geometry of a thermal sag basin (Morley, 1992). East of approximately 4° W the seafloor becomes significantly more irregular due to faulting and scattered Neogene volcanism (Tesson *et al.*, 1987). The dominant submarine feature is the northeast-southwest trending Alboran Ridge (see Figure 1a). Various models have been proposed for the origin of this relief, including uplift as a horst block (Comas *et al.*, 1992), sedimentary cover pierced by volcanic intrusions (Giermann *et al.*, 1964; Horvarth and Berckhemer, 1982) or a transpressive structure (Bourgois *et al.*, 1992; Woodside and Maldonado, 1992). Magmatic processes clearly play a role in the development of the ridge, its only subaerial exposure being the volcanic Alboran Island (dated as Miocene (7-18 Ma) in age by Apericio *et al.* (1991) (A.I. on Figure 1).

The Alboran Sea is bounded on three sides by the arcuate Moroccan Rif and Spanish Betic alpine-style fold and thrust belts. The Rif can be divided into three tectonic zones, the Internal Rif, External Rif and the Pre-Rif (Figure 1a) (Choubert and Faure-Muret, 1974). The Al-Hoceima region is located between the Jebha and Nekor strike-slip faults (Figure 2a), two major structural elements in the Rif. Both of these faults are interpreted to have left-lateral offsets of approximately 50 km (Leblanc and Olivier, 1984; Olivier, 1982). The Jebha fault was active from late Paleogene (Oligocene, possibly Eocene) to early Miocene (Burdigalian), resulting in the emplacement of the major Internal Rif unit (Leblanc *et al.*, 1984). Leblanc *et al.* (1984) suggested that the Jebha fault may continue offshore, along the Alboran Ridge, but such a connection has not been identified on seismic reflection data (Bourgois *et al.*, 1992). Strike-slip movement along the Nekor

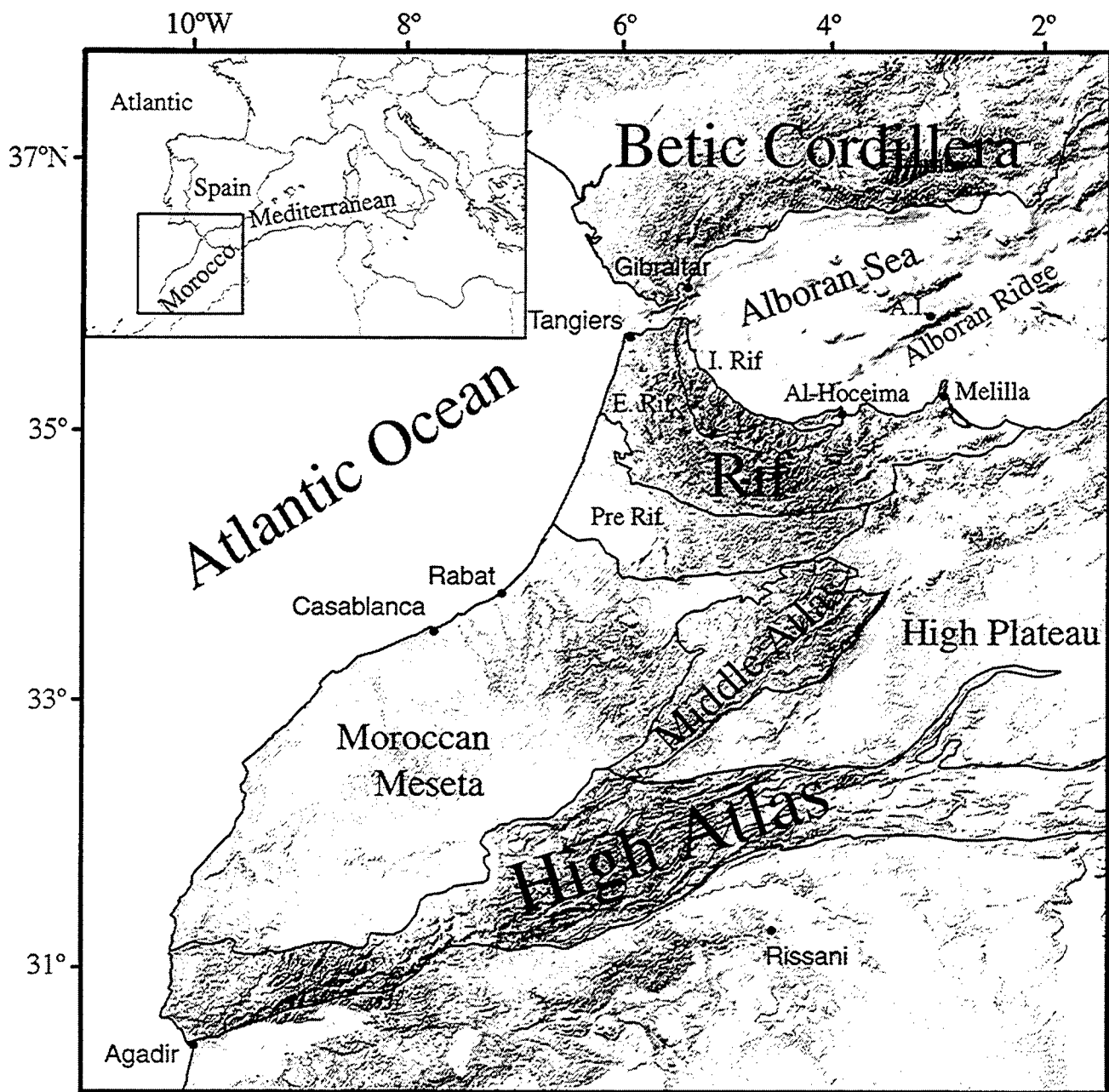


Figure 1a. Map showing north Morocco and the Alboran region: Alboran Island (A.I.), Internal Rif (I. Rif), External Rif (E. Rif). Note the differences in the seafloor morphology of the Alboran Sea between the regions east and west of approximately 4 ° W.

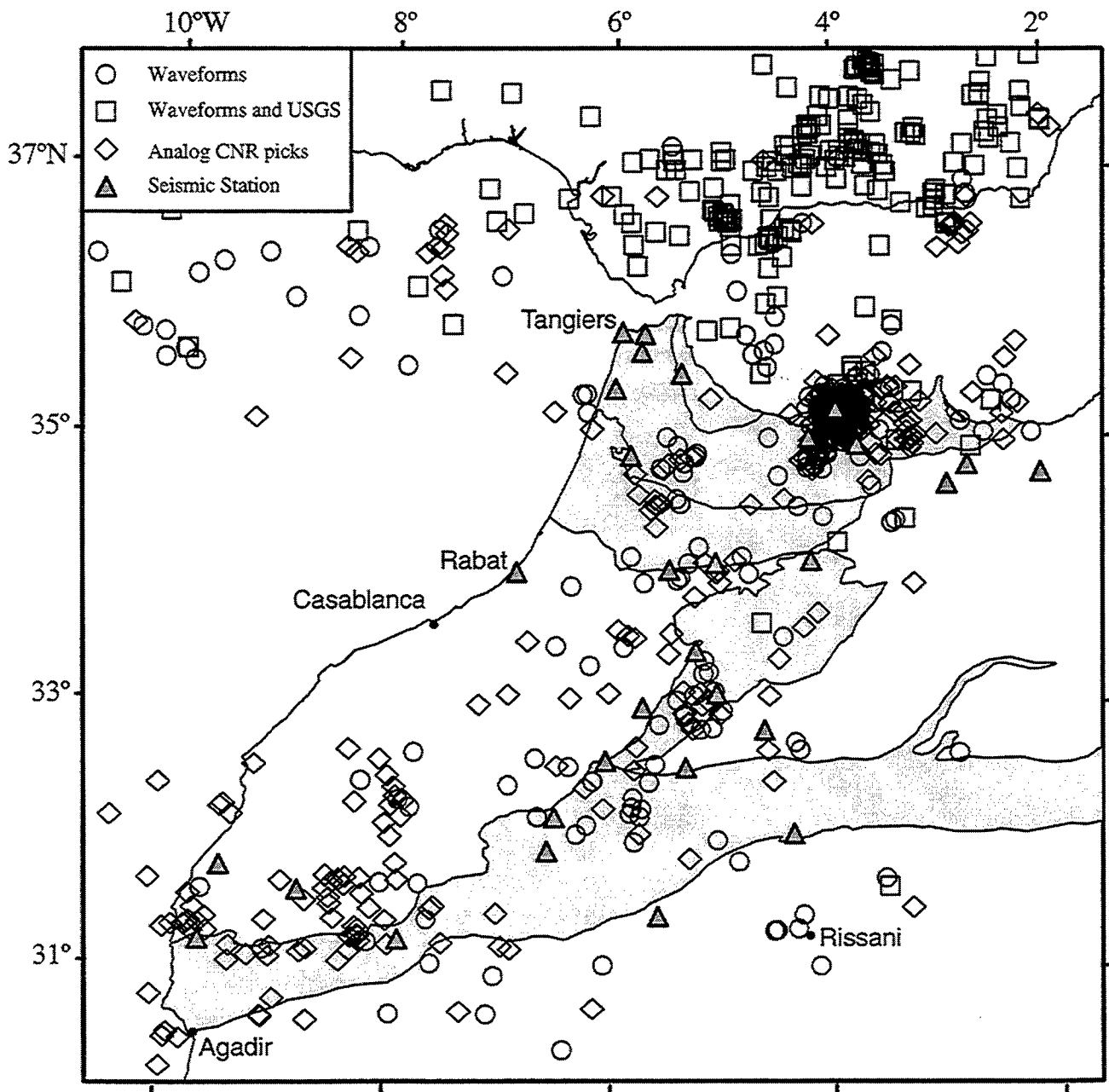


Figure 1b. Seismicity map of Morocco and Alboran region (1989-1995), and stations of the Moroccan National Seismological Network (filled triangles). Earthquakes were located using arrivals read from digital waveforms recorded by the network alone (circles), supplemented by USGS PDE readings (squares) (Seber et al., 1996), and reported in CNCPRST Seismological Bulletin (phases read from analog records) (diamonds). The Rif and Atlas mountain systems are shaded (see Fig. 1a).

fault in the Late Miocene (Tortonian) resulted in the WSW transport of the Rif (Leblanc, 1990). Further strike-slip movement and subsequent thrusting along relatively minor faults resulted in the emplacement of the southern section of the Internal Rif (Bokkoya unit) and the Tiziren nappe and Ketama metamorphic flysch units (Figure 2a) (Morel, 1989). Today the Nekor fault has a pronounced topographic expression (see Figure 2b), but no evidence of Quaternary slip along the Boudinar Basin section of the fault has been documented, and the fault could not be identified on seismic reflection profiles that cross its offshore projection (Gensous *et al.*, 1986). Meghraoui *et al.* (1996) report slip rates of 2 mm/yr on the Nekor and Jebha faults; however, it is not clear along which sections of the faults these slip rates were determined.

The Al-Hoceima region is fractured by distributed NE-SW to N-S striking high angle faults that exhibit apparent left-lateral strike-slip offsets and by a conjugate NW-SE oriented group of more minor faults with apparent right-lateral slip components (Ait Brahim *et al.*, 1990; Fetah *et al.*, 1987; Saadi *et al.*, 1984a). The lack of Plio-Quaternary cover prevents the determination of an accurate date for the most recent slip along these faults, but they do appear to offset the fault bounding the Tiziren and Ketama units. Quaternary structures documented as seismically active are the triangular Lower Nekor Basin (Figure 2a), bounded to the west by the Imzouren fault and to the east by the Trougout fault, and the N-S trending Jebel Hammam normal fault (Hatzfeld *et al.*, 1993). These faults are believed to have been active since the Late Miocene (Morel, 1989). The Lower Nekor basin is filled with ~400 meters of Quaternary sediments (Frizon de Lamotte, 1982), suggesting relatively recent subsidence. In contrast, Ras Tarf is reported by Meghraoui *et al.* (1996) to have been uplifted at an average rate of 2 mm/yr over the last 500 ka.

The structures visible in the Al-Hoceima region today are interpreted to result from changes in the principal stress direction from NE-SW in the Tortonian, to N-S at the Tortonian-Messinian boundary, to a Plio-Quaternary orientation of NNW-SSE (Ait Brahim, 1991; Medina, 1995). These proposed changes in the paleostress orientation are thought to result from variations in the gross relative plate motions of Africa and Iberia, perturbed by secondary processes (e.g., Ait Brahim, 1991). Plate reconstructions by Dewey *et al.* (1989) using mid-ocean ridge magnetic anomalies date a change in the motion of Africa relative to Eurasia from NNE-SSW to NW-SE in the Late Miocene. The NUVEL-1A (Demets *et al.*, 1994) plate motion model predicts continued NW-SE convergence of Africa and Eurasia today at a rate of 5 mm/yr when measured at 36°N, 4°W (center of Alboran Sea).

Seismological Observations

The earthquake locations presented in this paper were primarily determined using data produced by the Moroccan national network. The network coverage has continued to expand since installation began in 1989 with the most recent additions being stations PAL and TOU (1993) and JBB (1994) (Figure 2b) in the Al-Hoceima region. The network consists of short period (1 Hz) vertical-component seismometers linked by radio and telephone lines to the Centre National de Coordination et de Planification de la

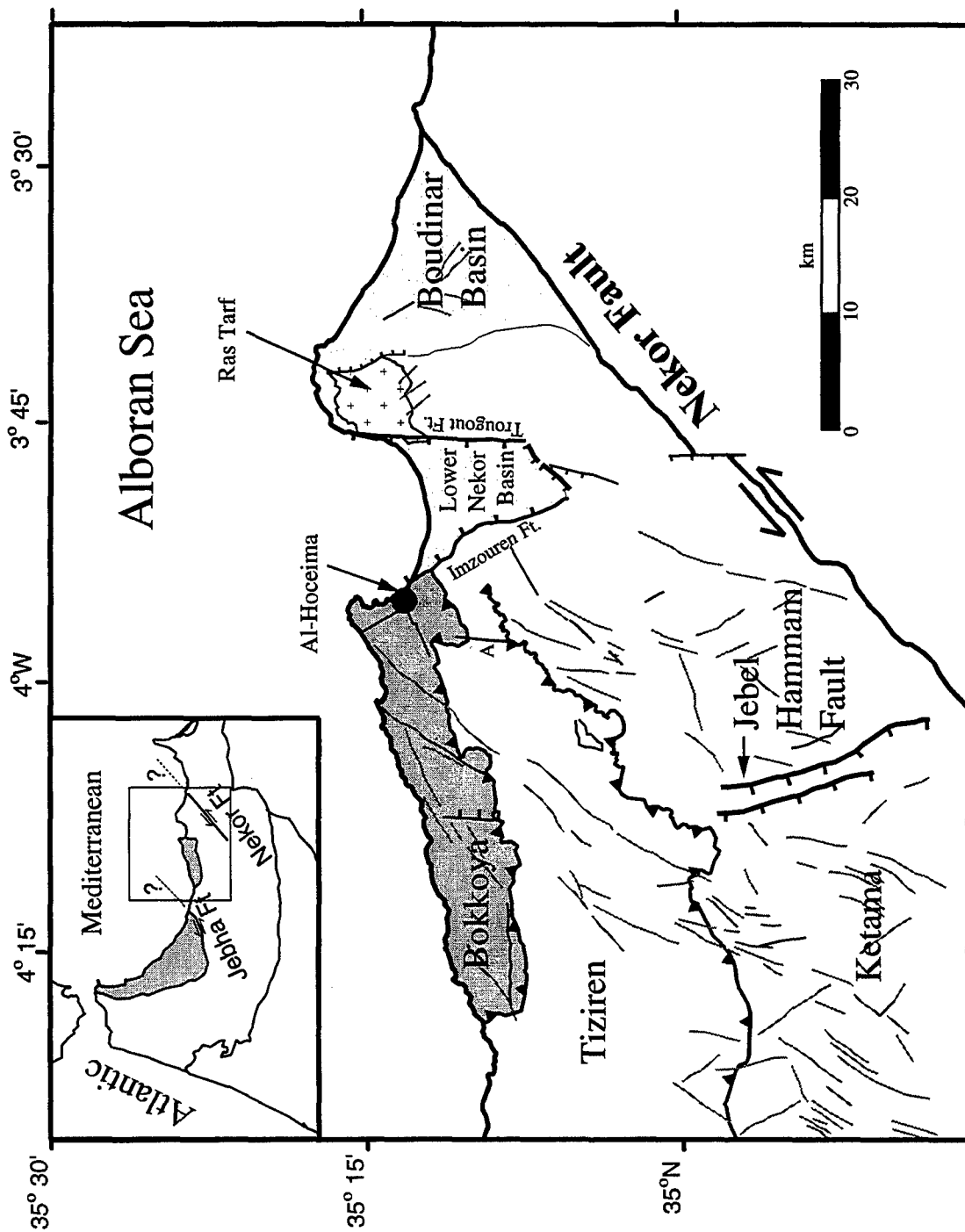


Figure 2a. Tectonic map of the Al-Hoceima region. Inset shows Jebha and Nekor faults. Internal Rif units are shaded. Major faults (black) were mapped from Thematic Mapper Landsat imagery, supplemented with 1:50,000 airphotos, and guided by geologic maps (1:50,000)(Fetah et al., 1987; Saadi et al., 1984a,b). Smaller faults (gray) digitized from Asebriy et al. (1993). A=Prominent lineament.

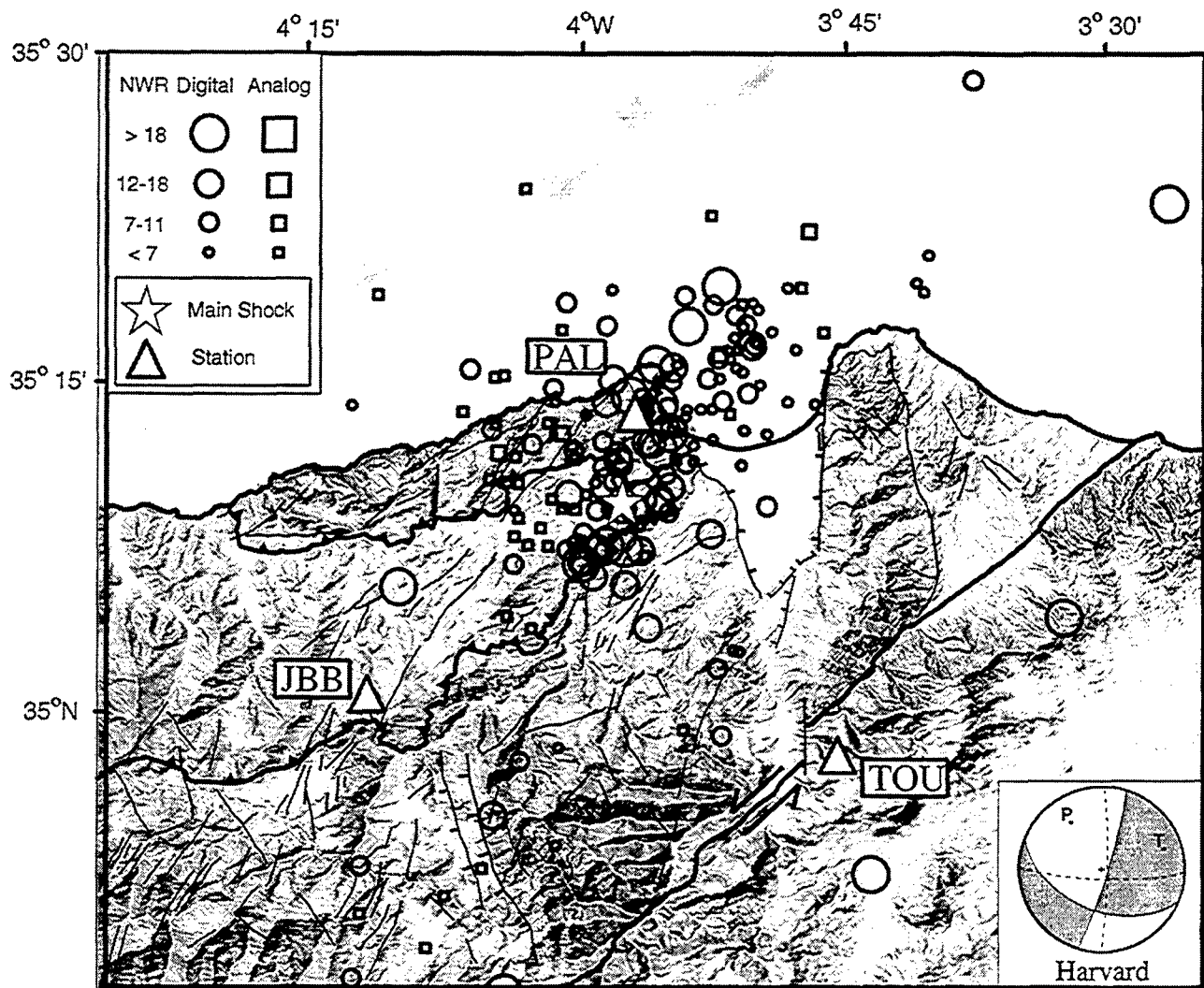


Figure 2b. Map showing location of the Al-Hoceima earthquake (May 26, 1994; $M_w=6.0$), associated seismicity (January 1994-June 1995), and Harvard CMT focal mechanism (with dashed nodal planes from USGS solution). Circles and squares denote locations determined using digital and analog records, respectively. The symbols are scaled by the number of arrivals contributing significantly to the location (NWR from Hypoinverse (see Klein, 1978)). PAL, TOU, and JBB are seismological stations (triangles). Shaded topography is based on a digital elevation model and bathymetry was digitized from the International Bathymetric Chart of the Mediterranean (I.O.C., 1981).

Recherche Scientifique et Technique (CNCPRST) in Rabat, where they are recorded in both analog and digital formats.

Figure 1b shows the epicenters of the most recent earthquakes (1989-1995), located using the data produced by the network, supplemented by phase readings from the USGS Preliminary Determination of Epicenter (PDE) bulletins. This map represents the most accurate locations presently available for earthquakes in Morocco. The crustal seismicity is not confined to linear belts either along the plate boundaries or in an intraplate setting. Significant levels of seismicity occur hundreds of kilometers from the diffuse plate boundary between Africa and Iberia. The seismicity tends to follow topographic trends, with concentrations in the Atlas, Betic, and Rif mountains. However, significant seismicity is also present in the relatively low-relief Moroccan Meseta and Pre Rif regions. Large events, such as two $M_b > 5$ earthquakes located near the town of Rissani (see Figure 1 for location) on October 23 and 30, 1992 even occur in what was considered the stable African platform. The map of recent seismicity (Figure 1b) is dominated by relatively minor clusters of events, especially the sequence associated with the 1994 Al-Hoceima earthquake. The Al-Hoceima region has historically been the site of large earthquakes (Ramdani *et al.*, 1989) and is the most seismically active region in Morocco, with the city reporting, on average, 2 to 3 intensity V (MSK) earthquakes per year (Cherkaoui, 1991). In May 1994, there was a marked increase in the seismicity of the area. However, owing to the lack of prior recordings, this was not interpreted as significant until after the $M_w=6.0$ event on May 26, 1994. A longer temporal record is required before changes in the level of background seismicity can be taken as an indication of an impending large earthquake. USGS PDE locations of the fore- and aftershocks delineate a broad NE-SW trending zone of seismicity extending from the Moroccan coast to the Alboran Ridge, with the main shock located off the coast of Morocco in close proximity to the Alboran Ridge. The ISC also located the epicenter offshore, approximately 4 km southwest of the PDE location. However, relocation of this event using arrival times from the Moroccan network (which did not report to the USGS at that time) places the epicenter onshore (35.159°N , 3.955°W at 4.4 km depth). Resolving the ambiguity in the location of the Al-Hoceima earthquake and associated shocks, and hence identifying possible seismogenic structures is of importance not only for the hazard assessment of Al-Hoceima, but also for improved understanding of the tectonic processes in this region.

The events in the Al-Hoceima sequence (January 1994 - June 1995) were relocated using the data from the Moroccan network in an effort to refine the PDE locations. P and S arrivals were picked from digital, and, where necessary, analog records. In addition to providing increased dynamic range and more precise arrival time picking, the digital records also allowed simple filtering to improve signal to noise ratios for small events. These filters were carefully checked to ensure that they did not introduce significant phase shifts to the data. The locations were determined using Hypoinverse (Klein, 1978) (Figure 2b), utilizing a 1-Dimensional velocity model adapted from a model proposed by Schwarz and Wigger (1988) on the basis of seismic refraction results.

Examination of location errors

The earthquake locations determined using the Moroccan national network, although similar in trend to USGS PDE locations, have an average displacement of 10 km to the SE, with the location of the main Al-Hoceima earthquake displaced by 20 km to the SE (Figure 3). The presence of nearby stations PAL, TOU, and JBB (Note: JBB only became operational on 10/94) (Figure 2b), renders the locations determined using the Moroccan network data relatively stable with respect to velocity models. To examine the sensitivity of the locations to the velocity model, the earthquakes were relocated using a number of simple three layer models (Layer 1: 0 to 5 ± 2.5 km, 5.0 km/s; Layer 2: 5 ± 2.5 to 30 ± 5 km, 6.0 km/s; Layer 3: 30 ± 5 km, 8.0 km/s), derived from refraction studies in the Alboran region (Hatzfeld and Ben Sari, 1977; Ben Sari, 1987; Tadili *et al.*, 1986; Ramdani and Tadili, 1988; Wigger *et al.*, 1992). Maximum shifts in the mean epicenter of 4 km and in the main shock epicenter of 6 km were obtained relative to the locations determined using the velocity model adapted from Schwarz and Wigger, with increased average RMS and standard horizontal and vertical errors. The velocity structure of the Alboran and Rif region is acknowledged to be heterogeneous (e.g., Blanco and Spakman, 1993; Seber *et al.*, 1996), with the Rifian crust thinning rapidly into the Alboran basin (W.G.D.S.S.A.S., 1978), and with zones of low velocity and high attenuation in the crust and uppermost mantle beneath the Rif region (Seber *et al.*, 1996). The average travel time residual for stations recording the Al-Hoceima sequence are all within one standard deviation of zero suggesting that there are no significant velocity variations across the Moroccan network relative to the 1-D velocity model used for the locations. The majority of stations used for the PDE locations are situated on the Spanish mainland on the opposite side of the Alboran Sea; the closest PDE station is situated 90 km away in the Spanish enclave of Mellila (See Figure 1a for location). In contrast, over 85% of the locations reported in this study were determined using stations PAL and TOU with average station-epicenter separations of 13 km and 37 km, respectively. Given the above facts, and from discussions with USGS seismologists (S. Koyanagi, USGS/NEIC, personal communication), we believe that the location of the Al-Hoceima sequence in an area of anomalous velocities, coupled with a relative dearth of seismic stations on the African continent for good azimuthal control, has lead to a systematic offset in the PDE locations. Unfortunately, owing to absolute timing problems, the digital readings from the Moroccan network during the Al-Hoceima earthquake sequence are an independent dataset. They cannot be merged with readings from surrounding countries to improve the available azimuthal coverage.

The effect of the distribution of Moroccan stations must also be considered. The majority of the stations are situated to the south of the Al-Hoceima region, and the smaller events are only recorded by a limited number of stations resulting in an average azimuthal gap in station coverage of 200 degrees. A particular concern is whether secondary RMS travel time residual (hereafter referred to simply as RMS) minima could exist that would not be identified by conventional inversion methods, resulting in an inaccurate standard error estimate, and potentially in a mislocation of the event. It is also important to understand the nature of the trade-off between depth and epicentral location.

A grid-search method was implemented to study these aspects. Hypoinverse was modified to minimize the RMS by adjusting only the origin time while keeping the trial earthquake location fixed in space. Minimum RMS values for a given set of arrival time data were then determined for trial locations placed on a 3-dimensional grid with a horizontal interval of 0.01° and depth intervals of 1.5 km to a maximum depth of 18 km, yielding a 3-dimensional matrix of RMS values. Following the method described by Sambridge and Kennett (1986), these RMS values were scaled by introducing a function Φ defined by

$$\Phi(\mathbf{h}) = (n - 4) \frac{[\text{RMS}(\mathbf{h}) - \text{RMS}(\mathbf{h}_0)]}{\text{RMS}(\mathbf{h}_0)}$$

where $\text{RMS}(\mathbf{h}_0)$ is the minimum RMS corresponding to the solution hypocentral parameters (\mathbf{h}_0), $\text{RMS}(\mathbf{h})$ is the RMS corresponding to a trial set of hypocentral parameters (\mathbf{h}), and n is the number of degrees of freedom (discussed below). Surfaces of constant $\Phi(\mathbf{h})$ are taken to represent surfaces of constant confidence. The value of $\Phi(\mathbf{h})$ that corresponds to the 95% confidence surface is determined using a chi-squared distribution. The values of \mathbf{h} that fall within the 95% region satisfy

$$\Phi(\mathbf{h}) \leq \chi^2_4(0.95)$$

The correct value to choose for the number of degrees of freedom (n) in equation (1) is not immediately clear. Sambridge and Kennett (1986) set n equal to the number of observed arrival times. However, tests conducted by adding random noise (evenly distributed within ± 0.5 sec for P and ± 1 sec for S) to synthetic arrival times suggest that this results in an overly conservative estimate of the 95% confidence region for these data. The overestimation may be occurring because the RMS calculated by Hypoinverse is weighted using 4 parameters: observer defined quality of arrival, magnitude of the travel time residual, station-epicenter separation, and whether the arrival is P or S (weight is lowered if the arrival is an S). This weighting results in considerable flattening of the variation in RMS with trial hypocenter location and is modeled as introducing additional degrees of freedom. It was found that setting n equal to twice the number of arrivals produced confidence contours that provided a good fit to the distribution of synthetic locations. Figure 4 shows the result of applying this method to the well constrained Al-Hoceima earthquake (15 P and 3 S arrivals) and a poorly constrained (4 P and 3 S) aftershock recorded on June 2, 1994. Figure 4a illustrates that large events recorded by many stations have elliptical confidence contours, but the epicentral location is reasonably well constrained. Figure 4b shows that smaller, poorly constrained events have elongate confidence contours and may even have multiple minima. The 95% region calculated by Hypoinverse is in agreement with the synthetic data for events located using a large numbers of arrivals. However, for poorly constrained events Hypoinverse overestimates the location accuracy. The horizontal and vertical standard errors are calculated using a combination of both an assumed reading precision of ± 0.05 seconds and the RMS residual (see Klein, 1978). Both events exhibit a similar depth/surface location trade-off with depth increasing towards the NE. Synthetics were also used to investigate the sensitivity of locations to S picks. Unsurprisingly, S picks for the close

stations have the most significant effect on location. We are confident that the S wave picks made at near stations are true S wave arrivals and not converted phases.

The fact that the seismicity distribution and the direction of maximum epicentral uncertainty, especially for poorly located events, are both approximately NE-SW is certainly a cause for concern. However, the location of larger events recorded by many stations defines a NE-SW trend, and furthermore the USGS locations determined using phase readings from different stations with a different geometry also have an underlying NE-SW trend. Therefore, we interpret this trend to be real and not an artifact of the station distribution.

Seismicity of the Al-Hoceima region

The earthquake locations for the period January, 1994 to June 1995 (Figure 2b) have a general NE-SW trend and extend over 30 km with significant seismicity occurring offshore. There is no obvious temporal trend in the location of the earthquakes. Seismicity is concentrated immediately to the northwest of the NE-SW striking thrust separating the Tiziren and Ketama units (Figure 2a), becoming increasingly diffuse farther to the NW. Both the Harvard (Dziewonski *et al.*, 1995) and NEIC moment tensors determined for the main event (Figure 2b) indicate predominantly strike-slip movement with high angle NNE-SSW oriented sinistral, and ESE-WNW oriented dextral nodal planes. The impulsive first motions recorded by the Moroccan network and reported by the ISC are in general agreement with those predicted by these focal mechanisms.

Figure 5 shows the seismicity distribution in three dimensions and standard location errors ERH and ERZ calculated by Hypoinverse. The block faces show projections of the events onto N-S and E-W oriented planes. The lower panels show projections of the seismicity and main shock Harvard focal mechanism onto NW-SE (perpendicular to trend of seismicity) and NE-SW (parallel to trend of seismicity) oriented cross sections. The seismicity distribution is diffuse and does not contain any obvious planar features that might be interpreted as a fault plane. The NE-SW trend visible in map view is found to be related to a dipping pipe-type geometry when examined in 3 dimensions. Aside from a concentration of shallow events in Al-Hoceima bay, the distribution appears to be essentially linear, dipping towards the NE at an angle of 30° to a maximum depth of 15 km. Although it is tempting to overinterpret this distribution, we do not believe that there are a large enough number of well-located events to be confident that details of this depth distribution are well-constrained. However, we are confident that the seismicity has a NE-SW trend and is limited to the upper 20 km of the crust.

A NNE-SSW oriented fault plane is preferred based on the seismicity distribution and strike of surface faulting in the area (Figure 2a). A particularly prominent lineament visible on Thematic Mapper imagery and airphotos (marked by A on Figure 2a) apparently offsets the thrust bounding the Tiziren and Ketama units in the region of the Al-Hoceima earthquake and the greatest concentration of epicenters. This lineament has been interpreted as a left-lateral strike-slip fault by Ait Brahim (1991).

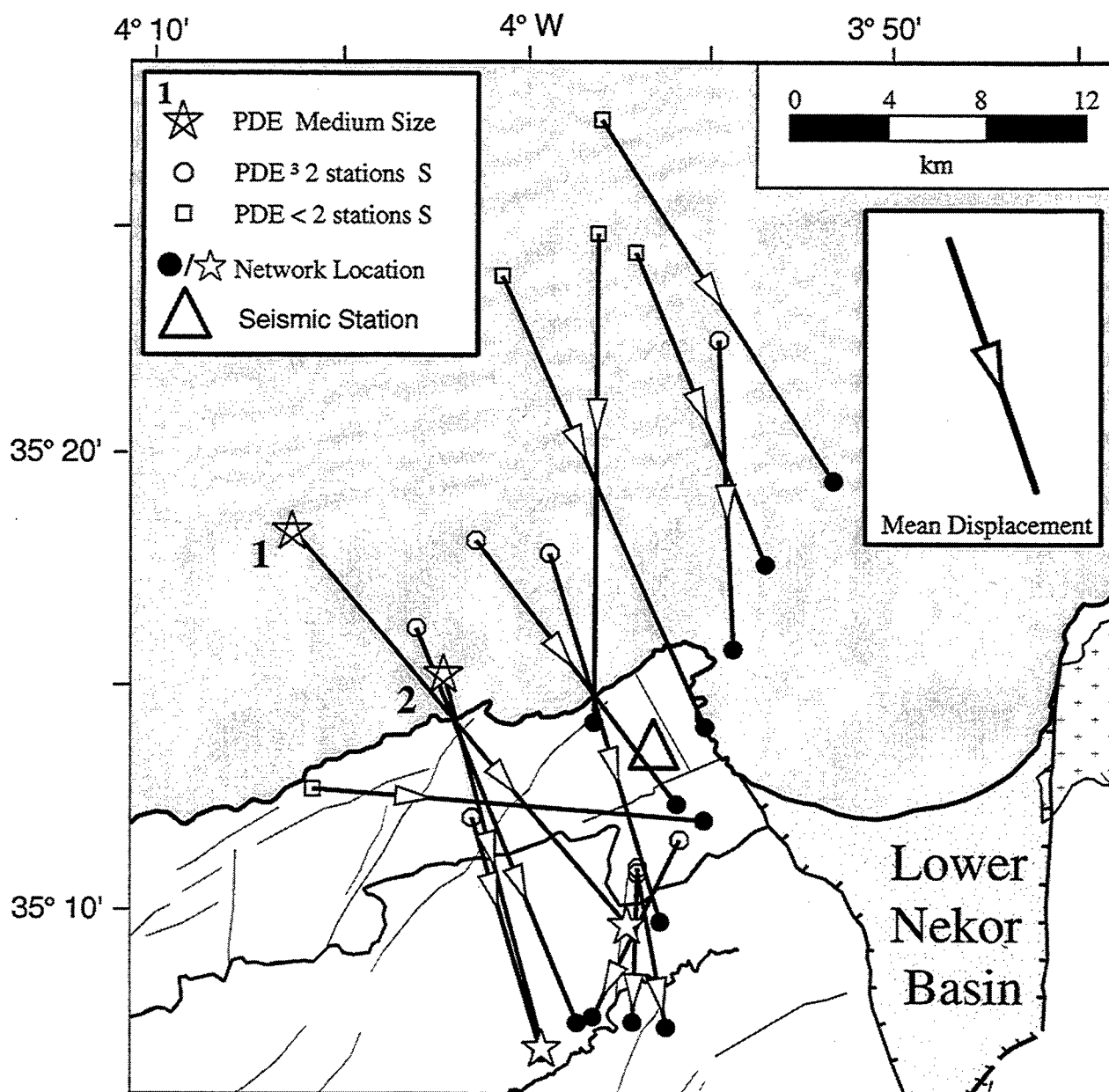


Figure 3. Comparison of USGS PDE locations to those determined using the Moroccan network. USGS locations are grouped by quality of azimuthal control into earthquakes recorded at: Teleseismic distances: (1) Al-Hoceima earthquake and (2) Largest aftershock (June 3, $M_b=4.6$) (stars), regional distances with two or more stations to the south of epicenter (octagon), and less than two stations to the south (squares). Mean vector for displacement of locations determined in this study relative to the PDE locations is shown. The apparent offset of the two distributions may be related to the anomalous seismic velocities in the region and to the limited station coverage available for the PDE locations.

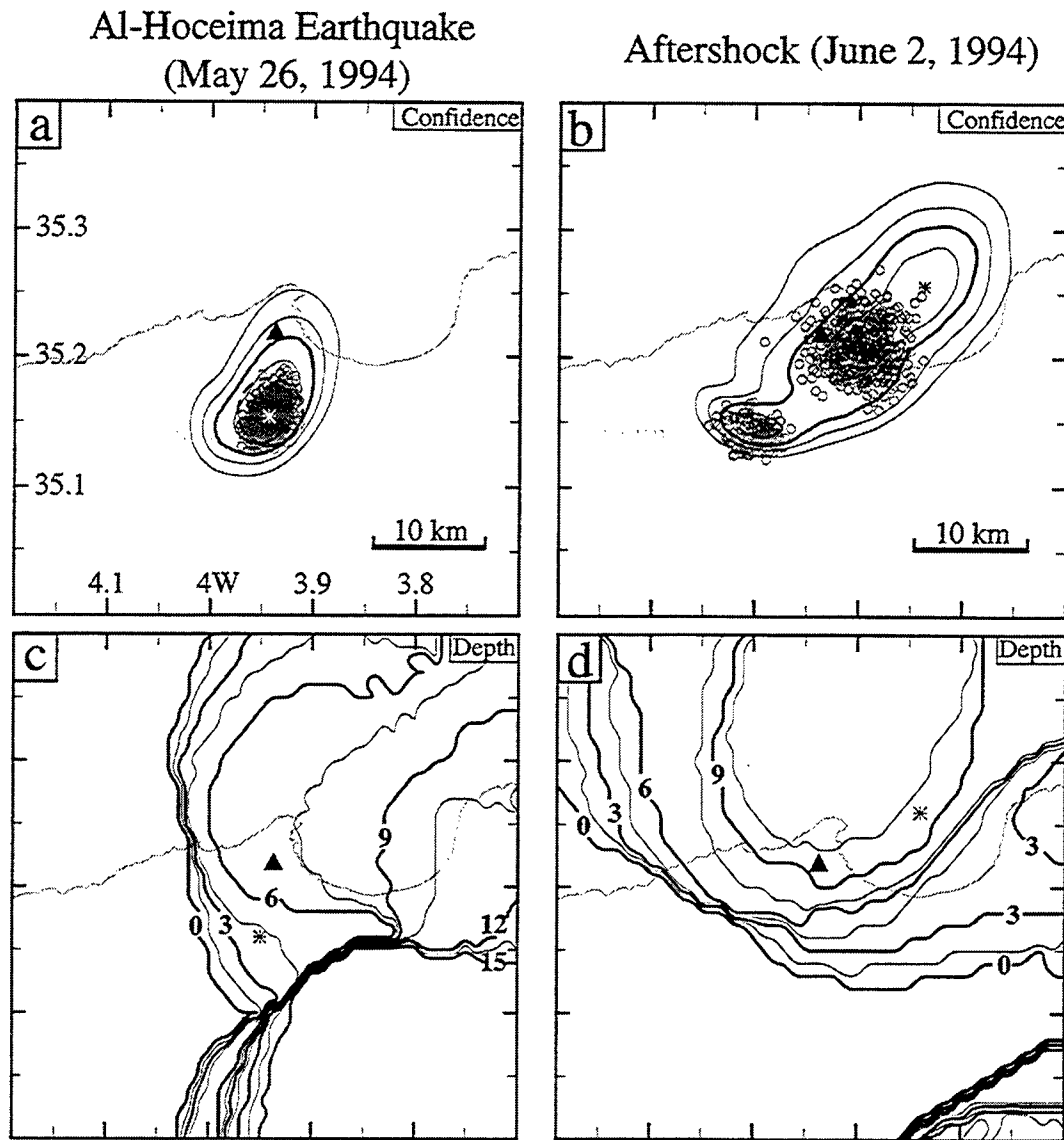


Figure 4. Results of applying a grid search method to the main Al-Hoceima earthquake (15 P and 3 S arrivals) and to a poorly constrained (4 P and 3 S) aftershock recorded on June 2, 1994. Figures 4a and 4b show contours of the 75% ,95% (bold), 99%, and 99.9% confidence regions for the epicenter based on the grid search. The dashed circle represents the 95% confidence region for the epicenter calculated by Hypoinverse. 500 relocations of a synthetic event at same location with random noise added to the arrival times (gray circles) give a further indication of the spread in possible locations. Figures 4c and 4d show contours of the best fit depth for a given trial epicentral location. The asterisk marks the earthquake location determined using the grid search. Large events are well constrained with elliptical confidence contours. Smaller events can be poorly constrained with elongate NE-SW trending minima owing to sparse station coverage.

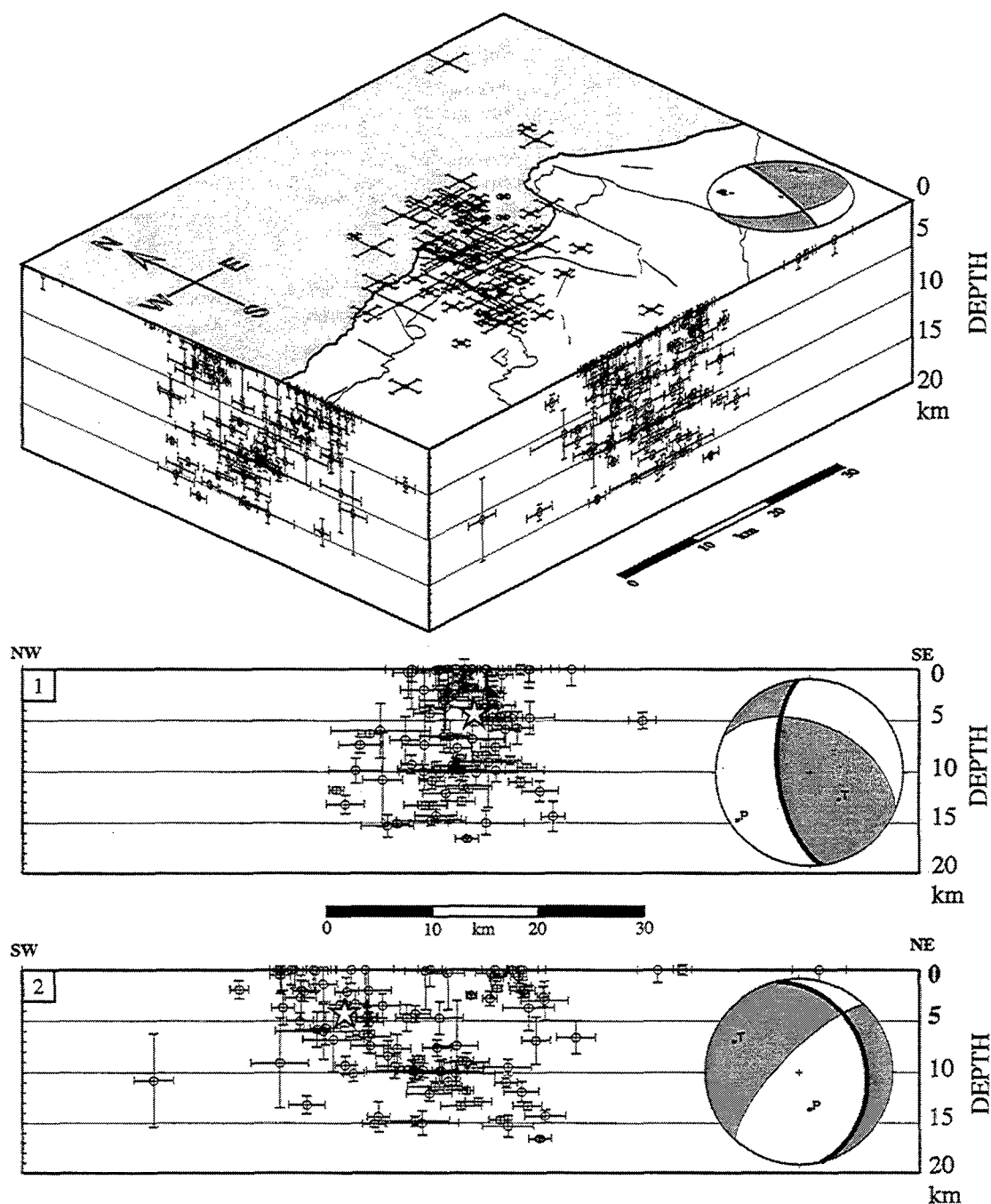


Figure 5. Three-dimensional distribution of Al-Hoceima earthquakes. The upper surface of the block shows the epicentral positions and the Harvard CMT focal mechanism (Dziewonski et al., 1995) for the main Al-Hoceima earthquake (lower hemisphere). The block faces show N-S and E-W projections of hypocenters. The lower panels show hypocenters and focal mechanism (back hemisphere) projected onto planes (1) perpendicular and (2) parallel to trend of seismicity. The preferred fault plane is marked by bold nodal plane. Star marks the hypocentral location determined for the main shock. Error bars are ERH and ERZ standard errors determined by the Hypoinverse location program (Klein, 1978).

Analysis of Marine Seismic Reflection Profiles

The continuation of the seismicity sequence offshore, into the vicinity of an oil industry seismic reflection survey (Figure 6), allows us to map the major marine structures in the region of seismicity and assess their present activity and relationship to onshore structures. The Moroccan National Oil Company (ONAREP) kindly provided a dense grid of migrated seismic reflection lines, supplemented by a more regional network of unmigrated lines for this study.

As onshore, the submarine area is structurally complex with a dominant group of NE-SW trending structures intersected by more northerly trending structures. The NE-SW oriented structures consist of an asymmetric elongate basin (termed the Bokkoya basin) bounded by the Bokkoya unit to the south and the Alboran Ridge to the north. This basin terminates to the east in a region of N-S trending block faulting associated with the Lower Nekor basin. Ties to the El Jebha-1 well (Figure 6) and the correlation of the seismic character of reflectors with those accurately dated in other parts of the Alboran Sea (Alonso and Maldonado, 1992; Campillo *et al.*, 1992; Jurado and Comas, 1992; Rodriguez Fernandez and Sanz de Galdeano, 1992) allow the identification of the strong reflector marking the base of coherent reflectivity (e.g., Figure 7) as the Messinian unconformity, in agreement with the interpretation made by Bourgois *et al.* (1992). This unconformity has been recognized throughout the Alboran basin and is believed to result from the evaporation of the Mediterranean during the Latest Miocene (Messinian salinity crisis) (Hsü *et al.*, 1973). The existence of an unconformity in this region between the Miocene and Pliocene is confirmed by stratigraphic contacts in the Boudinar basin (Guillemin and Houzay, 1982). The basin sediments consist of a seismically semi-transparent Pliocene unit, and a highly reflective Quaternary section.

Line 36 (Figure 7) provides a representative cross section across the NE-SW trending structures, extending from Al-Hoceima bay to the Alboran Ridge. Plio-Quaternary sediments are relatively thin inside the bay, and have been deformed by movement along high angle faults. The edge of the bay is marked by an apparent seabed offset and an acoustic basement high interpreted as the marine extension of the Bokkoya unit by Gensous *et al.* (1986) and Tesson *et al.* (1987) using high resolution seismic reflection profiles. The geometry of the fault causing this seabed offset is ambiguous owing to lack of reflectivity below the Messinian unconformity and the relatively large line spacing when compared to the scale of deformation seen onshore. Adjacent lines (34, 38, and 40) do not show seabed offsets but faulting appears to be traceable to Line 40, where normal offsets of the acoustic basement on a high angle fault are clearly imaged. A change in seafloor gradient and apparent drag folding along this fault suggest that this fault may have been reactivated as a reverse fault. Normal and reverse movement may represent scissoring along strike, which would imply strike-slip movement.

The Bokkoya basin floor is faulted, with the lowermost Pliocene reflectors onlapping Messinian topography. The Pliocene and Lower Quaternary units are clearly folded above these faults, suggesting post depositional reactivation of reverse slip on these faults in Quaternary time. The NW boundary of the basin with the Tofino bank section of the

Alboran Ridge differs significantly from its SE continental boundary. Mid Pliocene and older sediments are rotated, and Upper Pliocene and younger sediments thin significantly onto the ridge flank, suggesting progressive uplift of the Tofino bank relative to the basin center since the Late Pliocene. Truncation of the Pliocene units by the sea bed and the lack of similar truncations on the SE flank implies uplift of the Tofino bank during the Quaternary as opposed to accelerated subsidence of the basin. The fact that the youngest dated volcanism in the region is Miocene in age (e.g., Bellon and Brousse, 1977) and that the bank does not coincide with a gravity anomaly that could be considered indicative of diapirism, suggests that the uplift is tectonic in nature. Although no faults appear to offset the sediments draped on the SE flank of the bank, the Messinian unconformity appears to terminate on the bank's NW flank suggesting the presence of a bounding fault. The fault itself is not imaged, possibly owing to its steep dip, a lack of sufficient impedance contrast, or scattering of seismic energy by overlying Miocene volcanic structures. This uplift is not limited solely to the Tofino bank; similar structures related to Quaternary uplift are imaged along the entire length of the Alboran ridge in this region. The observations support the interpretation that the uplift of Alboran Ridge results from compressive tectonics, as proposed by Bourgois *et al.* (1992) and Woodside and Maldonado (1992).

Line 29 (Figure 8), oriented perpendicular to Line 36, illustrates the significantly different fault controlled structure exhibited by the Lower Nekor basin. The sea floor is relatively flat but the sedimentary layering is deformed, tilted, and affected by channel deposits. The Trougout fault (Figure 2a) may be traced off the coast but an offshore expression of the Imzouren fault cannot be identified. The lower Nekor basin has a graben structure with high angle normal faults dipping to the west on its eastern side and to the east dipping towards the western edge. These observations of distributed faulting are in agreement with results from water wells drilled in the graben floor that show approximately 400m of Quaternary fill overlying a faulted Ketama unit (Medina, 1995 from Thauvin, 1971). The faults have a generally north-south strike and the orientations shown on Figure 6 are probably close to their true strikes but it is possible that the faults in the center of the bay have a NNE-SSW strike as opposed to the NNW-SSW strike shown.

The seismic reflection profiles provide further evidence of the distributed nature of deformation in the region. No single master fault can be identified; rather, deformation is occurring along a number of smaller high angle faults that may have strike-slip components.

Discussion

Seismological observations provide a snapshot of the deformation occurring today in the Al-Hoceima region. Analysis of the seismic reflection profiles allows us to identify active structures, investigate their geometry, and examine their recent history from a regional perspective.

Analysis of the recent earthquake sequence in the Al-Hoceima region shows that these events are not directly related to either the geomorphically prominent Nekor fault or the submarine Alboran Ridge but occurred over an apparently diffuse NE-SW zone

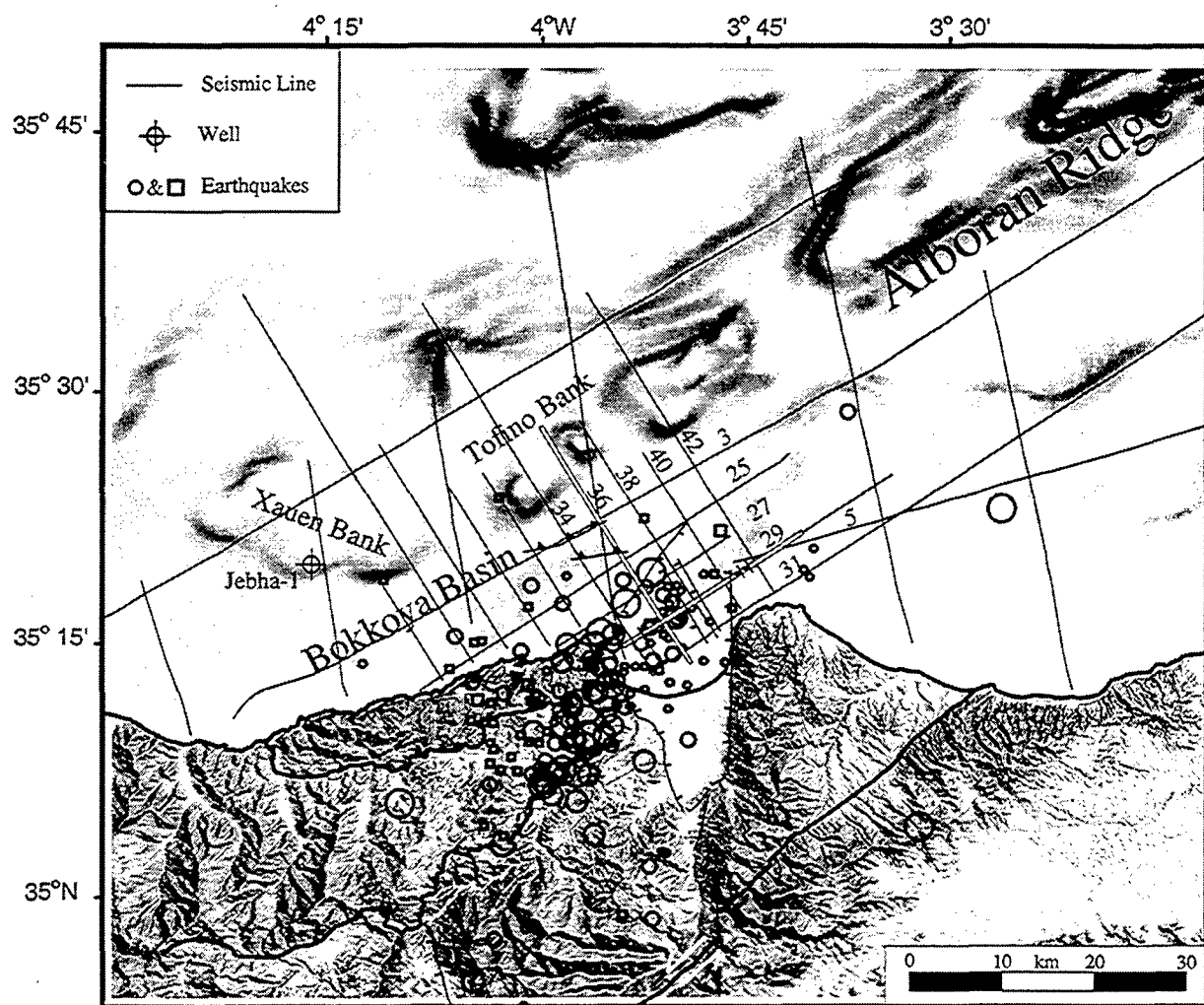


Figure 6. Map showing bathymetry and marine seismic reflection profiles examined for this study. The marine faults were mapped using the profiles shown. Lines 36 and 29 (highlighted) are shown in Figures 7 and 8, respectively.

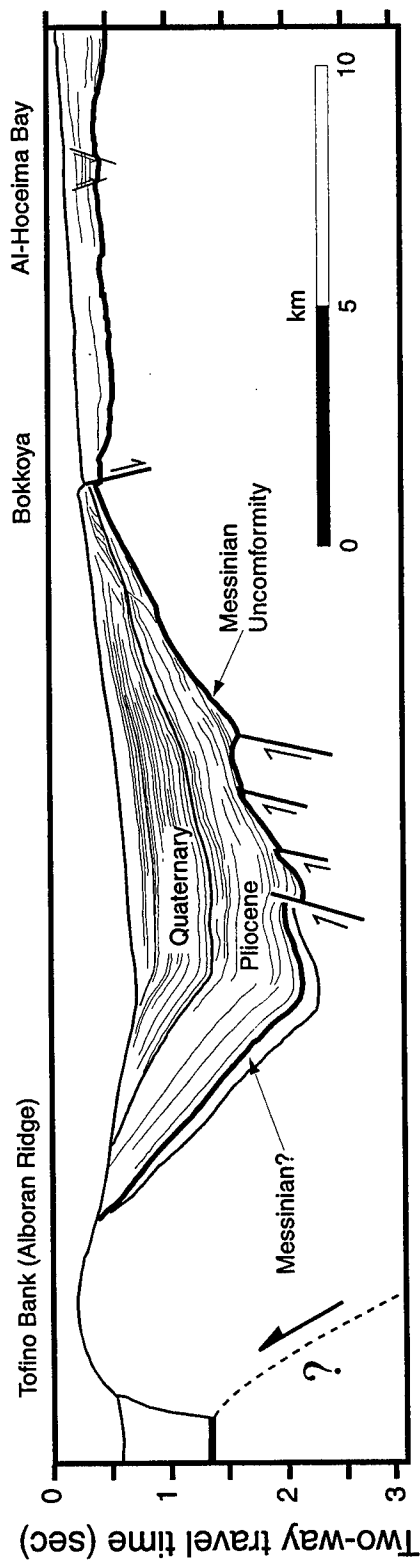
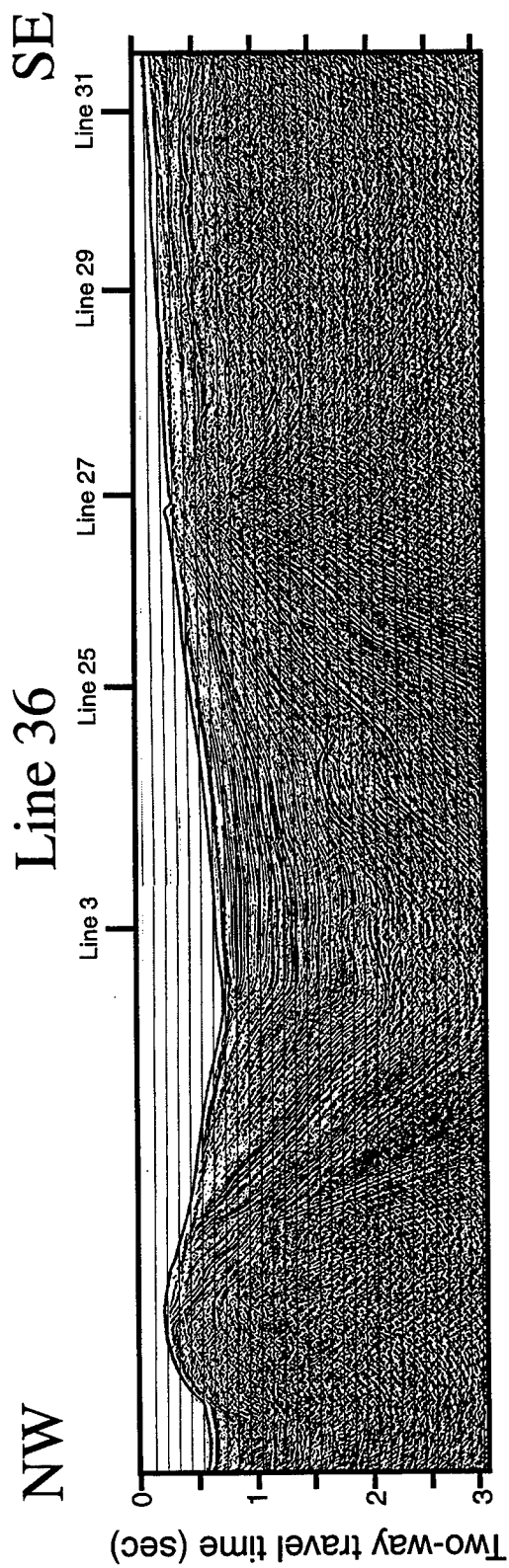


Figure 7. Migrated seismic reflection profile, Line 36, and interpretation across Bokkoya basin and Alboran Ridge (see Figure 6 for location). Note the seabed offset and deformation of Quaternary basin sediments by uplift of the ridge.

intersecting the marine extension of the Lower Nekor basin, and surface exposure of the Ketama, Tiziren, and Bokkoya tectonic units (Figures. 2a,b). Distributed seismic deformation in the Al-Hoceima region was identified in the microearthquake study conducted by Hatzfeld *et al.* (1993). However, the majority of the microearthquakes located by Hatzfeld *et al.* were in close proximity to the Lower Nekor basin and Jebel Hammam fault. This study and the results reported by Hatzfeld *et al.* (1993) together document the distributed nature of seismic deformation in the Al-Hoceima region.

The fault plane orientations for the main Al-Hoceima earthquake of May 26, 1994 are similar to those determined for both micro- and medium size earthquakes located in the region (Hatzfeld, 1978; Medina *et al.*, 1992; Hatzfeld *et al.*, 1993; Medina, 1995) (Figure 9). Both the larger and microearthquake events have focal mechanisms that indicate similar strike-slip faulting, with the majority of focal mechanisms having NNE-SSW to NNW-SSE oriented sinistral and ENE-WSW to ESE-WNW oriented dextral nodal planes. Rose diagrams (Figure 9) of the P and T axis orientations for all the focal mechanisms reported by Hatzfeld *et al.* (1993) in addition to those shown in Figure 9 illustrate the dominant trend of the P and T axis orientations. These focal mechanisms have a seismic consistency, C_s , (Frohlich and Apperson, 1992) of 0.73, suggesting a good consistency for these fault plane solutions. Seismicity in the region appears to be characterized by a diffuse pattern and have a characteristic strike-slip fault plane solution. This suggests that the distributed system of high angle NNE-SSW oriented sinistral surface faults mapped in the region may be active and represent the surface geological expression of this seismogenic deformation.

Analysis of the offshore seismic reflection profiles indicates that the Bokkoya and Lower Nekor basins are cut by high angle NNW-SSE to NNE-SSW striking faults. Whether these faults also cut the Alboran Ridge is equivocal. Identifying the strike-slip component of slip along faults is inherently difficult using two-dimensional seismic reflection profiles. High angle faults with normal offsets are imaged in Al-Hoceima bay, and possible strike-slip indicators (scissoring) are observed. Given the strike-slip focal mechanisms determined for earthquakes in this area, it seems likely that these faults may have a strike-slip component. The Alboran Ridge is also tectonically active, with slip occurring on high angle faults. However, in contrast to the normal offset of faults in the Lower Nekor basin, these faults exhibit a reverse component of slip. Strike-slip components of slip along faults bounding the ridge have been proposed (e.g., Woodside and Maldonado, 1992; Bourgois *et al.*, 1992). The faults identified as recently active appear to form two orientation dependent groups: (1) Distributed NNE-SSW striking faults exhibiting a left lateral sense of slip with a small normal component, and (2) NW-SE striking faults exhibiting reverse slip with possible strike-slip components. Analysis of the seismological and seismic reflection data suggests that deformation in the Al-Hoceima region today is occurring along high angle faults and is predominantly strike-slip, with normal or reverse components depending on the orientation of the fault.

Subsidiary synthetic and antithetic strike-slip faults are often associated with major strike-slip faults (e.g., Sylvester, 1988). The NNE-SSW oriented faulting has a similar strike and sense of shear to that expected for a synthetic fault related to movement along

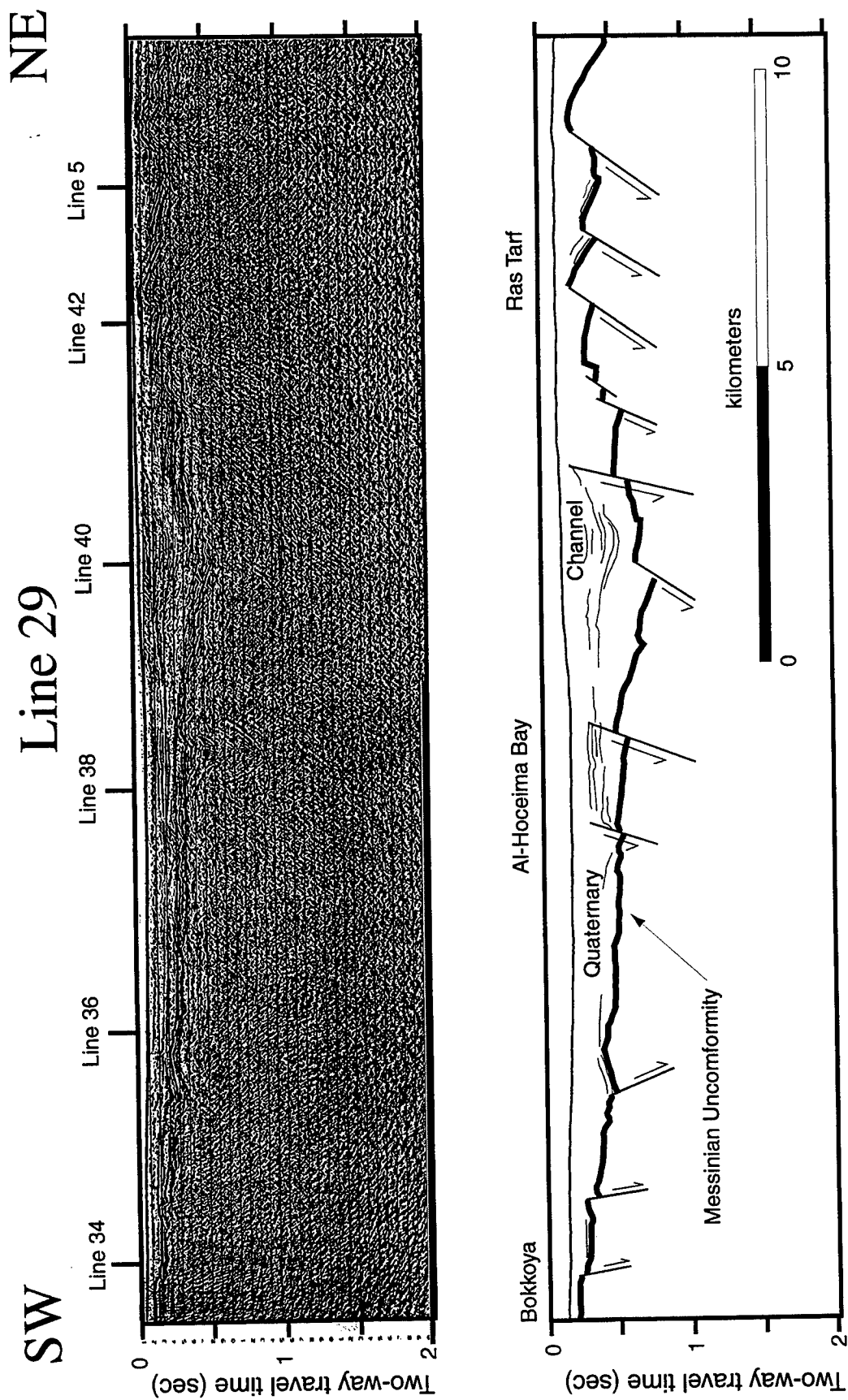


Figure 8. Migrated seismic reflection profile, Line 29, and interpretation across Lower Nekor basin. Note the faulted acoustic basement and deformed Quaternary sediments.

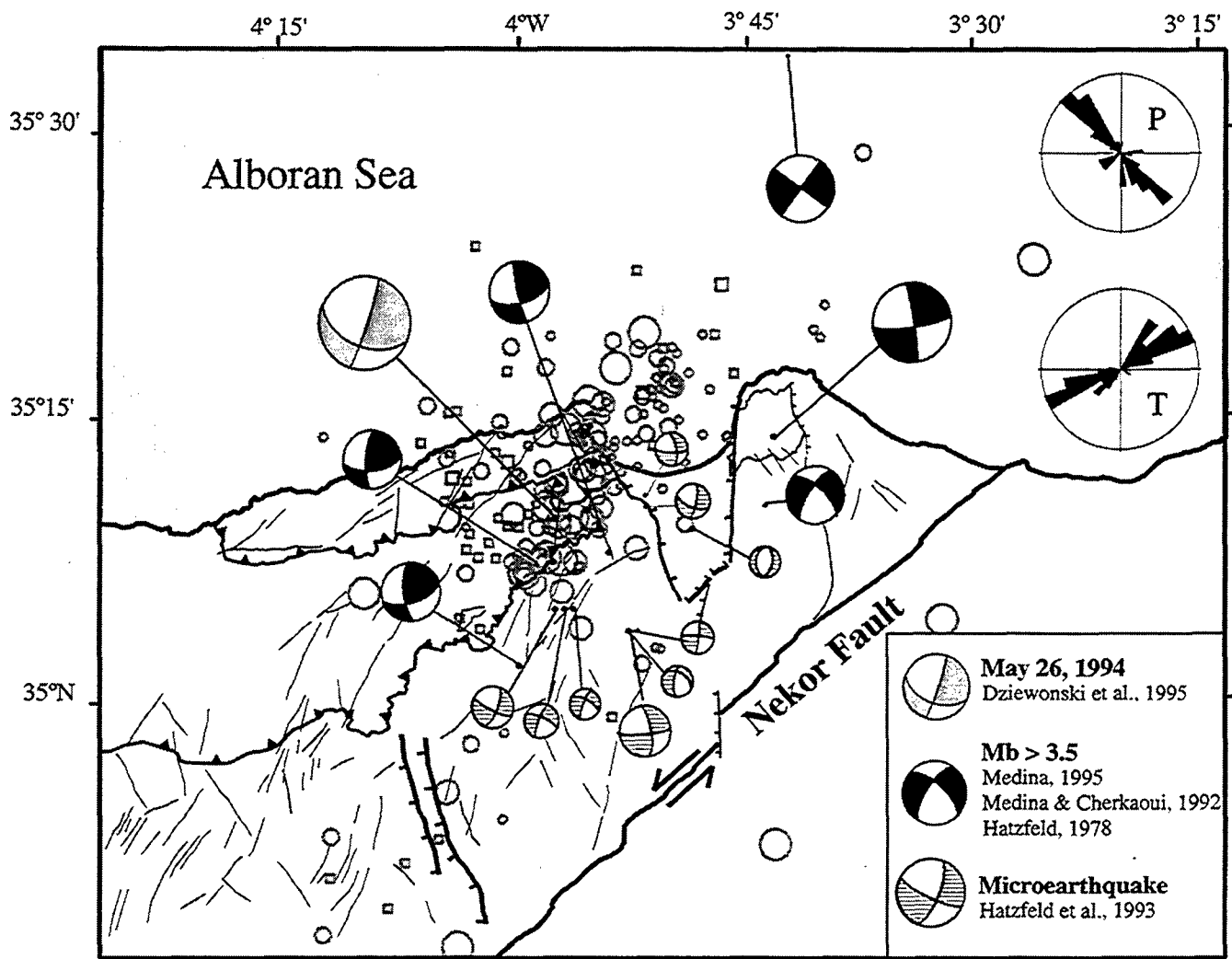


Figure 9. Focal Mechanisms of earthquakes ($M_b > 2.5$, 1968-1994) in the Al-Hoceima region (after Hatzfeld, 1978; Medina and Cherkaoui, 1992; Hatzfeld et al., 1993; Medina, 1995) and rose diagrams of P and T axes orientations for focal mechanisms determined in the region (49 events). Earthquakes are distributed and predominantly strike-slip with consistent P and T axes orientations.

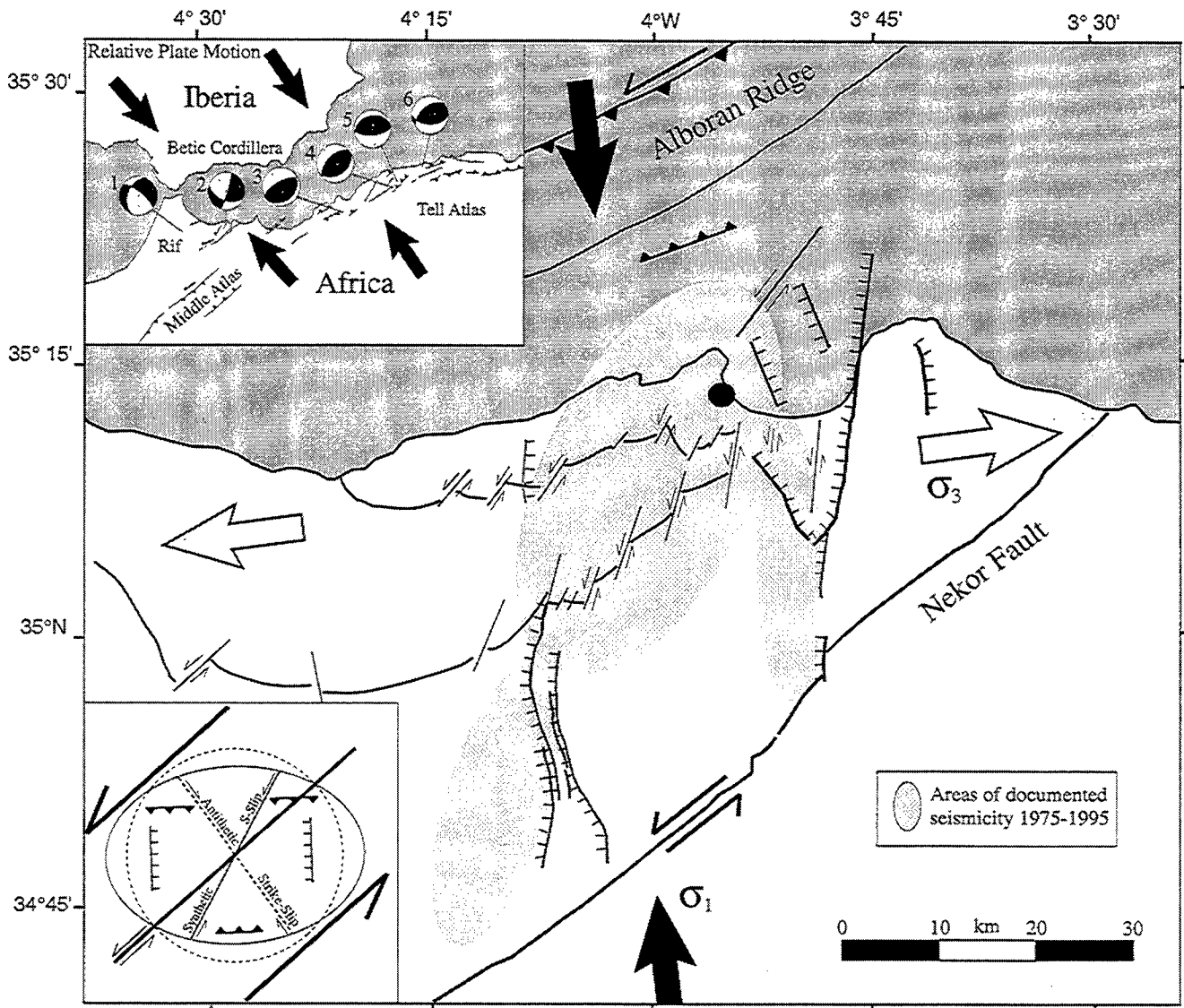


Figure 10. Zones of recent seismicity and model proposing that strike-slip movement along the Jebha and Alboran Ridge bounding faults has resulted in the formation of distributed synthetic strike-slip faults along which seismic deformation is now occurring. Large black and white arrows indicate present s_1 and s_3 directions determined by Medina (1995). Upper Inset: Focal Mechanisms of major earthquakes on the NW African margin and Neotectonic faults (adapted from Meghraoui et al., 1996): (1) Rif 11.15.64 (Medina et al., 1992), (2) Al-Hoceima 05.26.94 (Harvard), (3) Mascara 08.18.94 (Harvard), (4) El Asnam 10.10.80 (Deschamps et al., 1982), (5) El Asnam 09.09.54 (McKenzie, 1972), and (6) Cherrchell-Tifaza 10.29.89 (USGS). Black arrows show present plate convergence directions predicted by NUVEL-1A plate motion model (Demets et al., 1994). Lower inset: Strike-slip zone related fault orientations (adapted from Sylvester and Smith, 1976).

the Jebha and Nekor faults and the Alboran Ridge bounding fault (Figure 10, lower inset). Strike-slip movement along these major faults during the Neogene and Quaternary time, although not synchronous, may have resulted in distributed fracturing of the intervening region along this preferred orientation. The present NNW-SSE orientation of the principal stress (Medina, 1995) and the relative weakness of this zone, may account for the concentration of earthquakes in the region, with slip occurring preferentially along the subsidiary faults, and the relative inactivity of the major tectonic structures. An intriguing, but unproven, alternative hypothesis is that strike-slip movement is occurring along the northeastern section of the Alboran Ridge and is being transferred through the fractured Al-Hoceima region onto the south-western section of the Nekor fault, resulting in the subsidence of the lower Nekor basin as a pull-apart basin. Such a geometry would allow strike-slip movement to occur along the ridge fault and the southern section of the Nekor fault, without slip occurring along the Boudinar basin section (see Figure 2a) and offshore extensions of the Nekor and Jebha faults. Whether the absence of documented seismicity along the ridge or Nekor faults is a result of aseismic slip, an incomplete record, or a locking of the faults with an associated accumulation of strain is an important question that requires further study.

The strike-slip seismic deformation taking place in the Al-Hoceima region characterizes the Rif region as a whole (e.g., Medina and Cherkaoui, 1992), and contrasts with the predominant thrusting style of deformation in the Tell Atlas about 200 km farther to the east (Figure 10, upper inset). The orientation of the P axes for earthquakes in both regions is essentially NNW-SSE, owing to the general NW-SE convergence of Iberia and Africa, but the orientation of the T axes in the Rif region is subhorizontal as opposed to subvertical in the Tell Atlas (Rebaï *et al.*, 1992). The styles of deformation found in the Rif and Tell Atlas represent two different mechanisms for accommodating the collision of Africa and Iberia. The intracontinental deformation occurring in the Middle and High Atlas is also believed to be partially accommodating the convergent plate motion (e.g., Brede *et al.*, 1992). Although strain is being partitioned between the interplate Rif and Tell Atlas and the intraplate Middle and High Atlas the nature and mechanism for this partitioning is not well understood. Two kinematic models have been proposed specifically to explain the strike-slip deformation occurring in the Alboran region: (1) Trans-Alboran Shear zone model (e.g., Dillon *et al.*, 1980; De Larouziere *et al.*, 1988; Jacobshagen, 1992) proposing a crustal scale strike-slip fault zone extending from southern Spain, across the Alboran sea, through the eastern Rif, and possibly into the Middle Atlas, and (2) rotating block model (Meghraoui *et al.*, 1996) proposing that clockwise rotation of crustal blocks results in sinistral strike-slip deformation on their borders. The evidence for a connected fault system spanning the Alboran is equivocal. Further seismological observations over longer timescales are required to effectively evaluate these models. The various models proposed for the evolution of the western Mediterranean (see above, Tectonic summary) all suggest that the Rif and Tell Atlas regions, although both situated on the same convergent plate boundary, have been subject to differing geodynamic processes during Neogene and Quaternary time. The inheritance of controlling lithospheric structure, or the continuation of subcrustal processes such as delamination (e.g., Seber *et al.*, 1996) may provide an explanation for the distinct styles of deformation occurring in the two regions today.

Conclusions

The May 26, 1994 Al-Hoceima earthquake ($M_w=6.0$) is relocated onshore on the Mediterranean coast of Morocco and is associated with a 30 km, NE-SW oriented, fore- and aftershock distribution that extends partly offshore. Analysis of seismological data and seismic reflection profiles suggests that seismic deformation in the Al-Hoceima region is characterized by predominantly sinistral strike-slip and normal faulting. Deformation is occurring over a distributed zone with individual faults having a dominant NNE-SSW to N-S orientation. A simple model is suggested for the formation of this region of distributed shear: we propose that Miocene strike-slip movement on the Jebha and Nekor faults bounding the Al-Hoceima region has resulted in the formation of distributed synthetic strike-slip faults, along which seismic deformation is now occurring. The absence of documented seismicity along the Nekor and Alboran Ridge faults during this study and previous microearthquake studies may be an indication that slip is no longer occurring along these faults, possibly owing to the present plate convergence direction. Alternatively, the fractured Al-Hoceima region may be allowing the transfer of slip from along the Alboran Ridge fault to along the Nekor fault. If this is the case and slip is not occurring aseismically then strain may be accumulating along these major faults.

The Al-Hoceima earthquake provides a further example of the difference in style of present deformation of the Rif and Tell Atlas mountain belts, and the complex nature of the plate boundary between Africa and Iberia.

Acknowledgments. We would like to thank M. El Idrissi, A. A. El Mouraouah, M. Kasimi, A. W. Birrouk, and the other members of CNCPRST for their assistance and maintenance of the Moroccan seismological network, M. Ouazzaba and other members of ONAREP for the valuable discussions and assistance in obtaining the seismic reflection profiles, and T. Mourabit for sharing his knowledge of the Al-Hoceima region. We would also like to thank G. Brew, W. Beauchamp, and E. Sandvol at Cornell for their suggestions and ideas.

References

- Ait Brahim, L. (1991). Tectoniques cassantes et états de contraintes récents au Nord du Maroc, Ph.D. thesis, L'Université Mohammed V, Rabat, 244 pp.
- Ait Brahim, L., P. Chotin, B.A. Tadili, and M. Ramdani (1990). Failles actives dans le Rif central et oriental (Maroc), *C. R. Acad. Sci. Paris*, **310**, 1123-1129.
- Alonso, B. and A. Maldonado (1992). Plio-Quaternary margin growth patterns in a complex tectonic setting: Northeastern Alboran Sea, *Geo-Mar. Lett.*, **12**, 137-143.
- Andrieux, J., J.-M. Fontbote, and M. Mattauer (1971). Sur un modèle explicatif de l'Arc de Gibraltar, *Earth Planet. Sci. Lett.*, **12**, 191-198.
- Apericio, A., J.M. Mitjavila, V. Araña, and I.M. Villa (1991). La edad del volcanismo de las islas Columbreta Grande y Alborán (Mediterráneo occidental), *Bol. Geol. Min.*, **102-104**, 74-82.

- Asebriy, L., J. Bourgois, T.E. Cherkaoui, and A. Azdimousa (1993). Evolution tectonique récente de la zone de faille du Nekor: importance paléogéographique et structurale dans le Rif externe, Maroc, *J. Afr. Earth Sci.*, **17**, 65-74.
- Bellon, H. and R. Brousse (1977). Le magmatisme périméditerranéen occidental. Essai de synthèse, *Bull. Soc. Géol. Fr.*, **19**, 469-480.
- Ben Sari, D. (1987). *Connaissance Geophysique du Maroc*, Editions Marocaines et Internationales, Rabat, Morocco, 207 pp.
- Blanco, M.J. and W. Spakman (1993). The P-wave velocity of the mantle below the Iberian Peninsula: evidence for subducted lithosphere below southern Spain, *Tectonics*, **221**, 13-34.
- Brede, R., M. Hauptmann, and H-G. Herbig (1992). Plate tectonics and intracontinental mountain ranges in Morocco - The Mesozoic-Cenozoic development of the Central High Atlas and the Middle Atlas, *Geologische Rundschau*, **81**, 127-141.
- Bourgois, J., A. Mauffret, A. Ammar, and A. Demnati (1992). Multichannel seismic data imaging of inversion tectonics of the Alboran Ridge (Western Mediterranean Sea), *Geo-Mar. Lett.*, **12**, 117-122.
- Campillo, A.C., A. Maldonado, and A. Mauffret (1992). Stratigraphic and tectonic evolution of the western Alboran Sea: Late Miocene to Recent, *Geo-Mar. Lett.*, **12**, 165-172.
- Cherkaoui, T.-E. (1991). Contribution a l'etude de l'alea sismique au Maroc, etude detaillee du seisme d'Agadir (29/2/1960), etude de la microsismicite de la region d'Al Hoceima, Ph.D. thesis, L'Universite Joseph Fourier, Grenoble, France, 247 pp.
- Choubert, G. and A. Faure-Muret, (1974). Moroccan Rif, in *Mesozoic-Cenozoic Orogenic Belts*, A. Spencer (Editor), Scottish Academic Press, Edinburgh, Scotland, 37-46.
- Comas, M.C., V. Garcia-Duenas, and M.J. Jurado (1992). Neogene tectonic evolution of the Alboran sea from MCS data, *Geo-Mar. Lett.*, **12**, 157-164.
- Comas, M.C., R. Zahn, A. Klaus, and ODP Leg 161 Scientific Party (1995). ODP Leg 161 - Western Mediterranean: Overview and preliminary results, *Eos, Trans. Am. Geophys. Union*, Supplement 1995 Fall Meeting, **76**, F620.
- De Larouzière, F.D., J. Bolze, P. Bordet, J. Hernandez, C. Montenat, and P. Ott d'Estevou (1988). The Betic segment of the lithospheric Trans-Alboran shear zone during the Late Miocene, *Tectonophysics*, **152**, 41-52.
- Demets, C., R.G. Gordon, D.F. Argus, and S. Stein (1994). Effect of recent revisions to the geomagnetic reversal time scale on the estimate of current plate motions, *Geophys. Res. Lett.*, **21**, 2191-2194.
- Deschamps, A., Y. Gaudemer, and A. Cisternas (1982). The El Asnam, Algeria Earthquake of 10 October 1980: Multiple-source mechanism determined from long-period records, *Bull. Seism. Soc. Am.*, **72**, 1111-1128.
- Dewey, J., M. Helman, E. Turco, D. Hutton, and S. Knott, (1989). Kinematics of the western Mediterranean, in *Alpine Tectonics*, M. Coward, D. Dietrich, and R. Park (Editors), Royal Geological Society, Oxford, 265-283.
- Dillon, W.P., J.M. Robb, H.G. Greene, and J.C. Lucena (1980). Evolution of the continental margin of southern Spain and the Alboran sea, *Mar. Geol.*, **36**, 205-226.

- Docherty, C. and E. Banda (1995). Evidence for the eastward migration of the Alboran Sea based on regional subsidence analysis: A case for basin formation by delamination of the subcrustal lithosphere? *Tectonics*, **14**, 804-818.
- Dziewonski, A.M., G. Ekstrom, and M.P. Salganik (1995). Centroid-moment tensor solutions for April-June 1994, *Phys. Earth. Planet. Int.*, **88**, 69-78.
- Fetah, S.E.M., M. Bensaid, and M. Dahmani (1987). Carte géologique du Rif, Rouadi, *Notes Mem. Serv. Geol. Maroc*, **347**.
- Frizon de Lamotte, D. (1982). Contribution à l'étude de l'évolution structurale du Rif oriental, *Notes Mem. Serv. Geol. Maroc*, **314**, 7-238.
- Frohlich, C. and K.D. Apperson (1992). Earthquake focal mechanisms, moment tensors, and the consistency of seismic activity near plate boundaries, *Tectonics*, **11**, 279-296.
- Gensous, B., M. Tesson, and E. Winnock (1986). La Marge meridionale de la mer d'Alboran: Caracteres structuro-sedimentaires et evolution recente, *Mar. Geol.*, **72**, 341-370.
- Giermann, G., M. Pfannenstiel, and W. Wimmenauer (1968). Relations entre morphologie, tectonique et volcanisme en mer d'Alboran (Méditerranée occidentale). Résultats préliminaires de la campagne Jean-Charcot (1967), *C. R. Soc. Geol. Fr.*, **4**, 116-118.
- Guillemin, M. and J.P. Houzay (1982). La Néogène post-nappes et le Quaternaire du Rif nord-oriental stratigraphie et tectonique des bassins de Melilla, du Kert, de Boudinar et du piedmont des Kebdana, *Notes Mem. Serv. Geol. Maroc*, **314**, 7-238.
- Hatzfeld, D. and D. Ben Sari (1977). Grands profils sismiques dans la région de l'arc de Gibraltar, *Bull. Soc. Géol. Fr.*, **19**, 749-756.
- Hatzfeld, D. (1978). Etude sismotectonique de la zone de collision Ibéro-Maghrébine, Ph.D. thesis, Grenoble, 281 pp.
- Hatzfeld, D., V. Caillot, T.-E. Cherkaoui, H. Jebli, and F. Medina (1993). Microearthquake seismicity and fault plane solutions around the Nekor strike-slip fault, Morocco, *Earth Planet. Sci. Lett.*, **120**, 31-41.
- Horvarth, F. and H. Berckhemer, (1982). Mediterranean backarc basins, in *Alpine Mediterranean Geodynamics*, H. Berckhemer and K. Hsü (Editors), American Geophysical Union, 141-173.
- Hsü, K.J., M.B. Cita, and W.B.F. Ryan (1973). The origin of the Mediterranean evaporites, *Initial Rep. Deep Sea Drill. Proj.*, **13**, 1203-1231.
- Hsü, K.J. and W.B.F. Ryan (1973). Comments on Alboran basin "basement" samples, *Initial Rep. Deep Sea Drill. Proj.*, **13**, 762-766.
- Intergovernmental Oceanographic Commission (1981). International Bathymetric Chart of the Mediterranean, *Dept. Navigation and Oceanography*, Ministry of Defense (USSR), Leningrad.
- Jacobshagen, V. (1992). Major fracture zones of Morocco: The South Atlas and Transalboran fault systems, *Geologische Rundschau*, **81**, 185-197.
- Jurado, M.J. and M.C. Comas (1992). Well Log Interpretation and Seismic Character of the Cenozoic Sequence in the Northern Alboran Sea, *Geo-Mar. Lett.*, **12**, 129-136.

- Klein, F.W. (1978). Hypocenter Location Program, HYPOINVERSE, *U.S. Geol. Surv. Open-File Rept.* 78-694, 113 pp.
- Leblanc, D. and P. Olivier (1984). Role of strike-slip faults in the Betic-Rifian Orogeny, *Tectonophysics*, **101**, 345-355.
- Leblanc, D. (1990). Tectonic adaptation of the External Zones around the curved core of an orogen: the Gibraltar Arc, *J. Struct. Geol.*, **12**, 1013-1018.
- Loomis, T. (1975). Tertiary mantle diapirism, orogeny, and plate tectonics east of the Strait of Gibraltar, *Am. J. Sci.*, **275**, 1-30.
- McKenzie, D. (1972). Active tectonics of the Mediterranean region, *Geophys. J. R. Astron. Soc.*, **30**, 109-185.
- Medina, F. (1995). Present-day state of stress in northern Morocco from focal mechanism analysis, *J. Struct. Geol.*, **17**, 1035-1046.
- Medina, F. and T.-E. Cherkaoui (1992). Mécanismes au foyer des séismes du Maroc et des régions voisines (1959-1986). Conséquences tectoniques., *Eclogae Geol. Helv.*, **85**, 433-457.
- Meghraoui, M., J.-L. Morel, J. Andrieux, and M. Dahmani (1996). Tectonique Plio-Quaternaire de la chaîne Tello-Rifaine et de la mer d'Alboran. Une zone complexe de convergence continent-continent, *Bull. Soc. Géol. Fr.*, **167**, 141-157.
- Morel, J.-L. (1989). Evolution paléogéographique et tectonique du Rif (Maroc) du Tortonien à l'actuel, *C. R. Acad.Sci., Paris*, **309**, 2053-2059.
- Morley, C.K. (1992). Notes on the Neogene basin history of the western Alboran Sea and its implications for the tectonic evolution of the Rif-Betic orogenic belt, *J. Afr. Earth Sci.*, **14**, 57-65.
- Olivier, P. (1982). L'accident de Jebha-Chrafate (Rif, Maroc), *Rev. Géol. Dyn. Géogr. Phys.*, **23**, 97-106.
- Platt, J.P. and R.L.M. Vissers (1989). Extensional collapse of thickened continental lithosphere: A working hypothesis for the Alboran Sea and Gibraltar arc, *Geology*, **17**, 540-543.
- Ramdani, M. and B.A. Tadili (1988). Deep crustal structure in Morocco, *Gerlands Beitr. Geophys.*, **97**, 137-143.
- Ramdani, M., B. Tadili, and T.E. Mrabet, (1989). The present state of knowledge on historical seismicity of Morocco, in *Proceedings of the symposium on Calibration of Historical Earthquakes in Europe and Recent Developments in Intensity interpretation*, G. Payo, C. Radu, and D. Postpischl (Editors), European Seismological Commission, Madrid, 257-279.
- Rebaï, S., H. Philip, and A. Taboada (1992). Modern tectonic stress field in the Mediterranean region: evidence for variation in stress directions at different scales, *Geophys. J. Int.*, **110**, 106-140.
- Rodriguez Fernandez, J. and C. Sanz de Galdeano (1992). Onshore Neogene stratigraphy in the north of the Alboran sea (Betic Internal zones): Paleogeographic implications, *Geo-Mar. Lett.*, **12**, 123-128.
- Royden, L.H. (1993). Evolution of retreating subduction boundaries formed during continental collision, *Tectonics*, **12**, 629-638.
- Saadi, S.E.M., M. Bensaid, and M. Dahmani (1984a). Carte géologique du Rif, Al Hoceima, *Notes Mem. Serv. Geol. Maroc*, **302**.

- Saadi, S.E.M., M. Bensaid, and M. Dahmani (1984b). Carte géologique du Rif, Boudinar, *Notes Mem. Serv. Geol. Maroc*, **299**.
- Sambridge, M.S. and B.L.N. Kennett (1986). A novel method of hypocentre location, *Geophys. J. R. astr. Soc.*, **87**, 679-697.
- Schwarz, G. and P.J. Wigger, (1988). Geophysical studies of the earth's crust and upper mantle in the Atlas system of Morocco, in *The Atlas System of Morocco*, V. Jacobshagen (Editor), Springer-Verlag, Berlin, 339-357.
- Seber, D., M. Barazangi, A. Ibenbrahim, and A. Demnati (1996). Geophysical evidence for lithospheric delamination beneath the Alboran Sea and Rif-Betic mountains, *Nature*, **379**, 785-790.
- Sylvester, A.G. (1988). Strike-slip faults, *Geol. Soc. Am. Bull.*, **100**, 1666-1703.
- Sylvester, A.G. and R.R. Smith (1976). Tectonic transpression and basement-controlled deformation in San Andreas fault zone, Salton Trough California, *Am. Assoc. Pet. Geol. Bull.*, **60**, 2081-2102.
- Tadili, B., M. Ramdani, D. Ben Sari, K. Chapochnikov, and A. Bellot (1986). Structure de la croûte dans le nord du Maroc, *Ann. Geophysicae*, **4**, 99-104.
- Tesson, M., B. Gensous, and M. Labraim (1987). Seismic analysis of the southern margin of the Alboran Sea, *J. Afr. Earth Sci.*, **6**, 813-821.
- Thauvin, S. (1971). Ressources en eau du Maroc. Tome I: Domaines du Rif et du Maroc oriental, *Notes Mem. Serv. Geol. Maroc*, **231**, 69-79.
- Watts, A.B., J.P. Platt, and P. Buhl (1993). Tectonic evolution of the Alboran Sea, *Basin Res.*, **5**, 153-177.
- Wigger, P., G. Ash, P. Giese, W.-D. Heinshon, S.O. El Alami, and F. Ramdani (1992). Crustal structure along a traverse across the Middle and High Atlas mountains derived from seismic refraction studies, *Geol. Rundsch.*, **81**, 237-248.
- Woodside, J.M. and A. Maldonado (1992). Styles of compressional neotectonics in the eastern Alboran Sea, *Geo-Mar. Lett.*, **12**, 111-116.
- Working Group for Deep Seismic Sounding in the Alboran Sea (W.G.D.S.S.A.S) (1978). Crustal Seismic Profiles in the Alboran Sea- Preliminary Results, *Pageoph.*, **116**, 167-180.

E. REGIONAL DISCRIMINATION OF CHEMICAL EXPLOSIONS AND EARTHQUAKES: A CASE STUDY IN MOROCCO

Abstract

To examine the limitations in the techniques for discriminating between chemical explosions and earthquakes at local and regional distances, we applied several standard heuristics to seismic events in northwest Morocco where little *a priori* information was available. Although the 8 Oud Zem phosphate mine explosions have similar geographic locations, total charge size, and presumably ripple fired mechanisms, the seismic recordings are characterized by a surprising amount of diversity. Time and path independent modulations, owing to the periodic source mechanism of the ripple fired explosions, rarely unequivocally distinguish the explosions from the earthquakes. Our findings imply that, more often than the current literature suggests, source inconsistencies such as differing blasting arrangements play a role in the failure of common discriminants. Furthermore, crustal seismic velocity and the attenuation structure seemed to shape the seismic signals more than the nature of the source mechanism, although site effects could not be ruled out. The 10-15 Hz Pg/Sg ratio test proved to be the most precise and accurate discriminant. Popular intra-phase spectral and cross-spectral ratios performed considerably worse. Finally, we argue that a regional case-based approach requires extensive regional information to meet the demanding verification goals of the proposed Comprehensive Test Ban Treaty.

Introduction

A Comprehensive Test Ban Treaty (CTBT) verification system will strive to discriminate background events, such as earthquakes and chemical explosions, from an aggressively evasive nuclear test, such as a 1 kiloton decoupled nuclear explosion hidden within multiple large chemical explosions. The CTBT's rigorous verification requirements and today's more transparent security environment have brought regional discrimination and industrial explosions back to the foreground of seismic verification research.

Large industrial explosions for mining and excavating are almost always chemical explosions which can be as large as 500 metric tons (Smith, 1989). Usually chemical explosions over a few tons are actually a series of time-delayed sub-explosions, or *ripple fired explosions*, whose spatial and temporal layout are determined by the purpose of the explosion, the topography, and the equipment available for the blasts. The source multiplicity inherent in ripple fired explosions is often the characteristic used to discriminate large chemical explosions from nuclear explosions and earthquakes (e.g., Baumgardt and Ziegler, 1988; Smith, 1989; Kim *et al.*, 1994). Various compressional and shear wave ratios (amplitude and spectral) have been used to discriminate between all types of explosions and earthquakes, in an attempt to apply the basic physical premise that explosions excite more compressional waves than earthquakes relative to shear waves (e.g., Pomeroy *et al.*, 1982; Taylor *et al.*, 1989; Kim *et al.*, 1994; Walter *et al.*, 1995; Taylor, 1996).

In the recent literature, researchers have studied the regional discrimination of ripple fired explosions using three methodologies:

- By simulating ripple fired explosion spectra in order to predict spectral details indicative of ripple fired explosions and not of earthquakes or single-event explosions (e.g., Greenhalgh, 1980; Chapman *et al.*, 1992; Smith, 1989, 1993).
- By examining differences in observed compressional/shear wave amplitude ratios (e.g., Baumgardt and Young, 1990; Wuster, 1993).
- By analyzing observed spectra of ripple fired explosions, instantaneous explosions, and earthquakes and contrasting time-independent modulations, path independent modulations, spectral ratios, spectral slopes, and spectral maxima and minima (e.g., Baumgardt and Ziegler, 1988; Hedlin *et al.*, 1989, 1990; Baumgardt and Young, 1990; Smith, 1989, 1993; Wuster, 1993; Gitterman and van Eck, 1993; Kim *et al.*, 1994).

These researchers and others have often used different techniques (e.g., spectrograms, cepstral analysis, quadratic discrimination functions, linear discrimination functions) and have examined different frequency windows, but their general observations are the same. Time independent and path independent modulations can be used to identify ripple fired events. Spectral maxima and minima are influenced by the spatial-temporal pattern of the explosions and by the recording station's azimuth from that pattern. P/S ratios also can be used to discriminate chemical explosions from earthquakes. All of these heuristics, however, have their limits. First, heuristics that can be applied to ripple fired explosions may not be readily transferred to nuclear explosions (Baumgardt and Young, 1990; Walter *et al.*, 1995). Second, for the discrimination success often advertised for ripple fired explosions, a number of conditions are highly desirable, if not required, such as favorable geologic conditions (e.g., laterally homogeneous velocity structure and low anelastic attenuation), the use of a regional array, relatively high signal-to-noise ratios with a diverse calibration (or "training") set on which to base comparisons, or a combination of the above (e.g., Hedlin *et al.*, 1990; Smith, 1989, 1993; Wuster, 1993; Kim *et al.*, 1994). In order to arrive at the details behind some of the heuristics employed, some of the studies have required significant *a priori* information, such as meticulously kept blasting logs (e.g., Greenhalgh, 1980; Chapman *et al.*, 1992; Smith, 1989, 1993; Kim *et al.*, 1994). While these ideal conditions are very useful for experimentally confirming the basic phenomena of ripple fired explosions, these ideal conditions do not exist in a significant part of the world.

This study applies many of the techniques and tools mentioned above to a new geologic setting, Morocco, under less favorable circumstances. The constraints and limitations of spectral discrimination techniques will be qualitatively explored by examining source and path effects. Also, some of the previously cited discrimination methods will be employed in an attempt to develop a systematic discriminant that minimizes case-by-case analyses. To some extent, our study can serve as an assessment of current discrimination techniques in a complicated world of inadequate information. Attention will be paid to failures, particularly when those failures could be a result of geologic conditions, such as crustal structure.

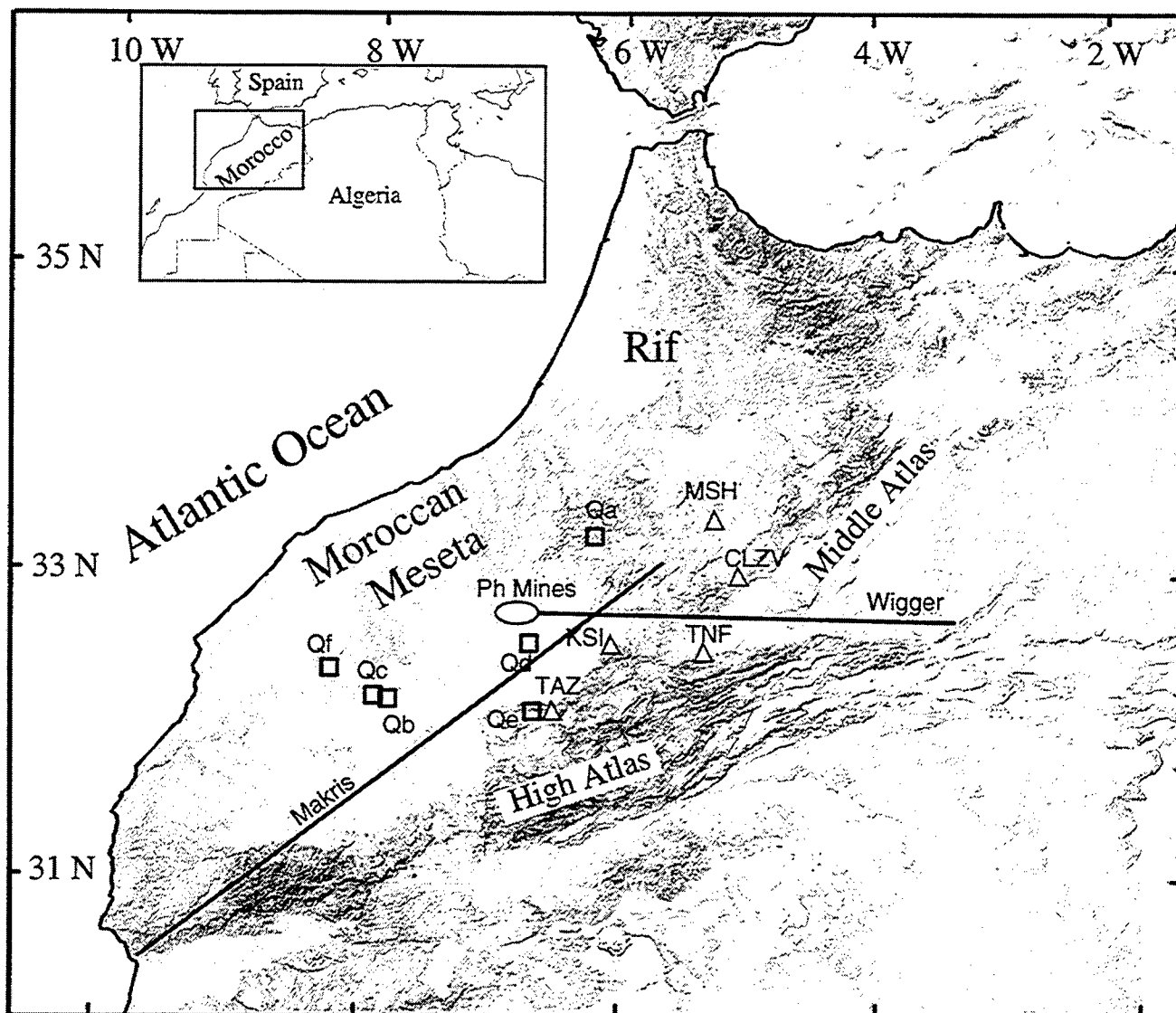


Figure 1. The seismic events and stations used in this study are located in northwest Morocco. The triangles denote the 1 Hz seismic stations; the 8 phosphate mine explosions are located inside the oval; the squares mark the epicenters of the earthquakes; and "Makris" and "Wigger" are the refraction profiles from which velocity information was obtained.

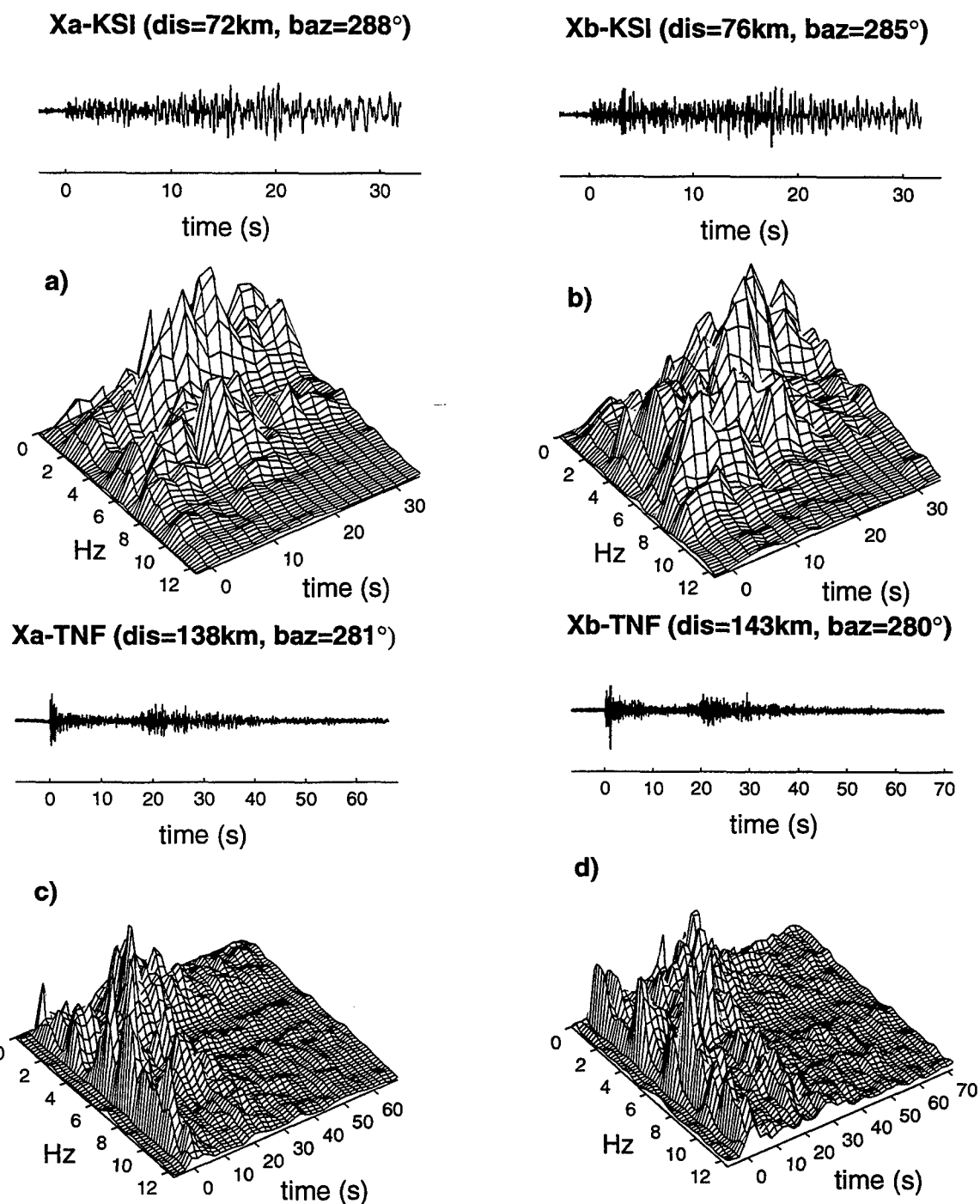


Figure 2. (a) Seismogram and filtered acceleration spectrogram for explosion Xa recorded at station KSI. Notice the two time independent modulations. (b) A different source of similar size, Xb, recorded after traveling about the same path and distance as Xa. Note what may be a second P_g arrival and its interference effects by comparing with the recorded Xa data. (c) Signal from Xa at TNF after crossing the Middle-High Atlas junction. (d) Explosion Xb after passing through the same crustal structure. Propagation or site effects seem to dominate the signal in comparison with source effects.

Crustal Structure of Northwest Morocco

The seismic events and stations used in this study are located in northwest Morocco (Figure 1). The collision of the African and Eurasian plates governs Morocco's geomorphology (e.g., Jacobshagen *et al.*, 1988). The Atlas mountains of Morocco are an active intracontinental mountain system composed of two inverted Mesozoic rift systems: the High Atlas that runs approximately east-west, and the Middle Atlas that trends northeast and merges into the interplate Betic-Rif mountain system.

Although most refraction velocity profile data for the Moroccan crust and uppermost mantle are not well established, two studies provide pertinent, but approximate, profile information about the two paths. The Makris *et al.* (1985) profile (labeled "Makris" in Figure 1) showed that the direct P-wave travels at a velocity of 5.5 km/s and is finally overtaken by Pg after nearly 40 km at an apparent velocity of 6.0 km/s, because the thickness of the sediments is almost 4 km and the velocity contrast is small. The Pn velocity is somewhat slow at 7.8 km/s and does not appear as the first arrival until approximately 140 km, if it can be seen over the background noise. Also, Makris *et al.* found an Sg apparent velocity to be approximately 3.3 km/s homogeneous along the profile, and the Moho to be about 30 km deep. Wigger *et al.* (1992) found from their profile (labeled "Wigger" in Figure 1) the Moho's depth to be approximately 35 km with an average Pn velocity at the uppermost mantle of about 7.7-7.9 km/s, also relatively slow, as was found in the Makris *et al.* profile. They also determined that the maximum thickness of the crust was under the northern border of the High Atlas at 38-39 km. Finally, both studies concluded that the Middle and High Atlas lack a substantial root. This point, however, is still contentious.

Data

The Oud Zem phosphate mines in the Moroccan Meseta provide an opportunity to analyze recordings produced by ripple fired explosions different than those already noted in the literature (Figure 1). Blasting engineers in Morocco may use different equipment and techniques for surface mining than either what the European engineers use for quarry mining in Norway, Sweden, and Germany or what the American engineers use for quarry mining in New York, Kentucky, and Minnesota (locations of ripple fired events in the literature cited above). As might frequently occur in a treaty verification scenario, these spatial-temporal variations were undocumented in the blasting logs. An explosion's geometrical layout and timing could directly influence the spectral details of a seismogram (e.g., Greenhalgh, 1980; Chapman *et al.*, 1992). As already discussed, the geologic setting is certainly different from previous investigations--for both the source and the propagation path. For instance, Greenhalgh's (1980) and Smith's (1989, 1993) propagation paths crossed a low-attenuating continental shield, as did the paths in the studies of Scandinavian events (e.g., Baumgardt and Ziegler, 1988; Baumgardt and Young, 1990; Hedlin *et al.*, 1990). Our analysis from events in the Moroccan Meseta complements this previous work.

The seismic stations of the Moroccan national network used in this study consist of short period (1 Hz), vertical-component, Ranger geophones that are linked through radio and

telephone telemetry to the Centre National de Coordination et de Planification de la Recherche Scientifique et Technique in Rabat. The instrument response of these geophones is considered flat for the bandwidth of primary interest in this study (1 - 12 Hz). The events are recorded by both analog and digital data acquisition systems; the digital data are sampled at 100 Hz. The earthquake magnitudes cited in Table 1 are duration magnitudes calculated by the Centre using the analog recordings. The other three non-explosion events, for which magnitudes are not listed, were not found in the Centre's bulletin. Precise magnitude information, however, is not required for our analysis; all of the events are comparable in size, roughly in the 2-3 magnitude range. For our locations and for our signal analysis, we used the digital recordings.

After subjecting all available explosion seismograms to a number of tests, described below in *Processing Methods*, the explosion population was trimmed down to 8 explosions (labeled Xa through Xh) with a total of 33 recordings. All available *a priori* information about the explosions from blasting logs is listed in Table 1. Because of their total charge size and their presumed purpose (phosphate surface mining), the explosions are assumed to be ripple fired. Spatial-temporal layout data independent of the seismic analysis were not available.

Although the orogenic regions of Morocco are seismically active, the same cannot be said of the Moroccan Meseta near the phosphate mines. After searching through a database of hundreds of recent seismic events recorded by the Moroccan national network (for database and event location methodology specifics, see Calvert *et al.*, 1997), only 6 (labeled Qa through Qf) crustal events were found that might have propagation paths similar to those of the known explosions, judging from the propagation distances, event-station azimuths, and associated topography. After subjecting the seismograms of these events to a number of tests like those of the explosions, the record population was reduced to only 13 recordings. Each of the non-Oud Zem phosphate mine events was located using about 5 or 6 recordings. Location information is listed in Table 1. Owing to typical errors found in hypocenter inversions, the locations could vary by several kilometers.

Table 1. Seismic Event Information

Event	Source Type	Date	Time	Latitude(N)	Long.(W)	Mag/Charge
Qa	Earthquake	07/13/92	06:12:48	33.295	6.183	2.0
Qb	Earthquake	07/14/92	19:34:35	32.210	7.783	-
Qc	Earthquake	07/21/92	18:31:45	32.226	7.889	-
Qd	Unknown	10/30/92	15:24:08	32.592	6.665	-
Qe	Earthquake	12/13/92	18:57:12	32.150	6.640	2.6
Qf	Earthquake	06/17/94	23:58:32	32.403	8.222	2.7
Xa	Surface Bl	01/12/93	17:25:--	32.768	6.767	26,750 kg
Xb	Surface Bl	01/16/93	14:06:--	32.756	6.824	20,000 kg
Xc	Surface Bl	01/18/93	15:29:--	32.751	6.836	35,000 kg

Xd	Surface Bl	01/19/93	15:45:--	32.752	6.838	33,100 kg
Xe	Surface Bl	01/20/93	14:13:--	32.760	6.818	20,000 kg
Xf	Surface Bl	01/21/93	12:49:--	32.759	6.819	20,000 kg
Xg	Surface Bl	01/21/93	14:35:--	32.820	6.719	30,000 kg
Xh	Surface Bl	01/23/93	12:48:--	32.787	6.846	07,750 kg

Unknown event Qd is most certainly an explosion.

As in most verification operations, not all of the seismic events labeled as earthquakes are actually earthquakes. At some point, they are determined to be earthquakes by excluding other sources, such as ripple fired explosions. Relevant ground-truth data are not available *a priori* for all events (in the CTBT system, seismic monitoring efforts trigger the search for ground-truth). Among our events, only the events labeled as explosions are confirmed identifications, based on their listings in blasting logs. Considering the mining practices in the Moroccan Meseta region, the other events can never be absolutely classified as earthquakes, because we cannot be certain that the blasting information for every explosion has been properly filed and distributed. Thus, as with many regions of verification interest, all events in the Meseta region should be treated with some skepticism, even those listed in local bulletins as earthquakes. For instance, Qb and Qc are located near a region known to have had phosphate mines at one time, but they are not located at the active phosphate mines themselves. The origin times of Qb and Qc are both in the early evening. Most of the known explosions, however, were blasted in mid-afternoon. Thus, *a priori* (before any processing other than their location), events Qb and Qc are probably earthquakes. Our analysis (discussed below) does not contradict this assumption, and with event Qc, our analysis supports this conclusion. On the other hand, Qd is most certainly an explosion, but it is still not labeled as such since it cannot be independently ruled out as an earthquake any more than the other earthquakes. It is located near the phosphate mines, but once again it is not at the known mines themselves. The Qd origin time is in mid-afternoon, prime time for the explosions. The *Results* section will provide more information to sort out these events, which are classified as earthquakes throughout all analyses. Readers should be aware of these complexities in constructing any "training" or "calibration" set for regions that provide the best opportunities for discrimination studies, that is, where seismic activity and mining activity coexist (cf. Baumgardt and Young, 1990).

Processing Methods

Only seismic stations that recorded both earthquakes and explosions in proportionate numbers were included in the analysis in order to account for station effects and thus to allow direct comparisons between events. Recordings that have under a 2:1 rms signal to noise ratio (or more accurately, $(S+N)/N$) were eliminated from the population. The noise was approximated from a 10 second window preceding the first motion of the seismogram. These two tests eliminated over 50 recordings for the events listed in Table 1 and disqualified 6 other events completely. Those disqualified events are not listed in Table 1.

For the purpose of this study, the Pg phase was defined by the 6.0 - 4.5 km/s apparent velocity window. Sg was in the 3.7 - 2.7 km/s velocity window. The Pg window always missed any possible Pn phase, but it sometimes did not capture the first motion of the Pg phase, usually in the case of distant events farther than 175 km. If the 6.0 km/s point was before the first motion of the seismogram (which was "hand" picked), then the velocity window did contain some noise. These two consequences were intentional in order to abide by a strict velocity window setup which allows for comparisons with other studies in the literature. The Sg velocity window was terminated at 2.7 km/s to eliminate any influences from Rg. Rg was visible in a few recordings but was not utilized systematically because of its uncertainty and because of its limited utility for regional verification efforts, since it is mostly used as a depth discriminant (cf., Taylor *et al.*, 1989; Kim *et al.*, 1994). The Pg and Sg windows were relatively long for two reasons: to encompass a significant portion of each phase's coda which might amplify the effects of time-independent modulation, and to allow for variations in apparent velocity with propagation distance. Velocities for the explosions were calibrated from the observational data of the earthquakes, since the explosion origin times were known only to the nearest minute. The explosion locations, however, were noted to a thousandth of a degree in the blasting logs.

In order to emphasize different properties such as time independent modulations and path independent modulations, spectra are displayed in a variety of ways. To highlight possible modulations, all spectra are calculated as acceleration amplitude spectra to enhance the higher frequencies relative to the lower frequencies. The basic computations and approximations behind the spectra displays for all phase windows are the same. The calculation of a spectrogram is given as an example. Each time-frequency distribution (i.e., spectrogram) is a compilation of acceleration spectra from 3.84 second windows centered around 1.92 second intervals (for 50% overlap) between 8.6 and 1.4 km/s group velocities. The acceleration spectrum mapped at each interval on the spectrogram was calculated in the following way. First, the entire velocity-response time series was differentiated and demeaned to give the acceleration-response. Each 3.84 second window was lengthened with alternating time-inverted copies, to about 80 seconds. The lengthening and flipping process minimizes any discontinuities and phase distortions from the filtering, facilitates the hanning, and reinforces a stationary signal assumption, all of which are described below. This lengthened series was filtered with a 2nd order zero phase Butterworth filter. The 3dB corner frequencies of the pass-band were 1 Hz and 25 Hz. This served both as an anti-aliasing filter for the appendage process (which introduced its own periodicity) and as a frequency response filter for the seismograph, although signal-to-noise ratios usually became unacceptable (less than 2:1) anywhere from 10 Hz to 20 Hz. After filtering, the "lengthened" time series was modeled as a stationary random signal, and its power spectrum was estimated using the Welch method with a 512 pt. fast-fourier transform, 100% hanning, and 50% overlap (Welch, 1967; Oppenheim and Schaffer, 1989). From experimentation with other lengths (e.g., 8, 30, and 61 seconds) the lengthening process does not significantly change the spectrum in the 1 - 25 Hz range, but it does smooth the spectrum below 1 Hz. The amplitude of the acceleration power spectrum was obtained by taking the square root of the power

spectrum, as is often used (e.g., Wuster, 1993). For the spectrograms, the log of the noise spectra was subtracted from the log of the signal spectrum. The noise spectra are generally subtracted out for all displayed spectra, unless the noise spectra are displayed underneath the signal spectra. All spectra were smoothed using a very conservative 3 point moving average filter.

Since frequency resolution is always inversely proportional to time resolution in Fourier analysis, compromises had to be made with the window lengths. With our data set, this spectral estimate method seemed to provide an optimal trade-off between resolution, spectral variance, and calculation speed for the windows of interest. The short windows (considering the 100 Hz sampling rate) were necessary to resolve the phases of the local events. Also, short windows are preferable so that the signal characteristics within the window may be approximated as stationary. These 3.84 second window lengths, however, should not conceal time independent modulations, that is, with this window length, time independent modulations should be observable throughout Pg, Sg, and their codas (cf. the 4 second windows of Kim *et al.*, 1994). The relatively low rms signal-to-noise ratios for our data (greater than 2) and the signals' frequency complexity were thought to be the limiting factors for spectral resolution, and not simply the dynamic range of the data. Under these circumstances, the conservative, stable, and readily available Welch method is adequate. This conclusion was supported by qualitatively comparing a variety of spectral estimation techniques with the Welch method, such as the methods of Blackman-Tukey (1958), Capon (1969), and the maximum-likelihood and maximum-entropy methods of SAC 2000, Lawrence Livermore National Laboratory's seismic analysis program (Lacoss, 1971; Kanasewich, 1981). For the few recordings compared, the variability of the spectral estimates were minimal. No estimator convincingly revealed time independent modulations where the others did not.

The calculation of the spectral discriminants was straightforward following previous spectral discrimination studies (e.g., Taylor *et al.*, 1989; Walter, 1995; Taylor, 1996). The spectral ratios were calculated by dividing the sums of the spectral amplitudes in each respective band. The amplitude spectra were calculated using the above Welch spectrum estimation technique on each complete phase window (6.0 - 4.5 km/s for Pg, and 3.7 - 2.7 km/s for Sg), but without the differentiation. Since the instrument response is considered to be essentially flat for the frequency range of interest in this paper, it is not deconvolved from the spectra, and noise is assumed to cancel out in the spectral ratios. The Pg/Sg maximum amplitude ratio was calculated by dividing the sums of the largest 1% of each phase window's amplitudes in the 1 - 25 Hz frequency band. Any first order dependency on propagation distance was removed from the ratios with a linear least squares fit. This correction slightly improved the performance of the discriminants (for all cases the slope of the fit was less than about five percent of the overall spread). The discriminant line was rather arbitrarily chosen as the median value of the earthquakes. The authors are aware of statistical methods for selecting the discriminant line (e.g., Elvers, 1974; Taylor *et al.*, 1989; Woodward and Gray, 1995; Fisk *et al.*, 1996;

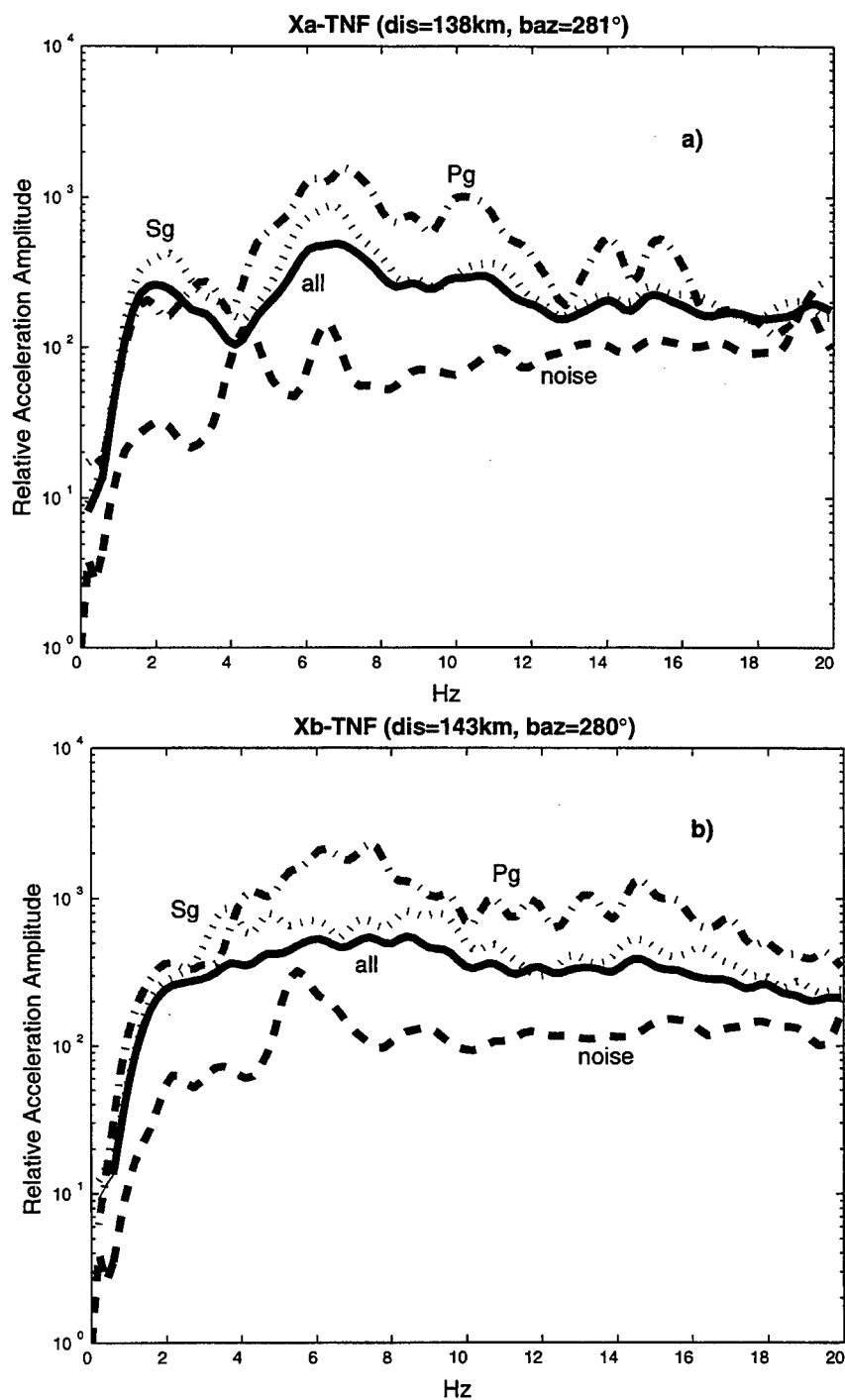


Figure 3. (a) Filtered acceleration spectra of Xa's phases as recorded at TNF. "All" is the logarithmic mean of the phase spectra. (b) Explosion Xb's acceleration spectra. Notice Xa's prominent time independent modulations in comparison with Xb's spectra.

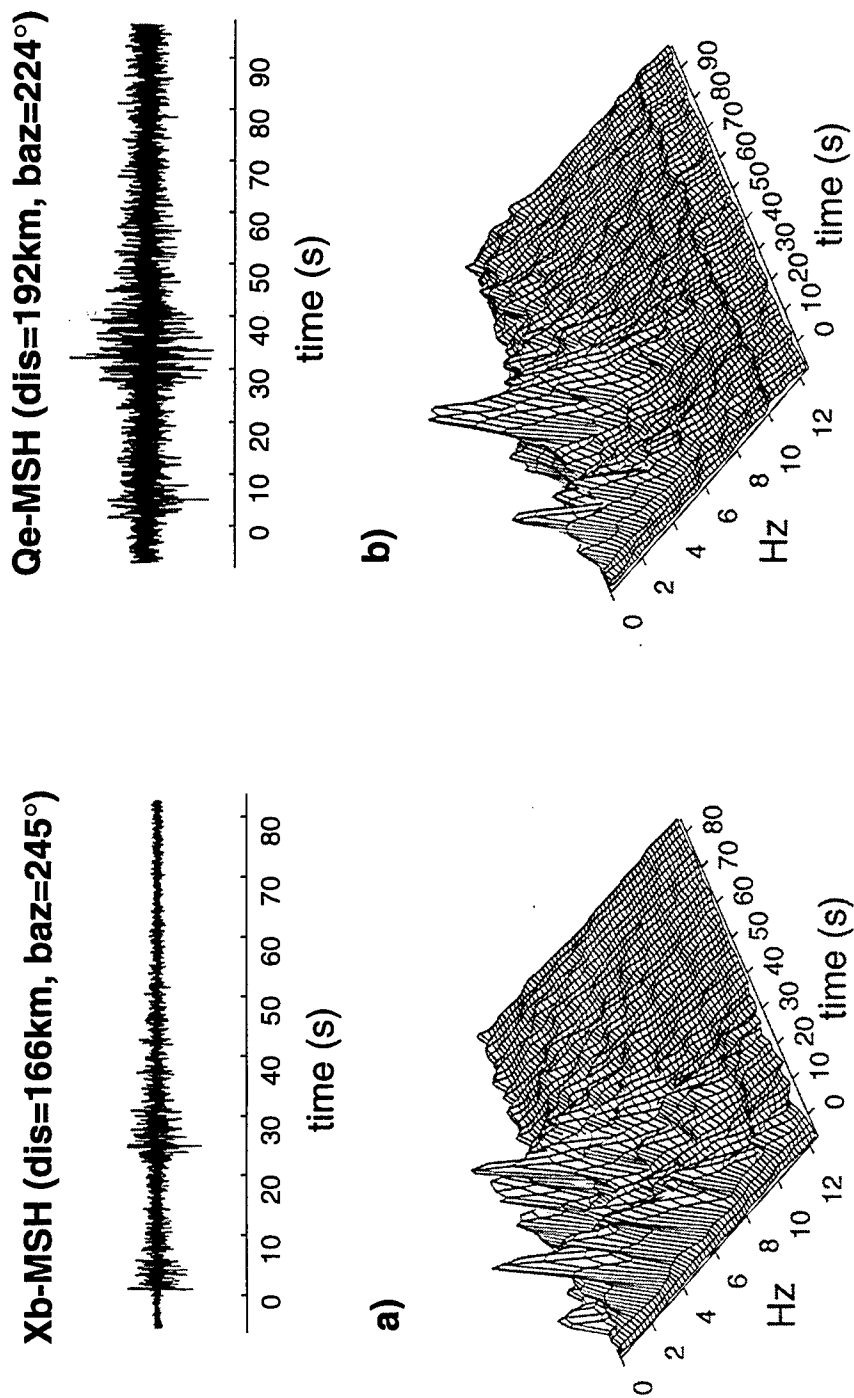


Figure 4. (a) Explosion Xb's seismogram and spectrogram recorded at MSH in the Middle Atlas. (b) Earthquake Qe's signal at MSH after traveling a comparable path. Although clearly Xb's signal has proportionally higher frequencies and is possibly more complex, both signals have similar distributions in time-frequency space in comparison to the spectrograms of Figure 2.

Taylor, 1996), but our small and uncertain training set does not warrant such approaches.

Analysis and Results

The seismic recordings of the 8 Oud Zem phosphate mine explosions were characterized by a surprising amount of variability in view of their similar purpose, total charge magnitude, ripple-fired mechanism, and location (Table 1). While phase and path independent spectral scalloping were noticeable in many of the signals to some extent, those features were hardly ubiquitous. Furthermore, among the signals for which spectral modulation was clearly evident, the frequencies of their maxima and minima were not correlated, even for those cases where the propagation path, recording station, and total charge size were similar. These observations suggest that the spatial-temporal arrangement of the source varied considerably, whether intentionally as a result of blast requirements or crew preferences, or as a result of misfirings. For example, Figure 2 shows the seismograms and velocity-frequency distributions for two explosions, Xa and Xb, both comparable in size (Table 1) and both exploded at the Oud Zem site. The signals shown in Figures 2a and 2b are recorded by the same seismograph station, KSI, within a week's time. From Xa's spectrogram, two phase independent modulations can be noted, one at about 3 Hz and the other at about 7 Hz. In other words, the spectrogram has a time independent "valley" at about 4 to 5 Hz. It should be noted that this feature could be emphasized by shading, color, or even a different spectrogram perspective, but that individualized analysis is impractical for any large-scale verification system (in the initial stages of characterization) and is beyond the scope of most previous discrimination studies that attempt to minimize case-by-case analyses. Turning to Xb's spectrogram, any phase independent modulations are not obvious. Xb's spectrogram is less coherent. The destructive interference apparent in Xb's spectrogram and seismogram could be the result of a second blast bench, if it is significant in charge size in relation to the initial rippled-fired blast. This hypothesis is supported by a large arrival on Xb's seismogram just after the first motion at zero time. The corresponding Sg doublet is not readily visible. The brief listing for Xb in the blast log only notes one blast bench. This abnormality is one of the more conspicuous variations among the observed ripple fired source mechanisms.

Surficial features such as topography, which could reflect crustal heterogeneity, seemed to affect the seismic signals. Figures 2c and 2d are the recorded signals of explosions Xa and Xb, respectively, at station TNF (Figure 1). The recordings' back-azimuths to the location of the explosions are comparable to those at the KSI station. The seismic signals from explosions Xa and Xb are similarly filtered presumably by their propagation through the Middle-High Atlas junction. The Sg phase is much more attenuated than the Pg phase. The resulting spectrograms are dramatically different than their counterparts constructed from the signals recorded at the KSI station. Note that at this distance, the effect of that postulated second blast bench on the time- frequency distribution are minimal, perhaps owing to both the change in time scale and path effects (in this case, we cannot separate path, distance, and site effects). Still, the relative acceleration spectra of each explosion's phases, shown in Figure 3a and 3b, do reveal some possible deconstructive interference. The "all" line is the logarithmic mean of the phase spectra. As expected from explosion Xa's spectrogram, Xa's modulations are much more

prominent than those of Xb. The phase independence of Xb's scalloping is still not apparent.

Propagation effects appear to conceal differences between the seismic signals of explosions and earthquakes. An explosion and earthquake which were quite distinguishable with spectral analysis at one station (whose back-azimuth and distance to each event were similar), were in some cases much less distinguishable when using recordings at other stations. A representative case is that of explosion Xb and earthquake Qe (Figure 4). For both events the Pg and Sg amplitudes recorded at MSH are of the same order of magnitude, and the energy of the phases is distributed similarly in frequency space (Figures 4a and 4b). The explosion's Pg / Sg ratio is larger than that of the earthquake, and more of the explosion's energy spills over into higher frequencies (Figures 4a and 4b). A comparison of explosion Xb's recording at MSH (Figure 4a) with that at KSI (Figure 2b) and TNF (Figure 2d) shows the importance of azimuthal and propagation effects, as well as highlights the similarities between Xb's and Qe's signal at MSH (possibly from site effects). For instance, contrasting Xb's recording at MSH (Figure 4a) and TNF (Figure 2d), which are at comparable distances, the TNF spectrogram has more high frequency energy relative to low frequency energy and has more Pg energy relative to Sg energy than the MSH spectrogram. As seen in Figure 5a, the scalloping of the explosion signal is relatively consistent for the lower frequencies within two path groups, that of CLZV and TNF, and that of KSI, MSH, and TAZ, whose paths differ significantly (Figure 1). Above 8 Hz, the frequency maxima and minima within these groups no longer correlate. As in Xb's case, for Qe's acceleration spectra the lower frequency maxima and minima of CLZV and TNF correlate (Figure 5b). Because of the above similarities, it is difficult to recognize path independent, source related modulations. These observations indicate that path dependencies, rather than source characteristics, seem to dominate the signal's form.

As discriminants, the most successful ratio tests were the 5-10 Hz Pg / 5-10 Hz Sg and 10-15 Hz Pg / 10-15 Hz Sg cross-phase tests (Figure 6). The variance in the ratios of both tests, due to differences in the recording station or in path effects (but not distance effects), was still considerable. The narrower cross-phase and cross-spectral ratio tests (e.g., 6-8 Hz Pg / 6-8 Hz Sg and 1-2 Hz Pg / 6-8 Hz Sg) were less effective (Figure 7), and the cross-spectral ratio tests within phases (e.g., the narrow versions, 1-2 Hz Sg / 6-8 Hz Sg, as well as the corresponding broader versions which are not displayed, e.g., 1-4 Hz Sg / 5-10 Hz Sg) were significantly less effective (Figure 8). The Pg/Sg maximum amplitude test was also ineffective (not displayed). If the two spectral discriminants of Figure 6 are integrated by a union (*vis-à-vis* intersection) and seismic information from only a single station is available, then a single explosion recording has a 12% probability of being classified as an earthquake, and a single earthquake recording has a 23% probability of being classified as an explosion. If all of the recordings of an event were used in the discrimination scheme (an unweighted network average for each event), then only "earthquake" Qd would be "misclassified." The other discriminants did not demonstrate such results (and in only one of the other discriminants, 6-8 Hz Pg / 6-8 Hz Sg, is Qd an outlier). As already mentioned in the *Data* section, judging from *a priori* information such as origin time and location, event Qd is most likely an explosion and

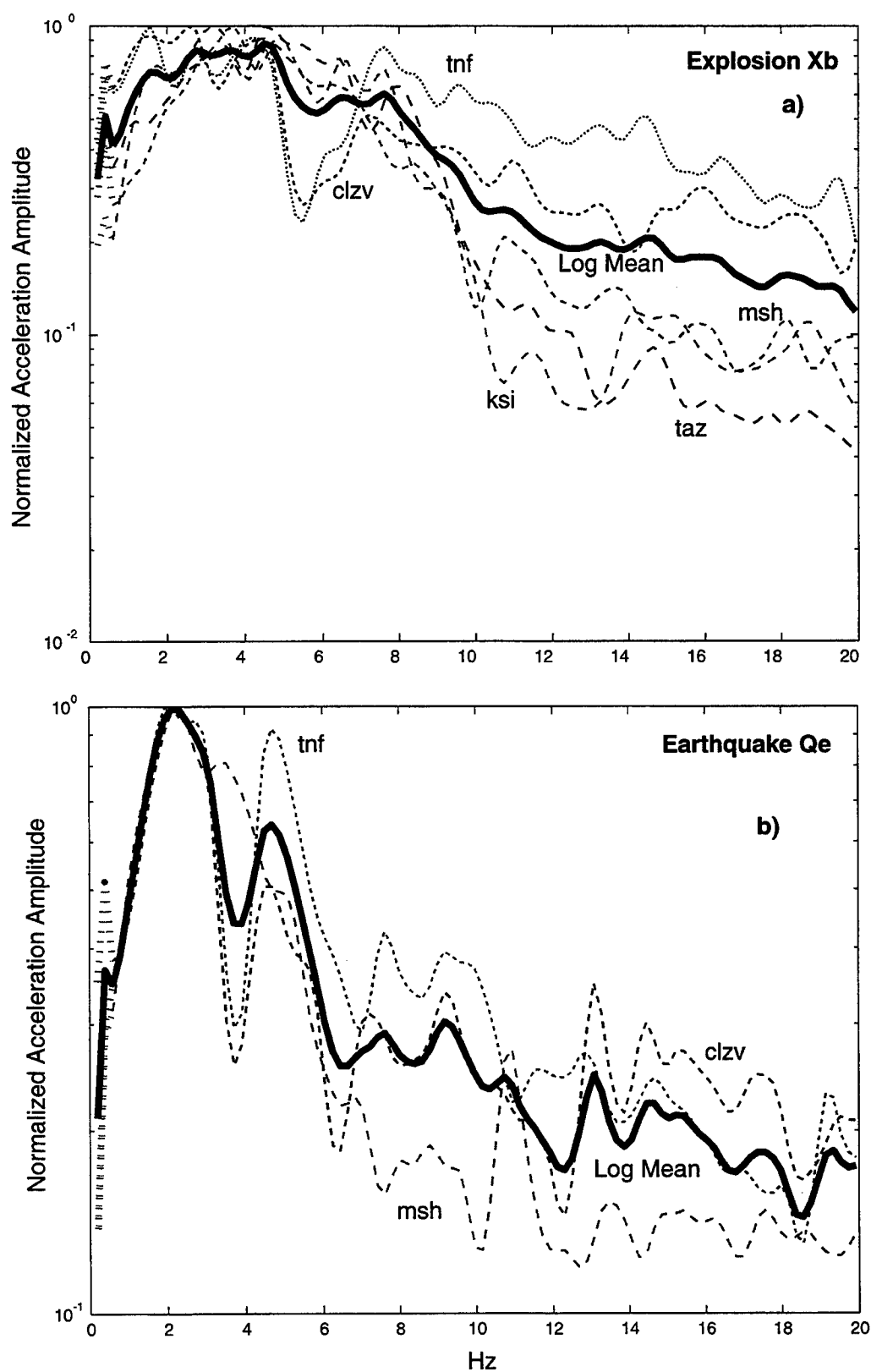


Figure 5. (a) The acceleration spectra of explosion Xb at different stations. (b) Earthquake Qe's acceleration spectra. Notice the correlation between the acceleration spectra of CLZV and TNF and their differences with that of MSH for both the explosion and earthquake, especially in the 3 to 6 Hz range.

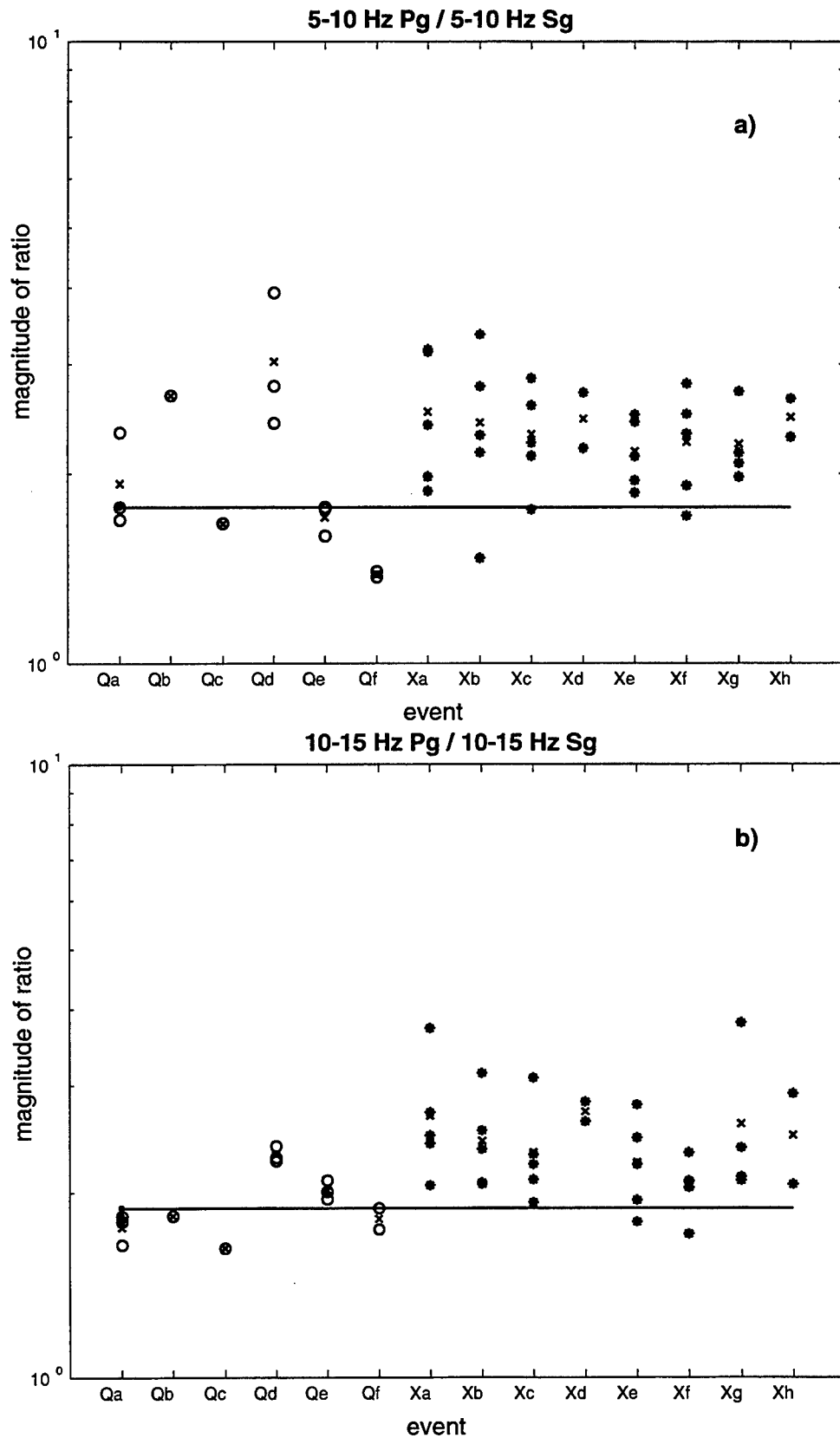


Figure 6. (a) The 5-10 Hz Pg/Sg ratio test sorted by source. (b) The more precise 10-15 Hz Pg/Sg ratio test. The o's mark the discriminant values for the earthquakes; the asterisks mark the values for the explosions; and the x's mark the unweighted, simple, network average for each event. See Table 1 and text for information about source Qd, which is most likely an explosion.

not an earthquake (but independent confirmation is not available through blasting logs, etc., so the event is assumed to be an earthquake). If Qd is considered an explosion in the training set, then the network approach using the 5-10 Hz Pg / 5-10 Hz Sg and 10-15 Hz Pg / 10-15 Hz Sg discriminants would classify every event correctly. Thus, since the original discriminant is based on a flawed training set, its results represent a worst case scenario which reflects some of the challenges of constructing a discriminant in a world of uncertain and incomplete information.

Discussion

The large regional variability of source mechanisms, source geologic conditions, and propagation paths and the geophysical and seismological community's relative lack of a comprehensive physical understanding of propagation effects, have encouraged site-dependent, case-based approaches for discriminating between earthquakes, industrial explosions, and nuclear explosions. As shown by our study, the empirical heuristics utilized in case-based approaches have limitations that must be considered by any CTBT verification system.

Our findings argue that more often than the current literature (reviewed above) suggests, source inconsistencies may result in the failure of time independent spectral modulations to discriminate between earthquakes and ripple-fired explosions. Specifically, we agree with the observations of Baumgardt and Young (1990) and Kim *et al.* (1994) that for some ripple fired explosions time independent spectral modulations may or may not exist, and that if they do exist, they need not be consistent among different explosions, even if those explosions originate from the same mine or quarry. Irregular source delays have been noted elsewhere (e.g., Richards *et al.*, 1991). Furthermore, as we have observed in this case, spectral banding in explosion spectra may not be any more visible than spectral banding in earthquakes. In fact, spectral banding has been clearly observed in a few earthquakes, possibly due to region-specific source-receiver paths (e.g., Richards *et al.*, 1991). As our results imply, the inability of time independent modulations to discriminate between earthquakes and explosions may not necessarily be the exception.

Low frequency path independent modulations advocated by Gitterman and van Eck (1993) also can be inconclusive for discrimination purposes, possibly as a result of the spatial-temporal layout of the explosion, the earthquake mechanism's radiation pattern, or disproportionate phase attenuation. We found that the travel path through the Middle-High Atlas junction significantly attenuates shear waves (in our case, Sg) with respect to the compressional waves. This observation agrees with, for example, the Kim *et al.* (1994) finding that Lg propagation was disrupted when significant structural variations were encountered, such as in their case the Appalachian platform in southern New York-New Jersey. We also found that in the low frequencies, earthquakes often seemed to demonstrate path independent spectral modulation similar to that of ripple fired explosions; at higher frequencies, the scalloping from ripple fired explosions was often incoherent among recording stations. As in the case of time independent modulations, path independent modulations might exist for a significant portion of the ripple fired explosion recordings, but they might not be conclusive enough in comparison to earthquake spectra data to use consistently and reliably as a discriminant.

Our attempts to discriminate between earthquakes and explosions using spectral ratios support several findings in the literature. First, for separating explosions from earthquakes the cross-phase discriminants (Pg/Sg) seem to perform better than discriminants within the same phase (Pg/Pg or Sg/Sg), especially for low-magnitude events. For our study, cross-phase spectral discriminants, especially the wider bands (e.g., 5-10 Hz Pg / 5-10 Hz Sg), were more effective at distinguishing between ripple fired explosions and earthquakes than same-phase cross-spectral discriminants (e.g., 1-2 Hz Sg / 6-8 Hz Sg). Baumgardt and Young (1990) noted that for the Baltic shield, amplitude ratios between compressional and shear waves were successful in separating the ripple fired blasts from the earthquakes, whereas a low-frequency to high-frequency Lg spectral ratio test (i.e., a same-phase cross-spectral test) provided no separation. For discriminating chemical or nuclear explosions from earthquakes (here, mixing the two types of explosions), Taylor (1996) notes in reviewing the past performance of Lg spectral ratios that in most regions other than the western United States the discriminant is "disappointing." In discriminating between nuclear explosions and earthquakes, none of Walter *et al.*'s (1995) same-phase low frequency to high frequency discriminants (Pn, Pg, Lg, and Lg coda) performed well below magnitude (m_b) 3.5. On the other hand, high frequency P/S ratios (in this study, 10-15 Hz Pg / 10-15 Hz Sg) have been relatively successful in a variety of geological environments. Richards *et al.* (1991), Kim *et al.* (1994), and Blandford (1995) demonstrated their effectiveness in discriminating between ripple fired explosions and earthquakes, and Walter *et al.* (1996) and Taylor (1996) convincingly distinguished between NTS nuclear explosions and western U.S. earthquakes also using high frequency (greater than 5 Hz) P/S ratios. Therefore, in contrast to same-phase discriminants, high frequency P/S discriminants, as a group, would appear to be relatively effective for different regions and paths within those regions.

The literature has been unclear about whether low frequency to high frequency P/S discriminants should be included in that group, because often the comparison is not made within the same study (e.g., Baumgardt and Young, 1990; Kim *et al.*, 1994; Walter *et al.*, 1995; Taylor, 1996). This study's admittedly small data set suggests that, for distinguishing between earthquakes and ripple fired explosion (versus nuclear explosions), the low frequency to high frequency Pg / Sg discriminant is not as effective as the high frequency cross-phase ratios (e.g., 5-10 Hz Pg / 5-10 Hz Sg and especially 10-15 Hz Pg / 10-15 Hz Sg). This finding is consistent with the work of Lynnes and Baumstark (1991).

Although Taylor *et al.* (1989) and Lynnes and Baumstark (1991) find increasing frequency to have little or no effect on the compressional to shear wave discriminant's performance in the western United States, we find the effectiveness of the same-bandwidth Pg / Sg test to increase with frequency, in agreement with, among others, Baumgardt and Young's (1990) Baltic shield study, Walter *et al.*'s (1995) Nevada Test Site study, and Taylor's (1996) study of the western United States (which, paradoxically, used the same recording stations and many of the events from Taylor *et al.* (1989)). The literature's only potentially portable spectral ratio test thus becomes less effective with

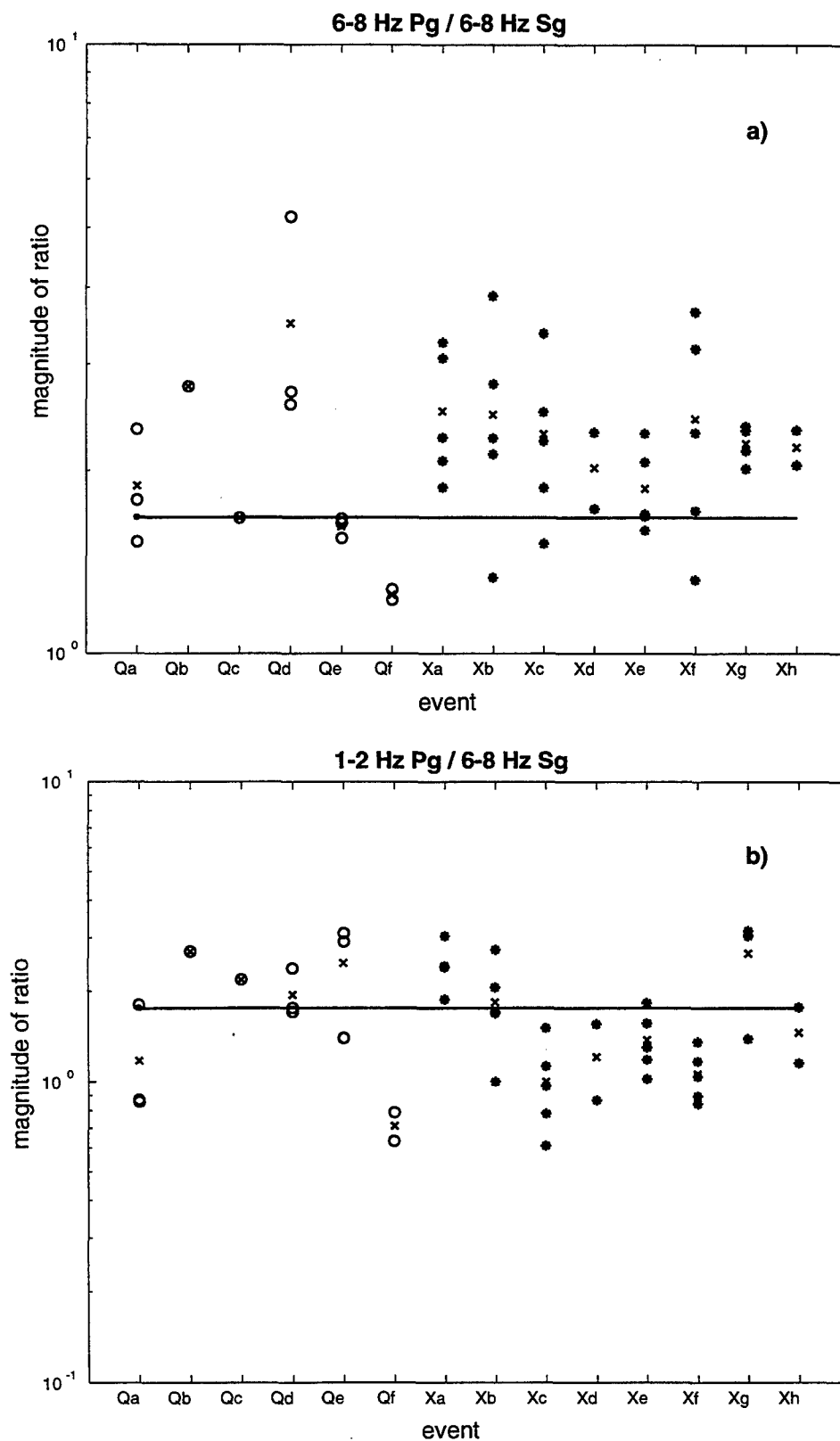


Figure 7. (a) The narrower 6-8 Hz Pg/Sg cross-phase ratio test is almost as effective as the broader 5-10 Hz test of Figure 6a. (b) The 1-2 Hz Pg / 6-8 Hz Sg cross-spectral ratio test shows to be a poor discriminant in this case.

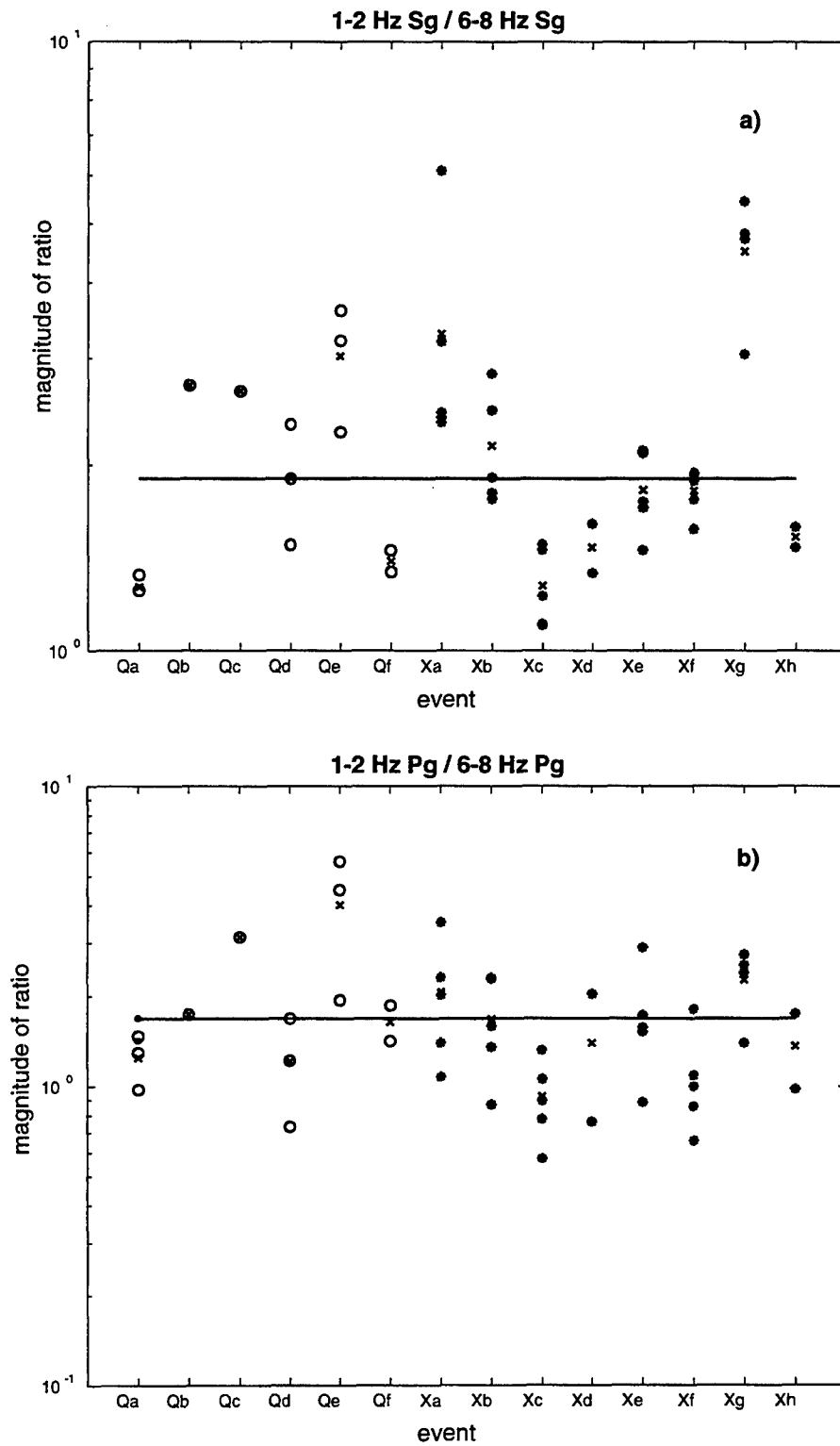


Figure 8. The low-frequency to high-frequency same-phase spectral ratio tests are unable to distinguish the ripple fired explosions from the earthquakes, even when the network averages are considered.

greater distances or in a lower-Q region. In addition, the Walter *et al.* (1995) analysis also suggests that variations in this discriminant might arise from source medium differences of velocity, density, and gas porosity.

This paper also argues that the discriminant's value will depend upon propagation path and/or site effects (our analysis does not separate these effects). For example, the TNF station recordings consistently had the highest Pg/Sg values. Also, the value of each event's discriminant varied substantially by recording site (each which used basically the same equipment). Even after Walter *et al.* (1995) considered the source medium, they still required path-dependent factors "other than a simple regional attenuation model. . . to explain the scatter in the data" (e.g., the discriminant values of the non-proliferation experiment's 1 kt chemical explosion). Our posited dependency on propagation path agrees with the findings of Lynnes and Baumstark (1991) for P/S discriminants for Nevada Test Site explosions. Finally, as Baumgardt and Young (1990) and Wuster (1993) have emphasized, empirical discriminants are fundamentally limited by their training sets. No doubt, this caveat is especially applicable for our small data set.

Conclusions

This study applied many of the standard methods for discriminating between earthquakes and ripple fired explosions to a new geologic setting (northwest Morocco) in an effort to examine the limitations of these techniques. We found that although time and path independent spectral modulations can be useful, they are far from ubiquitous. Source mechanisms for explosions may vary substantially even among events from the same quarry or mine. Furthermore, crustal structure and/or site effects determine the character of the seismic signal to a greater extent than the source mechanism, as demonstrated by spectrogram analysis. Despite the susceptibility of spectral discriminant values for a given event to propagation and/or site effects, we were able to construct a discrimination technique using two high-frequency, wide-band, Pg/Sg spectral ratio tests that could systematically discriminate the events in our data set. The training set's size, however, imposes fundamental constraints, especially since nuclear explosions are not a constituent of that data set.

Since the source, path, and site effects noted in this study are likely to play a role in all efforts to seismically discriminate among nuclear explosions, chemical explosions, and earthquakes, databases that organize regional geological, geophysical, seismological, and crustal information are critical components to the success of any seismic CTBT verification project. By recognizing the complexity of seismic discrimination, our study emphasizes that the regional case-based approach which has shown much promise requires nothing less than the best empirical information.

Acknowledgments

This research was sponsored and supported by the U.S. Department of Energy Contract #F19628-95-C-0092, issued by the Phillips Laboratory. We thank the Centre National de Coordination et de Planification de la Recherche Scientifique et Technique, and the Institut Scientifique, Departement de Physique du Globe for providing us with the data for this study. This manuscript greatly benefited from the suggestions of reviewers Won-

Young Kim and William R. Walter, and an anonymous reviewer. Institute for the Study of the Continents contribution No. 229.

References

- Baumgardt, D.R. and K.A. Ziegler (1988). Spectral evidence for source multiplicity in explosions: application to regional discrimination of earthquakes and explosions, *Bull. Seism. Soc. Am.* **78**, 1773-1795.
- Baumgardt, D.R. and G.B. Young (1990). Regional seismic waveform discriminants and case-based event discrimination using regional arrays, *Bull. Seism. Soc. Am.* **80**, 1874-1892.
- Bennett, T.J. and J.R. Murphy (1986). Analysis of seismic discrimination capabilities using regional data from western United States events, *Bull. Seism. Soc. Am.* **76**, 1069-1086.
- Blackman, R.B., and J.W. Tukey (1958). *The Measurement of Power Spectra From the Point of View of Communication Engineering*, Dover Publications, New York, 190 pp.
- Blandford, R.R. (1995). Discrimination of mining, cratering, tamped, and decoupled explosions using high frequency S-to-P ratios, AFTAC-TR-95-002, Patrick AFB, Florida, 34 pp.
- Capon, J. (1969). High-resolution frequency-wavenumber spectrum analysis, *Proc. IEEE* **57**, 1408-1418.
- Calvert, A., F. Gomez, D. Seber, M. Barazangi, N. Jabour, A. Ibenbrahim, and A. Demnati (1997). An integrated geophysical investigation of recent seismicity in the Al-Hoceima region of north Morocco, *Bull. Seism. Soc. Am.*, in press.
- Chapman, M.C., G.A. Bollinger, and M.S. Sibol (1992). Modeling delay-fired explosion spectra at regional distances, *Bull. Seism. Soc. Am.* **82**, 2430-2447.
- Elvers, E. (1974). Seismic event identification by negative evidence, *Bull. Seism. Soc. Am.* **64**, 1671-1683.
- Fisk, M.D., H.L. Gray, and G.D. McCartor (1996). Regional event discrimination without transporting thresholds, *Bull. Seism. Soc. Am.* **86**, 1545-1558.
- Gitterman, Y. and T. van Eck (1993). Spectra of quarry blasts and microearthquakes recorded at local distances in Israel, *Bull. Seism. Soc. Am.* **83**, 1799-1812.
- Greenhalgh, S.A. (1980). Effects of delay shooting on the nature of P-wave seismograms, *Bull. Seism. Soc. Am.* **70**, 2037-2050.
- Hedlin, M.A., J.B. Minster, and J.A. Orcutt (1989). The time-frequency characteristics of quarry blasts and calibration explosions recorded in Kazakhstan, USSR, *Geophys. J. Int.* **99**, 109-121.
- Hedlin, M.A., J.B. Minster, and J.A. Orcutt (1990). An automatic means to discriminate between earthquakes and quarry blasts, *Bull. Seism. Soc. Am.* **80**, 2143-2160.
- Jacobshagen, V., K. Gorler, and P. Giese (1988). Geodynamic evolution of the Atlas System (Morocco) in Post-Palaeozoic time, in *The Atlas System of Morocco*, Jacobshagen (Editor), Lecture Notes in Earth Sciences, **15**, Springer-Verlag, Berlin, 481-499.
- Kanasewich, E.R. (1981). *Time Sequence Analysis in Geophysics*, University of Alberta Press, Edmonton, 480 pp.

- Kim, W.Y., D.W. Simpson, and P.G. Richards (1994). High-frequency spectra of regional phases from earthquakes and chemical explosions, *Bull. Seism. Soc. Am.* **84**, 1365-1386.
- Lacoss, R.T. (1971). Data Adaptive Spectral Analysis Methods, *Geophy.* **36**, 661-675.
- Lynnes, C. and R. Baumstark (1991). Phase and spectral ratio discrimination in North America, Teledyne Technical Report TGAL-91-06.
- Makris, J., A. Demnati, and J. Klusmann (1985). Deep seismic soundings in Morocco and a crust and upper mantle model deduced from seismic and gravity data, *Annales Geophysicae* **3**, 369-380.
- Oppenheim, A.V., and R.W. Schaffer (1989). *Discrete-time signal processing*, Prentice Hall, New Jersey, 879 pp.
- Pomeroy, P.W., W.J. Best, and T.V. McEvilly (1982). Test ban treaty verification with regional data--a review, *Bull. Seism. Soc. Am.* **72**, S89-S129.
- Richards, P.G., W.Y. Kim, D.W. Simpson, and G. Ekstrom (1991). Chemical explosions and the discrimination problem, PL-TR-91-2285, Phillips Lab., Hanscom AFB, Massachusetts, 96 pp, ADA251594.
- Smith, A.T. (1989). High-frequency seismic observations and models of chemical explosions: implications for the discrimination of ripple-fired mining blasts, *Bull. Seism. Soc. Am.* **79**, 1089-1110.
- Smith, A.T. (1993). Discrimination of explosions from simultaneous mining blasts, *Bull. Seism. Soc. Am.* **83**, 160-179.
- Taylor, S.R., M.D. Denny, E.S. Vergino, and R.E. Glaser (1989). Regional discrimination between NTS explosions and western U.S. earthquakes, *Bull. Seism. Soc. Am.* **79**, 1142-1176.
- Taylor, S.R. (1996). Analysis of high-frequency Pg/Lg ratios from NTS explosions and western U.S. earthquakes, *Bull. Seism. Soc. Am.* **86**, 1042-1053.
- Walter, W.R., K.M. Mayeda, and H.J. Patton (1995). Phase and spectral ratio discrimination between NTS earthquakes and explosions. Part I: empirical observations, *Bull. Seism. Soc. Am.* **85**, 1050-1067.
- Welch, P.D. (1967). The use of fast fourier transform for the estimation of spectra: A method based on time averaging over short, modified periodograms, *IEEE Trans. Audio Electroacoust.*, Vol. AU-15, June, 70-74.
- Wigger, P., G. Asch, P. Giese, W. Heinsohn, S. El Alami, and F. Ramdani (1992). Crustal structure along a traverse across the Middle and High Atlas mountains derived from seismic refraction studies, *Geol. Rundschau*. **70**, 801-841.
- Wuster, J. (1993). Discrimination of chemical explosions and earthquakes in Central Europe--a case study, *Bull. Seism. Soc. Am.* **83**, 1184-1212.
- Woodward, W.A. and H.L. Gray (1995). A Hypothesis-Testing Approach to Outlier Detection, PL-TR-95-2141, Phillips Lab., Hanscom AFB, Massachusetts, 115 pp, ADA305773

APENDIX I: COLLECTED REFERENCES ON THE GEOLOGY/GEOPHYSICS OF THE MIDDLE EAST AND NORTH AFRICA

1. References for the Middle East

- Abbas, M.J. & Masin, J., 1975. New Geophysical Aspects Of The Basement Structure In Western Iraq. *Journal Of The Geological Society Of Iraq*, Special Issue: 1-13.
- Abdelhady, Y.E., Tealeb, A. & Ghaib, F.A., 1983. Tectonic Trends Inferred From Gravity Field Analysis In The Sinjar Area, Northwest Iraq. *International Basement Tectonics Association*, 4: 237-244.
- Abdula, S. & Valek, R. (1968). Patterns And General Properties Of The Gravity Field Of Iraq. XXIII International Geological Congress, Iraq.
- Abed, A.M., 1985. On The Supposed Precambrian Palaeosuture Along The Dead Sea Rift, Jordan. *Journal Of The Geological Society Of London*, 142: 527-531.
- Abu-Jaber, N.S., Kimberley, M.M. & Cavaroc, V.V., 1989. Mesozoic-Palaeogene Basin Development Within The Eastern Mediterranean Borderland. *Journal Of Petroleum Geology*, 12: 419-436.
- Adams, R.D. & Barazangi, M., 1984. Seismotectonics And Seismology In The Arab Region; A Brief Summary And Future Plans. *Bulletin Of The Seismological Society Of America*, 74: 1011-1030.
- Agar, R.A., 1987. The Najd Fault System Revisited; A Two-Way Strike-Slip Orogen In The Saudi Arabian Shield. *Journal Of Structural Geology*, 9: 41-48.
- Akinci, A., Delpezzo, E. & Ibanez, J.M., 1995. Separation Of Scattering And Intrinsic Attenuation In Southern Spain And Western Anatolia (Turkey). *Geophysical Journal International*, 121: 337-353.
- Aktas, G. & Robertson, A.H.F., 1984. The Maden Complex, Se Turkey: Evolution Of A Neotethyan Active Margin. the Maden Complex, Se Turkey: Evolution Of A Neotethyan Active Margin. In: J.E. Dixon And A.H.F. Robertson (Eds), *The Geological Evolution Of The Eastern Mediterranean*, Geological Society Of London, Blackwell Scientific Publications, Special Publication 17, 375-402.
- Al Mashadani, A. & Coustau, H., 1985. Oil Field Waters From Iraq. *Bull. Centres Rech. Explor.-Prod. Elf-Aquitaine*, 9: 405-425.
- Al-Gailani, M., 1996. Iraq's Significant Hydrocarbon Potential Remains Relatively Undeveloped. *Oil & Gas Journal*, July 29: 108-112.
- Al-Hashimi, H.A.J., 1975. Contribution To The Stratigraphy And Micropaleontology Of The Naopurdan Shaly Group In Chuwartz Area, Northeastern Iraq. *Journal Of The Geological Society Of Iraq*, Special Issue: 27-36.
- Al-Hashimi, A.R. & Al-Mehaidi, H.M., 1975. Cu, Ni, Cr Dispersion In Mawat Ophiolite Complex, Ne Iraq. *Journal Of The Geological Society Of Iraq*, Special Issue: 37-44.
- Al-Husseini, M., Ed. (1994). *Geo '94, The Middle East Petroleum Geosciences*. Manama, Bahrain, Gulf Petrolink.
- Al-Laboun, A., 1988. The Distribution Of Carboniferous-Permian Siliciclastic Rocks In The Greater Arabian Basin. *Geological Society Of America Bulletin*, 100: 362-373.
- Al-Maleh, A.K., The Mesozoic In The Palmyridean Region And Its Oil Potential (Middle Syria). Al-Maleh, A.K. & Mouty, M., 1984. *Les Grands Traits De L'evolution Sedimentologique Et Paleogeographique Du Bassin Palmyrien Pendant Le Senonien*. 27th International Geological Congress (Moscow), 2: 92-93.
- Al-Mashadani, 1986. Hydrodynamic Framework Of The Petroleum Reservoirs And Cap Rocks Of The Mesopotamian Basin Of Iraq. *Journal Of Petroleum Geology*, 9: 89-110.
- Al-Rahim, A.M.H., 1993. Geophysical Transect Project: North West- South East Iraq, College Of Science-University Of Baghdad.

- Al-Saad, D., Sawaf, T., Gebran, A., Barazangi, M., Best, J. & T. Chaimov, 1991. Northern Arabian Platform Transect Across The Palmyride Mountain Belt, Syrian Arab Republic, Global Geoscience Transect. Trans. Amer. Geophys. Union, 1.
- Al-Saad, D., Sawaf, T., Gebran, A., Barazangi, M., Best, J. & Chaimov, T., 1992. Crustal Structure Of Central Syria: The Intracontinental Palmyride Mountain Belt. *Tectonophysics*, 207: 345-358.
- Al-Saigh, N.H., Toffeq, A.N. & Abdul-Hameed, I., 1990. Crustal Structure Along Geotranssect Baghdad-Dohuk, Northern Iraq. *Pacific Rim Congress*, 3: 777.
- Al-Shanti, A.M. & Gass, I.G., 1983. The Upper Proterozoic Ophiolite Melange Zones Of The Easternmost Arabian Shield. *Journal Of The Geological Society Of London*, 140: 867-876.
- Al-Sulaimi, J. & El-Rabaa, S.M., 1994. Morphological And Morphostructural Features Of Kuwait. *Geomorphology*, 11: 151-167.
- Al-Swaidan, H.M., 1992. Determination Of Lead And Nickel In Saudi Arabian Crude Oils By Icp/Ms Using Mibk For Sample Pretreatment. *Analytical Letters*, 25: 2157-2163.
- Al-Tarazi, E., 1992. Investigation And Assessment Of Seismic Hazard In Jordan And Its Vicinity. 194.
- Ala, M.A. & Moss, B.J., 1979. Comparative Petroleum Geology Of Southeast Turkey And Northeast Syria. *Journal Of Petroleum Geology*, 1: 3-27.
- Alamri, A.M., Scholt, F.R. & Bufe, C.G., 1991. Seismicity And Aeromagnetic Features Of The Gulf Of Aqaba (Elat) Region. *Journal Of Geophysical Research*, 96: 20179-20185.
- Alavi, M., 1991. Sedimentary And Structural Characteristics Of The Paleo-Tethys Remnants In Northeastern Iran. *Geological Society Of America Bulletin*, 103: 983-992.
- Alavi, M., 1992. Thrust Tectonics Of The Binalood Region, NE Iran. *Tectonics*, 11: 360-370.
- Alavi, M., 1994. Tectonics Of The Zagros Orogenic Belt Of Iran: New Data And Interpretations. *Tectonophysics*, 229: 211-238.
- Alavi, M. & Mahdavi, M.A., 1994. Stratigraphy And Structures Of The Nahavand Region In Western Iran, And Their Implications For The Zagros Tectonics. *Geological Magazine*, 131: 43-47.
- Alhafidh, N.M. & Qasim, S.A., 1992. Petrochemistry And Geotectonic Setting Of The Shalair Granite, Ne Iraq. *Journal Of African Earth Sciences And The Middle East*, 14: 429-441.
- Ali, A.J. & Khoshaba, B.N., 1981. Petrography And Heavy Mineral Studies Of Lower Bakhtiari Formation. *Journal Of The Geological Society Of Iraq*, 14: 15-24.
- Ali, A.J. & Aziz, Z.R., 1993. The Zubair Formation, East Baghdad Oilfield, Central Iraq. *Journal Of Petroleum Geology*, 16: 353-364.
- Almond, D.C., 1986. The Relation Of Mesozoic-Cainozoic Volcanism To Tectonics In The Afro-Arabian Dome. *Journal Of Volcanology And Geothermal Research*, 28: 225-246.
- Alsdorf, D., Barazangi, M., Litak, R., Seber, D., Sawaf, T. & Al-Sadd, D., 1995. The Intraplate Euphrates Depression-Palmyrides Mountain Belt Junction And Relationship To Arabian Plate Boundary Tectonics. *Annali Di Geofisica*, 38: 385-397.
- Alsharhan, A.B. & Kendall, C.G.S.C., 1986. Precambrian To Jurassic Rocks Of Arabian Gulf And Adjacent Areas: Their Facies, Depositional Setting, And Hydrocarbon Habitat. *American Association Of Petroleum Geologists Bulletin*, 70: 977-1002.
- Alshdidi, S., Thomas, G. & Delfaud, J., 1995. Sedimentology, Diagenesis, And Oil Habitat Of Lower Cretaceous Qamchuqa Group, Northern Iraq. *American Association Of Petroleum Geologists Bulletin*, 79: 763-779.
- Alsinawi, S.A. & Al-Banna, A.S., 1990. An E-W Transect Section Through Central Iraq, In Australia And Other Regions. an E-W Transect Section Through Central Iraq, In Australia And Other Regions. In: M.J. Rickard, H.J. Harrington And P.R. Williams (Eds), *Basement Tectonics*, Kluwer Academic Publishers, 9, 191-196.
- Alsinawi, S.A. & Al-Heety, E.A. (1992). Crustal Structure Determinations In Iraq Using Teleseismic Travel Time Residuals And Converted Phase Methods. 29th International Geological Congress, Kyoto, Japan.
- Altarazi, E., 1994. Seismic Hazard Assessment In Jordan And Its Vicinity. *Natural Hazards*, 10: 79-96.

- Altiner, D., 1989. An Example For The Tectonic Evolution Of The Arabian Platform Margin (SE Anatolia) During The Mesozoic And Some Criticisms Of The Previously Suggested Models. In: C. Sengor (Eds), *Tectonic Evolution Of The Tethyan Region*, Kluwer Academic Publishers, 117-129.
- Ambraseys, N.N., 1978. The Relocation Of Epicenters In Iran. *Geophysical Journal Of The Royal Astronomical Society*, 53: 117-121.
- Ambraseys, N. & Barazangi, M., 1989. The 1759 Large Earthquake In The Bekaa Valley: Implications For Earthquake Hazard Assessment In Lebanon And Syria. *Journal Of Geophysical Research*, 94: 4007-4013.
- Ambraseys, N.N. & Melville, C.P., 1989. Evidence For Intraplate Earthquakes In Northwest Arabia. *Bulletin Of The Seismological Society Of America*, 79: 1279-1281.
- Ambraseys, N.N. & Adams, R.D., 1993. Seismicity Of The Cyprus Region. *Terra Nova*, 5: 85-94.
- Ambraseys, N.N., Melville, C.P. & Adams, R.D., 1994. *The Seismicity Of Egypt, Arabia, And The Red Sea*. Cambridge University Press, p. 181.
- Ambraseys, N.N. & Melville, C.P., 1995. Historical Evidence Of Faulting In Eastern Anatolia And Northern Syria. *Anali Di Geofisica*, 38, 337-343.
- Ambraseys, N.N. & Finkel, C.F., 1995. The Seismicity Of Turkey And Adjacent Areas: A Historical Review, 1500-1800. Muhittin Salih Eren Istanbul: 240.
- Ameen, M.S., 1991. Possible Forced Folding In The Taurus-Zagros Belt Of Northern Iraq. *Geological Magazine*, 128: 561-584.
- Ameen, M.S., 1992. Effect Of Basement Tectonics On Hydrocarbon Generation, Migration, And Accumulation In Northern Iraq. *American Association Of Petroleum Geologists Bulletin*, 76: 356-370.
- Amiran, D.H., 1951. A Revised Earthquake-Catalogue Of Palestine. *Isr. Explor. J.*, 1: 223-246.
- Angelier, J., 1985. Extension And Rifting: The Zeit Region, Gulf Of Suez. *Journal Of Structural Geology*, 7: 605-612.
- Ansari, Y.S., 1995. Seismic Risk Analysis Of Pakistan. *Individual Studies By Participants At The International Institute Of Seismology And Earthquake Engineering*, 31: 103-118.
- Arapat, E. & Sarogulu, F., 1972. The East Anatolian Fault System; Thoughts On Its Development. *Bulletin Of Mineral Research & Exploration Instit. Of Turkey*, 78: 33-39.
- Arieh, E., 1967. Seismicity Of Israel And Adjacent Areas. *Geologic Survey Of Israel Bulletin*, 43: 1-14.
- Arieh, E., Rotstein, Y. & Peled, U., 1982. The Dead Sea Earthquake Of 23 April 1979. *Bulletin Of The Seismological Society Of America*, 72: 1627-1634.
- Arieh, E. & Rotstein, Y., 1985. A Note On The Seismicity Of Israel (1900-1982). *Bulletin Of The Seismological Society Of America*, 75: 881-887.
- Arieh, E., Artzi, D., Benedik, N., Eckstein (Shapira), A., Issakow, R., Reich, B. & Shapira, A., 1985. Revised And Updated Catalog Of Earthquakes In Israel And Adjacent Areas, 1900-1980. The Institute For Petroleum Research And Geophysics.
- Arieh, E. & Rabinowitz, N., 1989. Probabilistic Assessment Of Earthquake Hazard In Israel. *Tectonophysics*, 167: 223-233.
- Arieh, E., Rotwain, I., Steinberg, J., Vorobieva, I. & Others, A., 1992. Diagnosis Of Time Of Increased Probability Of Strong Earthquakes In The Jordan-Dead Sea Rift Zone. *Tectonophysics*, 202: 351-359.
- Arkhangel'skaya, V.M., Gergau, A. & Shechkov, B.I., 1974. On The Structure Of The Earth's Crust In The Regions Of The Arabian Peninsula And The Iranian Highland According To Surface-Wave Dispersion. *Phys. Solid Earth (Engl. Ed.)*, 9: 60-66.
- Arkin, Y., 1989. Large-Scale Tensional Features Along The Dead Sea Jordan Rift Valley. *Tectonophysics*, 165: 143-154.
- Asudeh, I., 1982. Pn Velocities Beneath Iran. *Earth And Planetary Science Letters*, 61: 136-142.

- Asudeh, I., 1982. Seismic Structure Of Iran From Surface And Body Wave Data. *Geophysical Journal Royal Astronomical Society*, 71: 715-730. Asudeh, I., 1983. I.S.C. Mislocation Of Earthquakes In Iran And Geometrical Residuals. *Tectonophysics*, 95: 61-74.
- Atallah, M., 1992. Tectonic Evolution Of Northern Wadi-Araba, Jordan. *Tectonophysics*, 204: 17-26.
- Attanasi, E.D. & Root, D.H., 1993. Statistics Of Petroleum Exploration In The Caribbean, Latin America, Western Europe, The Middle East, Africa, Non-Communist Asia, And The Southwestern Pacific, U.S. Geological Survey.
- Avedik, F., Geli, L., Gaulier, J.M. & Formal, J.P.L., 1988. Results From Three Refraction Profiles In The Northern Red Sea (Above 25 Degrees N) Recorded With An Ocean Bottom Vertical Seismic Array. *Tectonophysics*, 153: 89-101.
- Bach Imam, I. & Sigal, J., 1985. Precisions Nouvelles Sur L'age Triasique Et Non Jurassique De La Majeure Partie Des Formations Evaporitiques Et Dolomitiques Des Forages De L'est Syrien. *Revue De Paleobiologie*, 4: 35-42.
- Badri, M. & Y., S., 1991. Qp Crustal Structure In Central Saudi-Arabia. *Journal Of African Earth Sciences And The Middle East*, 12: 561-568.
- Badri, M., 1991. Crustal Structure Of Central Saudi Arabia Determined From Seismic Refraction Profiling. *Tectonophysics*, 185: 357-374.
- Bahat, D. & Rabinovitch, A., 1983. The Initiation Of The Dead Sea Rift. *Journal Of Geology*, 91: 317-332.
- Baker, C., Jackson, J. & Priestly, K., 1993. Earthquakes On The Kazerun Line In The Zagros Mountains Of Iran: Strike-Slip Faulting Within A Fold-And-Thrust Belt. *Geophysical Journal International*, 115: 41-61.
- Baker, J., Snee, L. & Menzies, M., 1996. A Brief Oligocene Period Of Flood Volcanism In Yemen: Implications For The Duration Of The Continental Flood Volcanism At The Afro-Arabian Triple Junction. *Earth And Planetary Science Letters*, 138: 39-55.
- Banat, K.M. & Al-Dyni, N.K., 1981. Petrology And Mineralogy Of Selected Sections From The Euphrates And Jeribe Formations (Miocene), Iraq. *Journal Of The Geological Society Of Iraq*, 14: 1-9.
- Bandel, K. & Mikbel, S.M., 1985. Origin And Deposition Of Phosphate Ores From The Upper Cretaceous At Ruseifa (Amman, Jordan). *Mitteilungen Aus Dem Geologisch-Palaeontologischen Institut Der Universitat Hamberg*, 59: 167-188.
- Barazangi, M., 1983. A Summary Of The Seismotectonics Of The Arab Region. In: K. Cidlinsky And B. Rouhban (Eds), *Assessment And Mitigation Of Earthquake Risk In The Arab Region*, Unesco, 43-58.
- Barazangi, M., 1989. Continental Collision Zones: Seismotectonics And Crustal Structure. *continental Collision Zones: Seismotectonics And Crustal Structure*. In: D.E. James (Eds), *The Encyclopedia Of Solid Earth Geophysics*, Van Nostrand Reinhold Company, 58-74.
- Barazangi, M., Seber, D., Al-Saad, D. & Sawaf, T., 1992. Structure Of The Intracontinental Palmyride Mountain Belt In Syria And Its Relationship To Nearby Arabian Plate Boundaries. *Bulletin Of Earth Sciences, Cukurova University, Adana, Turkey*, 20: 111-118.
- Barazangi, M., Seber, D., Chaimov, T., Best, J., Litak, R., Al-Saad, D. & Sawaf, T., 1993. Tectonic Evolution Of The Northern Arabian Plate In Western Syria. *tectonic Evolution Of The Northern Arabian Plate In Western Syria*. In: E. Boschi And E. Al (Eds), *Recent Evolution And Seismicity Of The Mediterranean Region*, Kluwer Academic Publishers, 117-140.
- Barazangi, M., Fielding, E., Isacks, B. & Seber, D., 1996. Geophysical And Geological Databases And Cbdt Monitoring: A Case Study Of The Middle East. In: E.S. Husebye And A.M. Dainty (Eds), *Monitoring A Comprehensive Test Ban Treaty*, Kluwer Academic Publishers, 197-224.
- Barjous, M. & Mikbel, S., 1990. Tectonic Evolution Of The Gulf Of Aqaba-Dead Sea Transform Fault System. *Tectonophysics*, 180: 49-59.
- Barka, A.A. & Kadinsky-Cade, K., 1988. Strike-Slip Fault Geometry In Turkey And Its Influence On Earthquake Activity. *Tectonics*, 7: 663-684.
- Barton, P.J., Owen, T.R.E. & White, R.S., 1990. The Deep Structure Of The East Oman Continental Margin - Preliminary Results And Interpretation. *Tectonophysics*, 173: 319-331.

- Basha, S.H., 1980. Stratigraphy Of The Risha Area In Northeast Jordan. *Journal Of The Geological Society Of Iraq*, 13: 287-291.
- Beach, A., Bird, T. & Gibbs, A., 1987. Extensional Tectonics And Crustal Structure: Deep Seismic Reflection Data From The Northern North Sea Viking Graben. extensional Tectonics And Crustal Structure: Deep Seismic Reflection Data From The Northern North Sea Viking Graben. In: J.F.D. M. P. Coward, And P. L. Hancock (Eds), *Continental Extensional Tectonics*, Geological Society, Special Publication No.28, 467-476.
- Beaumont, C., Keen, C.E. & Boutilier, R., 1982. On The Evolution Of Rifted Continental Margins: Comparison Of Models And Observations From The Nova Scotian Margin. *Journal Of The Royal Astronomical Society*, 70: 667-715.
- Bebeshev, I.I., Dzhililov, Y.M., Portnyagina, L.A., Yudin, G.T., Mualla, A., Zaza, T. & Jusef, A., 1988. Triassic Stratigraphy Of Syria. *International Geology Review*, : 1292-1301.
- Becker, A. & Paladini, S., 1992. Intra-Plate Stresses In Europe And Plate-Driving Mechanisms. *Annales Tectonicae*, 6: 173-192.
- Beicip, 1975. Gravity Maps Of Syria: Damascus (Syria), Bur. Etud. Ind. Coop. Inst. Fr. Pet., Hauts De Seine: 96.
- Bein, A. & Binstock, R., 1985. Depositional Environments And Source Rock Potential Of The Jurassic Kidod Shales, Israel. *Journal Of Petroleum Geology*, 8: 187-198.
- Ben-Avraham, Z., 1978. The Structure And Tectonic Setting Of The Levant Continental Margin, Eastern Mediterranean. *Tectonophysics*, 46: 313-331.
- Ben-Avraham, Z., Almagor, G. & Garfunkel, Z., 1979. Sediments And Structure Of The Gulf Of Elat (Aqaba) - Northern Red Sea. *Sedimentary Geology*, 23: 239-267.
- Ben-Avraham, Z. & Nur, A., 1986. Collisional Processes In The Eastern Mediterranean. *Geologische Rundschau*, 75: 209-217.
- Ben-Avraham, Z. & Brink, U.T., 1989. Transverse Faults And Segmentation Of Basins Within The Dead Sea Rift. *Journal Of African Earth Sciences*, 8: 603-616.
- Ben-Avraham, Z., Brink, U.T. & Charrach, J., 1990. Transverse Faults At The Northern End Of The Southern Basin Of The Dead Sea Graben. *Tectonophysics*, 180: 37-47.
- Ben-Avraham, Z. & Ginzburg, A., 1990. Displaced Terranes And Crustal Evolution Of The Levant And The Eastern Mediterranean. *Tectonics*, 9: 613-622.
- Ben-Avraham, Z. & Grasso, M., 1991. Crustal Structure Variations And Transcurrent Faulting At The Eastern And Western Margins Of The Eastern Mediterranean. *Tectonophysics*, 196: 269-277.
- Ben-Avraham, Z. & Lyakhovsky, V., 1992. Faulting Processes Along The Northern Dead Sea Transform And The Levant Margin. *Geology*, 20: 1139-1142.
- Ben-Avraham, Z. & Zoback, M.D., 1992. Transform-Normal Extension And Asymmetric Basins: An Alternative To Pull-Apart Models. *Geology*, 20: 423-426.
- Ben-Avraham, Z., Ten Brink, U., Bell, R. & Reznikov, M., 1996. Gravity Field Over The Sea Of Galilee: Evidence For A Composite Basin Along A Transform Fault. *Journal Of Geophysical Research*, 101: 533-544.
- Ben-Gai, Y. & Ben-Avraham, Z., 1995. Tectonic Processes In Offshore Northern Israel And The Evolution Of The Carmel Structure. *Marine And Petroleum Geology*, 12: 533-548.
- Ben-Menahem, A. & Aboodi, E., 1971. Tectonic Patterns In The Northern Red Sea Region. *Journal Of Geophysical Research*, 76: 2674-2689.
- Ben-Menahem, A., A.N. & Vered, M., 1976. Tectonics, Seismicity, And Structure Of The Afro-Eurasian Junction - The Breaking Of An Incoherent Plate. *Physics Of The Earth And Planetary Interiors*, 12: 1-50.
- Ben-Menahem, A., Aboodi, E., Vered, M. & Kovach, R.L., 1977. Rate Of Seismicity Of The Red Sea Region Over The Past 4000 Years. *Physics Of The Earth And Planetary Interiors*, 14: P17-P27.
- Ben-Menahem, A., 1979. Earthquake Catalogue For The Middle East (92 B.C. - 1980 A.D.). *Boll. Geofis. Teor. Appl.*, 21: 245-310.

- Ben-Menahem, A. & Aboodi, E., 1981. Micro- And Macro- Seismicity Of The Dead Sea Rift And Off-Coast Eastern Mediterranean. *Tectonophysics*, 80: 199-233.
- Ben-Menahem, A., 1991. Four Thousand Years Of Seismicity Along The Dead Sea Rift. *Journal Of Geophysical Research*, 96: 20195-20216.
- Bender, V.F., 1968. On The Age And Evolution Of The Jordan Graben: An Example From The Southern Section (Wadi Arabia). *Geol. Jb. (German)*, 3: 177-196.
- Bender, D.F., 1968. Geologie Von Jordanien. *geologie Von Jordanien*. In: (Eds), *Beiträge Zur Regionalen Geologie Der Erde, Gebrüder Borntraeger*, 7, 187-190.
- Bender, F., 1975. *Geology Of The Arabian Peninsula (Jordan)*, Us Geological Survey.
- Bentor, Y., 1961. Some Geochemical Aspects Of The Dead Sea And The Question Of Its Age. *Geochimica Et Cosmochimica Acta*, 25: 239-260.
- Berberian, M., 1979. Discussion Of The Paper A.A. Nowroozi, 1976, "Seismotectonic Provinces Of Iran". *Bulletin Of The Seismological Society Of America*, 69: 293-297.
- Berberian, M., 1979. Evaluation Of The Instrumental And Relocated Epicenters Of Iranian Earthquakes. *Geophysical Journal Of The Royal Astronomical Society*, 58: 625-630.
- Berberian, F. & Berberian, M., 1981. Tectono-Plutonic Episodes In Iran, In Zagros, Hindu Kush, Himalaya, Geodynamic Evolution. In: H. Gupta And F. Delany (Eds), *Zagros-Hindu Kush-Himalaya Geodynamic Evolution*, American Geophysical Union, *Geodynamics Series* 3, 5-32.
- Berberian, M. & King, G.C.P., 1981. Towards A Paleogeography And Tectonic Evolution Of Iran. *Canadian Journal Of Earth Science*, 18: 210-265.
- Berberian, M., 1981. Active Faulting And Tectonics Of Iran. *active Faulting And Tectonics Of Iran*. In: H. Gupta And F. Delany (Eds), *Zagros-Hindu Kush-Himalaya Geodynamic Evolution*, American Geophysical Union, *Geodynamics Series* 3, 33-69.
- Berberian, F., Muir, I.D., Pankhurst, R.J. & Berberian, M., 1982. Late Cretaceous And Early Miocene Andean-Type Plutonic Activity In Northern Makran And Central Iran. *Journal Of The Geological Society Of London*, 139: 605-614.
- Berberian, M., 1983. The Southern Caspian: A Compressional Depression Floored By A Trapped, Modified Oceanic Crust. *Canadian Journal Of Earth Science*, 20: 163-183.
- Berberian, M., Qorashi, M., Jackson, J.A., Priestly, K. & Wallace, T., 1992. The Rudbar-Tarom Earthquake Of June 20, 1990 In Nw Iran: Preliminary Field And Seismotectonic Observations, And Its Tectonic Significance. *Bulletin Of The Seismological Society Of America*, 82: 1726-1755.
- Berberian, M. & Qorashi, M., 1994. Coseismic Fault Related Folding During The South Golbaf Earthquake Of November 20, 1989, In Southeast Iran. *Geology*, 22: 531-534.
- Berberian, M., 1995. Master "Blind" Thrust Faults Hidden Under The Zagros Folds: Active Basement Tectonics And Surface Morphotectonics. *Tectonophysics*, 241: 193-224.
- Best, J.A., Barazangi, M., Al-Saad, D., Sawaf, T. & Gebran, A., 1990. Bouguer Gravity Trends And Crustal Structure Of The Palmyride Mountain Belt And Surrounding Northern Arabian Platform In Syria. *Geology*, 18: 1235-1239.
- Best, J.A., 1991. Crustal Evolution Of The Northern Arabian Platform Beneath The Syrian Arab Republic. Department Of Geological Sciences. Ph.D. Thesis, Ithaca, NY, Cornell University.
- Best, J.A., Barazangi, M., Al-Saad, D., Sawaf, T. & Gebran, A., 1993. Continental Margin Evolution Of The Northern Arabian Platform In Syria. *American Association Of Petroleum Geologists Bulletin*, 77: 173-193.
- Bevis, M., Businger, S., Herring, T.A., Rocken, C., Anthes, R.A. & Ware, R.H., 1992. Gps Meteorology: Remote Sensing Of Atmospheric Water Vapor Using The Global Positioning System. *Journal Of Geophysical Research*, 97: 15787-15801.
- Beydoun, Z., 1977. The Levantine Countries: The Geology Of Syria And Lebanon (Maritime Regions). the Levantine Countries: The Geology Of Syria And Lebanon (Maritime Regions). In: A.E.M. Nairn, W.H. Kanes And F.G. Stehli (Eds), *The Ocean Basins And Margins, The Eastern Mediterranean*, Plenum Press, 319-353.

- Beydoun, Z.R., 1977. Petroleum Prospects Of Lebanon: Reevaluation. American Association Of Petroleum Geologists Bulletin, 19: 43-64.
- Beydoun, Z., 1981. Some Open Questions Relating To The Petroleum Prospects Of Lebanon. Journal Of Petroleum Geology, 3: 303-314.
- Beydoun, Z.R., 1986. The Petroleum Resources Of The Middle East: A Review. Journal Of Petroleum Geology, 9: 5-28.
- Beydoun, Z.R., 1991. Arabian Plate Hydrocarbon Geology And Potential - A Plate Tectonic Approach:. Arabian Plate Hydrocarbon Geology And Potential - A Plate Tectonic Approach:. In: (Eds), Studies In Geology, American Association Of Petroleum Geologists,, 33, 77.
- Beydoun, Z.R., 1992. Petroleum In The Zagros Basin: A Late Tertiary Foreland Basin Overprinted Onto The Outer Edge Of A Vast Hydrocarbon-Rich Paleozoic-Mesozoic Passive-Margin Shelf. In: R.M.A.D. Leckie (Eds), Foreland Basins And Foldbelts, Aapg Memoir 55, Beydoun, Z.R. & Sikander, A.H., 1992. The Red Sea - Gulf Of Aden: Re-Assesment Of Hydrocarbon Potential. Journal Of Petroleum Geology, 15: 245-246.
- Beydoun, Z.R., 1993. Evolution Of The Northeastern Arabian Plate Margin And Shelf: Hydrocarbon Habitat And Conceptual Future Potential. Revue De L'institut Francais Du Petrole, 48: 311-345.
- Beydoun, Z.R., Futyan, A. & Jawzi, A.H., 1994. Jordan Revisited - Hydrocarbons Habitat And Potential. Journal Of Petroleum Geology, 17: 177-194.
- Bijwaard, H., Spakman, W. & Van Eck, T., 1994. Tomographic Investigation Of Crustal Structure In Israel, Institute For Earth Sciences, Utrecht University.
- Bird, P., 1978. Finite Element Modeling Of Lithosphere Deformation: The Zagros Collisional Orogeny. Tectonophysics, 50: 307-336.
- Bishop, R.S. & McLaughlin, P.P., 1993. Thermo-Tectonic History Of The Eastern Mediterranean-Middle East Region Based On Geohistory Analysis, AAPG annual meeting, New Orleans, April 25-28.
- Bishop, R.S., 1994. Maturation History Of The Lower Paleozoic Of The Eastern Arabian Platform. maturation History Of The Lower Paleozoic Of The Eastern Arabian Platform. In: M. Al-Husseini (Eds), Geo '94, The Middle East Papers From The Middle East Geoscience Conference, Gulf Petrolink, 1, 180-189.
- Blank, H.R., Healy, J.H., Roller, J.C., Lamson, R., Fischer, F., Mcclearn, R. & Allen, S., 1979. Seismic Refraction Profile, Kingdom Of Saudi Arabia, Field Operations, Instrumentation, And Initial Results, U.S. Geological Survey, OF 79-1568.
- Bobsien, M., Egloff, R., Izzeldin, A.Y., Makris, J. & Rihm, R., 1989. Seismic Measurements On A Profile Across The Western Flank Of The Red Sea, Offshore Sudan. Technical Programme And Abstracts Of Papers - European Association Of Exploration Geophysicists, 51: 185.
- Bonatti, E., Ottonello, G. & Hamlyn, P.R., 1986. Peridotites From The Island Of Zabargad (St. John), Red Sea: Petrology And Geochemistry. Journal Of Geophysical Research, 91: 599-631.
- Bonnin, J. & Olivet, J.-L., 1988. Geodynamics Of The Mediterranean Regions. In: J.B.E. Al. (Eds), Seismic Hazard In Mediterranean Regions, Ecse, Eec, Eaec, 257-281.
- Bosworth, W., Strecker, M. R., Blisniuk, P. M., 1992. Integration Of East African Paleostress And Present-Day Stress Data: Implications For Continental Stress Field Dynamics. Journal Of Geophysical Research, 97: 11,851-11,865.
- Bosworth, W. & Taviani, M., 1996. Late Quaternary Reorientation Of Stress Field And Extension Direction In The Southern Gulf Of Suez, Egypt: Evidence From Uplifted Coral Terraces, Mesoscopic Fault Arrays, And Borehole Breakouts. Tectonics, 15: 791-802.
- Bou-Rabee, F., 1994. Earthquake Hazard In Kuwait. Journal Of The University Of Kuwait, 21: 253-264.
- Bou-Rabee, F., 1994. Earthquake Recurrence In Kuwait Induced By Oil And Gas Extaction. Journal Of Petroleum Geology, 17: 473-480.
- Bou-Rabee, F., 1996. Shallow Crustal Structure In Kuwait Based On Gravity Anomalies. Kuwait Journal Of Science And Engineering, 23: 305-322.
- Bou-Rabee, F., 1996. Shallow Crustal Structure In Kuwait Based On Gravity Anomalies.

- Bozkurt, E. & Park, R.G., 1994. Southern Menderes Massif - An Incipient Metamorphic Core Complex In Western Anatolia, Turkey. *Journal Of The Geological Society Of London*, 151: 213-216.
- Brew, G.E., Litak, R.K., Seber, D., Barazangi, M., Al-Imam, A. & Sawaf, T., 1997. Basement Depth And Sedimentary Velocity Structure In The Northern Arabian Platform, Eastern Syria. *Geophysical Journal International*, 128: 617-631.
- Brueckner, H.K., Zindler, A., Seyler, M. & Bonatti, E., 1987. Zabargad And The Pan-African And Miocene Isotopic Evolution Of The Sub-Red Sea Mantle And Crust. *Abstracts With Programs - Geological Society Of America*, 19: 603.
- Bruner, I. & Landa, E., 1991. Fault Interpretation From High-Resolution Seismic Data In The Northern Negev, Israel. *Geophysics*, 56: 1064-1070.
- Buday, T., 1975. The Two Main Structural Units Of The Tertiary Eugeosyncline Of Northeastern Iraq. *Journal Of The Geological Society Of Iraq*, Special Issue: 79-88.
- Burke, K. & Sengor, C., 1986. Tectonic Escape In The Evolution Of The Continental Crust. *tectonic Escape In The Evolution Of The Continental Crust*. In: M. Barazangi And L. Brown (Eds), *Reflection Seismology: The Continental Crust*, American Geophysical Union, 14, 41-53.
- Burov, E.B., Houdry, F., Diamant, M. & Deverchere, J., 1994. A Broken Plate Beneath The North Baikal Rift Zone Revealed By Gravity Modeling. *Geophysical Research Letters*, 21: 129-132.
- Burton, P.W., Mcgonigle, R., Makropulos, K.C. & Ucer, S.B., 1984. Seismic Risk In Turkey, The Aegean And The Eastern Mediterranean. *Geophysical Journal Of The Royal Astronomical Society*, 78: 475-506.
- Bushara, M.N., 1995. Subsurface Structure Of The Eastern Edge Of The Zagros Basin As Inferred From Gravity And Satellite Data. *American Association Of Petroleum Geologists Bulletin*, 79: 1259-1274.
- Buyukasikoglu, S. (1980). Euroasian-African Plate Boundary In Southern Turkey And Eastern Mediterranean. *Proceedings Of The 7th World Conference On Earthquake Engineering*, Istanbul.
- Byrne, D., Sykes, L.R. & Davis, D.M., 1992. Great Thrust Earthquakes And Aseismic Slip Along The Plate Boundary Of The Makran Subduction Zone. *Journal Of Geophysical Research*, 97: 449-478.
- Camp, V.E., 1984. Island Arcs And Their Role In The Evolution Of The Western Arabian Shield. *Geological Society Of America Bulletin*, 95: 913-921.
- Camp, V.E., Hooper, P.R., Roobol, M.J. & White, D.L., 1987. The Madinah Eruption, Saudi Arabia: Magma Mixing And Simultaneous Extrusion Of Three Basaltic Chemical Types. *Bulletin Of Volcanology*, 49: 489-508.
- Camp, V.E., Roobol, M.J. & Hooper, P.R., 1989. Intraplate Alkalic Volcanism And Magmatic Processes Along The 600-Km-Long Makkah-Madinah-Nafud Volcanic Line, Western Saudi Arabia. *Bulletin - New Mexico Bureau Of Mines & Mineral Resources*, 131: 39.
- Camp, V.E., Roobol, M.J. & Hooper, P.R., 1991. The Arabian Continental Alkali Basalt Province .2. Evolution Of Harrats Khaybar, Ithnayn, And Kura, Kingdom Of Saudi-Arabia. *Geological Society Of America Bulletin*, 103: 363-391.
- Camp, V.E. & Roobol, M.J., 1992. Upwelling Asthenosphere Beneath Western Arabia And Its Regional Implications. *Journal Of Geophysical Research*, 97: 15,255-15,271.
- Campos, J., Madariaga, R., Nabelek, J., Bukchin, B. & Others., 1994. Faulting Process Of The 1990 June 20 Iran Earthquake From Broad-Band Records. *Geophysical Journal International*, 118: 31-46.
- Capaldi, G., Manetti, P. & Piccardo, G.B., 1983. Preliminary Investigations On Volcanism Of The Sadah Region (Yemen Arabic Republic). *Bulletin Of Volcanology*, 46: 413-427.
- Cater, J.M.L. & Tunbridge, I.P., 1992. Paleozoic Tectonic History Of Se Turkey. *Journal Of Petroleum Geology*, 15: 35-50.
- Cemen, I. & Perincek, D. (1990). Late Cenozoic Tectonics In The Forelands Of The Southeastern Anatolia Fold And Thrust Belt. *Geological Society Of America, Annual Meeting*, Dallas, Texas.

- Chaimov, T., Barazangi, M., Al-Saad, D., Sawaf, T. & Gebran, A., 1990. Crustal Shortening In The Palmyride Fold Belt, Syria, And Implications For Movement Along The Dead Sea Fault System. *Tectonics*, 9: 1369-1386.
- Chaimov, T., Barazangi, M., Al-Saad, D., Sawaf, T. & Gebran, A., 1992. Mesozoic And Cenozoic Deformation Inferred From Seismic Stratigraphy In The Southwestern Intracontinental Palmyride Fold-Thrust Belt, Syria. *Geological Society Of America Bulletin*, 104: 704-715.
- Chaimov, T., Barazangi, M., Al-Saad, D. & Sawaf, T., 1993. Seismic Fabric And 3-D Upper Crustal Structure Of The Southwestern Intracontinental Palmyride Fold Belt, Syria. *American Association Of Petroleum Geologists Bulletin*, 77: 2032-2047.
- Chamot-Rooke, N., Truffert, C., Voogd, B.D., Huchon, P., Lallemand, S. & Pichon, X.L., 1990. Crustal Structure Of The Eastern Mediterranean Sea; Results Of The Pasiphae Cruise. *Eos, Transactions, American Geophysical Union*, 71: 1634.
- Chandra, U., McWhorter, J.C. & Nowroozi, A.A., 1979. Attenuation Of Intensities In Iran. *Bulletin Of The Seismological Society Of America*, 67: 237-250.
- Channell, J.E.T., Tuysuz, O., Bektas, O. & Sengor, A.M.C., 1996. Jurassic-Cretaceous Paleomagnetism And Paleogeography Of The Pontides (Turkey). *Tectonics*, 15: 201-212.
- Chen, C.Y., Chen, W.P. & Molnar, P., 1980. The Uppermost Mantle P Wave Velocities Beneath Turkey And Iran. *Geophys. Research Letters*, 7: 77-80.
- Chenet, P.Y., Colletta, B., Letouzey, J., Desforages, G., Ousset, E. & Zaghloul, E.A., 1987. Structures Associated With Extensional Tectonics In The Suez Rift. structures Associated With Extensional Tectonics In The Suez Rift. In: J.F.D. M. P. Coward, And P. L. Hancock (Eds), *Continental Extensional Tectonics*, Geological Society, Special Publication No. 28, 551-558.
- Chorowicz, J., Luxey, P., Lyberis, N., Carvalho, J. & Others, 1994. The Maras Triple Junction (Southern Turkey) Based On Digital Elevation Model And Satellite Imagery Interpretation. *Journal Of Geophysical Research-Solid Earth*, 99: 20225-20242.
- Clark, M.D., 1985. Late Proterozoic Crustal Evolution Of The Midyan Region, Northwestern Saudi Arabia. *Geology*, 13: 611-615.
- Cochran, J.R., 1983. Model For The Development Of The Red Sea. *American Association Of Petroleum Geologists Bulletin*, 67: 41-69.
- Cohen, Z., Flexer, A. & Kaptan, V., 1988. The Pleshet Basin: A Newly-Discovered Link In The Peripheral Chain Of Basins Of The Arabian Craton. *Journal Of Petroleum Geology*, 11: 403-414.
- Cohen, Z., Kaptan, V. & Flexer, A., 1990. The Tectonic Mosaic Of The Southern Levant: Implications For Hydrocarbon Prospects. *Journal Of Petroleum Geology*, 13: 437-462.
- Colletta, B., Le Quellec, P., Letouzey, J., And Moretti, I., 1995. Longitudinal Variation Of The Suez Rift Structure (Egypt). *Tectonophysics*, 153: 221-233.
- Coskun, B., 1994. Oil Possibilities Of Duplex Structures In The Amik-Reyhanli Basin, Se Turkey. *Journal Of Petroleum Geology*, 17: 461-472.
- Courtillot, V., Armijo, R. & Tapponnier, P., 1987. Kinematics Of The Sinai Triple Junction And A Two-Phase Model Of Arabia-Africa Rifting, In *Continental Extensional Tectonics. kinematics Of The Sinai Triple Junction And A Two-Phase Model Of Arabia-Africa Rifting*, In *Continental Extensional Tectonics*. In: M.P. Coward, J. Dewey And P. Hancock Geological Society Special Publication 28, 559-573.
- Craglietto, A., Panza, G.F., Mitchell, B.J. & Costa, G., 1989. Anelastic Properties Of The Crust In The Mediterranean Area. *Geophysical Monograph*, 51: 179-196.
- Coruh, C., 1990. Crustal Seismic Images From Part Of The Active Escape Of The Anatolia Block: Preliminary Results From The First Turkish Geotraverse. *Seismological Research Letters*, 61: 147-8.
- Darkal, A.N., Krauss, M. & Ruske, R., 1990. The Levant Fault Zone. *Zeitschrift Von Geologische Wissenschaft*, 18: 549-562.
- Darmoian, S.A., 1975. Stratigraphy And Micropaleontology Of The Upper Cretaceous Aruma Supergroup, Southeastern Iraq. *Journal Of The Geological Society Of Iraq*, Special Issue: 89-116.

- Davison, I., Alkadasi, M., Alkhirbash, S., Alsubbary, A.K. & Others, A., 1994. Geological Evolution Of The Southeastern Red Sea Rift Margin, Republic Of Yemen. *Geological Society Of America Bulletin*, 106: 1474-1493.
- De Ruiter, R.S.C., Lovelock, P.E.R. & Nabulsi, N., 1994. The Euphrates Graben, Eastern Syria: A New Petroleum Province In The Northern Middle East. In: M. Al-Husseini (Eds), *Geo '94, Middle East Petroleum Geosciences*, Gulf Petrolink, 1, 357-368.
- De Sitter, L., 1962. Structural Development Of The Arabian Shield In Palestine. *Geologie En Mijnbouw*, 41: 116-124.
- De Voogd, B., Truffert, C., Chamot-Rook, N., Huchon, P., Lallemand, S. & Pichon, X.L., 1992. Two-Ship Deep Seismic Soundings In The Basins Of The Eastern Mediterranean Sea (Pasiphae Cruise). *Geophysical Journal International*, 109: 536-552.
- Dehghani, G., 1981. Schwerefeld Und Krustenaufbau Im Iran (Gravimetric Field And Crustal Structure In Iran). *Hamburger Geophysikalische Einzelschriften*, 54: 74.
- Dehghani, G.A. & Makris, J., 1984. The Gravity Field And Crustal Structure Of Iran. *Neues Jahrbuch Fuer Geologie Und Palaeontologie, Abhandlungen*, 168: 215-229.
- Demirtas, R., 1995. Paleoseismicity Of The North Anatolian Fault: A Case Study Of The Mudurnu Valley Segment. *Individual Studies By The Participants At The International Institute Of Seismology And Earthquake Engineering*, 31.
- Demirtas, R., Karakisa, S. & Yilmaz, R., 1996. The October 1, 1995 Dinar Earthquake (M_L=5.9) In Southwestern Turkey. *Bulletin Of The International Institute Of Seismology And Earthquake Engineering*, 30: 45-58.
- Deniz, R., Aksoy, A., Yalin, D., Seeger, H., Franke, P., Hirsch, O. & Bartsch, P., 1993. Determination Of Crustal Movements In Turkey By Terrestrial Geodetic Methods. *J. Geodynamics*, 18: 13-22.
- Dercourt, J., Zonenshain, L.P., Ricou, L.-E., Kazmin, V.G., Lepichon, X., Knipper, A.L., Grandjacquet, C., Sbertshikov, I.M., Geysant, J., Lepvrier, C., Pechersky, D.H., Boulin, J., Sibuet, J.-C., Savostin, L.A., Sorokhtin, O., Westphal, M., Bazhenov, M.L., Lauer, J.P. & Biju-Duval, B., 1986. Geological Evolution Of The Tethys Belt From The Atlantic To The Pamirs Since The Lias. *Tectonophysics*, 123: 241-315.
- Dewey, J.F. & A.M. Sengor, 1979. Aegean And Surrounding Regions: Complex Multiplate And Continuum Tectonics In A Convergent Zone. *Geological Society Of American Bulletin*, 90: 84-92.
- Dilek, Y. & Moores, E.M., 1990. Regional Tectonics Of The Eastern Mediterranean Ophiolites. regional Tectonics Of The Eastern Mediterranean Ophiolites. In: (Eds), *Proceedings Of The Symposium On Ophiolites And Oceanic Lithosphere*, Troodos 87, Geol. Surv. Depart., 295-309. Dilek, Y. & Thy, P., 1990. Tectonic Evolution Of The Troodos Ophiolite Within The Tethyan Framework. *Tectonics*, 9: 811-823.
- Dilek, Y. & Thy, P. (1990). Structure And Petrology Of Mesozoic Peri-Arabian Ophiolites In The Eastern Mediterranean Region. *Geological Society Of America, Annual Meeting*, Dallas, Texas.
- Dilek, Y. & Delaloye, M., 1992. Structure Of The Kizildag Ophiolite, A Slow-Spread Cretaceous Ridge Segment North Of The Arabian Promontory. *Geology*, 20: 19-22.
- Dilek, Y. & Rowland, J.C., 1993. Evolution Of A Conjugate Passive Margin Pair In Mesozoic Southern Turkey. *Tectonics*, 12: 954-970.
- Dixon, T.H., Stern, R.J. & Hussein, I.M., 1987. Control Of Red Sea Rift Geometry By Precambrian Structures. *Tectonics*, 6: 551-571.
- Dorbath, L. & Montagner, J.P., 1983. Upper Mantle Heterogeneities In Africa Deduced From Rayleigh Wave Dispersion. *Physics Of The Earth And Planetary Interiors*, 32: 218-225.
- Drake, C.L., Girdler, R. W., 1964. A Geophysical Study Of The Red Sea. *The Geophysical Journal Of The Royal Astronomical Society*, 8: 473-495.
- Dubertret, L., 1932. Les Formes Structurales De La Syrie Et De La Palestine. *C. R. Acad. Sci. Colon.*, 195: 66.
- Dubertret, L., 1955. Carte Geologique Du Liban. Beyrouth, Ministere Des Travaux Publics.

- Dubertret, L., 1970. Review Of The Structural Geology Of The Red Sea And Surrounding Areas. Royal Society Of London Philosophical Transactions, Series A, 267.
- Dubray, E.A., Stoesser, D.B. & Mckee, E.H., 1991. Age And Petrology Of The Tertiary As-Sarat Volcanic Field, Southwestern Saudi-Arabia. *Tectonophysics*, 198: 155-180.
- Duncan, I.J., Rivard, B., Arvidson, R.E. & Sultan, M., 1990. Structural Interpretation And Tectonic Evolution Of A Part Of The Najd Shear Zone (Saudi-Arabia) Using Landsat Thematic-Mapper Data. *Tectonophysics*, 178: 309-335.
- Dunne, L.A. & Hempton, M.R., 1984. Strike-Slip Basin Sedimentation At Lake Hazar (Eastern Taurus Mountains). strike-Slip Basin Sedimentation At Lake Hazar (Eastern Taurus Mountains). In: O. Tekeli And M.C. Goncuoglu Mta, 229-235.
- Dunnington, H.V., 1958. Generation, Migration, Accumulation, And Dissipation Of Oil In Northern Iraq. generation, Migration, Accumulation, And Dissipation Of Oil In Northern Iraq. In: (Eds), Habitat Of Oil, American Association Of Petroleum Geologists, 1194-1250.
- Dunnington, H.V., 1967. Stratigraphical Distribution Of Oilfields In The Iraq-Iran-Arabia Basin. *Journal Of The Institute Of Petroleum*, 53: 129-161.
- Dzhabur, I., 1985. Seismological Description Of Latakia Region Of Syria According To Borehole And Surface Observations. *Vestnik Moskovskogo Universiteta. Geologiya.*, 40: 90-93.
- Dziewonski, A.M., Ekstrom, G. & Salganik, M.P., 1995. Centroid-Moment Tensor Solutions For October-December 1994. *Physics Of The Earth And Planetary Interiors*, 91: 187-201.
- Egloff, F., Rihm, R., Makris, J., Izzeldin, Y.A., Bobsien, M., Meier, K., Junge, P., Noman, T. & Warsi, W., 1991. Contrasting Structural Styles Of The Eastern And Western Margins Of The Southern Red Sea: The 1988 Sonne Experiment. *Tectonophysics*, 198: 329-353.
- El Harfi, A. & Et Jean Salomon, J.L., 1996. Cenozoic Continental Infilling Of The Ouarzazate Foreland Basin. Implications For The Structural Evolution Of The Central High Atlas Mountains (Morocco). *Geodynamics (Tectonics)*, 323: 623-630.
- El-Anbaawy, M.I.H. & Sadek, A., 1979. Paleogeology Of The Shiranish Formation (Maestrichtian) In Northern Iraq By Means Of Microfacies Analysis And Clay Mineral Investigation. *Palaeogeography, Palaeoclimatology, Palaeoecology*, 26: 173.
- El-Isa, Z.H., Marghelani, H.M. & Bazzari, M.A., 1984. The Tectonic Development Of The Western Margin Of The Gulf Of Eilat (Akaba) Rift. *Tectonophysics*, 80: 39-66.
- El-Isa, Z., Makris, J., Prodehl, C., 1986. A Deep Seismic Sounding Experiment In Jordan. *Dirasat*, 13: 271-281.
- El-Isa, Z.H., 1986. Earthquake Deformations In The Lisan Deposits And Seismotectonic Implications. *Geophysical Journal. R. Astr. Soc.*, 86: 413-424.
- El-Isa, Z., Mechie, J., Prodehl, C., Makris, J. & Rihm, R., 1987. A Crustal Structure Study Of Jordan Derived From Seismic Refraction Data. *Tectonophysics*, 138: 235-253.
- El-Isa, Z., Mechie, J. & Prodehl, C., 1987. Shear Velocity Structure Of Jordan From Explosion Seismic Data. *Geophysical Journal Of The Royal Astronomical Society*, 90: 265-281.
- El-Isa, Z.H. & Alshanti, A., 1989. Seismicity And Tectonics Of The Red Sea And Western Arabia. *Geophysical J.*, 97: 449-457.
- El-Isa, Z.H., 1990. Lithospheric Structure Of The Jordan-Dead Sea Transform From Earthquake Data. *Tectonophysics*, 180: 29-36.
- El-Isa, Z., 1992. Seismicity Of Wadi Araba-Dead Sea Region. *Geology Of The Arab World*, 1: 245-?
- El-Isa, Z.H., 1992. Seismicity Of Wadi Araba-Dead Sea Region. *Geology Of The Arab World (Cairo University)*, : 245-255.
- Elanbaawy, M.I.H., Alawah, M.A.H., Althour, K.A. & Tucker, M.E., 1992. Miocene Evaporites Of The Red Sea Rift, Yemen-Republic - Sedimentology Of The Salif Halite. *Sedimentary Geology*, 81: 61-71.

- Elramly, M.F., Greiling, R.O. & Rashwan, A.A., 1990. Extension Of The Najd Shear System From Saudi-Arabia To The Central Eastern Desert Of Egypt Based On Integrated Field And Landsat Observations - Comment. *Tectonics*, 9: 535-538.
- Emery, K.O., Heezen, Bruce C., Allan, T. D., 1966. Bathymetry Of The Eastern Mediterranean Sea. *Deep-Sea Research*, 13: 173-192.
- Erendil, M., 1984. Petrology And Structure Of The Upper Crustal Units Of The Kizildag Ophiolite. *petrology And Structure Of The Upper Crustal Units Of The Kizildag Ophiolite*. In: O. Tekeli And M.C. Goncuoglu (Eds), *Geology Of The Taurus Belt, Mta*, 269-284.
- Everett, J.R., 1991. Tectonic Context Of The Palmyrides Of Syria (Abstract). *American Association Of Petroleum Geologists*, .
- Eyal, M., Eyal, Y., Bartov, Y. & Steinitz, G., 1981. The Tectonic Development Of The Western Margin Of The Gulf Of Elat (Aqaba) Rift. *Tectonophysics*, 80: 39-66.
- Eyal, Y., 1983. Tectonic Analysis Of The Dead Sea Rift Region Since The Late-Cretaceous Based On Mesosstructures. *Tectonics*, 2: 167-185.
- Eyal, Y., 1996. Stress Field Fluctuations Along The Dead Sea Rift Since The Middle Miocene. *Tectonics*, 15: 157-170.
- Ezen, U., 1991. Surface Wave Dispersion And Upper Crustal Structure Along N-S Direction In Western Turkey From Burdur Earthquake Of 12 May 1971. *Bulletin Of The International Institute Of Seismology And Earthquake Engineering*, 25: 39-59.
- Fahmi, K.J., Al Salim, M.A. & Ayar, B.S., 1986. Recent Earthquake Activity In The Lesser Zab Region Of Northeastern Iraq. *Tectonophysics*, 131: 89-111.
- Fahmi, K.J. & Alabbasi, J.N., 1991. Application Of A Mixture Distribution Of Extreme Values To Earthquake Magnitudes In Iraq And Conterminous Regions. *Geophysical Journal International*, 107: 209-217.
- Fairhead, J.D., 1988. Late Mesozoic Rifting In Africa. *late Mesozoic Rifting In Africa*. In: W. Manspeizer (Eds), *Triassic-Jurassic Rifting; Continental Breakup And The Origin Of The Atlantic Ocean And Passive Margins*, Elsevier.
- Falcon, N.L., 1961. Major Earth-Flexing In The Zagros Mountains Of Southwest Iran. *Quarterly Journal Of The Geological Society Of London*, 117: 367-376.
- Falcon, N.L., 1969. Problems Of The Relationship Between Surface Structure And Deep Displacements Illustrated By The Zagros Range. *problems Of The Relationship Between Surface Structure And Deep Displacements Illustrated By The Zagros Range*. In: P.E. Kent, G.E. Satterthwaite And A.M. Spencer (Eds), *Time And Place In Orogeny*, Geological Society Of London, Special Publication 3, 9-22.
- Falcon, N.L., 1974. Southern Iran: Zagros Mountains. *southern Iran: Zagros Mountains*. In: A.M. Spencer (Eds), *Mesozoic-Cenozoic Orogenic Belts, Data For Orogenic Studies*, Geological Society Of London, Special Publication 4, 199-211.
- Farinacci, A. & Koyluoglu, M., 1982. Evolution Of The Jurassic-Cretaceous Taurus Shelf (Southern Turkey). *Ballettino Della Paleontologica Italiana*, 21: 267-276.
- Fat-Helbary, R., 1996. Land Use Planning And Seismic Microzonation Map Of The Northern Part Of Aswan High Dam Lake. *Bulletin Of The International Institute Of Seismology And Earthquake Engineering*, 30: 1-8.
- Feinstein, S., Kohn, B.P., Steckler, M.S. & Eyal, M., 1996. Thermal History Of The Eastern Margin Of The Gulf Of Suez, I. Reconstruction From Bore Hole Temperature And Organic Maturity Measurements. *Tectonophysics*, 266: 203-220.
- Feldman, L. & Shapira, A., 1994. Analysis Of Seismic Intensities Observed In Israel. *Natural Hazards*, 9: 287-301.
- Ferrucci, F., Gaudiosi, G., Hirn, A. & Nicolich, R., 1991. Ionian Basin And Calabria Arc; Some New Elements From Dss Data. *Tectonophysics*, 195: 411-419.
- Filatov, V. & Krasnov, A., 1959. On Aeromagnetic Surveys Carried Out Over The Syrian Territory, The United Arab Republic During 1958-1959, *Techonexport, Damascus*: 33.

- Fleck, R.J., Greenwood, W.R., Hadley, D.G., Anderson, R.E. & Schmidt, D.L., 1980. Rubidium-Strontium Geochronology And Plate-Tectonic Evolution Of The Southern Part Of The Arabian Shield. USGS Professional Paper, 1131.
- Folkman, Y., 1981. Structural Features In The Dead Sea- Jordan Rift Zone, Interpreted From A Combined Magnetic-Gravity Study. *Tectonophysics*, 80: 135-146.
- Fontaine, J.M., Monod, O., Braud, J. & Perincek, D., 1989. The Hezan Units: A Fragment Of The South Neo-Tethyan Passive Continental Margin In Southeastern Turkey. *Journal Of Petroleum Geology*, 12: 29-50.
- Freund, R., 1965. A Model Of The Structural Development Of Israel And Adjacent Areas Since Upper Cretaceous Times. *Geological Magazine*, 102: 189-205.
- Freund, R., Zak, I. & Garfunkel, Z., 1968. Age And Rate Of The Sinistral Movement Along The Dead Sea Rift. *Nature*, 220: 253-255.
- Freund, R., Garfunkel, Z., Zak, I., Goldberg, M., Weissbrod, T. & Derin, B., 1970. The Shear Along The Dead Sea Rift. *Phil. Trans. Roy. Soc. Lond.*, 267: 107-130.
- Gardosh, M., Reches, Z. & Garfunkel, Z., 1990. Holocene Tectonic Deformation Along The Western Margins Of The Dead Sea. *Tectonophysics*, 180: 123-137.
- Garfunkel, Z. & Horowitz, A., 1966. The Upper Tertiary And Quaternary Morphology Of The Negev, Israel. *Israel Journal Of Earth Sciences*, 15: 101-117.
- Garfunkel, Z., 1974. The Tectonics Of The Western Margins Of The South Arava, Hebrew University Of Jerusalem.
- Garfunkel, Z. & Bartov, Y., 1977. The Tectonics Of The Suez Rift. *Israel Geol. Surv. Bulletin*, 71: 44 pp.
- Garfunkel, Z., Arad, A. & Almagor, G., 1979. The Palmahim Disturbance And Its Regional Setting. *Israel Geol. Surv. Bulletin*, 72: 56 pp.
- Garfunkel, Z., 1981. Internal Structure Of The Dead Sea Leaky Transform (Rift) In Relation To Plate Kinematics. *Tectonophysics*, 80: 81-108.
- Garfunkel, Z., Zak, I. & Freund, R., 1981. Active Faulting In The Dead Sea Rift. *Tectonophysics*, 80: 1-26.
- Garfunkel, Z. & Derin, B., 1984. Permian-Early Mesozoic Tectonism And Continental Margin Formation In Israel And Its Implications For The History Of The Eastern Mediterranean. In: J.E. Dixon And A.H.F. Robertson (Eds), *The Geological Evolution Of The Eastern Mediterranean*, Blackwell Scientific Publications, 187-201.
- Garfunkel, Z. & Almagor, G., 1985. Geology And The Structure Of The Continental Margin Off Northern Israel And The Adjacent Part Of The Levantine Basin. *Marine Geology*, 62: 105-131.
- Garfunkel, Z. & Derin, B., 1988. Reevaluation Of Latest Jurassic-Early Cretaceous History Of The Negev And The Role Of Magmatic Activity. *Israel Journal Of Earth Science*, 37: 43-52.
- Garfunkel, Z., 1988. The Pre-Quaternary Geology Of Israel. In: Y. Yom-Tov And E. Tchernov (Eds), *Monographiae Biologicae, The Zoogeography Of Israel*, Dr. W. Junk Publishers, 627-634.
- Garfunkel, Z., 1989. Tectonic Setting Of Phanerozoic Magmatism In Israel. *Israel Journal Of Earth Science*, 38: 51-74.
- Garfunkel, Z. & Ben-Avraham, Z., 1996. The Structure Of The Dead Sea Basin. *Tectonophysics*, 266: 155-176.
- Gaulier, J.-M., Pichon, X.L., Lyberis, N., Avedik, F., Gely, L. & Moretti, I., 1986. New Refraction Data On The Northern Red Sea-Gulf Of Suez Area. *Eos, Transactions, American Geophysical Union*, 67: 1208-1209.
- Gaulier, J.M., Le Pichon, X., Lyberis, N., Avedik, F., Geli, L., Moretti, I., Deschamps, A. & Hafez, S., 1988. Seismic Study Of The Crust Of The Northern Red Sea And Gulf Of Suez. *Tectonophysics*, 153: 55-88.
- Gealey, W.K., 1988. Plate Tectonic Evolution Of The Mediterranean-Middle East Region. *Tectonophysics*, 155: 285-306.
- Geiss, E. & Drewes, H., 1985. Research On Kinematics And Structure Of The Mediterranean Sea. *Jahrestagung Der Deutschen Geophysikalischen Gesellschaft E.V.*, 45: 169.

- Geiss, E., 1987. The Lithosphere In The Mediterranean Region; A Contribution On Structure, Gravity Field And Deformation, University Of Munich, Ph.D. Thesis (in German)
- Gheitanchi, M.R., Kikuchi, M. & Mizoue, M., 1993. Teleseismic Interpretation Of The 1968 Dasht-E Bayaz, NE Iran, Earthquake. *Geophysical Research Letters*, 20: 245-248.
- Giannerini, G., Campredon, R., Feraud, G. & Zakhem, B.A., 1988. Intraplate Deformation And Associated Volcanism At The Northwestern Part Of The Arabian Plate (In French). *Bulletin de la Societe Geologique de France*, 4: 6937-6947.
- Giese, P., Makris, J., Akashe, B., Rower, P., Letz, H. & Mostaanpour, M., 1983. Seismic Crustal Studies In Southern Iran Between The Central Iran And Zagros Belt. In: V. Madelat (Eds), *Geological Survey Of Iran 51*, Geological Survey Of Iran, 71-89.
- Giese, P., Makris, J., Akasheh, B., Roewer, P., Letz, H. & Mostaanpour, M., 1984. The Crustal Structure In Southern Iran Derived From Seismic Explosion Data. *Neuer Jahrbuch Fuer Geologie Und Palaeontologie*, 168: 230-243.
- Ginzburg, A., Makris, J., Fuchs, K., Perathoner, B. & Prodehl, C., 1979. Detailed Structure Of The Crust And Upper Mantle Along The Jordan-Dead Sea Rift. *Journal Of Geophysical Research*, 84: 5605-5612.
- Ginzburg, A., Makris, J., Fuchs, K., Prodehl, C., Kaminski, W. & Amitai, U., 1979. A Seismic Study Of The Crust And Upper Mantle Of The Jordan-Dead Sea Rift And Their Transition Toward The Mediterranean Sea. *Journal Of Geophysical Research*, 84: 1569-1582.
- Ginzburg, A., Fuchs, K. & Makris, J., 1979. A Transition Zone In The Crust Along The Dead Sea - Gulf Of Elat Rift. In: (Eds), 25 Anniversary Of The Israel Geological Society; Annual Meeting; Abstracts Of Submitted Papers, Israel Geological Society, 24.
- Ginzburg, A. & Folkman, Y., 1980. The Crustal Structure Between The Dead Sea Rift And The Mediterranean Sea. *Earth Planet. Sci. Lett.*, 51: 181-188.
- Ginzburg, A., Makris, J., Fuchs, K. & Prodehl, C., 1981. The Structure Of The Crust And Upper Mantle In The Dead Sea Rift. *Tectonophysics*, 80: 109-119.
- Ginzburg, A. & Kashai, E., 1981. Seismic Measurements In The Southern Dead Sea. *Tectonophysics*, 80: 67-80.
- Ginzburg, A. & Ben-Avraham, Z., 1987. The Deep Structure Of The Central And Southern Levant Continental Margin. *Annales Tectonics*, 1: 105-115.
- Ginzburg, A., Benavraham, Z., Makris, J., Hubral, P. & Others, A., 1994. Crustal Structure Of Northern Israel. *Marine And Petroleum Geology*, 11: 501-506.
- Girdler, R.W., 1982. The Importance Of The Jordanian Rift To Studies Of The Red Sea And Gulf Of Aden. *Proceedings Of The First Jordanian Geological Conference*, 1: 503-522.
- Girdler, R.W., 1982. The Importance Of The Jordanian Rift To Studies Of The Red Sea And Gulf Of Aden. An Abridged Version Of The Lecture Given To The First Jordanian Conference In Amman On 7 September 1982.
- Girdler, R.W., 1985. Problems Concerning The Evolution Of Oceanic Lithosphere In The Northern Red Sea. *Tectonophysics*, 116: 109-122.
- Girdler, R.W. & Southren, T.C., 1987. Structure And Evolution Of The Northern Red Sea. *Nature*, 330: 716-721. Girdler, R.W., 1990. The Dead Sea Transform Fault System. *Tectonophysics*, 180: 1-13.
- Girdler, R.W., 1991. The Afro-Arabian Rift System - An Overview. *Tectonophysics*, 197: 139-153.
- Girdler, R.W., Mcconnell, D. A., 1994. The 1990 To 1991 Sudan Earthquake Sequence And The Extent Of The East African Rift System. *Science*, 264: 67-70.
- Gitterman, Y. & Van Eck, T., 1993. Spectra Of Quarry Blasts And Microearthquakes Recorded At Local Distances In Israel. *Bulletin Of The Seismological Society Of America*, 83: 1799-1812.
- Gitterman, Y. & Shapira, A., 1993. Spectral Discrimination Of Underwater Explosions. *Israel Journal Of Earth Science*, 42: 37-44.

- Gitterman, Y. & Van Eck, T., 1993. Low Frequency Spectra Of Quarry Blasts And Microearthquakes Recorded At Local Distances In Israel. *Bulletin Of The Seismological Society Of America*, 83: 1799-1812.
- Gitterman, Y. & Shapira, A., 1994. Spectral Characteristics Of Seismic Events Off The Coast Of The Levant. *Geophysical Journal International*, 116: 485-497.
- Goff, J.C., Jones, R.W. & Horbury, A.D., 1994. Cenozoic Basin Evolution Of The Northern Part Of The Arabian Plate And Its Control On Hydrocarbon Habitat. *Cenozoic Basin Evolution Of The Northern Part Of The Arabian Plate And Its Control On Hydrocarbon Habitat*. In: M. Al-Husseini (Eds), *Geo '94, The Middle East Petroleum Geosciences*, Gulf Petrolink, 1, 402-412.
- Gorin, G.E., Racz, L.G. & Walter, M.R., 1982. Late Precambrian-Cambrian Sediments Of Huqf Group, Sultanate Of Oman. *American Association Of Petroleum Geologists Bulletin*, 66: 2609-2627.
- Grabowski, J. & Norton, G.J.A.I.O., 1994. Tectonic Controls On The Stratigraphic Architecture And Hydrocarbon Systems Of The Arabian Plate. In: M. Al-Husseini (Eds), *Geo '94, The Middle East Petroleum Geosciences*, Gulf Petrolink, 1, 413-430.
- Gregor, C.B., Mertzman, S., A.E.M. & Negendank Nairn, J., 1974. The Paleomagnetism Of Some Mesozoic And Cenozoic Volcanic Rocks From The Lebanon. *Tectonophysics*, 21: 375-395.
- Greifswald, K., 1986. Zum Mechanismus Und Charakter Erste Plattentektonischer Prozesse Im Oberen Proterozoikum, Dargestellt Am Beispiel Der Hijaz-Tektogenese Im Ne-Afrikanisch-Arabischen Raum (Arabisch-Nubischer Schild) Teil I. *Zeitschrift Für Angewandte Geologie*, 32: 267-272.
- Group, G.S.O.L.P. (1995). First Symposium On The Hydrocarbon Geology Of North Africa, November 28-30 1995, Burlington House, London, Abstracts. First Symposium On The Hydrocarbon Geology Of North Africa, London, Bp Exploration.
- Guennoc, P., Pouit, Georges, Nawab, Zohair, The Red Sea: History And Associated Mineralization. the Red Sea: History And Associated Mineralization. In: W. Manspeizer (Eds), *Triassic-Jurassic Rifting; Continental Breakup And The Origin Of The Atlantic Ocean And Passive Margins*, Elsevier,
- Guillemot, J., 1987. La Geologie De La Region De Damas (Syria) D'apres Des Images Stereoscopiques Du Spot. *Photo-Interpretation*, 2: 17-33.
- Guirand, R. & Bellion, Y., 1996. Late Carboniferous To Recent Geodynamic Evolution Of The West Gondwanian, Cratonic, Tethyan Margins. late Carboniferous To Recent Geodynamic Evolution Of The West Gondwanian, Cratonic, Tethyan Margins. In: A.E.M.N.E. Al. (Eds), *The Ocean Basins And Margins: The Tethys Ocean*, Plenum Press, 8,
- Gurbuz, C. & Evans, J.R., 1991. A Seismic Refraction Study Of The Western Tuz Golu Basin, Central Turkey. *Geophysical Journal International*, 106: 239-251.
- Gvirtzman, G. & Weissbrod, T., 1984. The Hercynian Geanticline Of Helez And The Late Palaeozoic History Of The Levant. the Hercynian Geanticline Of Helez And The Late Palaeozoic History Of The Levant. In: J.E. Dixon And A.H.F. Robertson (Eds), *The Geological Evolution Of The Eastern Mediterranean*, Blackwell Scientific Publications, 177-186.
- Gvirtzman, Z. & Garfunkel, Z., 1997. Vertical Movements Following Intracontinental Magmatism: An Example From Southern Israel. *Journal Of Geophysical Research*, 102: 2645-2658.
- Hadiouche, O. & Jobert, N., 1988. Evidence For Anisotropy In North East Africa, From Geographical And Azimuthal Distribution Of Rayleigh Wave Velocities And Average Upper Mantle Structure. *Geophysical Research Letters*, 15: 365-368.
- Hadiouche, O. & Jobert, N., 1988. Geographical Distribution Of Surface-Wave Velocities And 3-D Upper Mantle Structure In Africa. *Geophys. J.*, 95: 87-110.
- Hadiouche, O., 1990. First Evidence For High Anelastic Attenuation Beneath The Red Sea From Love Wave Analysis. *Geophys. Res. Letters*, 17: 1973-1976.
- Hadiouche, O. & Walter Zuern, , (), ,, 1992. On The Structure Of The Crust And Upper Mantle Beneath The Afro-Arabian Region From Surface Wave Dispersion. *Tectonophysics*, 209: 179-196.
- Hadiouche, O. & Zurn, W., 1992. On The Structure Of The Crust And Upper Mantle Beneath The Afro-Arabian Region From Surface Wave Dispersion. *Tectonophysics*, 209: 179-196.

- Hall, R., 1976. Ophiolite Emplacement And The Evolution Of The Taurus Suture Zone, Southeastern Turkey. *Geological Society Of America Bulletin*, 87: 1078-1088.
- Hall, J.K., Schwartz, E. & Cleave, R.L.W., 1990. The Israeli Dtm (Digital Terrain Map) Project. the Israeli Dtm (Digital Terrain Map) Project. In: J.T. Hanley And D.F. Merriam (Eds), *Microcomputer Applications In Geology*, Ii, Pergamon Press, 111-118.
- Hall, J., K., 1996. Digital Topography And Bathymetry Of The Area Of The Dead Sea Depression. *Tectonophysics*, 266: 177-185.
- Halpern, M. & Tristan, N., 1981. Geochronology Of The Arabian-Nubian Shield In Southern Israel And Eastern Sinai. *Journal Of Geology*, 89: 639-648.
- Hamdi, B., Brasier, M.D. & Zhiwen, J., 1989. Earliest Skeletal Fossils From Precambrian-Cambrian Boundary Strata, Elburz Mountains, Iran. *Geological Magazine*, 126: 283-289.
- Hamid, S.H. & Aitani, A.M., 1995. Plentiful Natural Gas Headed For Big Growth In Mideast. *Oil And Gas Journal*, 93: 51-54.
- Hancock, P.L. & Atiya, M.S., 1979. Tectonic Significance Of Mesofracture Systems Associated With The Lebanese Segment Of The Dead Sea Transform Fault. *J. Struct. Geol.*, 1: 143-153.
- Hanna, S.S., 1990. The Alpine Deformation Of The Central Oman Mountains. the Alpine Deformation Of The Central Oman Mountains. In: A.H.F. Robertson, M.P. Searle And A.C. Ries (Eds), *The Geology And Tectonics Of The Oman Region*, The Geological Society, 846.
- Hartzell, S. & Mendoza, C., 1991. Application Of An Iterative Least-Squares Waveform Inversion Of Strong-Motion And Teleseismic Records To The 1978 Tabas, Iran, Earthquake. *Bulletin Of The Seismological Society Of America*, 81: 305-331.
- Hatcher, R.D., Zietz, I., Regan, R.D. & Abu-Ajamieh, M., 1981. Sinistral Strike-Slip Motion On The Dead Sea Rift: Confirmation From New Magnetic Data. *Geology*, 9: 458-462.
- Hatzor, Y. & Reches, Z., 1990. Structure And Paleostresses In The Gilboa Region, Western Margins Of The Central Dead Sea Rift. *Tectonophysics*, 180: 87-100.
- Healy, J.H., Mooney, W.D., Blank, H.R., Gettings, M.E., Kohler, W.M., Lamson, R.J. & L.E. Leone, T., 1982. Saudi Arabian Seismic Deep-Refraction Profile: Final Project Report, U. S. Geological Survey.
- Hearn, T.M. & Ni, J.F., 1994. Pn Velocities Beneath Continental Collision Zones: The Turkish-Iranian Plateau. *Geophysical Journal International*, 117: 273-283.
- Heimann, A., 1993. Geometric Changes Of Plate Boundaries Along Part Of The Northern Dead Sea Transform: Geochronologic And Paleomagnetic Evidence. *Tectonics*, 12: 477-491.
- Heimman, A., Eyal, M. & Eyal, Y., 1990. The Evolution Of Barahta Rhomb-Shaped Graben, Mount Hermon, Dead Sea Transform. *Tectonophysics*, 180: 101-110.
- Hempton, M., 1985. Structure And Deformation Of The Bitlis Suture Near Lake Hazar, Southeastern Turkey. *Geological Society Of America Bulletin*, 96: 233-243.
- Hempton, M., 1987. Constraints On Arabian Plate Motion And Extensional History Of The Red Sea. *Tectonics*, 6: 687-705.
- Hirsch, F. & Picard, L., 1988. The Jurassic Facies In The Levant. *Journal Of Petroleum Geology*, 11: 277-308.
- Hofstetter, A., Ron, H. & Van Eck, T., 1989. Mt. Carmel Earthquake Sequence, Seismological Division, Institute For Petroleum Research And Geophysics, Holon, Israel.
- Hofstetter, A., Feldman, L. & Rotstein, Y., 1990. Crustal Structure Of Israel: Constraints From Teleseismic And Gravity Data. *Geophysical Journal International*, 104: 371-379.
- Hofstetter, A., Feldman, L. & Rotstein, Y., 1991. Crustal Structure Of Israel: Constraints From Teleseismic And Gravity Data. *Geophysics Journal International*, 104: 371-379.
- Hofstetter, A., Van Eck, T. & Shapira, A., 1995. Seismic Activity Along Fault Branches Of The Jordan - Dead Sea Transform : The Carmel-Tirza Fault System. *Tectonophysics*, .
- Horowitz, A., 1979. Structure And Tectonic Development Of Israel (And) Pre-Quaternary Geology Of Israel. In: (Eds), *The Quaternary Of Israel*, Academic Press, 11-364.

- Hubbard, R.J., 1988. Age And Significance Of Sequence Boundaries On Jurassic And Early Cretaceous Rifted Continental Margins. *American Association Of Petroleum Geologists Bulletin*, 72: 49-72.
- Hussein, H.M., Korrat, I.M. & Fattah, A.K.A., 1996. The October 12, 1992 Cairo Earthquake: A Complex Multiple Shock. *Bulletin Of The International Institute Of Seismicity And Earthquake Engineering*, 30: 9-22.
- Husseini, M. & Husseini, S., 1988. Origin Of The Infracambrian Salt Basins Of The Middle East. Submitted To : The Geological Society Of London.
- Husseini, M., 1988. The Arabian Infracambrian Extensional System. *Tectonophysics*, 148: 93-103.
- Husseini, M.I., 1989. Tectonic And Deposition Model Of Late Precambrian-Cambrian Arabian And Adjoining Plates. *American Association Of Petroleum Geologist Bulletin*, 73: 1117-1131.
- Husseini, M.I., 1990. The Cambro-Ordovician Arabian And Ajoining Plates: A Glacio-Eustatic Model. *Journal Of Petroleum Geology*, 13: 267-288.
- Husseini, M.I., 1991. Tectonic And Depositional Model Of The Arabian And Adjoining Plates During The Silurian-Devonian. *American Association Of Petroleum Geologists Bulletin*, 75: 108-120.
- Husseini, M.I., 1992. Upper Palaeozoic Tectono-Sedimentary Evolution Of The Arabian And Adjoining Plates. *Journal Of The Geological Society Of London*, 149: 419-429.
- Ibrahim, M.W.I., 1978. *Petroleum Geology Of South Iraq*, University Of London, Imperial College.
- Ibrahim, M.W., 1979. Shifting Depositional Axes Of Iraq: An Outline Of Geosynclinal History. *Journal Of Petroleum Geology*, 2: 181-197.
- Ibrahim, E.M., 1985. Seismic Activity In The Different Tectonic Provinces Of Egypt. *Bulletin Of The International Institute Of Seismology And Earthquake Engineering*, 21: 139-176.
- Ibrahim, K.E., Alakhras, M.N. & Bazuhair, A.S., 1993. Combined Gravity And Aeromagnetic Surveys Of The Khulais Basin Of Western Saudi-Arabia. *Journal Of African Earth Sciences And The Middle East*, 17: 373-381.
- Ibrahim, M.W., 1994. Geothermal Gradient Anomalies Of Hydrocarbon Entrapment In The Middle East And North Africa. In: M. Al-Husseini (Eds), *Geo '94, The Middle East Petroleum Geosciences*, Gulf Petrolink, 1, 543-552.
- Ibrahim, M.W., 1996. Study Sizes Up Iraq's Reserves, Exploration Status, Production Potential. *Oil & Gas Journal*, June 24: 53-55.
- Ibrahim, E.M. & Fattah, K.A., 1996. Evaluation Of The Seismic Force Horizontal Acceleration Ratio Distribution An Seismic Zoning Maps For Egypt And Vicinities. *Bulletin Of The International Institute Of Seismicity And Earthquake Engineering*, 30: 23-28.
- IPRG Seismological Bulletins, 1982-1993. Earthquakes In And Around Israel. *Bulletin Of The International Seismological Centre, Edinburgh*, 1-11.
- Islami, A.A., 1972. A Study Of The Depth Of Mohorovicic Discontinuity In Western Iran And The Velocity Of P N Wave. *J. Earth Space Phys.*, 1: 1-12.
- Ismail, I.A.H., 1987. Iraq, Inter-Union Commission On The Lithosphere.
- Izzeldin, A.Y., 1987. Seismic, Gravity And Magnetic Surveys In The Central Part Of The Red Sea: Their Interpretation And Implications For The Structure And Evolution Of The Red Sea. *Tectonophysics*, 143: 269-306.
- Jackson, J.A. & Fitch, T., 1981. Basement Faulting And The Focal Depths Of The Larger Earthquakes In The Zagros Mountains (Iran). *Geophysical Journal Royal Astronomical Society*, 64: 561-586.
- Jackson, J.A., Fitch, T. & Mckenzie, D.P., 1981. Active Thrusting And The Evolution Of The Zagros Fold Belt Thrust And Nappe Tectonics. In: K. Mcclay And N. Price *Geological Society Of London, Special Publication 9*, 371-379.
- Jackson, N.J., 1981. A Note On The Geochemistry Of The Khumrah Metabasalts, Southern Arabian Shield, Saudi Arabia. *Bulletin Of King Abdulaziz Univ. Fac. Earth Science*, 4: 1599-166.
- Jackson, J. & Mckenzie, D., 1984. Active Tectonics Of The Alpine-Himalayan Belt Between Western Turkey And Pakistan. *Geophys. J. R. Astr. Soc.*, 77: 185-264.

- Jackson, J. & McKenzie, D., 1988. The Relationship Between Plate Motions And Seismic Moment Tensors, And The Rates Of Active Deformation In The Mediterranean And Middle East. *Geophysical Journal International*, 93: 45-73.
- Jackson, J.A., White, N.J., Garfunkel, Z. & Anderson, H., 1988. Relations Between Normal-Fault Geometry, Tilting And Vertical Motions In The Extensional Terrains: An Example From The Southern Gulf Of Suez. *J. Struct. Geol.*, 10: 155-170.
- Jackson, J., 1992. Partitioning Of Strike-Slip And Convergent Motion Between Eurasia And Arabia In Eastern Turkey And The Caucasus. *Journal Of Geophysical Research-Solid Earth*, 97: 12471-12479.
- Jassim, S.Z., Al-Shaibani, S.K. & Ajina, T.M., 1975. Possible Middle Eocene Movements In The Derbendikhan Area, Northeastern Iraq. *Journal Of The Geological Society Of Iraq*, Special Issue: 139-145.
- Jassim, S.Z., 1981. Early Pleistocene Gravel Fan Of The Tigris River From Al Fatha To Baghdad, Central Iraq. *Journal Of The Geological Society Of Iraq*, 14: 25-34.
- Jestin, F., Huchon, P., Gaulier, J. M., 1994. The Somalia Plate And The East African Rift System: Present-Day Kinematics. *Geophys. J. Int.*, 116: 637-654.
- Jih, R.S. & Lynnes, C.S., 1993. Regional Lg Q Variation In Iranian Plateau And Its Implication For Mb(Lg) Determination, Phillips Lab Report PL-TR-93-2003 (Tgal-93-01), ADA262801.
- Joffe, S. & Garfunkel, Z., 1987. Plate Kinematics Of The Circum Red Sea - A Re-Evaluation. *Tectonophysics*, 141: 5-22.
- Johnson, P.R., Scheibner, E. & Smith, E.A., 1987. Basement Fragments, Accreted Tectonostratigraphic Terranes And Overlap Sequences: Elements In The Tectonic Evolution Of The Arabian Shield. basement Fragments, Accreted Tectonostratigraphic Terranes And Overlap Sequences. In: A. Kroner (Eds), *Geodynamics Series, Proterozoic Lithospheric Evolution*, American Geophysical Union, 323-343.
- Johnson, P., Stewart, I., 1995. Magnetically Inferred Basement Structure In Central Saudi Arabia. *Tectonophysics*, 245. Kaddouri, N., 1982. Late Turonian-Early Campanian Sediments In Iraq. *Journal Of The Geological Society Of Iraq*, 15.
- Kader, A.B.S., And Marouf, N. Z., 1994. Tigris Structures In Iraq, And Example Of Fault Rejuvenation And Its Control Of Sedimentation And Hydrocarbon Accumulation. *tigris Structures In Iraq, And Example Of Fault Rejuvenation And Its Control Of Sedimentation And Hydrocarbon Accumulation*. In: (Eds), *Of Abstracts, Fifth Jordanian Geological Conference & Third Geological Conference On The Middle East*, Geocom, 3, 165-166.
- Kadinsky-Cade, K., Barazangi, M., Oliver, J. & Isacks, B., 1981. Lateral Variations Of High-Frequency Seismic Wave-Propagation At Regional Distances Across The Turkish And Iranian Plateaus. *Journal Of Geophysical Research*, 86: 9377-9396.
- Kadinsky-Cade, K. & Barazangi, M., 1982. Seismotectonics Of Southern Iran: The Oman Line. *Tectonics*, 1: 389-412.
- Kafri, U. & Shapira, A., 1990. A Correlation Between Earthquake Occurrence, Rainfall And Water Level In Lake Kinnereth, Israel. *Physics Of The Earth And Planetary Interiors*, 62: 277-283.
- Kamel, A.F. & Sokkary, E.L., 1994. Geologic Hazards Assessment Of Cairo And Vicinity. *Natural Hazards*, 13: 253-274.
- Karakaisis, G.F., 1994. Long-Term Earthquake Prediction In Iran Based On The Time- And Magnitude-Predictable Model. *Physics Of The Earth And Planetary Interiors*, 83: 129-145.
- Karaki, N.A., 1994. Analysis, Relocation And Focal Mechanism Of The Carmel Earthquake Swarm Of 1984. *Dirasat*, 21: 281.
- Karaki, N.A. (1995). Re-Evaluating The Seismicity Of The Jordan-Dead Sea Transform System. 5th Jordanian Geological Conference And 3rd Conference On The Geology Of The Middle East, Amman, Jordan.
- Karig, D.E. & Kozly, H., 1990. Late Paleogene-Neogene Evolution Of The Triple Junction Region Near Maras, South Central Turkey. *Geological Society Of London Journal*, 147: 1023-1034.

- Kasapoglu, K.E., 1984. Stress-Strain And Displacement Distributions In The Taurus Belt. stress-Strain And Displacement Distributions In The Taurus Belt. In: O. Tekeli And M.C. Goncuoglu (Eds), *Geology Of The Taurus Belt*, Mta, 295-301.
- Kashai, E.L., 1988, A Review Of The Relations Between The Tectonics, Sedimentation And Petroleum Occurrences Of The Dead Sea - Jordan Rift System. In: W. Manspeizer (Eds), *Triassic-Jurassic Rifting; Continental Breakup And The Origin Of The Atlantic Ocean And Passive Margins*, Elsevier,
- Kashai, E.L. & Croker, P.F., 1987. Structural Geometry And Evolution Of The Dead Sea-Jordan Rift System As Deduced From New Subsurface Data. *Tectonophysics*, 141: 33-60.
- Katzman, R., Ten Brink, U.S. & Lin, J., 1995. Three-Dimensional Modeling Of Pull-Apart Basins: Implications For The Tectonics Of The Dead Sea Basin. *Journal Of Geophysical Research*, 100: 6295-6312.
- Kawar, R., Girdler, R.W. & Kovach, R.L., 1995. The Dead Sea Transform Fault System. *International Union Of Geodesy And Geophysics, Abstracts Week B, XXI General Assembly*, : B345.
- Kebeasy, R.M., Maamoun, M., Albert, R.N.H. & Megahed, M., 1981. Earthquake Activity And Earthquake Risk Around Alexandria, Egypt. *Bulletin Of International Institute Of Seismology And Earthquake Engineering*, 19: 93-113.
- Kebeasy, R.M., 1990. Seismicity. In: R. Said (Eds), *The Geology Of Egypt*, A. A. Balkema, 51-59.
- Kelling, G., Gokcen, S., Floyd, P. & Gokcen, N., 1987. Neogene Tectonics And Plate Convergence In The Eastern Mediterranean: New Data From Southern Turkey. *Geology*, 15: 425-429.
- Kempler, D. & Ben-Avraham, Z., 1987. The Tectonic Evolution Of The Cyprean Arc. *Annales Tectonicae*, 1: 58-71.
- Kempler, D. & Garfunkle, Z., 1991. The Northeast Mediterranean Triple Junction From A Plate Kinematic Point Of View. *Bulletin Tech. Univ. Istanbul*, 44: 425-454.
- Kempler, D. & Garfunkel, Z., 1994. Structures And Kinematics In The Northeastern Mediterranean: A Study Of An Irregular Plate Boundary. *Tectonophysics*, 234: 19-32.
- Kenar, O., Osmansahin, I. & Ozer, M.F., 1996. Seismicity And Tectonics Of Eastern Anatolia. *Bulletin Of The International Institute Of Seismology And Earthquake Engineering*, 30: 59-76.
- Khair, K., Aker, N. & Zahrudinne, K., 1992. Hydrogeologic Units Of Lebanon. *Applied Hydrogeology*, 1: 34-49.
- Khair, K., 1992. A Review Of Geophysical Data In Lebanon And Their Significance To The Levantine Plate Structure. *Geology Of The Arab World*, 1: 231-?
- Khair, K., Khawlie, M., Haddad, F., Barazangi, M., Seber, D. & Chaimov, T., 1993. Bouguer Gravity And Crustal Structure Of The Dead Sea Transform Fault And Adjacent Mountain Belts In Lebanon. *Geology*, 21: 739-742.
- Khair, K., Aker, N., Haddad, F. & Hachach, A., 1994. The Environmental Impacts Of Humans On Groundwater In Lebanon. *Water, Air And Soil Pollution*, 77: 1-13.
- Khair, K., Tsokas, G.N. & Sawaf, T., 1997. Crustal Structure Of The Northern Levant Region: Multiple Source Werner Deconvolution Estimates For Bouguer Gravity Anomalies. *Geophysical Journal International*, 128: 605-616.
- Khalil, B., 1992. The Geology Of The Ar Rabba Area. Ammam, Jordon, Ministry Of Energy And Mineral Resources, Natural Resources Authority, Geological Mapping Division.
- Khattab, M.M., 1993. Interpretation Of Recent Gravity Profiles Over The Ophiolite Belt, Northern Oman Mountains, United-Arab-Emirates. *Journal Of African Earth Sciences And The Middle East*, 16: 319-327.
- Khattab, M.M., 1993. Interpretation Of Recent Gravity Profile Over The Ophiolite Belt, Northern Oman Mountains, United Arab Emirates. *Journal Of African Earth Sciences*, 16: 319-327.
- Khattab, M.M., 1994. Tectonics Of The North-Western Gulf Of Oman And The Arabian Continental Margin As Indicated By Magnetic Data. *Marine And Petroleum Geology*, 11: 116-123.

- Khatab, M.M., 1994. Tectonics Of The North-Western Gulf Of Oman And The Arabian Continental Margin As Indicated By Magnetic Data. *Marine And Petroleum Geology*, 11: 116-123.
- Khatab, M.M., 1995. Interpretation Of Magnetic And Gravity Surveys In The Southern Arabian Gulf, The Strait Of Hormuz, And The Northwesternmost Gulf Of Oman - Implications Of Pre-Permian Basement Tectonics. *Marine Geology*, 123: 105-116.
- Khawlie, M.R., 1992. Shaping The Eastern Mediterranean Coast By Earthquakes: Lebanon. *Geology Today*, : 58-61.
- Khoury, J., 1982. Hydrogeology Of The Syrian Steppe And Adjoining Arid Areas. *Quarterly Journal Of Engineering Geology (London)*, 15: 135-154.
- Kim, S.G. & Nuttli, O.W., 1977. Spectral Characteristics Of Anomalous Eurasian Earthquakes. *Bulletin Seismological Society Of America*, 67: 463-478.
- Kissel, C., Averbuch, O., De Lamotte, D., Monod, O. & Allerton, S., 1993. First Paleomagnetic Evidence For A Post-Eocene Clockwise Rotation Of The Western Taurides Thrust Belt East Of The Isparta Reentrant (Southwestern Turkey). *Earth And Planetary Science Letters*, 117: 1-14.
- Klinger, Y., Avouac, J.P. & Abou Karaki, N., Sismotectonic Of Wadi Araba Fault (Jordan). *Annales Geophysicae*, 15 (Supplement): C234.
- Knipper, A., Savelyev, A. & Ruklye, M., 1988. Ophiolitic Association Of Northwestern Syria. *Geotectonics*, 22: 73-82. Kocyigit, A., 1991. An Example Of An Accretionary Forearc Basin From Northern Central Anatolia And Its Implications For The History Of Subduction Of Neo-Tethys In Turkey. *Geological Society Of America Bulletin*, 103: 22-36.
- Kohn, B.P., Lang, B. & Steinitz, G., 1993. 40Ar/39 Ar Dating Of The Atlit-1 Volcanic Sequence. *Israel Journal Of Earth Sciences*, 42: 17-28.
- Kolars, J.F. & Mitchell, W.A., The Euphrates River And The Southeast Anatolia Development Project. Southern Illinois University Press Carbondale: 324.
- Koop, W.J. & Stoneley, R., 1982. Subsidence History Of The Middle East Zagros Basin, Permian To Recent. *Phil. Trans. R. Society Of London*, 305: 149-168.
- Korrat, I.M., Ibrahim, E.M., Shrief, R.M. & Abou Elenean, K.M., 1996. Earthquake Mechanisms In The Eastern Mediterranean Region And Their Tectonic Implications. *Bulletin Of The International Institute Of Seismology And Earthquake Engineering*, 30: 29-45.
- Kovach, R.L. & Ben-Avraham, Z., 1985. Gravity Anomalies Across The Dead Sea Rift And Comparison With Other Rift Zones. *Tectonophysics*, 111: 155-162.
- Kovach, R.L., Andreasen, G.E., Gettings, M.E. & El-Kaysi, K., 1990. Geophysical Investigations In Jordan. *Tectonophysics*, 180: 61-69.
- Krashennnikov, V., A. & Hall, J., K. (1994). *Geological Structure Of The North-Eastern Mediterranean, Jerusalem*.
- Lababidi, M.M. & Hamdan, A.N., 1985. Preliminary Lithostratigraphic Correlation Study In Oapec Member Countries. Kuwait, Organization Of Arab Petroleum Exporting Countries.
- Lamson, R.J., Blank, H.R., Mooney, W. & Healy, J.H., 1979. Seismic Refraction Observations Across The Oceanic-Continental Rift Zone, Southwest Saudi Arabia. *Eos (Am. Geophys. Union, Trans.)*, 60: 954. Lartet, L., 1879.
- La Geologie De La Palestine. *Ann. Sci. Geol.*, 1.
- Laughton, A.S. & Tramontini, C., 1969. Recent Studies Of The Crustal Structure In The Gulf Of Aden. *Tectonophysics*, 8: 359-375.
- Laws, E.D. & Wilson, M., 1997. Tectonics And Magmatism Associated With The Mesozoic Passive Continental Margin Development In The Middle East. *Journal Of The Geological Society*, 154: 459-464.
- Le Pichon, X. & Francheteau, J., 1978. A Plate-Tectonic Analysis Of The Red Sea- Gulf Of Aden Area. *Tectonophysics*, 46: 369-406.
- Le Pichon, X. & Gaulier, J.M., 1987. Plate Tectonics Of The Red Sea-Levant Area. plate Tectonics Of The Red Sea-Levant Area. In: T. Hilde And R. Carlson (Eds), *Silver Anniv. Celebration Of Plate*

- Tectonics, Geodynamics Research Institute Tamu, Program And Abstracts: 1987 Geodynamics Symposium, 42-44.
- Le Pichon, X. & Gaulier, J.M., 1988. The Rotation Of Arabia And The Levant Fault System. *Tectonophysics*, 153: 271-294.
- Leblanc, D., 1977. Stratigraphie Et Structure Du Rif Externe Oriental Au Nord De Taza (Maroc). *Bulletin: Societe Geologique De France*, 7: 319-330.
- Lenczowski, G., 1997. The Caspian Oil And Gas Basin: A New Source Of Wealth? *Middle East Policy*, V: 111-.
- Leonov, Y.G., Makarem, K. & Zaza, T., 1986. Olistostrome Origin For Rocks In The Core Of The Abd El Aziz Anticline, Syria. *Geotectonics*, 20: 142-146.
- Leonov, Y.G., Sigachev, S.P., Otri, M., Yusef, A., Zaza, T. & Sawaf, T., 1989. New Data On The Paleozoic Complex Of The Platform Cover Of Syria. *Geotectonics*, 23: 538-542.
- Lepine, J.-C. & Hirn, A., 1992. Seismotectonics In The Republic Of Djibouti, Linking The Afar Depression And The Gulf Of Aden. *Tectonophysics*, 209: 65-86.
- Lippard, S., Shelton, A. & Gass, I., 1986. The Ophiolite Of Northern Oman. *The Geological Society* 1-16.
- Litak, R.K., Barazangi, M., Beauchamp, W., Seber, D., Brew, G., Sawaf, T. & Al-Youssef, W., 1997. Mesozoic-Cenozoic Evolution Of The Intraplate Euphrates Fault System, Syria: Implications For Regional Tectonics. *Journal Of The Geological Society*, 154: 653-666.
- Litak, R.K., Barazangi, M., Brew, G., Sawaf, T., Al-Iman, A. & Al-Youssef, W., 1998. Structure And Evolution Of The Petroliferous Euphrates Graben System, Southeast Syria. *American Association Of Petroleum Geologists Bulletin*, 82, 1173-1190, 1998.
- Livermore, R.A. & Smith, A.G., 1984. Relative Motions Of Africa And Europe In Vicinity Of Turkey. In: O. Tekeli And M.C. Goncuoglu MTA Bulletin, 1-10.
- Livieratos, E. & Zadro, M., 1985. Multiple-Input Linear Systems In Geoprocesses; An Analysis Of Geophysical Data Across The Eastern Continental Hellenic Margin. *Acta Geophysica Polonica*, 33: 135-146.
- Lovelock, P.E.R., 1984. A Review Of The Tectonics Of The Northern Middle East Region. *Geological Magazine*, 121: 577-587.
- Lowell, J.D., Genik, G.J., Nelson, T.H. & Tucker, P.M., 1975. Petroleum And Plate Tectonics Of The Southern Red Sea. *petroleum And Plate Tectonics Of The Southern Red Sea*. In: A.G. Fischer And S. Judson (Eds), *Petroleum And Global Tectonics*, Princeton Univ. Press, 129-153.
- Lyberis, N., 1988. Tectonic Evolution Of The Gulf Of Suez And The Gulf Of Aqaba. *Tectonophysics*, 153: 209-220.
- Lyberis, N., Kasapoglu, E., Yurur, T. & Gundogdu, N., 1992. The East Anatolian Fault: An Oblique Collisional Belt. *Tectonophysics*, 204: 1-15.
- Mahfoud, R.F. & Beck, J.N., 1991. Inorganic Origin In Upper Mantle Seen Likely For Solid Hydrocarbon In Syria Plateau Basalt. *Oil & Gas Journal*, : 88-92.
- Mahfoud, R.F., Beck, James N., 1993. Petrographic Study Of, And Trace Element Distribution In, High-Mg, Transitional And High-Al₂O₃ Basalts From The Coastal Region And Sw-Central Syria: A Comparative Study With Similar Basalts From The Aleutian Island Arc. *J. Geodynamics*, 17: 57-76.
- Mahmoud, M.D. & Vaslet, D., 1992. The Lower Silurian Quabah Formation Of Saudi Arabia: An Important Hydrocarbon Source Rock. *The American Association Of Petroleum Geologists Bulletin*, 76: 1491-1506.
- Makhous, M., Galushkin, Y. & Lopatin, N., 1997. Burial History And Kinetic Modeling For Hydrocarbon Generation, Part I: The Galo Model. *American Association Of Petroleum Geologists*, 81: 1660-1677.
- Makris, J., Allam, A., Mokhtar, T., Basahel, A., Dehghani, G.A. & Bazari, M., 1983. Crustal Structure In The Northwestern Region Of The Arabian Shield And Its Transition To The Red Sea. *Bulletin Fac. Earth Sci.*, 6: 435-447.

- Makris, J., Ben Abraham, Z., Behle, A., Ginzburg, A., Giese, P., Steinmetz, L., Whitmarsh, R.B. & Eleftheriou, S., 1983. Seismic Refraction Profiles Between Cyprus And Israel And Their Interpretation. *Geophys. J. R. Astr. Soc.*, 75: 575-591.
- Makris, J., Nicolich, R. & Weigel, W., 1985. Crustal Structures In The Ionian Sea. *Rapports Et Proces Verbaux Des Reunions - Commission Internationale Pour L'exploration Scientifique De La Mer Mediterranee*, 29: 73-75.
- Makris, J. & Ginzburg, A., 1987. The Afar Depression: Transition Between Continental Rifting And Sea-Floor Spreading. *Tectonophysics*, 141: 199-214.
- Makris, J., Rihm, R. & Gotz, L.G., 1989. Heat Flow In The Central Red Sea. *European Association Of Exploration Geophysicists: 51st Meeting And Technical Exhibition; Technical Programme And Abstracts Of Papers*, 51: 194-195.
- Makris, J., Henke, C.H., Egloff, F. & Akamaluk, T., 1991. The Gravity Field Of The Red Sea And East Africa. *Tectonophysics*, 198: 369-381.
- Makris, J., Rihm, R., 1991. Shear-Controlled Evolution Of The Red Sea: Pull Apart Model. *Tectonophysics*, 198: 441-466.
- Makris, J. & Henke, C.H., 1992. Pull-Apart Evolution Of The Red Sea. *Journal Of Petroleum Geology*, 15: 127-134.
- Manetti, P., Capaldi, G., Chiesa, S., Civetta, L. & Others, 1991. Magmatism Of The Eastern Red Sea Margin In The Northern Part Of Yemen From Oligocene To Present. *Tectonophysics*, 198: 181-202.
- Marco, S., Stein, M., Agnon, A. & Ron, H., 1996. Long-Term Earthquake Clustering: A 50,000-Year Paleoseismic Record In The Dead Sea Graben. *Journal Of Geophysical Research*, 101: 6179-6191.
- Marcoux, J., Brun, J.-P., Burg, J.-P. & Ricou, L., 1987. Shear Structures In Anhydrite At The Base Of Thrust Sheets (Antalya, Southern Turkey). *Journal Of Structural Geology*, 9: 555-561.
- Marcoux, J., Ricou, L.E., Burg, J.P. & Brun, J.P., 1989. Shear-Sense Criteria In The Antalya And Alanya Thrust System (Southwestern Turkey): Evidence For A Southward Emplacement. *Tectonophysics*, 161: 81-91.
- Marquer, D., Peters, T. & Gnos, E., 1995. A New Structural Interpretation For The Emplacement Of The Masirah Ophiolites (Oman) - A Main Paleocene Intra-Oceanic Thrust. *Geodinamica Acta*, 8: 13-19.
- Mart, Y., 1990. The Dead Sea Rift: From Continental Rift To Incipient Ocean. *Tectonophysics*, 197: 155-179.
- Mart, Y., 1994. Ptolemais Basin: The Tectonic Origin Of A Senonian Marine Basin Underneath The Southeastern Mediterranean Sea. *Tectonophysics*, 234: 5-17.
- Marzouk, I.A., 1988. Study Of Crustal Structure Of Egypt Deduced From Deep Seismic And Gravity Data. *Hamburg, University Of*: pp. 118.
- Marzouk, I. & Sattar, M.A.E., 1994. Wrench Tectonics In Abu Dahbi, United Arab Emirates. In: M. Al-Husseini (Eds), *Geo '94, The Middle East Petroleum Geosciences*, Gulf Petrolink, 1, 655-668.
- Matar, A. & Mascle, G., 1993. Kinematic Of The Levant Fault In Northern Syria: Microtectonic Analysis Of The Alghab Rift. *Geodinamica Acta (Paris)*, 6: 153-160.
- May, P.R., 1991. The Eastern Mediterranean Mesozoic Basin: Evolution And Oil Habitat. *American Association Of Petroleum Geologists Bulletin*, 75: 1215-1232.
- Mcbride, J.H., Barazangi, M., Best, J., Al-Saad, D., Sawaf, T., Al-Otri, M. & Gebran, A., 1990. Seismic Reflection Structure Of Intracratonic Palmyride Fold-Thrust Belt And Surrounding Arabian Platform, Syria. *American Association Of Petroleum Geologists Bulletin*, 74: 238-259.
- Mcgillivray, J.G. & Hussein, M.I., 1992. The Paleozoic Petroleum Geology Of Central Arabia. *The American Association Of Petroleum Geologists Bulletin*, 76: 1473-1490.
- Mckenzie, D., Davies, D. & Molnar, P., 1970. Plate Tectonics Of The Red Sea And East Africa. *Nature*, 226: 243-248.
- Mckenzie, D.P., 1970. Plate Tectonics Of The Mediterranean Region. *Nature*, 226: 239-243.

- Mckenzie, D., 1978. Some Remarks On The Development Of Sedimentary Basins. *Earth And Planetary Science Letters*, 40: 25-32.
- Mechie, J., Prodehl, C. & Koptchalitsch, G., 1985. A Ray-Tracing And Ray Theoretical Seismograms Interpretation Of The U. S. G. S. Saudi Arabian Seismic Line. *Jahrestagung Der Deutschen Geophysikalischen Gesellschaft E.V.*, 45: 75.
- Mechie, J., Prodehl, C. & El-Isa, Z., 1986. P- And S-Wave Crustal Structure Beneath A Seismic-Refraction Line In Jordan. *Jahrestagung Der Deutschen Geophysikalischen Gesellschaft E.V.*, 46: 169.
- Mechie, J., Prodehl, C. & Koptchalitsch, G., 1986. Ray Path Interpretation Of The Crustal Structure Beneath Saudi Arabia. *Tectonophysics*, 131: 333-352.
- Megharaoui, M. & Doumaz, F., 1996. Earthquake-Induced Flooding And Paleoseismicity Of The El Asnam, Algeria, Fault-Related Fold. *Journal Of Geophysical Research*, 101: 17, 617-17, 644.
- Meghraoui, M., Morel, J.L., Andrieux, J. & Dahmani, M., 1996. Tectonique Plio-Quaternaire De La Chaîne Tello-Rifaine Et De La Mer D'alboran. Une Zone Complexe De Convergence Continent-Continent. *Bulletin: Societe Geologique De France*, 167: 141-157.
- Metwalli, M., Philip, G. & Moussly, M., 1974. Petroleum-Bearing Formations In Northeastern Syria And Northern Iraq. *American Association Of Petroleum Geologists Bulletin*, 58: 1781-1796.
- Meyerhoff, A.A., 1991. Energy Resources: Oil And Gas. *Geotimes*, .
- Michaelis, P.L. & Pauken, R.J., 1990. Seismic Interpretation Of The Structure And Stratigraphy Of The Strait Of Hormuz. seismic Interpretation Of The Structure And Stratigraphy Of The Strait Of Hormuz. In: A.H.F. Robertson, M.P. Searle And A.C. Ries (Eds), *The Geology And Tectonics Of The Oman Region*, The Geological Society, 846.
- Michard, A., Goffe, B., Saddiqi, O., Oberhansli, R. & Others, 1994. Late Cretaceous Exhumation Of The Oman Blueschists And Eclogites - A 2-Stage Extensional Mechanism. *Terra Nova*, 6: 404-413.
- Mikbel, S. & Zacher, W., 1986. Fold Structures In Northern Jordan. *Schweizerbart'sche Verlagsbuchhandlung*, : 248-256.
- Milkereit, B. & Flueh, E.R., 1985. Saudi Arabian Refraction Profile; Crustal Structure Of The Red Sea Arabian Shield Transition. *Tectonophysics*, 111: 283-298.
- Miller, J.J., Agena, W.F. & Lee, M.W., 1992. Reprocessing Of Reflection Seismic Lines R111 And R102, Risha Gas Field, Hashemite Kingdom Of Jordan. U.S. Department Of The Interior, U.S. Geological Survey; Open-File Report 92-680.
- Mindevalli, O.Y. & Mitchell, B.J., 1989. Crustal Structure And Possible Anisotropy In Turkey From Seismic Wave Dispersion. *Geophysical Journal International*, 98: 93-106.
- Minshull, T.A., White, R.S., Barton, P.J. & Collier, J.S., 1992. Deformation At Plate Boundaries Around The Gulf-Of-Oman. *Marine Geology*, 104: 265-277.
- Mohajer-Ashjai, A. & Nowroozi, A.A., 1978. Observed And Probable Intensity Zoning Of Iran. *Tectonophysics*, 29: 149-160.
- Mohamed, M.M., 1995. Spectral Analysis Of Microearthquakes Recorded By Aswan Telemetered Network. Individual Studies By Participants At The International Institute Of Seismology And Earthquake Engineering, 31: 33-44.
- Mokhtar, T.A., 1995. Phase Velocity Of The Arabian Platform And The Surface Waves Attenuation Characteristics By Wave Form Modeling. *Jkau: Earth Science*, 8: 23-45.
- Mokhtar, T.A., 1995. Phase Velocity Of The Arabian Platform And The Surface Waves Attenuation Characteristics By Wave Form Modeling. *Journal Of King Abel El Aziz University*, 8: 23-45.
- Mooney, W.D. & Gettings, M.E., 1983. Interpretation Of Seismic Deep-Refraction Line, U. S. Geological Survey Professional paper 289.
- Mooney, W.D. & Prodehl, C., 1984. Proceedings Of The 1980 Workshop Of The International Association Of Seismology And Physics Of The Earth's Interior On The Seismic Modeling Of Laterally Varying Structures: Contributions Based On Data From The 1978 Saudi Arabian Refraction Profile, U.S. Geological Survey.

- Mooney, W.D., Gettings, M.E., Blank, H.R. & Healy, J.H., 1985. Saudi Arabian Seismic-Refracton Profile: A Traveltime Interpretation Of Crustal And Upper Mantle Structure. *Tectonophysics*, 111: 173-246.
- Moore, E.M., Robinson, P.T., Malpas, J. & Xenophonotos, C., 1984. Model For The Origin Of The Troodos Massif, Cyprus, And Other Mideast Ophiolites. *Geology*, 12: 500-503.
- Morel, J.L. & Megharaoui, M., 1996. Goringe-Alboran-Tell Tectonic Zone: A Transpression System Along The Africa-Eurasia Plate Boundary. *Geology*, 24: 755-758.
- Moskalenko, V.N., Neprochnov, Y.P. & Sollogub, V.B., 1989. Structure Of The Consolidated Crust And Upper Mantle: Structure Of The Mohorovicic Surface. In: V.V. Belousov And B.S. Vol'vovskiy (Eds), *Structure And Evolution Of The Crust And Upper Mantle Of The Black Sea, Rezul'taty Issledovaniy Po Mezhdunarodnym Geofizicheskim Proyektam*, Izd. Nauka, 135-136.
- Moskalenko, V.N., 1991. Migration Of The Subduction Zone In The Eastern Mediterranean. *Geotectonics*, 24: 451-459.
- Moussaviharami, R. & Brenner, R.L., 1992. Geohistory Analysis And Petroleum Reservoir Characteristics Of Lower Cretaceous (Neocomian) Sandstones, Eastern Kopet-Dagh Basin, Northeastern Iran. *American Association Of Petroleum Geologists Bulletin*, 76: 1200-1208.
- Moustafa, A.R. & Khalil, M.H., 1994. Rejuvenation Of The Eastern Mediterranean Passive Continental Margin In Northern And Central Sinai: New Data From The Themed Fault. *Geological Magazine*, 131: 435-448.
- Moustafa, A.R. & Khaili, S.M., 1995. Rejuvenation Of The Tethyan Passive Continental Margin Of Northern Sinai: Deformation Style And Age (Gebel Yelleq Area). *Tectonophysics*, 241: 225-238.
- Moustafa, A.R., 1996. Internal Structure And Deformation Of An Accommodation Zone In The Northern Part Of The Suez Rift. *Journal Of Structural Geology*, 18: 93-107.
- Moustafa, A.R., 1996. Structural Setting And Tectonic Evolution Of The Northern Hammam Faraun Block (Wadi Wasit-Wadi Warden Area), Eastern Side Of The Suez Rift. *Kuwait Journal Of Science And Engineering*, 23: 105-131.
- Mouty, M., Delaloye, M., Fontignie, D., Piskin, O. & Wagner, J.-J., 1992. The Volcanic Activity In Syria And Lebanon Between Jurassic And Actual. *Schweiz. Mineral. Petrogr. Mitt.*, 72: 91-105.
- Mouty, M., 1997. The Jurassic In The Palmyrides Chain (Syria). 168: 181-186. Mouty, M. & Al-Maleh, A.K. (1997). The Mesozoic System In Syria. Peri-Tethys Programme - Onarep Annual Meeting, Rabat-Morocco.
- Muehlberger, W.R., 1981. The Splintering Of The Dead Sea Fault Zone In Turkey. *Yerbilimleri*, 8: 125-130.
- Muehlberger, W. & Gordon, M., 1987. Observations On The Complexity Of The East Anatolian Fault, Turkey. *Journal Of Structural Geology*, 9: 899-903.
- Murris, R.J., 1980. Middle East: Stratigraphic Evolution And Oil Habitat. *American Association Of Petroleum Geologists Bulletin*, 64: 597-618.
- Nakiboglu, S.M., Eren, K. & Shedayed, A.M., 1994. Analysis Of Distortions In The National Geodetic Network Of Saudi-Arabia. *Bulletin Geodesique*, 68: 220-229.
- Naoum, A.A., Atiya, M.S. & Al-Ubaidi, M.R., 1981. Mesoscopic Structures Associated With Sinjar Anticline. *Journal Of The Geological Society Of Iraq*, 14: 71-80.
- Nasir, S., 1990. K-Ar Age Determinations And Volcanological Evolution Of The Northwestern Part Of The Arabian Plate, Jordan. *European Journal Of Mineralogy*, 2: 188.
- Nasir, S., 1992. The Lithosphere Beneath The Northwestern Part Of The Arabian Plate (Jordan): Evidence From Xenoliths And Geophysics. *Tectonophysics*, 201: 357-370.
- Neev, D.N., 1975. Tectonic Evolution Of The Middle East And The Levantine Basin (Easternmost Mediterranean). : 683-686.
- Neev, D. & Ben-Avraham, Z., 1977. The Levantine Countries: The Israeli Coastal Region. In: A.E.M. Nairn, W.H. Kanes And F.G. Stehli (Eds), *The Ocean Basins And Margins, The Eastern Mediterranean*, Plenum Press, 4a, 319-353.

- Neugebauer, J., 1995. Structures And Kinematics Of The North Anatolian Fault Zone, Adapazarı-Bolu Region, Northwest Turkey. *Tectonophysics*, 243: 119-134.
- Ni, J. & Barazangi, M., 1986. Seismotectonics Of The Zagros Continental Collision Zone And A Comparison With The Himalayas. *Journal Of Geophysical Research*, 91: 8205-8218.
- Niazi, M., 1968. Crustal Thickness In Central Saudi Arabian Peninsula. *Geophysical Journal Of The Royal Astronomical Society*, 15: 545-547.
- Niazi, M., Asudeh, I., Ballard, G., Jackson, J., King, G. & McKenzie, D., 1978. The Depth Of Seismicity In The Kermanshah Region Of The Zagros Mountains (Iran). *Earth And Planetary Science Letters*, 40: 270-274.
- Niazi, M., Shimamura, H. & Matsuura, M., 1980. Microearthquakes And Crustal Structure Of The Makran Coast Of Iran. *Geophysical Research Letters*, 7: 297-300.
- Nishigami, K., Iio, Y., Gurbuz, C., Pinar, A., Aybey, N., Ucer, S.B., Honkura, Y. & Isikara, A.M., 1990. Microseismic Activity And Spatial Distribution Of Coda-Q In The Westernmost Part Of The North Anatolian Fault Zone, Turkey. *Bulletin Disas. Prev. Inst., Kyoto Univ.*, 40: 41-56.
- North, R.G., 1974. Seismic Slip Rates In The Mediterranean And Middle East. *Nature*, 252: 560-563.
- Nowroozi, A.A., 1972. Focal Mechanism Of Earthquakes In Persia, Turkey, West Pakistan, And Afghanistan And Plate Tectonics Of The Middle East. *Bulletin Of The Seismological Society Of America*, 62: 823-850.
- Nowroozi, A.A., 1976. Seismotectonic Provinces Of Iran. *Bulletin Of The Seismological Society Of America*, 66: 1249-1276.
- Nowroozi, A.A. & Mohajer-Ashjai, A., 1985. Fault Movements And Tectonics Of Eastern Iran: Boundaries Of The Lut Plate. *Geophys. J. Roy. Astr. Soc.*, 83: 215-237. Nowroozi, A.A., 1986. Discrimination Between Underground Explosions And Earthquakes Using Discriminant Functions: Examples For Eurasia And North America. *Annales Geophysicae*, 4: 577-588.
- Nowroozi, A.A., 1987. Tectonics And Earthquake Risk Of Iran. *Developments In Geotechnical Engineering*, 44: 59-75.
- Nur, A. & Ben-Avraham, Z., 1978. The Eastern Mediterranean And The Levant: Tectonics Of Continental Collision. *Tectonophysics*, 46: 297-311.
- Nuttli, O.W., 1980. The Excitation And Attenuation Of Seismic Crustal Phases In Iran. *Bulletin Of The Seismological Society Of America*, 70: 469-485.
- Okay, A.I. & Kelley, S.P., 1994. Tectonic Setting, Petrology And Geochronology Of Jadeite Plus Glaucophane And Chloritoid Plus Glaucophane Schists From North-West Turkey. *Journal Of Metamorphic Geology*, 12: 455-466.
- Omar, G.I. & Steckler, M.S., 1995. Fission Track Evidence On The Initial Rifting Of The Red Sea: Two Pulses, No Propagation. *Science*, 270: 1341-1344.
- Onalan, M., 1988. Geological Evolution Of The Kahramanmaraş Tertiary Peripheral Basin. *Geological Bulletin Of Turkey*, 31: 1-10.
- Orbay, N., Gundogdu, O., Kolcak, D., Duzgit, Z. & Others, 1994. Seismo-Magnetic Studies Between Dokurcun And Abant Area Along The North Anatolian Fault Zone, Turkey. *Journal Of Geomagnetism And Geoelectricity*, 46: 1095-1107.
- Oshiman, N., Tuncer, M.K., Honkura, Y., Baris, S. & Others, A., 1991. A Strategy Of Tectonomagnetic Observation For Monitoring Possible Precursors To Earthquakes In The Western Part Of The North Anatolian Fault Zone, Turkey. *Tectonophysics*, 193: 359-368.
- Osmansahin, I. & Sayil, N., 1996. Pn-Wave Velocity Beneath Anatolia From The First Arrivals. *Bulletin Of The International Institute Of Seismology And Earthquake Engineering*, 30: 77-?.
- Ouglanov, V., Tatlybayev, M. & Nutrobkin, V., 1974. Report On Seismic Profiling In The Syrian Arab Republic, (Unpublished), General Petroleum Company Report, Aleppo, Syria.
- Pallister, J.S., Stacey, J.S., Fischer, L.B. & Premo, W.R., 1987. Arabian Shield Ophiolites And Late Proterozoic Microplate Accretion. *Geology*, 15: 320-323.

- Panagiotopoulos, D.G. & Papazachos, B.C., 1985. Travel Times Of Pn-Waves In The Aegean And Surrounding Area. *Geophysical Journal International*, 80: 165-176.
- Patton, T. & O'connor, S., 1988. Cretaceous Flexural History Of Northern Oman Mountain Foredeep, United Arab Emirates. *American Association Of Petroleum Geologists Bulletin*, 72: 797-809.
- Patton, T.L., Moustafa, A. R., Nelson, R. A., & Abdine, S.A., 1994. Tectonic Evolution And Structural Setting Of The Suez Rift. *tectonic Evolution And Structural Setting Of The Suez Rift*. In: S.M. Landon (Eds), *Interior Rift Basins*, American Association Of Petroleum Geologists Memoir, 39, 9-55.
- Pauken, R.J. & Hemer, D.O., 1991. Tectonics, Stratigraphy, And Hydrocarbon Exploration In The Strait Of Hormuz. *Society Of Petroleum Engineers*, 21380: 369-380.
- Perincek, D. & Cemen, I., 1990. The Structural Relationship Between The East Anatolian And Dead Sea Fault Zones In Southeastern Turkey. *Tectonophysics*, 172: 331-340.
- Perrin, M., Prevot, M. & Bruere, F., 1994. Rotation Of The Oman Ophiolite And Initial Location Of The Ridge In The Hotspot Reference Frame. *Tectonophysics*, 229: 31-42.
- Perry, S.K. & Schamel, S., 1990. The Role Of Low-Angle Normal Faulting And Isostatic Response In The Evolution Of The Suez Rift, Egypt. *Tectonophysics*, 174: 159-173.
- Pinar, A., Honkura, Y. & Kikuchi, M., 1994. Rupture Process Of The 1992 Erzincan Earthquake And Its Implication For Seismotectonics In Eastern Turkey. *Geophysical Research Letters*, 21: 1971-1974.
- Pirazzoli, P.A., Laborel & Stiros, S.C., 1996. Earthquake Clustering In The Eastern Mediterranean During Historical Times. *Journal Of Geophysical Research*, 101: 6083-6097.
- Ponikarov, V.P., 1964. Tectonic Map Of Syria: Scale 1:1,000,000. Damascus, Syrian Arab Republic, Ministry Of Industry.
- Ponikarov, V.P., 1966. The Geological Map Of Syria: Scale 1:1,000,000. Syrian Arab Republic, Ministry Of Industry.
- Ponikarov, V.P., 1967. The Geology Of Syria: Explanatory Notes On The Geological Map Of Syria, Scale 1:500,000 Part I: Stratigraphy, Igneous Rocks And Tectonics. Damascus, Syrian Arab Republic, Ministry Of Industry.
- Powell, J.H. & Mohamed, B.K., 1993. Structure And Sedimentation Of Permo-Triassic And Triassic Rocks Exposed In Small-Scale Horsts And Grabens Of Pre-Cretaceous Age: Dead Sea Margin, Jordan. *Journal Of African Earth Sciences*, 17: 131-143.
- Powell John, H., 1988. The Geology Of The Karak Area. Amman, The Hashemite Kingdom Of Jordan, Geological Mapping Division, Ministry Of Energy And Mineral Resources.
- Pratt, B.R. & Smewing, J.D., 1993. Early Cretaceous Platform-Margin Configuration And Evolution In The Central Oman Mountains, Arabian Peninsula. *American Association Of Petroleum Geologists Bulletin*, 77: 225-244.
- Pratt, B.R. & Smewing, J.D., 1993. Early Cretaceous Platform-Margin Configuration And Evolution In The Central Oman Mountains, Arabian Peninsula. *American Association Of Petroleum Geologists Bulletin*, 77: 225-244.
- Price, S.P. & Scott, B., 1994. Fault-Block Rotations At The Edge Of A Zone Of Continental Extension - Southwest Turkey. *Journal Of Structural Geology*, 16: 381-392.
- Priestley, K., Baker, C. & Jackson, J., 1994. Implications Of Earthquake Focal Mechanism Data For The Active Tectonics Of The South Caspian Basin And Surrounding Regions. *Geophysical Journal International*, 118: 111-141.
- Prodehl, C., 1985. Interpretation Of A Seismic-Refraction Survey Across The Arabian Shield In Western Saudi Arabia. *Tectonophysics*, 111: 247-282.
- Quennell, A.M., 1956. Tectonics Of The Dead Sea Rift. *Proceedings Of The 20th Igc In Mexico*, : 385-403.
- Quennell, A.M., 1958. The Structural And Geomorphic Evolution Of The Dead Sea Rift. *Quarterly Journal Of The Geological Society Of London*, 114: 1-24.

- Quennell, A.M., 1984. The Western Arabia Rift System. In: J.E. Dixon And A.H.F. Robertson (Eds), *The Geological Evolution Of The Eastern Mediterranean*, Blackwell Scientific Publications, Geological Society Of London special Publication 17, 775-788.
- Rebai, S., Philip, H. & Taboada, A., 1992. Modern Tectonic Stress Field In The Mediterranean Region: Evidence For Variation In Stress Directions At Different Scale. *Geophysical Journal International*, 110: 106-140.
- Reches, Z.E. & Schubert, G., 1987. Models Of Post-Miocene Deformation Of The Arabian Plate. *Tectonics*, 6: 707-725.
- Reilinger, R.E., McClusky, S.C., Oral, M.B., King, R.W. & Toksoz, M.N., 1997. Global Positioning System Measurements Of Present-Day Crustal Movements In The Arabia-Africa-Eurasia Plate Collision Zone. *Journal Of Geophysical Research*, 102: 9983-9999.
- Riad, S. & Meyers, H., 1985. Earthquake Catalog For The Middle East Countries 1900-1983. *World Data Center-A For Solid Earth Geophysics* 127p.
- Ricateau, R. & Riche, P.H., 1980. Geology Of The Musandam Peninsula (Sultanate Of Oman) And Its Surroundings. *Journal Of Petroleum Geology*, 3: 139-152.
- Richter, H., Makris, J. & Rihm, R., 1991. Geophysical Observations Offshore Saudi-Arabia - Seismic And Magnetic Measurements. *Tectonophysics*, 198: 297-310.
- Ricou, L.E., 1996. The Plate Tectonic History Of The Past Tethys Ocean. In: A.E.M.N.E. Al. (Eds), *The Ocean Basins And Margins: The Tethys Ocean*, Plenum Press, 8,
- Rigo De Righi, M. & Cortesini, A., 1964. Gravity Tectonics In Foothills Structure Belt Of Southeast Turkey. *American Association Of Petroleum Geologists Bulletin*, 48: 1911-1937.
- Rigo De Righi, M. & Cortesini, A., 1964. Gravity Tectonics In Foothills Structure Belt Of Southeast Turkey. *Bulletin Of The American Association Of Petroleum Geologists*, 48: 1911.
- Rihm, R., Makris, J. & Moller, L., 1991. Seismic Survey In The Northern Red Sea: Asymmetric Crustal Structure. *Tectonophysics*, 198: 279-295.
- Robertson, A., 1987. The Transition From A Passive Margin To An Upper Cretaceous Foreland Basin Related To Ophiolite Emplacement In The Oman Mountains. *Geological Society Of America Bulletin*, 99: 633-653.
- Robertson, A.H.F. & Searle, M.P., 1990. The Northern Oman Tethyan Continental Margin: Stratigraphy, Structure, Concepts And Controversies. In: A.H.F. Robertson, M.P. Searle And A.C. Ries (Eds), *The Geology And Tectonics Of The Oman Region*, The Geological Society,
- Robertson, A.H.F., Clift, P.D., Degnan, P.J. & Jones, G., 1991. Palaeogeographic And Palaeotectonic Evolution Of The Eastern Mediterranean Neotethys. *Palaeogeography, Palaeoclimatology, Palaeoecology*, 87: 289-343.
- Rodgers, A.J., Ni, J., F. & Hearn, T., M., 1997. Propagation Characteristics Of Short-Period Sn And Lg In The Middle East. *Bulletin Of The Seismological Society Of America*, 87: 396-413.
- Rogers, A.J., Ni, J.F. & Hearn, T.M., 1995. Pn, Sn, And Lg Propagation In The Middle East. Ron, H., 1984. Paleomagnetic Investigation Of The Fault Structure Of Galilee - Northern Israel, Hebrew University Of Jerusalem.
- Ron, H., 1987. Deformation Along The Yammuneh, The Restraining Bend Of The Dead Sea Transform: Paleomagnetic Data And Kinematic Implications. *Tectonics*, 6: 653-666.
- Ron, H., Nur, A. & Hofstetter, A., 1990. Late Cenozoic And Recent Strike Slip Tectonics In Mt. Carmel Northern Israel. *Annales Tectonicae*, 4: 70-80.
- Roobol, M.J. & Camp, V.E., 1990. Structural Control Of Young Basaltic Fissure Eruptions In The Plateau Basalt Area Of The Arabian Plate, Northeast Jordan - Comment. *Journal Of Volcanology And Geothermal Research*, 43: 365-366.
- Roperch, P. & Bonhommet, N., 1986. Paleomagnetism Of Miocene Volcanism From South Syria. *Journal Of Geophysics*, 59: 98-102.
- Ross, D.A., Uchupi, E. & White, R.S., 1986. The Geology Of The Iran-Gulf Of Oman Region: A Synthesis. *Reviews Of Geophysics*, 24: 537-556.

- Rotstein, Y. & Kafka, A., 1982. Seismotectonics Of The Southern Boundary Of Anatolia, Eastern Mediterranean Region: Subduction, Collision, And Arc Jumping. *Journal Of Geophysical Research*, 87: 7694-7706.
- Rotstein, Y., 1984. Counterclockwise Rotation Of The Anatolian Block. *Tectonophysics*, 108: 71-91.
- Rotstein, Y. & Ben-Avraham, Z., 1985. Accretionary Processes At Subduction Zones In The Eastern Mediterranean. *Tectonophysics*, 112: 551-561.
- Rotstein, Y. & Ariei, E., 1986. Tectonic Implications Of A Recent Microearthquake Data From Israel And Adjacent Areas. *Earth Planet. Sci. Lett.*, 78: 237-244.
- Rotstein, Y., Yuval, Z. & Trachtman, P., 1987. Deep Seismic Reflection Studies In Israel -- An Update. *Journal Of Geophysical Research*, 89: 389-394.
- Rotstein, Y., 1987. Gaussian Probability Estimate For Large Earthquake Occurrence In The Jordan Valley, Dead Sea Rift. *Tectonophysics*, 6: 653-666.
- Rotstein, Y. & Bartov, Y., 1989. Seismic Reflection Across A Continental Transform: An Example From A Convergent Segment Of The Dead Sea Rift. *Journal Of Geophysical Research*, 94: 2902-2912.
- Sadooni, F.N., 1993. Stratigraphic Sequence, Microfacies, And Petroleum Prospects Of The Yamama Formation, Lower Cretaceous, Southern Iraq. *American Association Of Petroleum Geologists Bulletin*, 77: 1971-1988.
- Sage, L. & Letouzey, J., 1990. Convergence Of The African And Eurasian Plate In The Eastern Mediterranean. convergence Of The African And Eurasian Plate In The Eastern Mediterranean. In: J. Letouzey (Eds), *Petroleum And Tectonics In Mobile Belts; Proceedings Of The Ifp Exploration And Production Research Conference*, Editions Technip, 49-68.
- Said, R., 1962. *The Geology Of Egypt*. Elsevier
- Saikia, C.K., 1994. Modeling Of Strong Ground Motions From The 16 September 1978 Tabas, Iran, Earthquake. *Bulletin Of The Seismological Society Of America*, 84: 31-46.
- Saint-Marc, P., 1981. Lebanon. In: (Eds), *Aspects Of Mid-Cretaceous Regional Geology*, 103-131.
- Sakaguchi, Y., 1994. *Rise And Fall Of Palmyra, Syria: Physical - Geographical Considerations*, University Of Tokyo.
- Salamon, A., 1993. Seismotectonic Analysis Of Earthquakes In Israel And Adjacent Areas, Hebrew University Of Jerusalem.
- Salamon, A., Hofstetter, A., Garfunkel, Z. & Ron, H., 1996. Seismicity Of The Eastern Mediterranean Region: Perspective From The Sinai Subplate. *Tectonophysics*, 263: 293-305.
- Salel, J.F. & Seguret, M., 1994. Late Cretaceous To Palaeogene Thin-Skinned Tectonics Of The Palmyrides Belt (Syria). *Tectonophysics*, 234: 265-290.
- Savostin, L.A., Sibuet, J.-C., Zonenshain, L.P., Pichon, X.L. & Roulet, M.-J., 1986. Kinematic Evolution Of The Tethys Belt From The Atlantic Ocean To The Pamirs Since The Triassic. *Tectonophysics*, 123: 1-35.
- Sawaf, T., Zaza, T. & Sarriyah, O., 1988. The Distribution And Litho-Stratigraphic Base For The Sedimentary Formations In The Syrian Arab Republic. Damascus, Syria, Syrian Petroleum Company.
- Sawaf, T., Al-Saad, D., Gebran, A., Barazangi, M., Best, J.A. & Chaimov, T., 1993. Structure And Stratigraphy Of Eastern Syria Across The Euphrates Depression. *Tectonophysics*, 220: 267-281.
- Sayyab, A. & Valek, R. (1968). Patterns And General Properties Of The Gravity Field Of Iraq. XXIII International Geological Congress, Prague.
- Sbeinati, M.R., Darawchah, R. & Mouty, M., Field Archaeological Evidences Of Seismic Effects In Syria. Review Of Historical Seismicity In Europe (Materials Of The Cec Project), 2: 195.
- Schamel, S. & Resselar, R., 1986. Intraplate Shear: The Cause Of The Syrian Arc Fold Belt [Abs.]. In: Geological Society Of America Abstracts With Programs, Geological Society Of America, Annual Meeting, San Antonio, Texas, November 10-13, 740.
- Sclater, J.G. & Christie, P.A.F., 1980. Continental Stretching: An Explanation Of The Post-Mid-Cretaceous Subsidence Of The Central North Sea Basin. *Journal Of Geophysical Research*, 85: 3711-3739.

- Scott, B., 1981. The Eurasian-Arabian And African Continental Margin From Iran To Greece. *Journal Of The Geological Society Of London*, 138: 719-733.
- Searle, M.P., 1994. Structure Of The Intraplate Eastern Palmyride Fold Belt, Syria. *Geological Society Of America Bulletin*, 106: 1332-1350.
- Seber, D., Barazangi, M., Chaimov, T., Al-Saad, D., Sawaf, T. & Khaddour, M., 1992. Geometry And Velocity Structure Of The Palmyride Fold-Thrust Belt And Surrounding Arabian Platform In Syria. *Bulletin Of Earth Sciences, Cukurova University, Adana, Turkey*, 20: 103-110.
- Seber, D. & Mitchell, B.J., 1992. Attenuation Of Surface Waves Across The Arabian Peninsula. *Tectonophysics*, 204: 137-150.
- Seber, D., Barazangi, M., Chaimov, T., Al-Saad, D., Sawaf, T. & Khaddour, M., 1993. Upper Crustal Velocity Structure And Basement Morphology Beneath The Intracontinental Palmyride Fold-Thrust Belt And North Arabian Platform In Syria. *Geophysical Journal International*, 113: 752-766.
- Sengor, A.M.C. & Kidd, W.S.F., 1979. Post-Collisional Tectonics Of The Turkish-Iranian Plateau And A Comparison With Tibet. *Tectonophysics*, 55: 361-376.
- Sengor, A.M.C., Burke, K. & Dewey, J., 1980. Tectonics Of The North Anatolian Transform Fault. *tectonics Of The North Anatolian Transform Fault*. In: A.M. Isikara And A. Vogel (Eds), *Multidisciplinary Approach To Earthquake Prediction*, Freidr. Vieweg And Sohn, 3-22.
- Sengor, A.M.C. & Yilmaz, Y., 1981. Tethyan Evolution Of Turkey: A Plate Tectonic Approach. *Tectonophysics*, 75: 181-241.
- Sengor, A.M.C., Gorurand, N. & Saroglu, F., 1984. Strike-Slip Faulting And Related Basin Formation In Zones Of Tectonic Escape: Turkey As A Case Study. In: K.T. Biddle And N. Christie-Blick (Eds), *Strike-Slip Deformation, Basin Formation And Sedimentation*, Society Of Economic Paleontologists And Mineralogists, Special Publication, 37, 227-264.
- Serva, L., Brunamonte, F., Michetti, A.M. & Vittori, E., The Role Of Neotectonic And Palaeoseismic Data In Seismic Hazard Analyses: Case Studies From Central Italy And Middle East. .
- Seyitoglu, G. & Scott, B., 1991. Late Cenozoic Crustal Extension And Basin Formation In West Turkey. *Geological Magazine*, 128: 155-166.
- Seyitoglu, G., Scott, B.C. & Rundle, C.C., 1992. Timing Of Cenozoic Extensional Tectonics In West Turkey. *Journal Of The Geological Society Of London*, 149: 533-538.
- Seyitoglu, G. & Scott, B.C., 1994. Late Cenozoic Basin Development In West Turkey - Gordes Basin Tectonics And Sedimentation. *Geological Magazine*, 131: 631-637.
- Shalem, N., 1952. La Seismicite Au Levant. *Bulletin Res. Coun. Israel*, 2: 1-16.
- Shapira, A., 1979. Redetermined Magnitudes Of Earthquakes In The Afro-Eurasian Junction. *Israel Journal Of Earth Science*, 28: 107-109.
- Shapira, A. & Feldman, L., 1987. Microseismicity Of Three Locations Along The Jordan Rift. *Tectonophysics*, 141: 89-94.
- Shapira, A., 1990. Increasing Seismicity As An Earthquake Precursor In Israel. *Geophysical Journal International*, 101: 203-211.
- Shapira, A. & Hofstetter, A., 1993. Source Parameters And Scaling Relationships Of Earthquakes In Israel. *Tectonophysics*, 217: 217-226.
- Shapira, A., Avni, R. & Nur, A., 1993. Note: A New Estimate For The Epicenter Of The Jericho Earthquake Of 11 July 1927. *Israel Journal Of Earth Science*, 42: 93-96.
- Sharief, F.A., 1982. Lithofacies Distribution Of The Permian-Triassic Rocks In The Middle East. *Journal Of Petroleum Geology*, 4: 299-310.
- Sharp, I.R., Ustaomer, T., Degnan, P., Robertson, A.H.F. & Dixon, J.E., 1991. A Two Day Informal Workshop On The Evolution Of The Tethyan Belt, Tethyan Workshop. The Grant Institute Department Of Geology And Geophysics Edinburgh:

- Shelton, A.W., 1990. The Interpretation Of Gravity Data In Oman: Constraints On The Ophiolite Emplacement Mechanism. In: A.H.F. Robertson, M.P. Searle And A.C. Ries (Eds), *The Geology And Tectonics Of The Oman Region*, The Geological Society, 846.
- Shmuel, M. & Ron, H., 1996. Long-Term Earthquake Clustering: A 50,000-Year Paleoseismic Record In The Dead Sea Graben. *Journal Of Geophysical Research*, 101: 6179-6191.
- Shoja-Taheri, J. & Niazi, M., 1981. Seismicity Of The Iranian Plateau And Bordering Regions. *Bulletin Of The Seismological Society Of America*, 71: 477-489.
- Simms, S.C., 1994. Structural Style Of Recently Discovered Oil Fields, Central Saudi Arabia. structural Style Of Recently Discovered Oil Fields, Central Saudi Arabia. In: M. Al-Husseini (Eds), *Geo '94, The Middle East Petroleum Geosciences*, Gulf Petrolink, 1, 861-866.
- Smith, A., Taymaz, T. & Al., E., 1995. High Resolution Seismic Profiling In The Sea Of Marmara (Nw Turkey): Late Quaternary Sedimentation And Sea-Level Changes. *Bulletin Of Geological Society Of America*, 107: 923-936.
- Snyder, D.B. & Barazangi, M., 1985. Deep Crustal Structure And Flexure Of The Arabian Plate Beneath The Zagros Collisional Mountain Belt As Inferred From Gravity Observations [Abstract]. *Eos, Transactions, American Geophysical Union*, 66: 1074.
- Snyder, D.B. & Barazangi, M., 1986. Deep Crustal Structure And Flexure Of The Arabian Plate Beneath The Zagros Collisional Mountain Belt As Inferred From Gravity Observations. *Tectonics*, 5: 361-373.
- Soller, D.R., Ray, R.D. & Brown, R.D., 1982. A New Global Crustal Thickness Map. *Tectonics*, 1: 125-149.
- Spakman, W., 1991. Delay-Time Tomography Of The Upper Mantle Below Europe, The Mediterranean, And Asia Minor. *Geophysical Journal International*, 107: 309-332.
- Stahl, P. & Plassard, J., 1954. *Carte Gravimetrique Du Liban*, Ministere Des Travaux Publics, Republique Libanise.
- Stein, R.S., Barka, A. & Dieterich, J.H., 1997. Progressive Failure On The North Anatolian Fault Since 1939 By Earthquake Stress Triggering. *Geophysical Journal International*, 128: 594-604.
- Stern, R.J., 1985. The Najd Fault System, Saudi Arabia And Egypt: A Late Precambrian Rift-Related Transform System? *Tectonics*, 4: 497-511.
- Stocklin, J., 1968. Structural History And Tectonics Of Iran: A Review. *American Association Of Petroleum Geologists Bulletin*, 52: 1229-1258.
- Stocklin, J., 1981. A Brief Report On Geodynamics In Iran. In: H. Gupta And F. Delany (Eds), *Zagros-Hindu Kush-Himalaya Geodynamic Evolution*, American Geophysical Union, *Geodynamics Series* 3, 70-74.
- Stoesser, D.B. & Camp, V.E., 1985. Pan-African Microplate Accretion Of The Arabian Shield. *Geological Society Of America Bulletin*, 96: 817-826.
- Stoneley, R., 1990. The Arabian Continental Margin In Iran During The Late Cretaceous. the Arabian Continental Margin In Iran During The Late Cretaceous. In: A.H.F. Robertson, M.P. Searle And A.C. Ries (Eds), *The Geology And Tectonics Of The Oman Region*, The Geological Society, 846.
- Straub, C. & Kahle, H.-G., 1994. Global Positioning System (Gps) Estimates Of Crustal Deformation In The Marmara Sea Region, Northwestern Anatolia. *Earth And Planetary Science Letters*, 121: 495-502.
- Striem, H.L., 1991. The Association Of Seismicity With Fault Systems In Israel's Southern And Central Offshore, As Exemplified By The Palmahim Structure, Seismological Division, The Institute For Petroleum Research And Geophysics, Holon, Israel.
- Sultan, M., Duncan, I.J., Arvidson, R.E., Stern, R.J. & Others, A., 1990. Extension Of The Najd Shear System From Saudi-Arabia To The Central Eastern Desert Of Egypt Based On Integrated Field And Landsat Observations - Reply. *Tectonics*, 9: 539-543.
- Suzanne, P., Lyberis, N., Chorowicz, J., Nurlu, M., Yurur, T. & Kasapoglu, E., *Geometry Of The North Anatolian Fault From Landsat-Mss Images*. *Bulletin Of Soc. Geol. F.* (In Press), : 1-24.
- Takin, M., 1972. Iranian Geology And Continental Drift In The Middle East. *Nature*, 235: 147-150.

- Taviani, M., Bonatti, E., Colantoni, P. & Piermaria, L.R., 1984. Tectonically Uplifted Crustal Blocks In The Northern Red Sea: Data From The Brothers Islets. *Memorial Society Of Italian Geology*, 27: 47-50.
- Taymaz, T., Jackson, J. & Westaway, R., 1990. Earthquake Mechanisms In The Hellenic Trench Near Crete. *Geophysical Journal International*, 102: 695-731.
- Taymaz, T., Eyidogan, H. & Jackson, J.A., 1991. Source Parameters Of Large Earthquakes In The East Anatolian Fault Zone (Turkey). *Geophysical Journal International*, 106: 537-550.
- Taymaz, T., Jackson, J. & Mckenzie, D., 1991. Active Tectonics Of The North And Central Aegean Sea. *Geophysical Journal International*, 106: 433-490.
- Taymaz, T., 1992. Observations On Source Time Functions Of Earthquakes Obtained From Inversion Of Teleseismic Body Waveforms. *Geophysical Journal International*, 108: 273-280.
- Taymaz, T. & Price, S., 1992. The 1971 May 12 Burdur Earthquake Sequence, Sw Turkey: A Synthesis Of Seismological And Geological Observations. *Geophysical Journal International*, 108: 589-603.
- Taymaz, T., 1993. The Source Parameters Of Cubukdag (Western Turkey) Earthquake Of 11 October 1986. *Geophysical Journal International*, 113: 260-267.
- Tchalenko, J.S. & Braud, J., 1974. Seismicity And Structure Of The Zagros (Iran): The Main Recent Fault Between 33 And 35N. *Philosophical Transactions Royal Society London*, 272: 1-25.
- Tchalenko, J.S. & Berberian, M., 1975. Dasht-E-Bayaz Fault, Iran: Earthquake And Earlier Related Structures In Bedrock. *Geological Society Of America Bulletin*, 86: 703-709.
- Ten Brink, U.S. & Ben-Avraham, Z., 1989. The Anatomy Of A Pull-Apart Basin: Seismic Reflection Observations Of The Dead Sea Basin. *Tectonics*, 8: 333-350.
- Ten Brink, U.S., Schoenberg, N., Kovach, R.L. & Ben-Avraham, Z., 1990. Uplift And A Possible Moho Offset Across The Dead Sea Transform. *Tectonophysics*, 180: 71-85.
- Ten Brink, U.S., Ben-Avraham, Z., Bell, R.E., Hassouneh, M., Coleman, D.F., Andreasen, G., Tibor, G. & Coakley, B., 1993. Structure Of The Dead Sea Pull-Apart Basin From Gravity Analyses. *Journal Of Geophysical Research*, 98: 21,877-21,894.
- Tibor, 1975. Contribution To The Geology Of Shaqlawa-Harir Area. *Journal Of The Geological Society Of Iraq*, Special Issue: 55-67.
- Tibor, G. & Benavraham, Z., 1992. Late Tertiary Seismic Facies And Structures Of The Levant Passive Margin Off Central Israel, Eastern Mediterranean. *Marine Geology*, 105: 253-273.
- Tinkler, C., Wagner, J.J., Delaloye, M. & Selcuk, H., 1981. Tectonic History Of The Hatay Ophiolites (South Turkey) And Their Relation With The Dead Sea Rift. *Tectonophysics*, 72: 23-41.
- Toprak, V. & Goncuoglu, M.C., 1993. Tectonic Control On The Development Of The Neogene Quaternary Central Anatolian Volcanic Province, Turkey. *Geological Journal*, 28: 357-369.
- Trifonov, V.G., Trubikhin, V.M., Adzhanyan, Z., Dzhallad, S., El' Khair, Y. & Ayed, K., 1991. Levant Fault Zone In Northeast Syria. *Geotectonics*, 25: 145-154.
- Trifonov, V.G., Karakhanian, A.S. & Kozhurin, A.I., 1994. Major Active Faults Of The Collision Area Between The Arabian And The Eurasian Plates. In: B.A. Bolt And R. Amirbekian (Eds), *Continental Collision Zone Earthquakes And Seismic Hazard Reduction*, National Survey Of Seismic Protection Under The Government Of The Republic Of Armenia.
- Trifonov, V.G., Karakhanian, A.S., Assaturian, A.O. & Ivanova, T.P., 1994. Relationship Of Earthquakes And Active Faults In Anatolia, The Lesser Caucasus And The Middle East. In: B.A. Bolt And R. Amirbekian (Eds), *Continental Collision Zone Earthquakes And Seismic Hazard Reduction*, National Survey Of Seismic Protection Under The Government Of The Republic Of Armenia.
- Tromp, S.W., 1949. Blockfolding Phenomena In The Middle East. *Geologie En Mijnbouw*, 9: 273-278.
- Turcotte, D.L. & Schubert, G., 1982. *Geodynamics: The Applications Of Continuum Mechanics To Geological Problems*. John Wiley & Sons New York.
- Turcotte, D.L., 1983. Mechanisms Of Crustal Deformation. *Journal Of The Geological Society Of London*, 140: 701-724.

- Turcotte, T. & Ariei, E., 1986. Catalog Of Earthquakes In And Around Israel, Nuclear Power Plant - Shivta Site, The Israel Electric Corporation Ltd.
- Turkelli, N., 1995. Monitoring Of Earthquake Activity In Turkiye. *Bulletin Of Iisee*, 29: 191-208.
- Tuysuz, O., 1990. Tectonic Evolution Of A Part Of The Tethyside Orogenic Collage - The Kargi Massif, Northern Turkey. *Tectonics*, 9: 141-160.
- Tuysuz, O., Dellaloglu, A.A. & Terzioglu, N., 1995. A Magmatic Belt Within The Neo-Tethyan Suture Zone And Its Role In The Tectonic Evolution Of Northern Turkey. *Tectonophysics*, 243: 173-191.
- Ustaomer, T. & Robertson, A.H.F., 1993. A Late Palaeozoic Early Mesozoic Marginal Basin Along The Active Southern Continental Margin Of Eurasia - Evidence From The Central Pontides (Turkey) And Adjacent Regions. *Geological Journal*, 28: 219-238.
- Ustaomer, T. & Robertson, A.H.F., 1994. Late Palaeozoic Marginal Basin And Subduction-Accretion - The Palaeotethyan Kure Complex, Central Pontides, Northern Turkey. *Journal Of The Geological Society Of London*, 151: 291-305.
- Vail, J.R., 1985. Pan-African (Late Precambrian) Tectonic Terrains And The Reconstruction Of The Arabian- Nubian Shield. *Geology*, 13: 839-842.
- Van Dongen, P.G., Van Der Voo, R. & Raven, T., 1967. Paleomagnetic Research In The Central Lebanon Mountains And In The Tartous Area (Syria). *Tectonophysics*, 4: 35-53.
- Van Eck, T., 1988. Attenuation Of Coda In The Dead Sea Region. *Bulletin Of The Seismological Society Of America*, 78: 770-779.
- Van Eck, T. & Hofstetter, A., 1989. Microearthquake Activity In The Dead Sea Region. *Geophysical Journal International*, 99: 605-620.
- Van Eck, T. & Hofstetter, A., 1990. Fault Geometry And Spatial Clustering Of Microearthquakes Along The Dead Sea - Jordan Rift Fault Zone. *Tectonophysics*, 180: 15-27.
- Van Eck, T. & Hofstetter, A., 1990. Fault Geometry And Spatial Clustering Of Microearthquakes Along The Dead Sea-Jordan Rift Fault Zone. *Tectonophysics*, 180: 15-27.
- Vanderbeek, J.W., 1994. Introduction To Exploration In The Gulf Of Suez. introduction To Exploration In The Gulf Of Suez. In: S.M. Landon (Eds), *Interior Rift Basins*, American Association Of Petroleum Geologists Memoir, 39, 7-8.
- Vered, M. & Striem, H.L., 1976. A Macroseismic Study Of The July 1, 1927 Earthquake, Israel Atomic Energy Commission Licensing Division.
- Vered, M., 1978. The Probable Maximum Earthquake Magnitude Associated With The Jordan Rift. *Israel Journal Of Earth Science*, 27: 82-84.
- Visser, W., 1991. Burial And Thermal History Of Proterozoic Source Rocks In Oman. *Precambrian Research*, 54: 15-36.
- Vita-Finzi, C., 1978. 14c Deformation Chronologies In Coastal Iran. *Journal Geological Society London*, 144: 553-560.
- Vita-Finzi, C., 1979. Rates Of Holocene Folding In The Coastal Zagros Near Bandar Abbas, Iran. *Nature*, 278: 632-634.
- Vroman, A., 1973. Is A Compromise Between The Theories Of Tension And Of Shear For The Origin Of The Jordan-Dead Sea Trench Possible? *Israel Journal Of Earth-Sciences*, 22: 141-156.
- Walley, C., 1988. A Braided Strike-Slip Model For The Northern Continuation Of The Dead Sea Fault And Its Implications For Levantine Tectonics. *Tectonophysics*, 145: 63-72.
- Wdowinski, S. & Zilberman, E., 1996. Kinematic Modelling Of Large Scale Structural Asymmetry Across The Dead Sea Rift. *Tectonophysics*, 266: 187-201.
- Wdowinski, S. & Zilberman, E., 1997. Systematic Analyses Of The Large-Scale Topography And Structure Across The Dead Sea Rift. *Tectonics*, 16: 409-424.
- Weissbrod, T., 1976. The Permian In The Near East. In: H. Falke (Eds), *The Continental Permian In Central, West, And South Europe*, D. Reidel Publishing Co., 200-214.
- Westaway, R., 1990. Block Rotation In Western Turkey .1. Observational Evidence. *Journal Of Geophysical Research-Solid Earth And Planets*, 95: 19857-19884.

- Westaway, R., 1992. Kinematics Of The Middle East And Eastern Mediterranean. *Earth And Planetary Science Letters* (Submitted), .
- Westaway, R., 1993. Neogene Evolution Of The Denizli Region Of Western Turkey. *Journal Of Structural Geology*, 15: 37-53.
- Westaway, R., 1994. Evidence For Dynamic Coupling Of Surface Processes With Isostatic Compensation In The Lower Crust During Active Extension Of Western Turkey. *Journal Of Geophysical Research-Solid Earth*, 99: 20203-20223.
- Westaway, R., 1994. Present-Day Kinematics Of The Middle East And Eastern Mediterranean. *Journal Of Geophysical Research*, 99: 12,071-12,090.
- Willis, B., 1928. Earthquakes In The Holy Land. *Bulletin Of The Seismological Society Of America*, 18: 72-103.
- Windley, B.F., Whitehouse, M.J. & Ba-Bttat, M.A.O., 1996. Early Precambrian Gneiss Terranes And Pan-African Island Arcs In Yemen: Crustal Accretion Of The Eastern Arabian Shield. *Geology*, 24: 131-134.
- Winter, T., Avouac, J.-P. & Lavenu, A., 1993. Late Quarternary Kinematics Of The Pallatanga Strike-Slip Fault (Central Ecuador) From Topographic Measurements Of Displaced Morphological Features. *Geophysical Journal International*, 115: 905-920.
- Woodside, J.M., 1977. Tectonic Elements And Crust Of The Eastern Mediterranean. *Marine Geophysics*, 3: 317-354.
- Wu, F.T., Karcz, I., Ariei, E., Kafri, U. & Peled, U., 1973. Microearthquakes Along The Dead Sea Rift. *Geology*, 1: 159-161.
- Wyllie, M.R., Gregory, A.R. & Gardner, G.H.F., 1958. An Experimental Investigation Of Factors Affecting Elastic Wave Velocities In Porous Media. *Geophysics*, 23.
- Yaroshenko, O.P. & Bach Imam, I., 1994. Palynology Of The Lower Permian Deposits In Northeastern Syria. *Stratigraphy And Geological Correlation*, 2: 56-67.
- Yaroshenko, O.P. & Imam, I.B., 1995. Age Variability Of Palynomorph Compositions Of The Middle And Late Triassic Of Syria And Their Relation To Climate And Facies. *Stratigraphy And Geological Correlation*, 3: 375-392.
- Yilmaz, P.O. & Maxwell, J.C., 1982. K-Ar Investigations From The Antalya Complex Ophiolites, SW Turkey. *Ofioliti*, 2-3: 527-530.
- Yilmaz, S., Boztug, D. & Ozturk, A., 1993. Geological Setting, Petrographic And Geochemical Characteristics Of The Cretaceous And Tertiary Igneous Rocks In The Hekimhan Hasancelebi Area, North-West Malatya, Turkey. *Geological Journal*, 28: 383-398.
- Yilmaz, Y., 1993. New Evidence And Model On The Evolution Of The Southeast Anatolian Orogen. *Geological Society Of America Bulletin*, 105: 251-271.
- Yilmaz, R., 1995. Seismic Network In Turkiye. *Bulletin Of IISSE*, 29: 209-222.
- Yuval, Z., 1985. Preliminary Results Of A Deep Seismic Reflection Profile From Zohar To Ashqelon. *Israel Geological Society Annual Meeting*, 1985, : 107.
- Yuval, Z. & Rotstein, Y., 1987. Deep Crustal Reflection Survey In Central Israel. *Journal Of Geodynamics*, 8: 17-31.
- Zak, I. & Bendor, Y.K., 1972. Some New Data On The Salt Deposits Of The Dead Sea Area, Israel. some New Data On The Salt Deposits Of The Dead Sea Area, Israel. In: (Eds), *Geology Of Saline Deposits, Proceedings Of The Hanover Symposium, 1968, Earth Sciences*, 7, 137-146.
- Zak, I. & Freund, R., 1981. Asymmetry And Basin Migration Of The Dead Sea Rift. *Tectonophysics*, 80: 27-38.
- Zanchi, A. & Angelier, J., 1993. Seismotectonics Of Western Anatolia: Regional Stress Orientation From Geophysical And Geological Data. *Tectonophysics*, 222: 259-274.
- Zijderveld, J.D.A. & Van Der Voo, R., Palaeomagnetism In The Mediterranean Area. *palaeomagnetism In The Mediterranean Area*. In: 133-161.

- Zoback, M.L., 1992. First- And Second-Order Patterns Of Stress In The Lithosphere: The World Stress Map Project. *Journal Of Geophysical Research*, 97: 11703-11728.
- Zwain, J.A. & Majeed, B.S., 1988. Structural Analysis Of Fracturing In Sinjar Anticline Using Remote Sensing Technique. *Technical Papers Of The American Society Of Photogrammetry*, 4: 181-190.

2. References for North Africa

- Abdel-Monem, A.A., And M.A. Heikel (1981). Major Element Composition, Magma Type And Tectonic Environment Of The Mesozoic To Recent Basalts, Egypt: A Review, *Bulletin Of The Faculty Earth Sciences, Assiut University*, 4, 121-148.
- Abdel-Rahman, E.M., And R.I. Rizkalla (1984). Crustal Structure Of The Northern Western Desert Of Egypt As Derived From Gravity Data, *Bulletin Of The Faculty Of Science, Assiut University*, 52, 601-615.
- Adams, R.D., And M. Barazangi (1984). Seismotectonics And Seismology In The Arab Region; A Brief Summary And Future Plans, *Bulletin Of The Seismological Society Of America*, 74, 1011-1030.
- Ait Brahim, L., (1990). Role Of The Atlasic Trends In The Neotectonic And Present Evolution Of The Rif And Its Foreland (Morocco) In *Structure And Evolution Of The Atlas Mountain System In Morocco*, Berlin, 1990, 42.
- Ait Brahim, L., And P. Chotin (1990). Oriental Moroccan Neogene Volcanism And Strike-Slip Faulting, *Journal Of African Earth Sciences*, 11, 273-280.
- Ait Brahim, L., P. Chotin, B. Tadili, And M. Ramdani, (1990). The Targuist Seismogenic Zone And Its Relation With The Thrust Front Of The External Domain On The Foreland (Rif, Morocco) In *Structure And Evolution Of The Atlas Mountain System In Morocco*, Berlin, 1990, 43.
- Ait Brahim, L., P. Chotin, B.A. Tadili, And M. Ramdani (1990). Failles Actives Dans Le Rif Central Et Oriental (Maroc), *C. R. Acad. Sci. Paris*, 310, 1123-1129.
- Ait Brahim, L., (1991). *Tectoniques Cassantes Et Etats De Contraintes Recents Au Nord Du Maroc*, L'universite Mohammed V, Rabat, 244 Pp.
- Akinci, A., E. Delpezzo, And J.M. Ibanez (1995). Separation Of Scattering And Intrinsic Attenuation In Southern Spain And Western Anatolia (Turkey), *Geophysical Journal International*, 121, 337-353.
- Albritton, C.C., J.E. Brooks, B. Issawi, And A. Swedan (1990). Origin Of The Qattara Depression, Egypt, *Geological Society Of America Bulletin*, 102, 952-960.
- Allam, A., And H. Khalil (1989). Geology And Stratigraphy Of Gebel-Qabeliat Area, Southwestern Sinai, Egypt, *Journal Of African Earth Sciences And The Middle East*, 9, 59-67.
- Allerton, S., L. Lonergan, J.P. Platt, E.S. Platzman, And E. McClelland (1993). Palaeomagnetic Rotations In The Eastern Betic Cordillera, Southern Spain, *Earth And Planetary Science Letters*, 119, 225-241.
- Alonso, B., And A. Maldonado (1992). Plio-Quaternary Margin Growth Patterns In A Complex Tectonic Setting: Northeastern Alboran Sea, *Geo-Marine Letters*, 12, 137-143.
- Ambraseys, N.N., And R.D. Adams (1986). Seismicity Of West Africa, *Annales Geophysicae*, 4, 679-702.
- Ammar, A.A., And S.I. Rabie (1992). Schematic Relief Of The Near-Surface And Deep-Seated Magnetic Basement, Using Local-Power Spectra, Gabal El-Erediya Area, Eastern Desert, Egypt, *Journal Of African Earth Sciences And The Middle East*, 14, 147-152.
- Andrieux, J., J.-M. Fontbote, And M. Mattauer (1971). Sur Un Modele Explicatif De L'arc De Gibraltar, *Earth And Planetary Sciences Letters*, 12, 191-198.
- Aoudia, A., And M. Meghraoui (1995). Seismotectonics In The Tell Atlas Of Algeria: The Cavaignac (Abou El Hassan) Earthquake Of 25.08.1922 (M(S) = 5.9), *Tectonophysics*, 248, 263-276.
- Apericio, A., J.M. Mitjavila, V. Araña, And I.M. Villa (1991). La Edad Del Volcanismo De Las Islas Columbretes Grande Y Alborán (Mediterráneo Occidental), *Boletín Geológico Y Minero*, 102-104, 74-82.

- Asebriy, L., J. Bourgois, T.E. Cherkaoui, And A. Azdimousa (1993). [Recent Tectonic Evolution Along The Nekor Fault - Paleogeographic And Structural Importance In The External Rif (Morocco)], *Journal Of African Earth Sciences And The Middle East*, 17, 65-74.
- Asfaw, L.M., (1981). On The Seismicity Of The Western Afar Margin In Proceedings Of The First International Symposium On Crustal Movements In Africa, A.M. Wassef, 1981, 61-83.
- Auzende, J.M., J. Bonnin, And J.L. Olivet (1973). The Origin Of The Western Mediterranean Basin, *Journal Geol. Soc. Lond.*, 129, 607-620.
- Azdimousa, A., And J. Bourgois (1993). The Atlantic-Mediterranean Gateway Via The South Riffian Strait Since The Tortonian: Sequential Stratigraphy Of Neogenic Basins Of Des Trois Fourches (Eastern Rif, Morocco), *Journal Of African Earth Sciences And The Middle East*, 17, 233-240.
- Badawi, H.S., And S.A. Mourad (1994). Observations From The 12 October 1992 Dahshour Earthquake In Egypt, *Natural Hazards*, 10, 261-274.
- Bahmad, A., H. Chariai, A. Djerrari, A.E. Kochri, E.A. Hilali, D. Ratz, T. Saqalli, And A.L.G. Tamain (1982). Remote Sensing Applied To Basement Tectonics Of The Calcareous High Atlas (Morocco), *Photogrammetria*, 37, 131-150.
- Banda, E., A. Udias, S. Mueller, J. Mezcua, M. Boloix, J. Gallart, And A. Aparicio (1983). Crustal Structure Beneath Spain From Deep Seismic Sounding Experiments, *Physics Of The Earth And Planetary Interiors*, 31, 277-280.
- Baraza, J., G. Ercilla, And H.J. Lee (1992). Geotechnical Properties And Preliminary Assessment Of Sediment Stability On The Continental Slope Of The Northwestern Alboran Sea, *Geo-Marine Letters*, 12, 150-156.
- Barazangi, M., (1983). A Summary Of The Seismotectonics Of The Arab Region In Assessment And Mitigation Of Earthquake Risk In The Arab Region, K. Cidlinsky, And B. Rouhban (Editor), Unesco, Paris, France, 1983, 43-58.
- Bayoumi, A.I., And H.I. Lotfy (1989). Modes Of Structural Evolution Of Abu-Gharadig Basin, Western Desert Of Egypt As Deduced From Seismic Data, *Journal Of African Earth Sciences And The Middle East*, 9, 273-287.
- Beauchamp, J., (1988). Triassic Sedimentation And Rifting In The High Atlas (Morocco) In Triassic-Jurassic Rifting, W. Manspeizer (Editor), Elsevier, 1988, 477-497.
- Bedir, M., F. Zargouni, S. Tlig, And C. Bobier (1992). Subsurface Geodynamics And Petroleum Geology Of Transform Margin Basins In The Sahel Of Mahdia And El Jem (Eastern Tunisia), *American Association Of Petroleum Bulletin*, 76, 1417-1442.
- Belazi, H.S. (1989). The Geology Of The Nafoora Oilfield, Sirte Basin, Libya, *Journal Of Petroleum Geology*, 12, 353-366.
- Bellon, H., And R. Brousse (1977). Le Magmatisme Périméditerranéen Occidental. Essai De Synthèse, *Bull. Soc. Géol. France*, 19, 469-480.
- Bellot, A., (1985). Gravimétrie Du Rif Paléozoïque Maroc, These Docteur Ingenieur, Université De Montpellier II, Montpellier, France, 140 Pp.
- Ben Sari, D., (1978). Connaissance Géophysique Du Maroc, L'université Grenoble I Scientifique Et Médicale, Grenoble, France, 262 Pp.
- Ben Sari, D. (1987). Connaissance Géophysique Du Maroc, Centre National De Coordination Et De Planification De La Recherche Scientifique Et Technique 207 Pp, From Cornell Database.
- Ben Sari, D., (1991). Latest Developments Of Seismology In Morocco In Mednet: The Broad-Band Seismic Network For The Mediterranean, E. Boschi, D. Giardini, And A. Morelli (Editor), Istituto Nazionale Di Geofisica, 1991, 502-510.
- Bendhia, H. (1991). Thermal Regime And Hydrodynamics In Tunisia And Algeria, *Geophysics*, 56, 1093-1102.
- Bensaid, M., J. Kutina, A. Mahmood, And M. Saadi (1985). Structural Evolution Of Morocco And New Ideas On Basement Controls Of Mineralization, *Global Tectonics And Metallogeny*, 3, 59-69.
- Bergerat, F. (1987). Stress Fields In The European Platform At The Time Of Africa-Eurasia Collision, *Tectonics*, 6, 99-132.

- Bezzeghoud, M., A. Ayadi, A. Sebai, And H. Benhallou (1993). Seismogenic Zone Survey By Algerian Telemetered Seismological Network Case-Study Of Rouina Earthquake January 19, 1992 $M=5.2$, *Physics Of The Earth And Planetary Interiors*.
- Black, R., And J. Fabre, (1983). A Brief Outline Of The Geology Of West Africa In *West Africa: Geological Introduction And Stratigraphic Terms*, J. Fabre (Editor), Pergamon Press, Oxford, 1983, 17-26.
- Blanco, M.J., And W. Spakman (1993). The P-Wave Velocity Of The Mantle Below The Iberian Peninsula: Evidence For Subducted Lithosphere Below Southern Spain, *Tectonics*, 221, 13-34.
- Bobier, C., C. Viguier, A. Chaari, And A. Chine (1991). The Post-Triassic Sedimentary Cover Of Tunisia - Seismic Sequences And Structure, *Tectonophysics*, 195, 371+.
- Boccaletti, M., G. Cello, And L. Tortorici (1988). Structure And Tectonic Significance Of The North-South Axis Of Tunisia, *Annales Tectonicae*, 2, 12-20.
- Bockel, M. (1972). Structure De La Crote In Algerie D'apres Les Ondes Seismiques, *Annales Geofisica*, 25, 339-358.
- Boschi, E., D. Giardini, And A. Morelli (1991). Mednet: The Broad-Band Seismic Network For The Mediterranean, *Istituto Nazionale Di Geofisica*.
- Bosworth, W. (1989). Basin And Range Style Tectonics In East Africa, *Journal Of African Earth Sciences*, 8, 191-201. Bosworth, W., (1995). A High-Strain Rift Model For The Southern Gulf Of Suez (Egypt) In *Hydrocarbon Habitat In Rift Basins*, J.J. Lambaise (Editor), Geological Society, 1995, 75-102.
- Bouillin, J.P., M. Durand-Delga, And P. Olivier Betic-Rifian And Tyrrhenian Arcs : Distinctive Features, Genesis, And Development Stages, .
- Bounif, A., H. Haessler, And M. Meghraoui (1987). The Constantine (Northeast Algeria) Earthquake Of October 27, 1985: Surface Ruptures And Aftershock Study, *Earth And Planetary Science Letters*, V. 85, 451-460.
- Bourgois, J., A. Mauffret, A. Ammar, And A. Demnati (1992). Multichannel Seismic Data Imaging Of Inversion Tectonics Of The Alboran Ridge (Western Mediterranean Sea), *Geo-Marine Letters*, 12, 117-122.
- Brechbuhler, Y.A., R. Bernasconi, And J. Schaer, (1988). Jurassic Sediments Of The Central High Atlas Of Morocco: Deposition, Burial And Erosion History In The Atlas System Of Morocco- Studies On Its Geodynamic Evolution - Lecture Notes In Earth Science, V. Jacobshagen (Editor), Springer-Verlag, Berlin, 1988, 201-215.
- Brede, R., M. Hauptmann, And H.G. Herbig (1992). Plate Tectonics And Intracratonic Mountain Ranges In Morocco - The Mesozoic-Cenozoic Development Of The Central High Atlas And The Middle Atlas, *Geologische Rundschau*, 81, 127-141.
- Broughton, P., And A. Trepanier (1993). Hydrocarbon Generation In The Essaouira Basin Of Western Morocco, *American Association Of Petroleum Geologists Bulletin*, 77, 999-1015.
- Buform, E., A. Udias, And M.A. Colombas (1988). Seismicity, Source Mechanisms And Tectonics Of The Azores-Gibraltar Plate Boundary, *Tectonophysics*, 152, 89-118.
- Buform, E., C. Sanz De Galdeano, And A. Udias (1995). Seismotectonics Of The Ibero-Maghrebian Region, *Tectonophysics*, 248, 247-261.
- Buhl, P., M. Torne, A. Watts, A. Mauffret, And G. Pascal (1990). Wide Aperture Seismic Profiling In The Gulf Of Valencia; Young Moho And Constraints On Modes Of Extension, *Eos, Transactions, American Geophysical Union*, 71, 1634.
- Buness, H., P. Giese, C. Bobier, C. Eva, F. Merlanti, R. Pedone, L. Jenatton, D.T. Nguyen, F. Thouvenot, F. Egloff, J. Makris, A. Lozej, M. Maistrello, S. Scarascia, I. Tabacco, P.F. Burollet, C. Morelli, R. Nicholich, T. Zaghouni, A. Egger, R. Freeman, And S. Mueller (1992). The Egt'85 Seismic Experiment In Tunisia; A Reconnaissance Of The Deep Structures, *Tectonophysics*, 207, 245-267.
- Burollet, P.F. (1991). Structures And Tectonics Of Tunisia, *Tectonophysics*, 195, 359+.
- Cahen, L., And N.J. Snelling (1984). *The Geochronology And Evolution Of Africa*, Clarendon Press, Oxford, 512.

- Caire, A. (1974). Eastern Atlas, In *Mesozoic-Cenozoic Orogenic Belts*, Scottish Academic Press, Edinburgh, 47-59.
- Campbell, A.E., And J. Stafleu (1992). Seismic Modeling Of An Early Jurassic, Drowned Carbonate Platform - Djebel Bou Dahar, High Atlas, Morocco, *American Association Of Petroleum Geologists Bulletin*, 76, 1760-1777.
- Campillo, A.C., M. A., And A. Mauffret (1992). Stratigraphic And Tectonic Evolution Of The Western Alboran Sea: Late Miocene To Recent, *Geo-Marine Letters*, 12, 165-172.
- Campos, J., A. Maldonado, And A.C. Campillo (1992). Post-Messinian Patterns Of The Central Alboran Sea, *Geo-Marine Letters*, 12, 173-178.
- Carmignani, L., S. Giammarino, G. Giglia, And P.C. Pertusati (1990). The Qasr-As-Sahabi Succession And The Neogene Evolution Of The Sirte Basin (Libya), *Journal Of African Earth Sciences And The Middle East*, 10, 753-769.
- Casas, A., And A. Carbo (1990). Deep Structure Of The Betic Cordillera Derived From The Interpretation Of A Complete Bouguer Anomaly Map, *Journal Of Geodynamics*, 12, 137-147.
- Chekhovich, V.D., And L.P. Zonenshayn (1976). Main Features Of Structure And Tectonic Development Of The North African Folded Region In The Mesozoic And Cenozoic, *Geotectonics*, 10, 178-188.
- Cherkaoui, T.-E., D. Hatzfeld, H. Jebli, F. Medina, And V. Caillot (1990). Etude Microsismique De La Région D'al Hoceima, *Bull. Inst. Sci., Rabat*, 14, 25-34.
- Cherkaoui, T.-E., (1991). Contribution A L'etude De L'alea Sismique Au Maroc, Etude Detaillee Du Seisme D'agadir (29/2/1960), Etude De La Microsismicite De La Region D'al-Hoceima, Thèse Docteur Es-Sciences, Université Joseph Fourier, Grenoble, France, 247 Pp.
- Cherkaoui, T.-E., F. Medina, And D. Hatzfeld, (1991). The Agadir Earthquake Of February 29, 1960. Examination Of Some Of The Parameters, In *Seismicity, Seismotectonics And Seismic Risk Of The Ibero-Maghrebian Region* In J. Mezcuca, And A. Udias (Editor), Instituto Geografico Nacional, Madrid, Spain, 1991, 133-148.
- Chihi, L. (1992). Seismotectonic Study In Central And Southern Tunisia, *Tectonophysics*, 209, 175-178.
- Chorowicz, J., E.M. Alem, A. Bahmad, H. Chariai, A. El Kochri, F. Medina, And G. Tamain (1982). Les Anticlinaux Éjectifs Du Haut Atlas: Résultat De Tectoniques Atlasiques Superposées, *C. R. Acad. Sc. Paris*, 294, 271.
- Choubert, G., And A. Faure-Muret, (1974). Moroccan Rif In *Mesozoic-Cenozoic Orogenic Belts*, A. Spencer (Editor), Scottish Academic Press, Edinburgh, 1974, 37-46.
- Choubert, G., And A. Faure-Muret, (1983). Anti-Atlas, In *West Africa: Geological Introduction And Stratigraphic Terms*, J. Fabre (Editor), Pergamon Press, Oxford, 1983, 80-95.
- Church, W.R. (1991). Precambrian Accretionary Tectonics In The Bou-Azzer-El-Graara Region, Anti-Atlas, Morocco - Comment, *Geology*, 19, 285-286.
- Cloetingh, S., P.A. Van Der Beek, D. Van Rees, T.B. Roep, C. Biermann, And R.A. Stephenson (1992). Flexural Interaction And The Dynamics Of Neogene Extensional Basin Formation In The Alboran-Betic Region, *Geo-Marine Letters*, 12, 66-75.
- Cohen, C.R. (1980). Plate Tectonic Model For The Oligo-Miocene Evolution Of The Western Mediterranean, *Tectonophysics*, 68, 283-311.
- Comas, M.C., V. Garcia-Duenas, And M.J. Jurado (1992). Neogene Tectonic Evolution Of The Alboran Sea From Mcs Data, *Geo-Marine Letters*, 12, 157-164.
- Conant, L.C., And G. H.Gondarzi (1967). Stratigraphic And Tectonic Framework Of Libya, *American Association Of Petroleum Geologists Bulletin*, 51, 719-730.
- Console, R., And Rovelli (1981). Attenuation Parameters For The Friuli Region From Strong-Motion Accelerogram Spectra, *Bulletin Of The Seismological Society Of America*, 71, 1981-1991.
- Crespo-Blanc, A., M. Orozco, And V. Garcia-Duenas (1994). Extension Versus Compression During The Miocene Tectonic Evolution Of The Betic Chain. Late Folding Of Normal Fault Systems, *Tectonics*, 13, 78-88.

- Danobeitia, J.J., M. Arguedas, J. Gallart, E. Banda, And J. Makris (1992). Deep Crustal Configuration Of The Valencia Trough And Its Iberian And Balearic Borders From Extensive Refraction And Wide-Angle Reflection Seismic Profiling, *Tectonophysics*, 203, 37-55.
- Dautria, J.M., And A. Lesquer (1989). An Example Of The Relationship Between Rift And Dome - Recent Geodynamic Evolution Of The Hoggar Swell And Of Its Nearby Regions (Central Sahara, Southern Algeria And Eastern Niger), *Tectonophysics*, 163, 45-61.
- Davidson, J.P., And Ian R. Wilson, ,, (1989). Evolution Of An Alkali Basalt-Trachyte Suite From Jebel Marra Volcano, Sudan, Through Assimilation And Fractional Crystallization, *Earth And Planetary Science Letters*, 95, 141-160.
- Deffontaines, B., P. Chotin, L.A. Brahim, And M. Rozanov (1992). Investigation Of Active Faults In Morocco Using Morphometric Methods And Drainage Pattern Analysis, *Geologische Rundschau*, 81, 199-210.
- Demnati, A. (1972). Krustenstruktur In Rif-Bereich Von Nord-Marokko Aus Gravimetrischen Und Aeromagnetischen Regionalmessungen, *Bollettino Di Geofisica Teorica Ed Applicata*, 14, 203-236.
- Dennison, B., And V.N. Mansfield (1976). Proterozoic Oceanic Crust At Bou Azzer, *Nature*, 261, 34-35.
- Dercourt, J., L.P. Zonenshain, L.-E. Ricou, V.G. Kazmin, X. Lepichon, A.L. Knipper, C. Grandjacquet, I.M. Shoroshikov, J. Geyssant, C. Lepvrier, D.H. Pechersky, J. Boulain, J.-C. Sibuet, L.A. Savostin, O. Sorokhtin, M. Westphal, M.L. Bazhenov, J.P. Lauer, And B. Biju-Duval (1986). Geological Evolution Of The Tethys Belt From The Atlantic To The Pamirs Since The Lias, *Tectonophysics*, 123, 241-315.
- Dewey, J.F., W.C. Pitman, W.B.F. Ryan, And J. Bonnin (1973). Plate Tectonics And The Evolution Of The Alpine System, *Bull. Geological Society Of America*, 84, 3137-3180.
- Dewey, J., M. Helman, E. Turco, D. Hutton, And S. Knott, (1989). Kinematics Of The Western Mediterranean In Alpine Tectonics, M. Coward, D. Dietrich, And R. Park (Editor), *Royal Geological Society, Oxford*, 1989, 265-283.
- Diot, H., And J.-L. Bouchez (1991). Structure Des Massifs Granitiques De La Meseta Marocaine, Marquers Geodynamiques: Aouli-Bou-Mia (Haute-Moulouya), Zaër (Massif Central) Et Sebt De Brikiine (Rehamna), *Géologie Méditerranéenne*, 18, 81-97.
- Dlala, M. (1992). Seismotectonic Study In Northern Tunisia, *Tectonophysics*, 209, 171-174.
- Doblas, M., And R. Oyarzun (1989). Neogene Extensional Collapse In The Western Mediterranean (Betic-Rif Alpine Orogenic Belt): Implications For The Genesis Of The Gibraltar Arc And Magmatic Activity, *Geology*, 17, 430-433.
- Docherty, J.I.C., And E. Banda (1992). A Note On The Subsidence History Of The Northern Margin Of The Alboran Basin, *Geo-Marine Letters*, 12, 82-87.
- Docherty, C., And E. Banda (1995). Evidence For The Eastward Migration Of The Alboran Sea Based On Regional Subsidence Analysis: A Case For Basin Formation By Delamination Of The Subcrustal Lithosphere?, *Tectonics*, 14, 804-818.
- Dresnay, R.D. (1971). Extension Et Development Des Phenomenes Recifaux Jurassiques Dans Le Domaine Atlasique Marocain, Particulierement Au Lias Moyen., *Bull. Soc. Geol*, 13, 46-56.
- Dresnay, R., (1988). Recent Data On The Geology Of The Middle-Atlas (Morocco) In The Atlas System Of Morocco, V. Jacobshagen (Editor), *Springer-Verlag, Berlin*, 1988, 293-320.
- Durand-Delga, M., And P. Olivier (1988). Evolution Of The Alboran Block Margin From Early Mesozoic To Early Miocene Time, The Atlas System Of Morocco, 15, 465-480.
- Düringer, P., M. Ais, And A. Chahi (1995). Geodynamic Context And Depositional Sedimentary Environment Of The Miocene Stevensite (Rhassoul) Of Morocco: Lacustrine Or Evaporitic Environment?, *Bull. Soc. Geol. Fr.*, 2.
- Ellella, R.A. (1990). Maturation History Of Neogene-Quaternary Sediments, Nile Delta Basin, Egypt, *American Association Of Petroleum Bulletin*, 74, 77-84.
- Elmrabet, T., A. Levret, M. Ramdani, And B. Tadili, (1991). Historical Seismicity In Morocco: Methodological Aspects And Cases Of Multidisciplinary Evaluation In Seismicity,

- Seismotectonics And Seismic Risk Of The Ibero-Maghrebian Region, J. Mezcua, And A. Udias (Editors), Instituto Geografico Nacional, Madrid, Spain, 1991, 115-129.
- Elsayed, A., R. Wahlstrom, And O. Kulhanek (1994). Seismic Hazard Of Egypt, *Natural Hazards*, 10, 247-259.
- Elsirafe, A.M., And S.I. Abie (1990). Contribution Of Aeromagnetism To Structural Mapping Of Gabal Gattar Area, North Eastern Desert, Egypt, *Journal Of African Earth Sciences And The Middle East*, 11, 119-128.
- Ercilla, G., B. Alonso, And J. Baraza (1992). Sedimentary Evolution Of The Northwestern Alboran Sea During The Quaternary, *Geo-Marine Letters*, 12, 144-149.
- Fauremuret, A., J.L. Morel, M. Dahmani, And M. Demnati (1990). Morocco, African Promontory Between The Mediterranean And The Atlantic - Rabat, Morocco, 27 April 11 May 1990, *Episodes*, 13, 277-278.
- Ferrucci, F., G. Gaudiosi, N.A. Pino, G. Luongo, A. Hirn, And L. Mirabile (1989). Seismic Detection Of A Major Moho Upheaval Beneath The Campania Volcanic Area (Naples, Southern Italy), *Geophysical Research Letters*, 16, 1317-1320.
- Fetah, S.E.M., M. Bensaid, And M. Dahmani (1987). Carte Géologique Du Rif, Rouadi, Editions Du Service Geologique Du Maroc.
- Fraissinet, C., E.M. Zouine, J.L. Morel, A. Poisson, J. Andrieux, And A. Faure-Muret, (1988). Structural Evolution Of The Southern And Northern Central High Atlas In Paleogene And Mio-Pliocene Times In The Atlas System Of Morocco, V. Jacobshagen (Editor), Springer-Verlag, Berlin, 1988, 273-291.
- Frei, L.S., And R. Freund (1990). Spatial And Temporal Relationships Between Two Sets Of Strike-Slip Faults In Southeastern Sinai, *Tectonophysics*, 180, 111-122.
- Frizon De Lamotte, D. (1982). Contribution À L'étude De L'évolution Structurale Du Rif Oriental, *Notes Et Memoires Du Service Geologique*, 314, 7-238.
- Froitzheim, N., J. Stets, And P. Wurster, (1988). Aspects Of Western High Atlas Tectonics, In The Atlas System Of Morocco In V. Jacobshagen (Editor), Springer-Verlag, Berlin, 1988, 219-244.
- Gaffet, S., B. Massinon, J.-L. Plantet, And Y. Cansi (1994). Modelling Local Seismograms Of French Nuclear Test In Taourirt Tan Afella Massif, Hoggar, Algeria, *Geophysical Journal International*, 119, 964-974.
- Galdeano, A., V. Courtillot, E. Le Borgne, J.L. Le Mouel, And J.C. Rossignol (1974). An Aeromagnetic Survey Of The Southwest Of The Western Mediterranean: Description And Tectonic Implications, *Earth And Planetary Science Letters*, 23, 323-336.
- Garcia-Duenas, V., J.C. Balanya, And J.M. Martinez-Martinez (1992). Miocene Extensional Detachments In The Outcropping Basement Of The Northern Alboran Basin (Betics) And Their Tectonic Implications, *Geo-Marine Letters*, 12, 88-95.
- Geiss, E. (1987). A New Compilation Of Crustal Thickness Data For The Mediterranean Area, *Annales Geophysicae, Series B: Terrestrial And Planetary Physics*, 5, 623-630.
- Gensous, B., M. Tesson, And E. Winnock (1986). La Marge Meridionale De La Mer D'alboran: Caracteres Structuro-Sedimentaires Et Evolution Recente, *Marine Geology*, 72, 341-370.
- Giardini, D., E. Boschi, S. Mazza, A. Morelli, D.B. Sari, D. Najid, H. Benhallou, M. Bezzeghoud, H. Trabelsi, M. Hfaïdh, R.M. Kebeasy, And E.M. Ibrahim (1992). Very-Broad-Band Seismology In Northern Africa Under The Mednet Project, *Tectonophysics*, 209, 17-30.
- Giardini, D., E. Boschi, And B. Palombo (1993). Moment Tensor Inversion From Mednet Data (2) Regional Earthquakes Of The Mediterranean, *Geophysical Research Letters*, 20, 273-276.
- Giermann, G., M. Pfannenstiel, And W. Wimmenauer (1964). Relations Entre Morphologie, Tectonique Et Volcanisme En Mer D'alboran (Méditerranée Occidentale). Résultats Préliminaires De La Campagne Jean-Charcot (1967), *Comptes Rendu De La Société Géologique Du France*, 4, 116-118.
- Giese, P., V. Haak, V. Jacobshagen, And K.J. Reutter (1987). Mobilization Of A Continental Margin; A Subduction-Induced Process, *Forschung (Boppard)*, 16, 115-134.

- Giese, P. (1990). Structure And Evolution Of The Atlas Mountain System In Morocco And Structure And Evolution Of The Central Andes In Northern Chile, Southern Bolivia And Northwestern Argentina, 104.
- Giese, P., And V. Jacobshagen (1992). Inversion Of Intracontinental Ranges: High And Middle Atlas, *Geologische Rundschau*, 81, 249-259.
- Gindy, A.R. (1991). Origin Of The Qattara Depression, Egypt - Discussion, *Geological Society Of America Bulletin*, 103, 1374-1375.
- Grimson, N.L., And W. Chen (1986). The Azores-Gibraltar Plate Boundary: Focal Mechanism, Depths Of Earthquakes And Their Tectonic Implications, *Journal Of Geophysical Research*, 92, 2029-2047.
- Grimson, N.L., And W. Chen (1988). Source Mechanism Of Four Recent Earthquakes Along The Azores-Gibraltar Plate Boundary, *Geophys. J. R. Astr. Soc.*, 92, 391-401.
- Guillemin, M., And J.P. Houzay (1982). La Néogène Post-Nappes Et Le Quaternaire Du Rif Nord-Oriental Stratigraphie Et Tectonique Des Bassins De Melilla, Du Kert, De Boudinar Et Du Piedmont Des Kebbana, *Notes Et Memoires Du Service Geologique*, 314, 7-238.
- Guiraud, R., Y. Bellion, J. Benkhelil, And C. Moreau (1987). Post-Hercynian Tectonics In Northern And Western Africa, *Geological Journal*, 22, 433-466.
- Gumati, Y.D., And A.E.M. Nairn (1991). Tectonic Subsidence Of The Sirte Basin, Libya, *Journal Of Petroleum Geology*, 14, 93-102.
- Gumpert, F., And P.W. Pomeroy (1970). Seismic Wave Velocities And Earth Structure On The African Continent, *Bulletin Of The Seismological Society Of America*, 60, 651-688.
- H'faiedh, M., J. Dorel, And J. Dubois (1985). Crustal Anomalies Under The Tunisian Seismograph Array Using Teleseismic P Waves, *Tectonophysics*, 118, 131-141.
- Harjes, H.-P., And H. Krummel (1989). Combined Processing Of Seismic Reflection And Borehole Measurements In The Moroccan Basin Offshore NW-Africa At Dsdp-Site 416, *Geologische Rundschau*, 78, 691-703.
- Harmand, C., And J.M. Cantagrel (1984). Le Volcanisme Alcalin Tertiaire Et Quaternaire Du Moyen Atlas (Maroc): Chronologie K/Ar Et Cadre Géodynamique, *Journal Of African Earth Sciences*, 2, 51-55.
- Harrell, J.A., And V.M. Brown (1992). The Worlds Oldest Surviving Geological Map - The 1150 Bc Turin Papyrus From Egypt, *Journal Of Geology*, 100, 3-18.
- Hartley, R., A.B. Watts, And J.D. Fairhead (1996). Isostasy Of Africa, *Earth And Planetary Science Letters*, 137, 1-18.
- Hatzfeld, D., And D.B. Sari (1977). Grands Profils Sismiques Dans La Région De L'arc De Gibraltar, *Bull. Soc. Géol. Fr.*, 19, 749-756.
- Hatzfeld, D., And M. Frogneux (1981). Intermediate Depth Seismicity In The Western Mediterranean Unrelated To Subduction Of Oceanic Lithosphere, *Nature*, 292, 443-445.
- Hatzfeld, D., V. Caillot, T.-E. Cherkaoui, H. Jebli, And F. Medina (1993). Microearthquake Seismicity And Fault Plane Solutions Around The Nekor Strike-Slip Fault, Morocco, *Earth And Planetary Science Letters*, 120, 31-41.
- Hatzidimitriou, P.M., E.E. Papadimitriou, D.M. Mountrakis, And B.C. Papazachos (1985). The Seismic Parameter B Of The Frequency-Magnitude Relation And Its Association With The Geological Zones In The Area Of Greece, *Tectonophysics*, 120, 141-151.
- Herbig, H.G., (1988). Synsedimentary Tectonics In Northern Middle Atlas (Morocco) During The Late Cretaceous And Tertiary In The Atlas System Of Morocco-Studies On Its Geodynamic Evolution-Lecture Notes In Earth Science, V. Jacobshagen (Editor), Springer, Berlin-Heidelberg-Newyork, 1988, 321-337.
- Hildenbrand, T., R. Kucks, M. Hamouda, And A. Bellot (1988). Bouguer Gravity Map And Related Filtered Anomaly Maps Of Morocco, U.S. Geological Survey Open-File Report 88-517, 15 pp.
- Hinz, K., H. Dostmann, And J. Fritsch, (1982). The Continental Margin Of Morocco: Seismic Sequences, Structural Elements, And Geological Development In Geology Of The Northwest African Continental Margin, E.A. U. Von Rad (Editor), Springer-Verlag, Berlin, 1982, 34-60.

- Hurley, P.M., A. Boudda, W.H. Kanes, And A.E.M. Nairn (1974). A Plate Tectonics Origin For Late Precambrian-Paleozoic Orogenic Belt In Morocco, *Geology*, 2, 343-344.
- Jabaloy, A., J. Galindo-Zaldivar, And Gonzalez-Lodeiro (1992). The Mecina Extensional System: Its Relation With The Post-Aquitania Piggy-Back Basins And The Paleostresses Evolution (Betic Cordilleras, Spain), *Geo-Marine Letters*, 12, 96-103.
- Jabour, H., And K. Nakayama (1988). Basin Modeling Of Tadla Basin, Morocco, For Hydrocarbon Potential, *American Association Of Petroleum Geologists Bulletin*, 72, 1059-1073.
- Jacobshagen, V., (1988). Geodynamic Evolution Of The Atlas System, Morocco: An Introduction In The Atlas System Of Morocco, V. Jacobshagen (Editor), Springer-Verlag, Berlin, 1988, 3-9.
- Jacobshagen, V., R. Brede, M. Hauptmann, W. Heinritz, And R. Zylka, (1988). Structure And Post-Paleozoic Evolution Of The Central High Atlas, In The Atlas System Of Morocco In The Atlas System Of Morocco, V. Jacobshagen (Editor), Springer-Verlag, Berlin, 1988, 245-271.
- Jacobshagen, V., K. Görler, And P. Giese, (1988). Geodynamic Evolution Of The Atlas System (Morocco) In Post-Paleozoic Times In The Atlas System Of Morocco, V. Jacobshagen (Editor), Springer-Verlag, Berlin, 1988, 481-499.
- Jacobshagen, V., R. Brede, M. Hauptmann, W. Heinritz, And R. Zylka, (1988). Structure And Post-Paleozoic Evolution Of The Central High Atlas In The Atlas System Of Morocco-Studies On Its Geodynamic Evolution-Lecture Notes In Earth Science, V. Jacobshagen (Editor), Springer, Berlin-Heidelberg- New York, 1988, 245-271.
- Jacobshagen, V., And P. Giese (1990). The Atlas System Of Morocco: Geodynamic Evolution In Post-Paleozoic Times, In Structure And Evolution Of The Atlas Mountain System In Morocco, Springer Verlag, Berlin.
- Jacobshagen, V. (1992). Major Fracture Zones Of Morocco - The South Atlas And The Transalboran Fault Systems, *Geologische Rundschau*, 81, 185-197.
- Jacobshagen, V. (1992). Major Fracture Zones Of Morocco: The South Atlas And The Transalboran Fault Systems, *Geologische Rundschau*, 81, 185-197.
- Jaffrezo, M., F. Medina, And J. Chorowicz (1985). Données Microbiostratigraphiques Sur Le Jurassique Supérieur Du Bassin De L'ouest Marocain. Comparaison Avec Les Résultats Du Leg 79 D.S.D.P. Et De La Campagne Cyamaz (1982), *Bull. Soc. Géol. France*, 1, 875-884.
- Jurado, M.J., And M.C. Comas (1992). Well Log Interpretation And Seismic Character Of The Cenozoic Sequence In The Northern Alboran Sea, *Geo-Marine Letters*, 12, 129-136.
- Kamel, A.F. (1994). Regional Fracture Analysis South Latitude 29-Degrees-N Of Egypt And Their Influence On Earthquakes, *Natural Hazards*, 9, 235-245.
- Kanes, W., M. Saadi, E. Ehrlich, And A. Alem (1973). Moroccan Crustal Response To Continental Drift, *Science*, 180, 950-952.
- Keeley, M.L. (1994). Phanerozoic Evolution Of The Basins Of Northern Egypt And Adjacent Areas, *Geologische Rundschau*, 83, 728-742.
- King, G.C.P., And C. Vita-Finzi (1981). Active Folding In The Algerian Earthquake Of 10 October 1980, *Nature*, 292, 22-26.
- Klein, F.W. (1978). Hypocenter Location Program, Hypoinverse (Usgs Open File Report 78-694), U.S. Geological Survey
- Knopoff, L., And J.W. Schlue (1972). Rayleigh Wave Phase Velocities For The Path Addis-Abeba-Nairobi, *Tectonophysics*, 15, 157-163.
- Kovachev, S.A., I.P. Kuzin, O.Y. Shoda, And S.L. Soloviev (1991). Attenuation Of S-Waves In The Lithosphere Of The Sea Of Crete According To Observations, *Physics Of The Earth And Planetary Interiors*, 69, 101-111.
- Kroner, A., J. Kruger, And A.A.A. Rashwan (1994). Age And Tectonic Setting Of Granitoid Gneisses In The Eastern Desert Of Egypt And South-West Sinai, *Geologische Rundschau*, 83, 502-513.
- Lagarde, J.L., And A. Michard (1986). Stretching Normal To The Regional Thrust Displacement In A Thrust-Wrench Shear Zone, Rehamna Massif, Morocco, *Journal Of Structural Geology*, 8, 483-492.

- Laville, E., And J.-P. Petit (1984). Role Of Synsedimentary Strike-Slip Faults In The Formation Of Moroccan Triassic Basins, *Geology*, 12, 424-427.
- Laville, E., And A. Piqué, (1990). Structural And Orogenic Inversions In The Central High Atlas (Morocco): A Tectonic Model In Structure And Evolution Of The Atlas Mountain System In Morocco, Berlin, 1990, 13.
- Laville, E., Piqué, Alain (1991). La Distension Crustale Atlantique Et Atlasique Au Maroc Au Début Du Mésozoïque: Le Rejeu Des Structures Hercyniennes, *Bull. Soc. Géol. France*, 162, 1161-1171.
- Laville, E., And A. Pique (1992). Jurassic Penetrative Deformation And Cenozoic Uplift In The Central High Atlas (Morocco): A Tectonic Model., *Geologische Rundschau*, 81, 157-170.
- Laville, E., A. Charroud, B. Fedan, M. Charrouds, And A. Pique (1995). Negative Inversion In Atlasic Domain (Morocco) : The Kerrouchen Triassic Basic, A Structural Element Of The Atlasic Rift, *Buil. Soc. Geol. Fr.*, 4, `.
- Le Pichon, X., Bergerat, Françoise, Roulet, Marie-José (1988). Plate Kinematics And Tectonics Leading To The Alpine Belt Formation; A New Analysis, *Geological Society Of America, Special Paper* 218, 111-131.
- Leblanc, M. (1976). Proterozoic Oceanic Crust At Bou Azzer, *Nature*, 261, 34-35.
- Leblanc, M., (1981). The Late Proterozoic Ophiolites Of Bou Azzer (Morocco): Evidence For Pan-African Plate Tectonics In Precambrian Plate Tectonics, A. Kröner (Editor), Elsevier Scientific Publishing Co., Amsterdam, New York, 1981, 435-451.
- Leblanc, D., And P. Olivier (1984). Role Of Strike-Slip Faults In The Betic-Rifian Orogeny, *Tectonophysics*, 101, 345-355.
- Leblanc, D. (1990). Tectonic Adaptation Of The External Zones Around The Curved Core Of An Orogen: The Gibraltar Arc, *Journal Of Structural Geology*, 12, 1013-1018.
- Lesquer, A., D. Takherist, J.M. Dautria, And O. Hadiouche (1990). Geophysical And Petrological Evidence For The Presence Of An Anomalous Upper Mantle Beneath The Sahara Basins (Algeria), *Earth And Planetary Science Letters*, 96, 407-418.
- Levret, A. (1991). The Effects Of The November 1, 1755 "Lisbon" Earthquake In Morocco, *Tectonophysics*, 193, 83-94.
- Lonergan, L., And J.P. Platt (1994). The Internal-External Zone Boundary In The Eastern Betic Cordillera, Se Spain, *Journal Of Structural Geology*, 16, 175-188.
- Loomis, T. (1975). Tertiary Mantle Diapirism, Orogeny, And Plate Tectonics East Of The Strait Of Gibraltar, *Amer. J. Sci.*, 275, 1-30.
- Lopez Casado, C., C. Sanz De Galdeano, J. Delgado, And M.A. Peinado (1995). The B Parameter In The Betic Cordillera, Rif And Nearby Sectors. Relations With The Tectonics Of The Region, *Tectonophysics*, 248, 277-292.
- Madeira, J., And A. Ribeiro (1990). Geodynamics Models For The Azores Triple Junction: A Contribution From Tectonics, *Tectonophysics*, 184, 405-415.
- Makris, J., H. Menzel, J. Zimmermann, And P. Gouin, (1975). Gravity Field And Crustal Structure Of North Ethiopia In Afar Depression Of Ethiopia, A. Pilger, And A. Roesler (Editors), E. Schweizer. Verlagsbuchhandl. (Naegle U. Obermiller), Stuttgart, Deu, 1975, 135-144.
- Makris, J., And V. Niemann (1981). Deep Seismic Sounding In Southern Morocco, *Jahrestagung Der Deutschen Geophysikalischen Gesellschaft E.V.*, 41, 85.
- Makris, J., A. Demnati, And J. Klubmann (1985). Deep Seismic Soundings In Morocco And A Crust And Upper Mantle Model Deduced From Seismic And Gravity Data, *Annales Geophysicae*, 3, 369-380.
- Makris, J., Rihm, R., Allam, A., (1988). Some Geophysical Aspects Of The Evolution And Structure Of The Crust In Egypt In The Pan-African Belt Of Northeast Africa And Adjacent Areas, *Tectonic Evolution And Economic Aspects Of A Late Proterozoic Orogen*, S.E.-G.A.R.O. Greiling (Editor), Friedr. Vieweg & Sohn, Braunschweig, 1988, 345-369.
- Maldonado, A., A.C. Campillo, A. Mauffret, B. Alonso, J. Woodside, And J. Campos (1992). Alboran Sea Late Cenozoic Tectonic And Stratigraphic Evolution, *Geo-Marine Letters*, 12, 179-186.

- Maldonado, A., And M.C. Comas (1992). Geology And Geophysics Of The Alboran Sea: An Introduction, *Geo-Marine Letters*, 12, 61-65.
- Manspeizer, W., J. Puffer, And H. Cousminer (1978). Separation Of Morocco And Eastern North America: A Triassic-Liassic Stratigraphic Record, *Geological Society Of America Bulletin*, 89, 901-920.
- Mantovani, E., D. Albarello, And M. Mucciarelli (1989). Evidence Of Interconnection Between Seismic Activity In The Iberian Peninsula And North African Belts, *Physics Of The Earth And Planetary Interiors*, 54, 116-119.
- Mariller, F., And S. Mueller (1982). Structure Of The Upper Mantle In The Northeastern Atlantic Close To The Azores-Gibraltar Ridge From Surface-Wave And Body-Wave Observations, *Tectonophysics*, 90, 195-213.
- Mattauer, M., F. Proust, And P. Tapponnier (1972). Major Strike-Slip Fault Of Late Hercynian Age In Morocco, *Nature*, 237, 160-162.
- Mattauer, M., P. Tapponnier, And F. Proust (1977). Sur Les Mécanismes De Formation Des Chaînes Intracontinentales. L'exemple Des Chaînes Atlasiques Du Maroc, *Bull. Soc. Géol. France*, 7, 521-526.
- Mauffret, A., A. Maldonado, And A.C. Campillo (1992). Tectonic Framework Of The Eastern Alboran And Western Algerian Basins, Western Mediterranean, *Geo-Marine Letters*, 12, 104-110.
- Mckenzie, D. (1972). Active Tectonics Of The Mediterranean Region, *Geophysical Journal Of The Royal Astronomical Society*, 30, 109-185.
- Mclaughlin, K.L., And R.-S. Jih (1988). Scattering From Near-Source Topography: Teleseismic Observations And Numerical Simulations, *BSSA*, 78, 1399-1414.
- Mclaughlin, K.L., A.C. Lees, Z.A. Der, And M.E. Marshall (1988). Teleseismic Spectral And Temporal M_0 And Chi Infinity Estimates For Four French Explosions In Southern Sahara, *BSSA*, 78, 1580-1596.
- Medina, F. (1988). Tilted-Blocks Pattern, Paleostress Orientation, And Amount Of Extension Related To Triassic Early Rifting Of The Central Atlantic In The Amzri Area (Argana Basin, Morocco), *Tectonophysics*, 148, 229-233.
- Medina, F. (1989). Landsat Imagery Interpretation Of Essaouira Basin (Morocco): Comparison With Geophysical Data And Structural Implications, *Journal Of African Earth Sciences*, 9, 69-75.
- Medina, F. (1989). Extensional Tectonics In The El Jadida-Agadir (Morocco) Triassic-Liassic Basin During The Early Rifting Of The Central Atlantic, *Garcia De Orta, Sér. Geol.*, Lisboa, 12, 21-36.
- Medina, F. (1989). Le Jurassique Des Régions D'imi N'tanout Et Chichaoua: Lithostratigraphie Et Corrélatons, *Bull. Inst. Sci.*, Rabat, 13, 5-16.
- Medina, F. (1991). Superimposed Extensional Tectonics In The Argana Triassic Formations (Morocco), Related To The Early Rifting Of The Central Atlantic, *Geol. Mag.*, 128, 525-536.
- Medina, F., And T.-E. Cherkaoui (1992). Focal Mechanisms Of The Earthquakes Of Morocco And Adjacent Areas (1959-1986) - Tectonic Implications, *Eclogae Geologicae Helveticae*, 85, 433-457.
- Medina, F. (1995). Present-Day State Of Stress In Northern Morocco From Focal Mechanism Analysis, *Journals Of Structural Geology*, 17, 1035-1046.
- Meghraoui, M., A. Cisternas, And H. Philip (1986). Seismotectonics Of The Lower Cheliff Basin: Structural Background Of The El Asnam (Algeria) Earthquake, *Tectonics*, 5, 809-836.
- Meghraoui, M., (1988). Paleoseismic Study On The El Asnam (Algeria) Thrust Fault In Seismic Hazard In Mediterranean Regions, J. Bonnin, Et Al. (Editor), Kluwer Academic Publishers, Dordrecht/Boston/London, 1988, 333-346.
- Meghraoui, M. (1991). Blind Reverse Faulting System Associated With The Mont Chenoua-Tipaza Earthquake Of 29 October 1989 (North-Central Algeria), *Terra Nova*, 3, 84-93.
- Mezcua, J., And A. Udias (1991). Seismicity, Seismotectonics And Seismic Risk Of The Ibero-Maghrebian Region, Instituto Geografico Nacional Monografia No. 8, 390 Pp., From Cornell Database.
- Michard, A. (1976). *Eléments De Géologie Marocaine*, Rabat, 408.

- Michard, A., B. Goffé, A. Chalouan, And O. Saddiqi (1991). Les Corrélations Entre Les Chaînes Bético-Rifaines Et Les Alpes Et Leurs Conséquences, *Bull. Soc. Géol. France*, 162, 1151-1160.
- Michard, A., H. Feinberg, D. El-Azzab, M. Bouybaouene, And O. Saddiqi (1992). A Serpentine Ridge In A Collisional Paleomargin Setting: The Beni Malek Massif, External Rif, Morocco, *Earth And Planetary Science Letters*, 113, 435-442.
- Milano, G., And I. Guerra (1989). Dss Profiling Across The Eolian Islands Volcanic Region (Tyrrhenian Sea, Italy), *Bulletin - New Mexico Bureau Of Mines & Mineral Resources*, 131, 190.
- Miranda, J.M., J.F. Luis, I. Abreu, L.A. Mendes Victor, A. Galdeano, And J.C. Rossignol (1991). Tectonic Framework Of The Azores Triple Junction, *Geophysical Research Letters*, 18, 1421-1424.
- Morel, J.-L. (1989). Evolution Paléogéographique Et Tectonique Du Rif (Maroc) Du Tortonien À L'actuel, *Comptes Rendu Académie Sciences Paris*, 309, 2053-2059.
- Morel, J.-L., E.M. Zouine, And A. Poisson (1993). Relations Entre La Subsidence Des Bassins Moulouyens Et La Création Des Reliefs Atlasiques (Maroc): Un Exemple D'inversion Tectonique Depuis Le Néogène, *Bull. Soc. Géol. France*, 164, 79-91.
- Morel, J., And B. Cabanis (1993). Mise En Evidence D'une Association Magmatique Dans Le Volcanisme Plio-Quaternaire Du Moyen-Atlas Marocain, *Comptes Rendus De L'académie Des Sciences, Sciences De La Terre Et Des Planètes*, 316, 357-362.
- Morelli, C., F. Barberi, E. Locardi, C. Morelli, A. Praturlon, P. Scandone, L. Vezzani, And F.-C. Wezel (1982). Geophysical Knowledge Of Italy And Surrounding Seas, *Memorie Della Società Geologica Italiana*, 24, 521-530.
- Morelli, C., And R. Nicolich (1990). A Cross Section Of The Lithosphere Along The European Geotransverse Southern Segment (From The Alps To Tunisia), *Tectonophysics*, 176, 229-243.
- Morley, C.K. (1987). Origin Of A Major Cross-Element Zone: Moroccan Rif, *Geology*, 15, 761-764.
- Morley, C.K., R.A. Nelson, T.L. Patton, And S.G. Munn (1990). Transfer Zones In The East African Rift System And Their Relevance To Hydrocarbon Exploration In Rifts, *American Association Of Petroleum Geologists Bulletin*, 74, 1234-1253.
- Morley, C.K. (1992). Notes On The Neogene Basin History Of The Western Alboran Sea And Its Implications For The Tectonic Evolution Of The Rif-Betic Orogenic Belt, *Journal Of African Earth Sciences*, 14, 57-65.
- Morley, C.K. (1993). Discussion Of Origins Of Hinterland Basins Of The Rif-Betic Cordillera And Carpathians, *Tectonophysics*, 226, 359-376.
- Moukadiri, A., (1983). Ultramafic Xenoliths Related To Alkalic Basalts In The Azrou-Timahdite Volcanic District, Middle Atlas, Morocco, Doctoral, Univ. Clermont-Ferrand 2, Pp.
- Moustafa, A.R., And K. Mosbah (1988). Late Cretaceous-Early Tertiary Dextral Transpression In North Sinai: Reactivation Of The Tethyan Continental Margin, *American Association Of Petroleum Geologists Bulletin*, 72, 1015.
- Moustafa, A.R., And M.H. Khalil (1989). North Sinai Structures And Tectonic Evolution,, Middle East Research Center, Ain Shams University, 3, 215-231.
- Moustafa, A.R. (1992). The Feiran Tilted Blocks: An Example Of A Synthetic Transfer Zone, Eastern Side Of Suez Rift, *Annales Tectonicae*, 6, 193-201.
- Moustafa, A., And M. Khalil (1994). Rejuvenation Of The Eastern Mediterranean Passive Continental Margin In Northern And Central Sinai; New Data From The Themed Fault, *Geology Magazine*, 131, 435-448.
- Moustafa, A., And S. Khalil (1995). Rejuvenation Of The Tethyan Passive Continental Margin Of Northern Sinai; Deformation Style And Age (Gebel Yelleq Area), *Tectonophysics*, 241, 225-238.
- Mulder, C.J., And G.R. Parry, Late Tertiary Evolution Of The Alboran Sea At The Eastern Entrance Of The Straits Of Gibraltar, In *International Symposium On The Structural History Of The Mediterranean Basins*, Edited By B. Bijou-Duval, And L. Montadert, Pp. 401-410, Editions Technip, Yugoslavia, 1976.

- Nairn, E.A.M., H.C. Noltimier, And B. Nairn (1980). Surface Magnetic Survey Of The Souss Basin, Southwestern Morocco: Evaluation Of The Tectonic Role Postulated For The Agadir And Tarfaya Fault Zones And The South Atlas Flexure, *Tectonophysics*, 64, 235-248.
- Najid, D., M. Westphal, And J. Hernandez (1981). Paleomagnetism Of Quaternary And Miocene Lavas From North-East And Central Morocco, *J. Geophys*, 49, 149-152.
- Ocal, N. (1964). Fault Plane Solutions For Agadir, Morocco, Earthquake Of February 29, 1960 And Skoplje, Yugoslavia, Earthquake Of July 26, 1963, *Bull. Inter. Inst. Seismol. Earthquake Eng.*, 1, 1-7.
- Omara, S. (1964). Diapiric Structures In Egypt And Syria, *American Association Of Petroleum Geologists Bulletin*, 48, 1116-1125.
- Oukemeni, D., Bourne, J. H. (1993). Etude Geochimique Des Granitoides Du Pluton D'aouli, Haute Moulouya, Maroc, *Journal Of African Sciences*, 17, 429-443.
- Oukemeni, D., J. Bourne, And T.E. Krogh (1995). U-Pb Geochronology On Zircon From The Aouli Pluton, Haute Moulouya Area, Morocco, *Bull. Soc. Geol. Fr.*, 1.
- Ouyed, M., M. Meghraoui, A. Cisternas, A. Deschamps, J. Dorel, J. Frechet, R. Gaulon, D. Hatzfeld, And H. Philip (1981). Seismotectonics Of The El Asnam Earthquake, *Nature*, 292, 26-.
- Pinet, B., L. Montadert, A. Mascle, M. Cazes, And C. Bois, (1987). New Insights Of The Structure And Formation Of Sedimentary Basins From Deep Seismic Profiling In Western Europe In *Petroleum Geology Of North West Europe*, J. Brooks, And K.W. Glennie (Editor), Graham & Trotman, London, 1987, 11-31.
- Pique, A., M. Dahmani, D. Jeannette, And L. Bahi (1987). Permanence Of Structural Lines In Morocco From Precambrian To Present, *Journal Of African Earth Sciences*, 6, 247-256.
- Pique, A., And A. Michard (1989). Moroccan Hercynides: A Synopsis. The Paleozoic Sedimentary And Tectonic Evolution At The Northern Margin Of West Africa, *American Journal Of Science*, 289, 286-330.
- Piqué, A., D. Jeannette, And A. Michard (1980). The Western Meseta Shear Zone, A Major And Permanent Feature Of The Hercynian Belt In Morocco, *Journal Of Structural Geology*, 2, 55-61.
- Platt, J.P., And R.L.M. Vissers (1989). Extensional Collapse Of Thickened Continental Lithosphere: A Working Hypothesis For The Alboran Sea And Gibraltar Arc, *Geology*, 17, 540-543.
- Platzman, E.S. (1992). Paleomagnetic Rotations And The Kinematics Of The Gibraltar Arc, *Geology*, 20, 311-314.
- Poupinet, G., A. Souriau, And L. Jenatton (1993). A Test On The Earths Core Mantle Boundary Structure With Antipodal Data - Example Of Fiji-Tonga Earthquakes Recorded In Tamanrasset, Algeria, *Geophysical Journal International*, 113, 684-692.
- Press, F., M. Ewing, And J. Oliver (1956). Crustal Structure And Surface-Wave Dispersion In Africa, *BSSA*, 46, 97-103.
- Rabchevsky, G.A. (1979). Tectonic Evolution Of The Moroccan Landscape, *Earth Science*, 153-155.
- Rabie, S.I., And A.A. Ammar (1990). Pattern Of The Main Tectonic Trends From Remote Geophysics, Geological Structures And Satellite Imagery, Central Eastern Desert, Egypt, *International Journal Of Remote Sensing*, 11, 669-683.
- Ragab, A.I. (1993). A Geodynamic Model For The Distribution Of The Oceanic Plate Slivers Within A Pan-African Orogenic Belt, Eastern Desert, Egypt, *J. Geodynamics*, 17, 21-26.
- Ramdani, M., G. Herquel, And B. Tadili, (1985). Etude Du Risque Sismique Au Maroc In *Sci. De La Terre*, , Nancy, France, 1985, 103-113.
- Ramdani, M., B. Tadili, A.E. Mouraouah, And L.A. Brahim, (1987). Etude De La Crise Sismique De La Région De Moulay Driss Zerhoun In *Centre National De Coordination Et De Planification De La Recherche Scientifique Et Technique*, 1987.
- Ramdani, M., And B.A. Tadili (1988). Deep Crustal Structure In Morocco, *Gerlands Beitrage Zur Geophysik*, 97, 137-143.

- Ramdani, M., B. Tadili, And T.E. Mrabet, (1989). The Present State Of Knowledge On Historical Seismicity Of Morocco In Proceedings Of The Symposium On Calibration Of Historical Earthquakes In Europe And Recent Developments In Intensity I Interpretation, G. Payo, C. Radu, And D. Postpischl (Editor), European Seismological Commission, Madrid, 1989, 257-279.
- Ramdani, M., (1991). Etude Sismotectonique Du Nord Du Maroc, Thèse Docteur Es-Sciences, Université Mohammed I, Morocco, 248 Pp.
- Rebai, S. (1993). Recent Tectonics In Northern Tunisia: Coexistence Of Compressive And Extensional Structures, *Annales Tectonicae*, 7, 129-141.
- Rebai, S., H. Philip, And A. Taboada (1992). Modern Tectonic Stress Field In The Mediterranean Region: Evidence For Variation In Stress Directions At Different Scales, *Geophysical Journal International*, 110, 106-140.
- Research Group For Lithospheric Structure In Tunisia (1992). The Egt'85 Seismic Experiment In Tunisia: A Reconnaissance Of The Deep Structures, *Tectonophysics*, 207, 245-267.
- Reuber, I., A. Michard, A. Chalouan, T. Juteau, And B. Jermoumi (1982). Structure And Emplacement Of The Alpine-Type Peridotites From Beni Bousera, Rif, Morocco: A Polyphase Tectonic Interpretation, *Tectonophysics*, 82, 231-251.
- Rimi, A. (1990). Geothermal Gradients And Heat Flow Trends In Morocco, *Geothermics*, 19, 443-454.
- Rod, E. (1962). Fault Pattern, Northwest Corner Of Sahara Shield, *American Association Of Petroleum Geologists Bulletin*, 46, 529-552.
- Rodriguez Fernandez, J., And C. Sanz De Galdeano (1992). Onshore Neogene Stratigraphy In The North Of The Alboran Sea (Betic Internal Zones): Paleogeographic Implications, *Geo-Marine Letters*, 12, 123-128.
- Rondeel, H.E., And O.J. Simon, (1974). Betic Cordilleras, In *Mesozoic-Cenozoic Orogenic Belts* In A. Spencer (Editor), Scottish Academic Press, Edinburgh, 1974, 23-35.
- Royden, L.H. (1993). Evolution Of Retreating Subduction Boundaries Formed During Continental Collision, *Tectonics*, 12, 629-638.
- Saadi, S.E.M., M. Bensaid, And M. Dahmani (1984). Carte Géologique Du Rif, Al Hoceima, Editions Du Service Géologique Du Maroc.
- Saadi, M., (1988). Les Grandes Fractures Du Maroc Et Leurs Relations Avec La Structure Géologique, La Sismicité, Le Volcanisme Et Les Gîtes Minéraux In Notes Et Mémoires Du Service Géologique, Editions Du Service Géologique Du Maroc, Rabat, 1988, 123pp.
- Sanz De Galdeano, C. (1990). Geologic Evolution Of The Betic Cordilleras In The Western Mediterranean, Miocene To The Present, *Tectonophysics*, 172, 107-119.
- Sanz De Galdeano, C., C. Lopez Casado, J. Delgado, And M.A. Peinado (1995). Shallow Seismicity And Active Faults In The Betic Cordillera. A Preliminary Approach To Seismic Sources Associated With Specific Faults, *Tectonophysics*, 248, 293-302.
- Savostin, L.A., J.-C. Sibuet, L.P. Zonenshain, X.L. Pichon, And M.-J. Roulet (1986). Kinematic Evolution Of The Tethys Belt From The Atlantic Ocean To The Pamirs Since The Triassic, *Tectonophysics*, 123, 1-35.
- Schaer, J.P., (1987). Evolution And Structure Of The High Atlas Of Morocco In The Anatomy Of Mountain Ranges, J.P. Schaer, And J. Rodgers (Editor), Princeton University Press, New Jersey, 1987, 107-127.
- Schwarz, G., And P.J. Wigger, (1988). Geophysical Studies Of The Earth's Crust And Upper Mantle In The Atlas System Of Morocco In The Atlas System Of Morocco, V. Jacobshagen (Editor), Springer-Verlag, Berlin, 1988, 339-357.
- Schwarz, G., P.J. Wigger, G. Asch, S.O.E. Alami, H.G. Mehl, F. Ramdani, And V. Rath, (1990). A Geophysical Traverse Across The Atlas Mountain System Of Morocco: Data And Interpretation In Structure And Evolution Of The Atlas Mountain System In Morocco, Berlin, 1990, 18.
- Schwarz, G., H.-G. Mehl, F. Ramdani, And V. Rath (1991). Electrical Resistivity Structure Of The Eastern Moroccan Atlas System And Its Tectonic Implications, *Geol. Rundsch.* (In Press).

- Seber, D., M. Barazangi, B.A. Tadili, M. Ramdani, A. Ibenbrahim, D.B. Sari, And S.O.E. Alami (1993). Sn To Sg Conversion And Focusing Along The Atlantic Margin, Morocco: Implications For Earthquake Hazard Evaluation, *Geophys. Res. Letters*, 20, 1503-1506.
- Seber, D., M. Barazangi, A. Ibenbrahim, And A. Demnati (1996). Geophysical Evidence For Lithospheric Delamination Beneath The Alboran Sea And Rif-Betic Mountains, *Nature*, 379, 785-790.
- Seno, T., And A. Saito (1994). Recent East African Earthquakes In The Lower Crust, *Earth And Planetary Science Letters*, 121, 125-136.
- Sichler, B., J.-L. Olivet, J.-M. Auzende, H. Jonquet, J. Bonnin, And A. Bonifay (1980). Mobility Of Morocco, *Can. J. Earth Sci*, 17, 1546-1558.
- Snoke, A., S. Schamel, And R. Karasek (1988). Structural Evolution Of Djebel Debadib Anticline: A Clue To The Regional Tectonic Style Of The Tunsian Atlas, *Tectonics*, 7, 497-516.
- Stanley, D.J. (1990). Recent Subsidence And Northeast Tilting Of The Nile-Delta, Egypt, *Marine Geology*, 94, 147-154.
- Stets, J., And P. Wurster, (1982). Atlas And Atlantic - Structural Relations In Geology Of The Northwest African Continental Margin, U. Von Rad, Et Al. (Editor), Springer-Verlag, Berlin, 1982, 69-85.
- Studer, M., And R. Du Dresnay (1980). Deformations Synsedimentaires En Compression Pendant Le Lias Superior Et Le Dogger, Au Tizi N'irhil (Haut- Atlas Central De Midelt, Maroc), *Soc. Geol. France Bull.*, 22, 391-397.
- Suleiman, A.S., And D.I. Doser (1995). The Seismicity, Seismotectonics And Earthquake Hazards Of Libya, With Detailed Analysis Of The 1935 April 19, M = 7.1 Earthquake Sequence, *Geophysical Journal International*, 120, 312-322.
- Sultan, M., R.E. Arvidson, N.C. Sturchio, And E.A. Guinness (1987). Lithologic Mapping In Arid Regions With Landsat Thematic Mapper Data: Meatiq Dome, Egypt, *Geological Society Of America Bulletin*, 99, 748-762.
- Tadili, B., And M. Ramdani (1983). Computer File Of Moroccan Earthquakes, *Bulletin Of The Seismological Society Of America*, 73, 653-654.
- Tadili, B., M. Ramdani, And L.A. Brahim, (1985). Etude De L'activité Sismique De La Région De Missour In Rapport Sismo Cnr/N°2/85, Centre National De Coordination Et De Planification De La Recherche Scientifique Et Technique, 1985.
- Tadili, B.A., M. Ramdani, D. Ben-Sari, K. Chapochnikov, And A. Bellot (1986). Crustal Structure In Northern Morocco, *Gerlands Beitrage Zur Geophysik*, 95, 477-485.
- Tadili, B., M. Ramdani, D.B. Sari, K. Chapochnikov, And A. Bellot (1986). Structure De La Croûte Dans Le Nord Du Maroc, *Annales Geophysicae*, 4, 99-104.
- Tadili, B., M. Ramdani, D.B. Sari, K. Chapochnikov, And A. Bellot (1986). Structure Of The Crust In Northern Morocco, *Annales Geophysicae, Series B: Terrestrial And Planetary Physics*, 4, 99-104.
- Tadili, B., (1991). Etude Du Risque Sismique Au Nord Du Marco, Docteur Es-Sciences, Université Mohammed I, Morocco, 229 Pp.
- Tesson, M., B. Gensous, And M. Labraim (1987). Seismic Analysis Of The Southern Margin Of The Alboran Sea, *Journal Of African Earth Sciences*, 6, 813-821.
- Tesson, M., And B. Gensous (1989). Les Bases D'une Stratigraphie Sismique Du Neogene Post-Nappes En Mer D'alboran, Au Large Du Maroc. Implications Structurales Et Paleogeographiques., *Journal Of African Earth Sciences*, 9, 421-433.
- Thauvin, S. (1971). Ressources En Eau Du Maroc. Tome I: Domaines Du Rif Et Du Maroc Oriental, Notes Et Mém. Serv. Géol. Maroc, 231, 69-79.
- Thorpe, R.S., And K. Smith (1974). Distribution Of Cenozoic Volcanism In Africa, *Earth And Planetary Science Letters*, 22, 91-95.
- Torne, M., G. Pascal, P. Buhl, A.B. Watts, And A. Mauffret (1992). Crustal And Velocity Structure Of The Valencia Trough (Western Mediterranean); Part I, A Combined Refraction/Wide-Angle Reflection And Near-Vertical Reflection Study, *Tectonophysics*, 203, 1-20.

- Torne, M., And E. Banda (1992). Crustal Thinning From The Betic Cordillera To The Alboran Sea, *Geo-Marine Letters*, 12, 76-81.
- Torres-Roldan, R.L., G. Poli, And A. Peccerillo (1986). An Early Miocene Arc-Tholeiitic Magmatic Dike Event From The Alboran Sea- Evidence For Precollision Subduction And Back-Arc Crustal Extension In The Westernmost Mediterranean, *Geologische Rundschau*, 75, 219-234.
- Touzani, A., Timoulali, Y. Etude De La Qualité De L'eau Cotière Marine (Casablanca-El Jadida) Par Traitement Numérique D'images Landsat, 245-250.
- Tricart, P., L. Torelli, A. Argani, F. Rekhiss, And A. Others (1994). Extensional Collapse Related To Compressional Uplift In The Alpine Chain Off Northern Tunisia (Central Mediterranean), *Tectonophysics*, 238, 317-329.
- Udias, A., A.L. Arroyo, And J. Mezcuca (1976). Seismotectonic Of The Azores-Alboran Region, *Tectonophysics*, 31, 259-289.
- Van Den Bosch, J.W.H., (1981). Mémoire Explicatif De La Carte Gravimétrique Du Maroc (Provinces Du Nord) Au 1/500 000 In Notes Et Mémoires Du Service Géologique, Editions Du Service Géologique Du Maroc, Rabat, 1981, 219.
- Van Der Wal, D., And R.L.M. Vissers (1993). Uplift And Emplacement Of Upper Mantle Rocks In The Western Mediterranean, *Geology*, 21, 1119-1122.
- Van Houten, F.B. (1977). Triassic-Liassic Deposits Of Morocco And Eastern North America: Comparison, *American Association Of Petroleum Geologists Bulletin*, 61, 79-99.
- Vandermeer, F., And S. Cloetingh (1993). Intraplate Stresses And The Subsidence History Of The Sirte Basin (Libya), *Tectonophysics*, 226, 37-58.
- Verzhbitsky, E.V., And V.G. Zolotarev (1989). Heat Flow And The Eurasian-African Plate Boundary In The Eastern Part Of The Azores-Gibraltar Fracture Zone, *Journal Of Geodynamics*, 11, 267-273.
- Vissers, R.L.M., J.P. Platt, And D. Van Der Wal (1995). Late Orogenic Extension Of The Betic Cordillera And The Alboran Domain: A Lithospheric View, *Tectonics*, 14, 786-803.
- Vita-Finzi, C. (1989). Temporal Clustering Of Paleoseismic Events On The Oued Fodda Fault, Algeria - Comment, *Geology*, 17, 865-865.
- Vogt, J. (1993). Further Research On The Historical Seismicity Of Tunisia, *Terra Nova*, 5, 475-476.
- Wallbrecher, E., (1988). The Anti-Atlas System: An Overview In The Atlas System Of Morocco, V. Jacobshagen (Editor), Springer-Verlag, Berlin, 1988, 13-17.
- Warme, J., (1988). Jurassic Carbonate Facies Of The Central And Eastern High Atlas Rift, Morocco In The Atlas System Of Morocco, V. Jacobshagen (Editor), Springer-Verlag, Berlin, 1988, 169-199.
- Watts, A.B., And M. Torne (1992). Subsidence History, Crustal Structure, And Thermal Evolution Of The Valencia Trough; A Young Extensional Basin In The Western Mediterranean, *Journal Of Geophysical Research*, B, Solid Earth And Planets, 97, 20,021-20,041.
- Watts, A.B., J.P. Platt, And P. Buhl (1993). Tectonic Evolution Of The Alboran Sea, *Basin Research*, 5, 153-177.
- Weigel, W., G. Wissmann, And P. Goldflam, (1982). Deep Seismic Structure (Mauritania And Central Morocco) In *Geology Of The Northwest African Continental Margin*, U. Von Rad, Et Al. (Editor), Springer-Verlag, Berlin, 1982, 132-159.
- Weijermars, R. (1985). In Search For A Relationship Between Harmonic Resolutions Of The Geoid, Convective Stress Patterns And Tectonics In The Lithosphere: A Possible Explanation For The Betic-Rif Orocline, *Physics Of The Earth And Planetary Interiors*, 37, 135-148.
- Weijermars, R. (1985). Uplift And Subsidence History Of The Alboran Basin And A Profile Of The Alboran Diapir (W-Mediterranean), *Geologie En Mijnbouw*, 64, 349-356.
- Weisrock, A. (1981). Neotectonic And Coastal Morphology In The Atlantic Atlas (Morocco), *Z. Geomorph. N.F.*, 40, 175-182.
- Westaway, R. (1990). Present-Day Kinematics Of The Plate Boundary Zone Between Africa And Europe, From The Azores To The Aegean, *Earth Planetary Science Letters*, 96, 393-406.
- Westaway, R. (1990). The Tripoli, Libya, Earthquake Of September 4, 1974 - Implications For The Active Tectonics Of The Central Mediterranean, *Tectonics*, 9, 231-248.

- Wigger, P., G. Ash, P. Giese, W.-D. Heinshon, S.O. El Alami, And F. Ramdani (1992). Crustal Structure Along A Traverse Across The Middle And High Atlas Mountains Derived From Seismic Refraction Studies, *Geologische Rundschau*, 81, 237-248.
- Wissmann, G., And U. Von Rad (1979). Seismic Structure, Continental Basement, And Mesozoic Sediments From The Mazagan Plateau Off Morocco, *Meteor Forsch.-Ergebnisse*, 31, 1-20.
- Woodside, J.M., And A. Maldonado (1992). Styles Of Compressional Neotectonics In The Eastern Alboran Sea, *Geo-Marine Letters*, 12, 111-116.
- Working, G.F.D.S.S.I.T.A.S. (1978). Crustal Seismic Profiles In The Alboran Sea- Preliminary Results, *Pageoph.*, 116. Working Group For Deep Seismic Sounding In Spain 1974-1975 (1977). Deep Seismic Soundings In Southern Spain, *Pageoph.*, 115, 721-735.
- Yielding, G., J.A. Jackson, G.C.P. King, H. Sinval, C. Vita-Finzi, And R.M. Wood (1981). Relations Between Surface Deformation, Seismicity, Rupture Characteristics And Fault Geometry During The El Asnam (Algeria) Earthquake Of 10 October 1980, *Earth Planetary Science Letters*, 56, 287-304.
- Young, M.E., H.G. Izzeldin, And A.F. Burr (1989). Bouguer And Isostatic Gravity Anomalies In NW Sudan And Their Implication For Petroleum Exploration, European Association of Exploration Geophysicists; 51st meeting and technical exhibition, Berlin, DEU, Federal Republic of Germany, 19890529, May 29-June 2, 1989.
- Zhang, T.R., S.Y. Schwartz, And T. Lay (1994). Multivariate Analysis Of Waveguide Effects On Short-Period Regional Wave Propagation In Eurasia And Its Application In Seismic Discrimination, *Journal Of Geophysical Research, Solid Earth*, 21929-21946.

THOMAS AHRENS
SEISMOLOGICAL LABORATORY 252-21
CALIFORNIA INST. OF TECHNOLOGY
PASADENA, CA 91125

AIR FORCE RESEARCH LABORATORY
ATTN: VSOP
29 RANDOLPH ROAD
HANSCOM AFB, MA 01731-3010 (2 COPIES)

AIR FORCE RESEARCH LABORATORY
ATTN: RESEARCH LIBRARY/TL
5 WRIGHT STREET
HANSCOM AFB, MA 01731-3004

AIR FORCE RESEARCH LABORATORY
ATTN: AFRL/SUL
3550 ABERDEEN AVE SE
KIRTLAND AFB, NM 87117-5776 (2 COPIES)

RALPH ALEWINE
- NTPO
1901 N. MOORE STREET, SUITE 609
ARLINGTON, VA 22209

G. ELI BAKER
MAXWELL TECHNOLOGIES
8888 BALBOA AVE.
SAN DIEGO, CA 92123-1506

MUAWIA BARAZANGI
INSTOC
3126 SNEE HALL
CORNELL UNIVERSITY
ITHACA, NY 14853

DOUGLAS BAUMGARDT
ENSCO INC.
5400 PORT ROYAL ROAD
SPRINGFIELD, VA 22151

THERON J. BENNETT
MAXWELL TECHNOLOGIES
11800 SUNRISE VALLEY
SUITE 1212
RESTON, VA 22091

WILLIAM BENSON
NAS/COS
ROOM HA372
2001 WISCONSIN AVE. NW
WASHINGTON DC 20007

JONATHAN BERGER
UNIV. OF CALIFORNIA, SAN DIEGO
SCRIPPS INST. OF OCEANOGRAPHY IGPP, 0225
9500 GILMAN DRIVE
LA JOLLA, CA 92093-0225

ROBERT BLANDFORD
AFTAC
1300 N. 17TH STREET
SUITE 1450
ARLINGTON, VA 22209-2308

LESLIE A. CASEY
DEPT. OF ENERGY/NN-20
1000 INDEPENDENCE AVE. SW
WASHINGTON DC 20585-0420

CENTER FOR MONITORING RESEARCH
ATTN: LIBRARIAN
1300 N. 17th STREET, SUITE 1450
ARLINGTON, VA 22209

FRANCESCA CHAVEZ
LOS ALAMOS NATIONAL LAB
P.O. BOX 1663, MS-D460
LOS ALAMOS, NM 87545 (5 COPIES)

ANTON DAINTY
DTRA/PMA
45045 AVIATION DRIVE
DULLESVA 20166-7517

CATHERINE DE GROOT-HEDLIN
UNIV. OF CALIFORNIA, SAN DIEGO
IGPP
8604 LA JOLLA SHORES DRIVE
SAN DIEGO, CA 92093

DIANE DOSER
DEPT. OF GEOLOGICAL SCIENCES
THE UNIVERSITY OF TEXAS AT EL PASO
EL PASO, TX 79968

DTIC
8725 JOHN J. KINGMAN ROAD
FT BELVOIR, VA 22060-6218 (2 COPIES)

MARK D. FISK
MISSION RESEARCH CORPORATION
735 STATE STREET
P.O. DRAWER 719
SANTA BARBARA, CA 93102-0719

LORI GRANT
MULTIMAX, INC.
311C FOREST AVE. SUITE 3
PACIFIC GROVE, CA 93950

HENRY GRAY
SMU STATISTICS DEPARTMENT
P.O. BOX 750302
DALLAS, TX 75275-0302

I. N. GUPTA
MULTIMAX, INC.
1441 MCCORMICK DRIVE
LARGO, MD 20774

DAVID HARKRIDER
BOSTON COLLEGE
24 MARTHA'S PT. RD.
CONCORD, MA 01742

THOMAS HEARN
NEW MEXICO STATE UNIVERSITY
DEPARTMENT OF PHYSICS
LAS CRUCES, NM 88003

MICHAEL HEDLIN
UNIVERSITY OF CALIFORNIA, SAN DIEGO
SCRIPPS INST. OF OCEANOGRAPHY
9500 GILMAN DRIVE
LA JOLLA, CA 92093-0225

DONALD HELMBERGER
CALIFORNIA INST. OF TECHNOLOGY
DIV. OF GEOL. & PLANETARY SCIENCES
SEISMOLOGICAL LABORATORY
PASADENA, CA 91125

EUGENE HERRIN
SOUTHERN METHODIST UNIVERSITY
DEPT. OF GEOLOGICAL SCIENCES
DALLAS, TX 75275-0395

ROBERT HERRMANN
ST. LOUIS UNIVERSITY
DEPT. OF EARTH & ATMOS. SCIENCES
3507 LACLEDE AVENUE
ST. LOUIS, MO 63103

VINDELL HSU
HQ/AFTAC/TTR
1030 S. HIGHWAY A1A
PATRICK AFB, FL 32925-3002

RONG-SONG JIH
DTRA/PMA
45045 AVIATION DRIVE
DULLES, VA 20166-7517

THOMAS JORDAN
MASS. INST. OF TECHNOLOGY
BLDG 54-918
CAMBRIDGE, MA 02139

LAWRENCE LIVERMORE NAT'L LAB
ATTN: TECHNICAL STAFF (PLS ROUTE)
PO BOX 808, MS L-208
LIVERMORE, CA 94551

LAWRENCE LIVERMORE NAT'L LAB
ATTN: TECHNICAL STAFF (PLS ROUTE)
PO BOX 808, MS L-205
LIVERMORE, CA 94551

LAWRENCE LIVERMORE NAT'L LAB
ATTN: TECHNICAL STAFF (PLS ROUTE)
PO BOX 808, MS L-200
LIVERMORE, CA 94551

THORNE LAY
UNIV. OF CALIFORNIA, SANTA CRUZ
EARTH SCIENCES DEPARTMENT
EARTH & MARINE SCIENCE BUILDING
SANTA CRUZ, CA 95064

ANATOLI L. LEVSHIN
DEPARTMENT OF PHYSICS
UNIVERSITY OF COLORADO
CAMPUS BOX 390
BOULDER, CO 80309-0309

JAMES LEWKOWICZ
WESTON GEOPHYSICAL CORP.
325 WEST MAIN STREET
NORTHBORO, MA 01532

LOS ALAMOS NATIONAL LABORATORY
ATTN: TECHNICAL STAFF (PLS ROUTE)
PO BOX 1663, MS D460
LOS ALAMOS, NM 87545

LOS ALAMOS NATIONAL LABORATORY
ATTN: TECHNICAL STAFF (PLS ROUTE)
PO BOX 1663, MS F665
LOS ALAMOS, NM 87545

SANDIA NATIONAL LABORATORY
ATTN: TECHNICAL STAFF (PLS ROUTE)
DEPT. 9311
MS 1159, PO BOX 5800
ALBUQUERQUE, NM 87185-1159

SANDIA NATIONAL LABORATORY
ATTN: TECHNICAL STAFF (PLS ROUTE)
DEPT. 5736
MS 0655, PO BOX 5800
ALBUQUERQUE, NM 87185-0655

AVI SHAPIRA
SEISMOLOGY DIVISION
IPRG
P.O.B. 2286 NOLON 58122 ISRAEL

MATTHEW SIBOL
ENSCO, INC.
445 PINEDA CT.
MELBOURNE, FL 32940

JEFFRY STEVENS
MAXWELL TECHNOLOGIES
8888 BALBOA AVE.
SAN DIEGO, CA 92123-1506

TACTEC
BATTELLE MEMORIAL INSTITUTE
505 KING AVENUE
COLUMBUS, OH 43201 (FINAL REPORT)

LAWRENCE TURNBULL
ACIS
DCI/ACIS
WASHINGTON DC 20505

FRANK VERNON
UNIV. OF CALIFORNIA, SAN DIEGO
SCRIPPS INST. OF OCEANOGRAPHY
9500 GILMAN DRIVE
LA JOLLA, CA 92093-0225

RU SHAN WU
UNIV. OF CALIFORNIA, SANTA CRUZ
EARTH SCIENCES DEPT.
1156 HIGH STREET
SANTA CRUZ, CA 95064

JAMES E. ZOLLWEG
BOISE STATE UNIVERSITY
GEOSCIENCES DEPT.
1910 UNIVERSITY DRIVE
BOISE, ID 83725

SANDIA NATIONAL LABORATORY
ATTN: TECHNICAL STAFF (PLS ROUTE)
DEPT. 5704
MS 0655, PO BOX 5800
ALBUQUERQUE, NM 87185-0655

THOMAS SERENO JR.
SAIC
10260 CAMPUS POINT DRIVE
SAN DIEGO, CA 92121

ROBERT SHUMWAY
410 MRAK HALL
DIVISION OF STATISTICS
UNIVERSITY OF CALIFORNIA
DAVIS, CA 95616-8671

DAVID SIMPSON
IRIS
1200 NEW YORK AVE., NW
SUITE 800
WASHINGTON DC 20005

BRIAN SULLIVAN
BOSTON COLLEGE
INSITUTE FOR SPACE RESEARCH
140 COMMONWEALTH AVENUE
CHESTNUT HILL, MA 02167

NAFI TOKSOZ
EARTH RESOURCES LABORATORY
M.I.T.
42 CARLTON STREET, E34-440
CAMBRIDGE, MA 02142

GREG VAN DER VINK
IRIS
1200 NEW YORK AVE., NW
SUITE 800
WASHINGTON DC 20005

TERRY WALLACE
UNIVERSITY OF ARIZONA
DEPARTMENT OF GEOSCIENCES
BUILDING #77
TUCSON, AZ 85721

JIAKANG XIE
COLUMBIA UNIVERSITY
LAMONT DOHERTY EARTH OBSERV.
ROUTE 9W
PALISADES, NY 10964

LOS ALAMOS NATIONAL LABORATORY
ATTN: TECHNICAL STAFF (PLS ROUTE)
PO BOX 1663, MS C335
LOS ALAMOS, NM 87545

GARY MCCARTOR
SOUTHERN METHODIST UNIVERSITY
DEPARTMENT OF PHYSICS
DALLAS, TX 75275-0395

KEITH MCLAUGHLIN
CENTER FOR MONITORING RESEARCH
SAIC
1300 N. 17TH STREET, SUITE 1450
ARLINGTON, VA 22209

BRIAN MITCHELL
DEPT OF EARTH & ATMOSPHERIC SCIENCES
ST. LOUIS UNIVERSITY
3507 LACLEDE AVENUE
ST. LOUIS, MO 63103

RICHARD MORROW
USACDA/IVI
320 21ST STREET, N.W.
WASHINGTON DC 20451

JOHN MURPHY
MAXWELL TECHNOLOGIES
11800 SUNRISE VALLEY DRIVE
SUITE 1212
RESTON, VA 22091

JAMES NI
NEW MEXICO STATE UNIVERSITY
DEPARTMENT OF PHYSICS
LAS CRUCES, NM 88003

ROBERT NORTH
CENTER FOR MONITORING RESEARCH
1300 N. 17th STREET, SUITE 1450
ARLINGTON, VA 22209

OFFICE OF THE SECRETARY OF DEFENSE
DDR&E
WASHINGTON DC 20330

JOHN ORCUTT
INST. OF GEOPH. & PLANETARY PHYSICS
UNIV. OF CALIFORNIA, SAN DIEGO
LA JOLLA, CA 92093

PACIFIC NORTHWEST NAT'L LAB
ATTN: TECHNICAL STAFF (PLS ROUTE)
PO BOX 999, MS K5-12
RICHLAND, WA 99352

FRANK PILOTTE
HQ AFTAC/TT
1030 S. HIGHWAY A1A
PATRICK AFB, FL 32925-3002

KEITH PRIESTLEY
DEPARTMENT OF EARTH SCIENCES
UNIVERSITY OF CAMBRIDGE
MADINGLEY RISE, MADINGLEY ROAD
CAMBRIDGE, CB3 0EZ UK

JAY PULLI
BBN SYSTEMS AND TECHNOLOGIES, INC.
1300 NORTH 17TH STREET
ROSSLYN, VA 22209

DELAINE REITER
WESTON GEOPHYSICAL CORP.
73 STANDISH ROAD
WATERTOWN, MA 0472

PAUL RICHARDS
COLUMBIA UNIVERSITY
LAMONT-DOHERTY EARTH OBSERV.
PALISADES, NY 10964

MICHAEL RITZWOLLER
DEPARTMENT OF PHYSICS
UNIVERSITY OF COLORADO
CAMPUS BOX 390
BOULDER, CO 80309-0309

DAVID RUSSELL
HQ AFTAC/TTR
1030 SOUTH HIGHWAY A1A
PATRICK AFB, FL 32925-3002

CHANDAN SAIKIA
WOODWARD-CLYDE FED. SERVICES
566 EL DORADO ST., SUITE 100
PASADENA, CA 91101-2560

SANDIA NATIONAL LABORATORY
ATTN: TECHNICAL STAFF (PLS ROUTE)
DEPT. 5704
MS 0979, PO BOX 5800
ALBUQUERQUE, NM 87185-0979